



**11<sup>th</sup> International Conference on  
Luminescent Detectors and  
Transformers of Ionizing Radiation**

**BOOK OF ABSTRACTS**

**12-17.09.2021, Bydgoszcz, Poland**

The LUMDETR 2021 Committees thank their partners:

**Kazimierz Wielki University in Bydgoszcz**  
**Oncology Center - prof. Łukaszczyk Memorial Hospital in Bydgoszcz**  
**Polish Physical Society (PPS)**  
**Polish Society of Medical Physics (FSMP)**  
**Office of the Marshal of the Kuyavian-Pomeranian Voivodeship**  
**Office of the President of Bydgoszcz**  
**Crystals and Materials, an open access journals by MDPI**  
**Firms: MEDSON Ltd, Poland, Czylok Ltd., Poland,**  
**RADPRO and VERITAS-Medical solution Ltd., Poland**

**LUMDETR 2021 will be held under the patronage of Mr Piotr Całbecki**  
**- the Marshal of the Kuyavian-Pomeranian Voivodeship and Mr Rafał**  
**Bruski - the President of Bydgoszcz**

## CONTENTS

Committies	4
Programme	5
Oral Session	13
Radioluminescence and scintillation mechanisms - 1	16
Radioluminescence and scintillation mechanisms - 2	22
Energy transfer and storage in the luminescent detectors	29
Technology and methods of luminescent material preparation: <i>Crystal growth 1</i>	35
Technology and methods of luminescent material preparation: <i>Crystal growth 2</i>	41
Technology and methods of luminescent material preparation: <i>Film     preparation</i>	48
Technology and methods of luminescent material preparation: Detectors based on the nanophosphors and nanocomposites	55
Defects and their role in performance of luminescence material - 1	61
Defects and their role in performance of luminescence material - 2	67
Luminescent spectroscopy of materials for detectors of ionization radiation: conventional methods and synchrotron radiation	73
Optically and thermally stimulated luminescence in solids - 1	80
Application of scintillators and detectors for medical diagnostics and biological research - 1	86
Application of scintillators and detectors for medical diagnostics and biological research - 2	92
Optically and thermally stimulated luminescence in solids - 2	96
Radiation dosimetry	102
Other phosphor applications	108
Poster session	112
Poster session - 1	113
Poster session - 2	140
Author index	165

## COMMITTEES LUMDETR 2021

### Conference Chairpersons

Chair – Prof. Dr. Yuriy Zorenko

Vice-Chair – Dr. Janusz Winiecki

Vice-Chair – Prof. Dr. Andrzej Suchocki

Vice-Chair – Prof. Dr. Kazimierz Fabisiak

Conference secretary – Dr. Karol Bartosiewicz

### LUMDETR 2021 Honor Committee

J. Woźny, Rector of Kazimierz Wielki University in Bydgoszcz

J. Kowalewski, Director of Oncology Center - prof Franciszek Łukaszczyk Memorial Hospital  
M. Adamski, Rector of Bydgoszcz University of Science and Technology

A. Gadomski, Chair of Bydgoszcz branch of Polish Physical Society (PPS)

K. Śłosarek, Chair of Polish Society of Medical Physics (FSMP)

R. Bruski, The President of Bydgoszcz

### International Advisory Committee

M. Akselrod (USA)

C. Andersen (Denmark)

A. Belsky (France)

P. Bilski (Poland)

A. Bos (The Netherlands)

R. Chen (Israel)

C. Dujardin (France)

A. Gektin (Ukraine)

B. Grinyov (Ukraine)

M. Kirm (Estonia)

A. Lushchik (Estonia)

A. Mandowski (Poland)

S.W.S. McKeever (USA)

M. Moszynski (Poland)

M. Nikl (Czech Republic)

A. Popov (Latvia)

W. Ryba-Romanowski (Poland)

P. Rodnyi (Russia)

S. Schweizer (Germany)

A. Vedda (Italy)

A. Voloshinovskii (Ukraine)

R.T. Williams (USA)

A. Winnacker (Germany)

A. Wojtowicz (Poland)

A. Yoshikawa (Japan)

Yu. Zorenko (Poland)

### Programme Committee

M. Nikl (Czech Republic)

A. Vedda (Italy)

C. Dujardin (France)

A. Yoshikawa (Japan)

E.G. Yukihara (Switzerland)

P. Bilski (Poland)

Yu. Zorenko (Poland)

A. Suchocki (Poland)

K. Śłosarek (Poland)

T. Piotrowski (Poland)

J. Winiecki (Poland)

### Local Organizing Committee

#### Institute of Physics UKW and PPS (Bydgoszcz branch)

Yu. Zorenko – conference Chair

A. Suchocki – conference vice Chair

K. Fabisiak – conference vice Chair

K. Bartosiewicz – conference secretary

G. Czerniak – PPS, Bydgoszcz branch

S. Witkiewicz-Łukaszek V. Gorbenko

P. Popielarski T. Zorenko

A. Markovskiy Y. Syrotych

A. Shakhno A. Majewski-Napierkowski

#### Oncology Center in Bydgoszcz

J. Winiecki – conference vice Chair

K. Klawińska-Knach

E. Woźniak

A. Madaj

P. Korowiecki

S. Nowakowski

# PROGRAMME

**Monday, 13.09.2021**

**08.00- 09.00** Registration of the participants

**09:00–09.40** OPENING ceremony

**Yu. Zorenko**, conference Chairman, *welcome speech*

**J. Woźny**, Rector Kazimierz Wielki University in Bydgoszcz, *welcome speech*

**J. Kowalewski**, Director of Oncology Centers in Bydgoszcz, *welcome speech*

**M. Adamski**, Rector of Bydgoszcz University of Science and Technology, *welcome speech*

**Person**, represented the Marshal of Kujawsko-Pomorske Wojewodship Office, *welcome speech*

**Person**, represented the President of Bydgoszcz, *welcome speech*

**09.40-10.00** In memoriam: R. Williams (M. Nikl) and M. Grinberg (S. Mahlik)

**10.00–10:15** MoS0-K1 A. Gadomski *Bydgoszcz Chapter of the Polish Physical Society: Past and Present*

**10:15–10:30** MoS0-K2 K. Śłosarek *Polish Society of Medical Physics - professional and scientific activity*

**10:30–11:00** Coffeee-break

**11:00–13:00** S1 Radioluminescence and scintillation mechanisms - 1

Chairman: Christophe Dujardin

**11:00–11:30** MoS1-K3 M. Nikl *Composition engineering in multicomponent garnets: new demands*

**11:30–12:00** MoS1-K4 A. Vasil'ev *Scintillation properties in connection with material structure and track fluctuations (remote presentation)*

**12:00–12:15** MoS1-O1 M. Yoshino *Scintillation properties and particle identification capability of (Li,Ca)I<sub>2</sub> solid solution (remote presentation)*

**12:15–12:30** MoS1-O2 L. Martinazzoli *Scintillation properties and timing performance of state-of-the-art Gd<sub>3</sub>Al<sub>2</sub>Ga<sub>3</sub>O<sub>12</sub> Single Crystals*

**12:30–12:45** MoS1-O3 V. Vaněček *Novel cross-luminescence scintillators: an exploration of CsMCl<sub>3</sub> perovskite matrix*

**12:45–13:00** MoS1-O4 S. Kurosawa *Fast Neutron Imaging using carbazole and p-terphenyl scintillator (remote presentation)*

**13:00–14:00** Lunch

**14:00–16:05** S2 Radioluminescence and scintillation mechanisms - 2

Chairman: Mauro Fassoli

**14:00 –14:25** MoS2-K5 M. Brik *First-principles calculations of electronic properties of scintillating materials*

**14:25–14:50** MoS2-K6 A. Wojtowicz *Radiative and nonradiative recombination in β-Ga<sub>2</sub>O<sub>3</sub> scintillator crystals*

**14:50–15:05** MoS2-O5 W. Drozdowski *Heading for brighter and faster β-Ga<sub>2</sub>O<sub>3</sub> Scintillator Crystals*

**15:05–15:20** MoS2-O6 S. Mann *Timing properties of radioluminescence in nanoparticle ZnS:Ag scintillators (remote presentation)*

**15:20–15:35** MoS2-O7 A. Monguzzi *Sensitization of scintillation in multicomponent polymeric composites*

**15:35–15:50** MoS2-O8 N. Galunov *Organic heterostructured scintillators with a high pulse shape discrimination capability (remote presentation)*

**15:50–16:05** MoS2-O9 C. Fujiwara *Scintillation properties for Cs<sub>2</sub>Hf(l,Br)<sub>6</sub> with red emission for real-time high dose rate monitor (remote presentation)*

**16:05–16:30** Coffeee-break

**16:30–18:30 S3 Energy transfer and storage in the luminescent detectors**

**Chairman: Andrzej Suchocki**

- 16:30 –17:00 MoS3-K7 S. Tanabe** *Energy transfer and NIR luminescence in lanthanoid and transition metal codoped storage phosphors (remote presentation)*
- 17:00 –17:30 MoS3-K8 S. Mahlik** *Broadband near-Infrared phosphors for light emitting diodes*
- 17:30 –17:45 MoS3-10 M. Danilkin** *Accelerated radiative transitions in impurities due to energy transfer from impurity-bound excitons (remote presentation)*
- 17:45 –18:00 MoS3-O11 G. Tamulaitis** *Excitation relaxation via intra- and intercenter transitions of Pr<sup>3+</sup> ion in garnet-type scintillator*
- 18:00 –18:15 MoS3-O12 S. Nargelas** *Relaxation of electronic excitation at cerium ions in GAGG matrix studied using transient absorption technique*
- 18:15 –18:30 MoS3-O13 E. Trofimova** *Luminescence properties and energy transfer processes in LiSrPO<sub>4</sub>:Pr<sup>3+</sup>,Na<sup>+</sup>, Mg<sup>2+</sup>(remote presentation)*
- 18:30–21:00 Welcome party**

**Tuesday, 14.09.2021**

**8:30–10:30 S4 Technology and methods of luminescent material preparation: Crystal growth 1**

**Chairman: Martin Nikl**

- 08:30–09:00 TuS4-K9 A. Yoshikawa** *A rapid screening method for novel scintillator crystals (remote presentation)*
- 09:00–09:30 TuS4-K10 O. Sidletskiy** *Advances in technologies of bulk crystal growth from non-precious metal crucibles*
- 09:30–09:45 TuS4-O14 K. Bartosiewicz** *La codoping strategy for modifying atoms segregation and luminescence and scintillation properties of LuAG:Pr single crystals*
- 09:45–10:00 TuS4-O15 F. Zajić** *Single crystal growth of garnets by floating zone method in laser furnace*
- 10:00–10:15 TuS4-O16 Ia. Gerasymov** *Effects of co-doping on optical and scintillation properties of YAG:Ce,C crystals*
- 10:15–10:30 TuS4-O17 D. Kofanov** *Growth and characterization of mixed LuYAG:Ce crystals under reducing atmosphere (remote presentation)*

**10.30–11.00 Coffee-break**

**11:00–13:00 S5 Technology and methods of luminescent material preparation: Crystal growth 2**

**Chairman: Miroslav Kucera**

- 11:00–11:30 TuS5-K11 J. Pejchal** *Luminescence mechanism and Ce incorporation in LaAP:Ce single crystals*
- 11:30 –11:45 TuS5-O18 K. Kamada** *Growth and scintillation properties of rare-earth doped SrO and CaO by core heating method (remote presentation)*
- 11:45–12:00 TuS5-O19 R. Král** *Cs<sub>2</sub>Hf<sub>x</sub>Zr<sub>1-x</sub>Cl<sub>6</sub> mixed crystals, their growth by vertical Bridgman method and characterization of luminescent and scintillation properties*
- 12:00–12:15 TuS5-O20 E. Galenin** *Crystallization of Y<sub>2</sub>O<sub>3</sub> melt in tungsten crucibles (remote presentation)*
- 12:15–12:30 TuS5-O21 Y. Takizawa** *Growth and scintillation properties of CsI/CsCl/KCl eutectics for radiation imaging applications*
- 12:30–12:45 TuS5-O22 R. Yajima** *Melt growth of Zn<sub>3</sub>Ta<sub>2</sub>O<sub>8</sub> crystal by core heating method and its scintillation properties (remote presentation)*
- 12:45–13:00 TuS5-O23 O. Lalinsky** *Optimization of cathodoluminescence efficiency of scintillators for low-energy electron detectors*
- 13:00–14:00 Lunch**

14:00–16:05 S6 Technology and methods of luminescent material preparation: Film preparation

Chairman: Yuriy Zorenko

- 14:00 –14:25 TuS6-K12 M. Kucera *Growth and properties of multicomponent garnet and perovskite films for low afterglow scintillators*
- 14:25–14:50 TuS6-K13 T. Runka *Raman spectroscopy of single crystalline films of perovskites*
- 14:50–15:05 TuS6-O24 Yu. Zorenko *Growth and luminescent properties of Bi<sup>3+</sup>, Tb<sup>3+</sup> and Eu<sup>3+</sup> doped Lu<sub>2</sub>O<sub>3</sub> single crystalline films and composites on their base*
- 15:05–15:20 TuS6-O25 J.A. Mares *Investigation of scintillating properties of single crystalline films and composite scintillators based on simple and mixed garnets*
- 15:20–15:35 TuS6-O26 A. Suchocki *High pressure studies of Ce<sup>3+</sup> luminescence in epitaxial LuAlO<sub>3</sub> single crystalline film*
- 15:35–15:50 TuS6-O27 V. Gorbenko *Development of composite scintillators based on the Ce<sup>3+</sup> doped single crystalline films and single crystals of orthosilicate compounds.*
- 15:50–16:05 TuS6-O28 M. Buryi *Optical and magnetic properties of epitaxially grown GaN:Ge(Si) thin films*

16:05–16:30 Coffee-break

16:30–18:30 S7 Technology and methods of luminescent material preparation: Detectors based on the nanophosphors and nanocomposites

Chairman: Marco Kirm

- 16:30 –17:00 TuS7-K14 C. Dujardin *Scintillation mechanisms of II-VI nano-semiconductor heterostructure*
- 17:00–17:30 TuS7-K15 I. Villa *Scintillation properties of advanced nanocomposite materials*
- 17:30–17:45 TuS7-O29 E. Mihóková *The role of Cs<sub>4</sub>PbBr<sub>6</sub> phase in the luminescence performance of bright CsPbBr<sub>3</sub> nanocrystals*
- 17:45–18:00 TuS7-O30 V. Jarý *Modification of optical properties of the GaN nanostructures via annealing in various atmospheres*
- 18:00–18:15 TuS7-O31 M. Chylii *The influence of precursor ratio in the Cd-Zn-S quantum dots synthesis on their morphological and optical properties*
- 18:15–18:30 TuS7-O32 R. Crapanzano *Radio- and Photo-luminescence of ZnO nanoparticles with different morphologies and functionalization.*

18:30–19:20 Poster session I with refreshment

Wednesday, 15.09.2021

8:30–10:30 S8 Defects and their role in performance of luminescence material - 1

Chairman: Anna Vedda

- 08:30–09:00 WeS8-K16 V. Laguta *Electron and hole trapping in wide band-gap oxide scintillation crystals*
- 09:00–09:30 WeS8-K17 A. Lushchik *Detection of uncatchable oxygen interstitials in neutron-irradiated corundum crystals (remote presentation)*
- 09:30 –09:45 WeS8-O33 E. Radzhabov *Fine structure of 4f-5d absorption spectra of MeF<sub>2</sub>-Yb<sup>3+</sup> in the vacuum ultraviolet region under synchrotron excitation (remote presentation)*
- 09:45–10:00 WeS8-O34 E. Zabelina *Gadolinium-aluminum-gallium garnet single crystals with partial substitution of gallium with aluminum and their optical characterization (remote presentation)*
- 10:00 –10:15 WeS8-O35 Y. Hizhnyi *Band gap engineering of RAlO<sub>3</sub> (R = Y, La, Gd, Yb, Lu) perovskites*
- 10:15–10:30 WeS8-O36 S. Kiselev *Influence of irradiation with fast electron beam on energy transport in praseodymium-ion doped phosphates (remote presentation)*

10.30–11.00 Coffee-break

11:00–13:30	<b>S9 Defects and their role in performance of luminescence material – 2</b>		
	Chairman: Valentyn Laguta		
11:00–11:30	WeS9-K18	M. Kitaura	<i>Gamma-ray-induced positron annihilation lifetime spectroscopy for characterization of Imperfections in scintillator crystals (remote presentation)</i>
11:30–12:00	WeS9-K19	A. Popov	<i>Detailed analysis of self-trapped hole <math>V_k</math> center mobility in binary and complex halides as a function of lattice parameters</i>
12:00–12:15	WeS9-O37	V. Nagirnyi	<i>Inter-configurational <math>4f5d \rightarrow f</math> radiative transitions of <math>Pr^{3+}</math> ions doped in <math>Li_6Y(BO_3)_3</math> single crystals</i>
12:15–12:30	WeS9-O38	V. Tsiumra	<i>Spectroscopic studies of <math>Bi^{3+}</math> - doped <math>Ca_3Ga_2Ge_3O_{12}</math> garnet</i>
12:30–12:45	WeS9-O39	D. Stefańska	<i>Luminescence and thermal behavior of <math>La_2MgTiO_6</math>- <math>Ba_2MgWO_6</math> solid solution (remote presentation)</i>
12:45–13:00	WeS9-O40	N. Majewska	<i>The broadband IR emission from <math>Cr^{3+}</math> ions in magnetoplumbite</i>
13:00–14:00	Lunch		
14:00–22:00	Excursion with bonfire		

### Thursday, 16.09.2021

08:30–10:35	<b>S10 Luminescent spectroscopy of materials for detectors of ionization radiation: conventional methods and synchrotron radiation</b>		
	Chairman: Vitaliy Nagirnyi		
08:30–08:55	ThS10-K20	M. Kirm	<i>Time-resolved luminescence spectroscopy in studies of ultrafast processes in wide gap materials using advanced light sources</i>
08:55–09:20	ThS10-K21	W. Stręk	<i>Emission properties of rare earth doped materials under high power excitation</i>
09:20–09:35	ThS10-O41	V. Pankratov	<i>Time-resolved luminescence and VUV excitation spectroscopy of GGAG:Ce single crystals</i>
09:35–09:50	ThS10-O42	D. Włodarczyk	<i>Structural and optical studies of novel, cerium-tungstate double perovskites doped with rare-earth ions</i>
09:50–10:05	ThS10-O43	D. Spassky	<i>Luminescence properties of GAGG:Ce scintillator under intense laser irradiation (remote presentation)</i>
10:05–10:20	ThS10-O44	L.-I. Bulyk	<i>Pressure induced blue luminescence in <math>CsPbBr_3</math> single crystals</i>
10:20–10:35	ThS10-O45	J. Saaring	<i>Relaxation of anion and cation electronic excitations in hexafluorogermanates</i>
10:35–11:00	Coffee-break		
11:00–13:00	<b>S11 Optically and thermally stimulated luminescence in solids - 1</b>		
	Chairman: Paweł Olko		
11:00–11:30	ThS11-K22	A. Mandowski	<i>Theory and a novel approach to optically stimulated luminescence in complex systems</i>
11:30–12:00	ThS11-K23	E. Yukihiro	<i>The still unexplained mechanism of the UV emission of <math>Al_2O_3:C</math>: what do we know and how do we move forward?</i>
12:00–12:15	ThS11-O46	P. Bilski	<i>Infrared-stimulated luminescence of garnets</i>
12:15–12:30	ThS11-O47	Ł. Kapłon	<i>Green-emitting polystyrene scintillators for plastic scintillation dosimetry</i>
12:30–12:45	ThS11-O48	M. Orfano	<i>Photoluminescence and radioluminescence properties of hafnium oxide-based Metal Organic Framework (MOF) nanocrystals and composites.</i>
12:45–13:00	ThS11-O49	R. Cala	<i>Characterization of BSO and mixed BGSO crystals for future dual-readout calorimetry</i>
13:00–14:00	Lunch		



**14:00–16:00 S12 Application of scintillators and detectors for medical diagnostics and biological research - 1**

**Chairman: Janusz Winięcki**

- 14:00–14:30 ThS12-K24 M. Maryański *Mechanisms of radiochromic response in polymer gel dosimeters***  
**14:30–15:00 ThS12-K25 P. Olko *Luminescence dosimetry in proton therapy***  
**15:00–15:15 ThS12-O50 S. Ishizawa *Development of red-emitting oxide scintillator for decommissioning Fukushima Daiichi nuclear power plant (remote presentation)***  
**15:15–15:30 ThS12-O51 K. Fabisiak *UV detector based on polycrystalline CVD diamonds***  
**15:30–15:45 ThS12-O52 O. V. Pakari *Investigation of the UV emission mechanism in Al<sub>2</sub>O<sub>3</sub>:C using pulsed OSL and photo-transfer experiments***  
**15:45–16:00 ThS12-O53 J.B. Christensen *Improving linear energy transfer measurements using automated OSL readers***

**16:00–16:30 Coffee-break**

**16:30–18:00 S13 Application of scintillators and detectors for medical diagnostics and biological research – 2**

**Chairman: Marek Maryański**

- 16:30–17:00 ThS13-K26 J. Winięcki *The purposes, principles and common techniques used in radiation therapy***  
**17:00–17:30 ThS13-K27 T. Piotrowski *What is plan quality in radiotherapy?***  
**17:30–17:45 ThS13-O54 S. Witkiewicz-Łukaszek *Basic characteristics of dose distributions of photons beam for radiotherapeutic applications using YAG:Ce crystal detectors***  
**17:45–18:00 ThS13-O55 O. Rebane *Time-resolved fluorescence study of bacterial spores treated by hydrogen peroxide vapour for monitoring decontamination process***

**18:00–19:00 Poster session II with refreshment**

**20:00–22:30 Concert and conference banquet**

**Friday, 17.09.2021**

**08:30–10:30 S14 Optically and thermally stimulated luminescence in solids – 2**

**Chairman: Arkadiusz Mandowski**

- 08:30–09:00 FrS14-K28 W. Gieszczyk *LiMgPO<sub>4</sub>:RE - review of the results of 7-years investigations on new dosimetric crystals***  
**09:00–09:30 FrS14-K29 Y. Zhydachevskyy *Trapping and recombination mechanisms in YAP:Mn<sup>2+</sup> crystals as promising TL/OSL detectors***  
**09:30–09:45 FrS14-O56 M. Sądel *2D OSL dosimetry based on LiMgPO<sub>4</sub> powder embedded into the flat sheet silicone foils***  
**09:45–10:00 FrS14-O57 R.R. Ruiz-Torres *Thermoluminescence of beta irradiated CaAl<sub>2</sub>O<sub>4</sub>:Eu<sup>2+</sup>,Dy<sup>3+</sup> synthesized by combustion method: thermal quenching and thermal cleaning studies***  
**10:00–10:15 FrS14-O58 K. Lemański *Luminescent properties of Ba<sub>2</sub>MgWO<sub>6</sub> polycrystals and ceramics doped with the Eu<sup>3+</sup> ions***  
**10:15–10:30 FrS14-O59 A. Shyichuk *Electron traps in Lu<sub>2</sub>O<sub>3</sub>:Hf from density functional calculations***

**10:30–11:00 Coffee-break**

**11:00–13:00 S15 Radiation dosimetry**

**Chairman: Paweł Bilski**

- 11:00–11:30 FrS15-K30 M. Martini *Natural radiation dosimetry applications: dating ancient bronze statue by luminescence***  
**11:30–12:00 FrS15-K31 A. Chruścińska *New challenges and problems in the field of luminescence dating***

<b>12:00–12:15</b>	FrS15-O60	M. Discher	<i>Temperature assisted OSL measurements of display glass from mobile phones for retrospective dosimetry</i>
<b>12:15–12:30</b>	FrS15-O61	A. Mrozik	<i>Common medicines as emergency dosimeters</i>
<b>12:30–12:45</b>	FrS15-O62	H. Kim	<i>Dose recovery test using a TA-OSL protocol of display glass for accident dosimetry (remote presentation)</i>
<b>12:45–13:00</b>	FrS15-O63	N. Miniajluk-Gawel	<i>Influence of sintering parameters on spectroscopic properties of BMW:Eu<sup>3+</sup> ceramic materials (remote presentation)</i>
<b>13:00–14:00</b>	<b>Lunch</b>		
<b>14:00–16:05</b>	<b>S16 Other phosphor applications</b>		
	Chairman: Andrzej Wojtowicz		
<b>14:00–14:30</b>	FrS16-K32	M. Batentschuk	<i>New phosphors for high temperature thermometry</i>
<b>14:30–15:00</b>	FrS16-K33	S. Schweizer	<i>Light guides based on lanthanide-doped borate glass (remote presentation)</i>
<b>15:00–15:15</b>	FrS16-O64	A. Markovskiyi	<i>Composite color converters based on Tb<sub>1.5</sub>Gd<sub>1.5</sub>Al<sub>5</sub>O<sub>12</sub>:Ce single crystalline films and Y<sub>3</sub>Al<sub>5</sub>O<sub>12</sub>:Ce crystal substrates</i>
<b>15:15–15:30</b>	FrS16-O65	T. H. Q. Vu	<i>Ba<sub>2</sub>MgWO<sub>6</sub>:Er<sup>3+</sup> as a novel bifunctional double perovskites for white-light emitting phosphor and low-temperature optical thermometer</i>
<b>15:45–16:00</b>	<b>Coffee-break</b>		
<b>16:00–16:30</b>	<b>Conference closing</b>		

# POSTER PRESENTATIONS

Tuesday, 14.09.2021, 18:30-19:30

PARIS center, posters hall

Chairmen's: Miroslaw Batentschuk; Winićjusz Drozdowski

- |         |                        |   |
|---------|------------------------|---|
| TuP1-1  | V.A. Pustovarov        | <i>Site-selective luminescence of solid solutions based on silicate-tungstates doped with <math>\text{Eu}^{3+}</math> ions (remote presentation)</i>  |
| TuP1-2  | E.V. Tishchenko        | <i>Scattering of hot charge carriers in solid solutions of dielectric crystals with substitutional disorder (remote presentation)</i>   |
| TuP1-3  | A. Bachiri             | <i>Scintillation yield of Czochralski-grown <math>\beta\text{-Ga}_2\text{O}_3</math> and <math>\beta\text{-Ga}_2\text{O}_3\text{:Si}</math> crystals</i>  |
| TuP1-4  | A. Romet               | <i>Developing UV emitters based on undoped <math>\text{ZnAl}_2\text{O}_4</math> nanofibers</i>  |
| TuP1-5  | V. Pankratov           | <i>Time-resolved luminescence spectroscopy of rare-earth doped <math>\text{SrMoO}_4</math> single crystals</i>  |
| TuP1-6  | M. Yoshino             | <i>Crystal growth, scintillation property, and pulse shape discrimination of <math>\text{Ca}(\text{Br},\text{I})_2</math> scintillators (remote presentation)</i>   |
| TuP1-7  | C. Dujardin            | <i>Purification, growth and optical properties of large <math>{}^6\text{Li}_2\text{MoO}_4</math> for scintillating bolometer</i>  |
| TuP1-8  | K. Kamada              | <i>Fabrication of <math>{}^6\text{LiBr}</math> and <math>\text{BaBr}_2</math> based eutectic scintillator and its radiation response (remote presentation)</i>  |
| TuP1-9  | Y. Takizawa            | <i>Growth and scintillation properties of <math>\text{Ce}:\text{LaBr}_3/\text{LiBr}</math> eutectics (remote presentation)</i>  |
| TuP1-10 | Y. Syrotych            | <i>New types of composite scintillators based on the single crystalline films and crystals of <math>\text{Gd}_3\text{Al}_{5-x}\text{Ga}_x\text{O}_{12}:\text{Ce}</math> garnets</i>   |
| TuP1-11 | P. Popielarski         | <i>Luminescent properties of <math>\text{YAG}:\text{Ce}</math> and <math>\text{TbAG}:\text{Ce}</math> nanopowder thin films in polycarbonate (PC) and polystyrene (PS) matrices</i>   |
| TuP1-12 | A. Mrozik              | <i>Analysis of TL signals from SCF/SC composite detectors (<math>\text{LuAG}:\text{Ce}/\text{YAG}</math>) for distinguishing radiation field components</i>   |
| TuP1-13 | Yu. Zorenko            | <i><math>\text{Ce}^{3+}</math> to <math>\text{Ce}^{4+}</math> recharge in Ce doped <math>\text{Y}_{3-x}\text{Ca}_x\text{Al}_{5-x}\text{Si}_x\text{O}_{12}</math> and <math>\text{Y}_3\text{Al}_{5-2y}\text{Mg}_y\text{Si}_y\text{O}_{12}</math> single crystalline films: EPR and optical studies</i> |
| TuP1-14 | S. Witkiewicz-Lukaszek | <i>Three-layered composite scintillator based on the <math>\text{YAG}</math> and <math>\text{LuAG}</math> garnets for simultaneous registration of <math>\alpha</math>-, <math>\beta</math>-particles and <math>\gamma</math>-quanta</i>  |
| TuP1-15 | M. Makowski            | <i>Scintillation time profiles of Czochralski-grown <math>\beta\text{-Ga}_2\text{O}_3</math> and <math>\beta\text{-Ga}_2\text{O}_3\text{:Si}</math> crystals</i>  |
| TuP1-16 | W. Dewo                | <i>Raman and luminescent spectroscopy of <math>\text{TbAG}:\text{Mn}</math> garnet single crystalline film phosphor</i>   |
| TuP1-17 | A. Voloshinovskii      | <i>Polymer nanocomposites with embedded <math>\text{CsPbBr}_3</math> nanoparticles (remote presentation)</i>  |
| TuP1-18 | V. Vistovskyy          | <i>Temperature behavior of the near band edge luminescence in <math>\text{CsPbBr}_3</math> single crystals, microcrystals and nanoparticles (remote presentation)</i>   |
| TuP1-19 | A. Akhmetova           | <i>Synthesis and characterization 2D <math>\text{CdTe}</math> nanoplatelets for PV application (remote presentation)</i>  |
| TuP1-20 | A. Shakhno             | <i>Micro-powder phosphors based on the <math>\text{Ce}^{3+}</math> and <math>\text{Mn}^{2+}</math> doped <math>\text{Ca}_2\text{YMgScSi}_3\text{O}_{12}</math> silicate garnet for WLED application</i>   |
| TuP1-21 | T. Zorenko             | <i><math>\text{Ce}^{3+}</math> doped <math>\text{Al}_2\text{O}_3\text{-YAG}</math> eutectics as converters for WLED application</i>   |
| TuP1-22 | O. Zapadlík            | <i>Engineering of <math>\text{YAG}:\text{Ce}</math> to improve its scintillation properties</i>   |
| TuP1-23 | Y. Hizhnyi             | <i>Electronic properties of Mn-related defects in <math>\text{YAlO}_3</math> perovskite crystal</i>   |
| TuP1-24 | V. Pankratova          | <i>Comparative study on the influence of swift heavy ions on structural and luminescent properties of several important optical and scintillator materials</i>  |
| TuP1-25 | O. Chukova             | <i>Synthesis and properties of luminescent glass-ceramics composed of vanadate-borate glass filled with vanadate nanoparticles</i>  |
| TuP1-26 | S. Nagorny             | <i>Scintillation and charge trapping properties of <math>\text{Cs}_2\text{HfCl}_6</math> and <math>\text{Cs}_2\text{ZrCl}_6</math> single crystals in a wide temperature range (remote presentation)</i>  |
| TuP1-27 | V. Gayshan             | <i>New type of ultra-high (&lt;3%) energy resolution gamma spectrometry using traditional scintillators (remote presentation)</i>   |

**Thursday, 16.09.2021, 18:00-19:00**

**PARIS center, posters hall**

**Chairmen's: Eduardo Yukichara, Kazimierz Fabisiak**

ThP2-1	A. Krasnikov	<i>Electron and hole centers in the UV-irradiated Bi<sup>3+</sup>-doped Ca<sub>3</sub>Ga<sub>2</sub>Ge<sub>3</sub>O<sub>12</sub> garnet</i>
ThP2-2	M. Buryi	<i>Charge trapping in Li doped Y<sub>3</sub>Al<sub>5</sub>O<sub>12</sub> single crystals: correlated EPR and TSL investigation</i>
ThP2-3	M. Sankowska	<i>The influence of temperature on the photoluminescence of lithium fluoride crystals</i>
ThP2-4	M. E. Witkowski	<i>Low temperature thermoluminescence of β-Ga<sub>2</sub>O<sub>3</sub> scintillator – new results and new interpretations</i>
ThP2-5	N. Krutyak	<i>Novel NASICON-type phosphors doped with RE ions: structure and luminescence (remote presentation)</i>
ThP2-6	S. Ubizskii	<i>Luminescence Response of YAP:Mn crystal to the ionizing and visible radiation</i>
ThP2-7	D. Spassky	<i>Luminescent and structural properties of Sc<sub>x</sub>Y<sub>1-x</sub>VO<sub>4</sub>:Eu<sup>3+</sup> solid solutions (remote presentation)</i>
ThP2-8	D. Daurenbekov	<i>Recombination emission and electron trapping centers in irradiated BaSO<sub>4</sub> and CaSO<sub>4</sub> (remote presentation)</i>
ThP2-9	A. Luchechko	<i>TL and OSL studies of Mn<sup>2+</sup> and Eu<sup>3+</sup>-doped MgGa<sub>2</sub>O<sub>4</sub> phosphor</i>
ThP2-10	S. Motta	<i>Characterization of Leksyg Smart automated reader for TL and OSL dosimetry using various materials</i>
ThP2-11	A. Maratova	<i>Effect of exciton-like luminescence flare-up in the field of homologous cations in KCl matrix (remote presentation)</i>
ThP2-12	A. Majewski-Napierkowski	<i>Regularities of manganese charge state formation and luminescent properties of Mn doped Al<sub>2</sub>O<sub>3</sub>, YAlO<sub>3</sub> and Y<sub>3</sub>Al<sub>5</sub>O<sub>12</sub> single crystalline films</i>
ThP2-13	V. Chernov	<i>Evaluation thermal quenching parameters from a series of experimental thermoluminescence curves recorded with variable heating rates</i>
ThP2-14	A. K. Somakumar	<i>Temperature dependent photoluminescence studies on Mn doped Y<sub>3</sub>Al<sub>5</sub>O<sub>12</sub> single crystalline films</i>
ThP2-15	M.-Y. Shih	<i>Execution of personal and extremity dosimeters proficiency tests regarding dose equivalent for beta particles (remote presentation)</i>
ThP2-16	M. Discher	<i>ProGlaDos Project: TL study of protective glasses of mobile phones for retrospective dosimetry</i>
ThP2-17	K. Szufa	<i>Optically stimulated luminescence properties of commercially available KCl dietary supplement as retrospective dosimeter</i>
ThP2-18	M. Biernacka	<i>Investigations of the thermal stability of the OSL main trap in quartz from sediments</i>
ThP2-19	N. Pawlak	<i>Thermal depletion curve of the complex OSL signal</i>
ThP2-20	R. Smyka	<i>Luminescent properties of microcline from the granite pegmatite of the Strzegom Massif</i>
ThP2-21	C. Bassinet	<i>ProGlaDos Project - Mobile phone screen protector glass for radiation accident dosimetry: TL investigation of the intrinsic background signal (remote presentation)</i>
ThP2-22	R. Majgier	<i>Comparison of OSL properties of sodium sulfate and potassium sulfate</i>
ThP2-23	E. Mandowska	<i>Investigation of feldspar luminescence decay using pulsed IRSL measurement</i>
ThP2-24	L. Oster	<i>Investigation of the Dose-Rate Effects in the Thermoluminescence of LiF:Mg,Ti (TLD-100) (remote presentation)</i>
ThP2-25	B. Rikhotso	<i>Atomistic simulation synthesis of Li<sub>x</sub>TiO<sub>2</sub> nanoporous as anode electrode materials for energy storage in lithium ion batteries (remote presentation)</i>

# Oral presentations

## **Bydgoszcz Chapter of the Polish Physical Society: Past and Present**

**A. Gadomski**<sup>1</sup>

<sup>1</sup> *Institute of Mathematics and Physics, Faculty of Chemical Technology and Engineering,  
Bydgoszcz University of Technology, al. Kaliskiego 7, PL85-796 Bydgoszcz, Poland*

Bydgoszcz Chapter of the PPS (BCh-PPS) has commenced its activity in the 1970s of the past millennium. The members of BCh-PPS are mainly physicists of three public universities located in Bydgoszcz. These are: UTP University of Science and Technology (UTP), Kazimierz Wielki University (UKW) and Collegium Medicum of the UMK in Bydgoszcz. The members body is complemented by physics teachers from the city and the region, and physicists from non-public universities.

Bydgoszcz is the capital and the biggest city of the Kujawy and Pomorze Voivodeship. This region is characteristic of certain personal historical facts. Namely, many distinguished physicists and natural sciences researchers were born in this region. The talk shall emphasize that the BCh-PPS rests on giants' shoulders, such as Copernicus, Michelson, Nernst, Czochralski, Regener and Hergesell, to name but a few. A current activity of the BCh-PPS, culminating at the General Meeting of the PPS in Bydgoszcz (September 19-23, 2021) <https://47zfp.utp.edu.pl/>, will be presented as well.

## **Polish Society of Medical Physics - professional and scientific activity**

**K. Ślosarek**<sup>1</sup>

*<sup>1</sup>Polish Society of Medical Physics Maria Skłodowska-Curie National Research Institute of Oncology, Gliwice Branch 44-101 Gliwice, Wybrzeże AK 15 Street*

Polish Society of Medical Physics (PSMP) was founded in 1965, three years after the formation of the International Organization for Medical Physics (IOMP). In the late 1980s, PSMP became a member of the European Federation of Organisations for Medical Physics (EFOMP). The interests of PSMP cover the full range of physics in medicine.

The organizational structure of the Society will be presented, its activity in the field of professional training and research, the cooperation with international organizations and publishing activities. Legal regulations concerning the profession of medical physicist in Poland will be discussed.

PSMP currently consists of 11 branches and has about 300 members. The work of the society is managed by the nine-person Main Board. Trainings are conducted as part of specialization in the field of medical physics (medical profession). Medical physicists from Poland are members of several committees of European Federation of Organisations for Medical Physics. The Society organizes the Autumn School of Medical Physics in Bydgoszcz, Section Meetings and Scientific Congresses. The Polish Journal of Medical Physics and Engineering journal, the publisher of which is PTFM, is rapidly gaining the market of scientific journals related to medical physics. This journal is the successor to *Postępy Fizyki Medycznej* which has been published since 1966.

## Composition engineering in multicomponent garnets: New demands

**M. Nikl<sup>1</sup>, J. Pejchal<sup>1</sup>, P. Bohacek<sup>1</sup>**

<sup>1</sup>*Institute of Physics, Czech Academy of Sciences, Na Slovance 1999/2, Prague, Czech Republic*

**E-mail: nikel@fzu.cz**

Single crystals of multicomponent garnets scintillators were reported for the first time in 2011 [1,2] as a result of combinatorial search within the cerium doped  $(\text{Gd,Y,Lu})_3(\text{Ga,Al})_5\text{O}_{12}$  compositions prepared by micropulling down technique. The balanced Gd-(Lu,Y) and (Ga,Al) content ensured immersion of shallow electron traps into conduction band and high enough ionization barrier of  $5d_1$  excited state of  $\text{Ce}^{3+}$  around room temperature. The most studied composition based on  $\text{Gd}_3\text{Ga}_3\text{Al}_2\text{O}_{12}:\text{Ce}$ , so called GAGG:Ce has shown light yield (LY) up to nearly 60 000 phot/MeV; two inch Czochralski grown single crystal was reported in 2012 [3]. Improvement of timing characteristics of these scintillators was achieved by divalent ion codoping at the expense of LY value [4,5]. The Mg codoping was found more effective for this purpose [5] and the leading decay time in scintillation response was shortened down to 45 ns with a slower tail with few-several hundreds ns decay time and similar share on total intensity of both components was reported [4,5]. The explanation of such improved timing was based on the stabilization of  $\text{Ce}^{4+}$  which competes for electrons from conduction band with any electron traps and effectively transforms very slow components in the decay into the fast one determined by the photoluminescence (PL) decay time of  $\text{Ce}^{3+}$  itself (about 60 ns in GAGG host) [5]. Furthermore, a detailed study performed later on a selected set of the codoped samples [6] revealed that the Ce-Mg pairs are responsible for the decay constants below PL decay time of  $\text{Ce}^{3+}$  due to the decreased energy barrier for quenching  $\text{Ce}^{3+}$  emission in such pairs. This effect and the overlap of  $\text{Gd}^{3+}$  emission at 312 nm with the CT absorption of  $\text{Ce}^{4+}$  center can explain the observed noticeable decrease of LY values.

There are two pressing questions nowadays regarding further tuning of properties of these multicomponent garnets using the industrial scale growth methods: (i) Given the demand coming mainly from high energy physics there is an open question up to which values the dominant decay constant can be shortened and slower components incl. afterglow suppressed with yet affordable LY. Together with the codoping mentioned above, the composition tuning of YAGG host towards more Ga-rich one provided the dominant decay constant of 21 ns [7]; (ii) Given the necessity to use Ir-crucible for garnets containing Ga cation [8] the price of the crystal remains very high. The question arises, if a multicomponent garnet hosts can be modified towards the Ga-free composition and if such a composition could be grown using a cheaper crucible material and keep high enough the values of light yield and other advantageous characteristics of GAGG:Ce scintillator. This presentation will address both these questions.

### References:

- [1] K. Kamada et al, *Crystal Growth & Design* **11** (2011) 4484
- [2] K. Kamada et al, *J. Phys. D: Appl. Phys.* **44** (2011) 505104
- [3] K. Kamada et al, *J. Cryst. Growth* **352**, (2012) 88
- [4] M. Tyagi et al, *J. Phys. D: Appl. Phys.* **46** (2013) 475302
- [5] K. Kamada et al, *Optical Materials* **41** (2015) 63
- [6] V. Babin et al, *Optical Materials* **83** (2018) 290
- [7] O. Sidletskiy et al, *CrystEngComm*. **19** (2017) 1001
- [8] K. Kamada et al, *J. Cryst. Growth* **535** (2020) 125510



## Scintillation properties in connection with material structure and track fluctuations

A. Gektin<sup>1</sup>, A.N. Vasil'ev<sup>2</sup>

<sup>1</sup>*Institute for Scintillation Materials, NAS of Ukraine, 60 Nauki Avenue, 61001 Kharkov, Ukraine*

<sup>2</sup>*Skobeltsyn Institute of Nuclear Physics, Lomonosov Moscow State University, Leninskie Gory, 1-2, 119991 Moscow, Russia*

**E-mail: [anv@sinp.msu.ru](mailto:anv@sinp.msu.ru)**

Scintillation pulse is formed by the excited region of the material. The formation of the spatial structure of initial distribution of excitations and temporal evolution of this region is controlled by the structure of material and the transport and interaction of excitations. An example of a system with high non-uniformity is a nanoscale composite material with embedded nanoparticles [1], in which processes of conversion of gamma-quanta into photoelectrons, multiplication cascade, energy transfer and scintillation photon emission may occur in different parts of the composite. Widely used crystalline solid solutions often demonstrate better scintillation properties in comparison with initial materials [2] not only due to change of e.g. effective bandgap but also due to strong modification of transport properties during carrier thermalization [3]. Even in highly uniform crystals tracks are characterised by strongly nonuniform structure resulting in large track-to-track fluctuations and the corresponding influence on scintillator energy resolution [4]. We discuss here how all these non-uniformities influence on different stages of the scintillation response development.

### References

- [1] R. M. Turtos, S. Gundacker, S. Omelkov et al, *npj 2D Materials and Applications*, 3 (2019), 37.
- [2] A. Belsky, A. Gektin, A. Vasil'ev, *IEEE Transactions on Nuclear Science*, 61 (2013) 262-270.
- [3] A. Belsky, A. Gektin, A. Vasil'ev, *Physica status solidi (b)*, 257 (2020) 1900535.
- [4] A. Gektin, A.N. Vasil'ev, V. Suzdal, and A. Sobolev, *IEEE Transactions on Nuclear Science*, 67 (2020) 880–887.

### Acknowledgments

This work is partially supported by the Russian Science Foundation under grant 21-12-00219.

## Scintillation properties and particle identification capability of (Li,Ca)I<sub>2</sub> solid solution

**M. Yoshino<sup>1</sup>, K. Kamada<sup>2,3</sup>, Y. Takizawa<sup>1</sup>, T. Iida<sup>4</sup>, K. Mizukoshi<sup>5</sup>, A. Yoshikawa<sup>1,2,3</sup>**

<sup>1</sup>Tohoku University, Institute for Materials Research, 2-1-1 Katahira, Aoba-ku, Sendai, 980-8577, Japan

<sup>2</sup>Tohoku University, New Industry Creation Hatchery Center, 6-6-10 Aoba, Aramaki, Aoba-ku, Sendai, 980-8579, Japan

<sup>3</sup>C&A Corporation, 1-16-23 Ichiban-cho, Aoba-ku, Sendai, 980-0811, Japan

<sup>4</sup>University of Tsukuba, 1-1-1 Tennodai, Tsukuba, Ibaraki, 305-8571, Japan

<sup>5</sup>Kobe University, Department of Physics, 1-1 Rokkodai, Nada-ku, Kobe, 657-8501, Japan

**E-mail: yoshino.masao@imr.tohoku.ac.jp**

Scintillators are used as radiation detectors in many fields, such as high-energy physics, medical imaging, and homeland security. Homeland security, underground physics, and space-based applications often require the detection of both neutron and gamma-ray. In the case of scintillators, Li-containing materials have good thermal neutron detection efficiency through the <sup>6</sup>Li(n, α)<sup>3</sup>H capture reaction, and gamma rejection from neutron signal may be accomplished by pulse shape discrimination (PSD).

CaI<sub>2</sub> scintillator crystals were discovered by Hofstadter et al. in the 1960s [1] and high light yield – double those of Tl doped NaI – was reported. We have grown a 1-inch diameter of CaI<sub>2</sub> single crystal by the vertical Bridgeman-Stockbarger (VB) method in a previous study. Grown crystals showed a high light yield of 107,000 photons/MeV [2] and excellent particle identification (PI) capability between alpha and gamma, even using a simple pulse shape ratio analysis [3].

In this study, to apply this excellent PI capability of CaI<sub>2</sub> to gamma/neutron separation, we prepared a solid solution of (Li<sub>x</sub>Ca<sub>1-x</sub>)I<sub>2-x</sub> as neutron scintillators. The crystal growth was performed by the VB method. PSD performance is evaluated using <sup>60</sup>Co, <sup>241</sup>Am, and <sup>252</sup>Cf as gamma, alpha, and neutron sources. Fig. 1 shows a 2D plot of energy versus PSD performance. The neutron/alpha and gamma are well separated. The best value of F-measure between alpha and gamma is 0.998 in the energy range of > 200 keVee. In this conference, the scintillation properties and PI capability of grown crystals will be discussed.

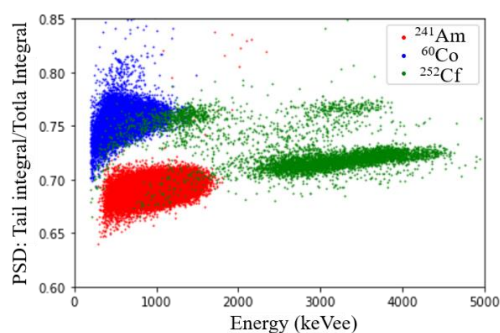


Fig. 1 2D-plot of energy versus PSD performance.

### References

- [1] R. Hofstadter, Alkali Halide Scintillation Counters, Phys Rev. 74 (1948) 100–101.
- [2] K. Kamada et al., Single crystal growth and scintillation properties of Ca(Cl, Br, I) 2 single crystal, Ceram Int. 43 (2017) S423–S427.
- [3] T. Iida et al., High-light-yield calcium iodide (CaI<sub>2</sub>) scintillator for astroparticle physics, Nucl Instruments Methods Phys Res A. 958 (2020) 162629.

# Scintillation properties and timing performance of state-of-the-art $\text{Gd}_3\text{Al}_2\text{Ga}_3\text{O}_{12}$ single crystals

**L. Martinazzoli**<sup>1,2</sup>, **N. Kratochwil**<sup>1,3</sup>, **S. Gundacker**<sup>4</sup>, **E. Auffray**<sup>1</sup>

<sup>1</sup>European Organization for Nuclear Research, Geneva, Switzerland

<sup>2</sup>Università degli Studi di Milano-Bicocca, Milan, Italy

<sup>3</sup>University of Vienna, Vienna, Austria

<sup>4</sup>PMI ExMI RWTH Aachen University, Aachen, Germany

**E-mail: [loris.martinazzoli@cern.ch](mailto:loris.martinazzoli@cern.ch)**

The High-Luminosity phase of the LHC collider will set stringent requirements on the performance of detector materials in terms of time resolution and radiation hardness. Cerium-doped scintillating garnet crystals proved to satisfy the latter [1, 2], while the former can be improved through technological developments [3]. Amongst them,  $\text{Gd}_3\text{Al}_2\text{Ga}_3\text{O}_{12}$  (GAGG) has better stopping power than  $\text{Y}_3\text{Al}_5\text{O}_{12}$  (YAG), and, unlike  $\text{Lu}_3\text{Al}_5\text{O}_{12}$  (LuAG), does not present a radioactive background, which is convenient for X-ray and gamma spectroscopy. Moreover, it is under consideration for thermal-neutron detection thanks to the large neutron-capture cross-section of the Gd isotopes.

We performed a characterization campaign of the optical and scintillation properties of single crystals of GAGG from several producers. The samples were characterised in terms of photoluminescence and optical transmission, light output, energy resolution, scintillation kinetics, and coincidence time resolution (CTR). Large differences were observed between them, depending on composition and growth conditions. Then, correlations between the measurements were examined. The effect of scintillation properties on CTR was analysed and quantitatively compared to theoretical predictions [4].

Employing ray-tracing Monte Carlo simulations, the performance of GAGG was investigated in the environment of a high-luminosity collider, in particular studying the effect of the high-rate as a function of scintillation rise and decay times.

This contribution presents the study of the GAGG properties giving an overview of the current state of the art for this material, and explores the requirements for the new generation of garnets crystals for future HEP experiments.

## References

- [1] V. Alenkov, et al., NIM A, 916 (2019) 226-229
- [2] M. T. Lucchini, et al., IEEE Trans. on Nucl. Sci., 63, 2, 2016
- [3] K. Kamada, et al., Opt. Mater. 41 (2015), 63-66
- [4] S. Vinogradov, NIM A, 912 (2018), 149-153

## Acknowledgments

This work was performed in the framework of the Crystal Clear Collaboration.

## Novel cross-luminescence scintillators: an exploration of CsMCl<sub>3</sub> perovskite matrix

**V. Vaněček<sup>1,2</sup>, R. Král<sup>1</sup>, J. Pátěrek<sup>1,2</sup>, V. Babin<sup>1</sup>, M. Nikl<sup>1</sup>**

<sup>1</sup> Institute of Physics, Czech Academy of Sciences, Na Slovance 1999/2, Prague, Czech Republic

<sup>2</sup> Faculty of Nuclear Sciences and Physical Engineering, Czech Technical University in Prague, Břehová 7, Prague, Czech Republic

**E-mail: vanecekv@fzu.cz**

Cross-luminescence (CL) is a fast radiative transition between a hole in the uppermost core band with an electron in the valence band. This type of luminescence was first observed in 1982 in the crystal of BaF<sub>2</sub>. Since then CL was observed in a wide range of materials mostly based on halides of alkali and alkali earth metals. However, due to a low light yield and emission in the UV region, CL materials were usually unsuitable for most of the fast timing applications.

Recent developments in fast timing applications including high energy physics and medical imaging have raised a demand for detectors of ionizing radiation with coincidence time resolution (CTR) < 20 ps. The best CTR achieved with conventional scintillators based on 5d-4f transitions of rare earth metals reach 60 ps. Such materials are a result of long and intense research and development. Therefore, significant improvement of timing characteristics is improbable. Thus, new materials based on faster phenomena should be investigated.

Cesium-based ternary chlorides of general formulas CsMCl<sub>3</sub> where M corresponds to a divalent cation are perspective CL materials due to the red-shift of CL emission compared to BaF<sub>2</sub> and possible tunability via M site substitution. The red-shift of CL results in a better spectral match between the scintillator and the photodetector (e. g. PMT or SiPM). While the M site substitution allows modification of the valence band which plays a significant role in the CL mechanism.

In this study, we report on the scintillation properties of several crystals from the CsMCl<sub>3</sub> family. These materials crystallize in perovskite (or distorted perovskite) structure and exhibit CL in 250 – 300 nm region. All presented crystals were grown by the vertical Bridgman method. Cut and polished samples were prepared for further optical characterizations. The prepared samples were studied by the means of absorbance, radioluminescence, and photoluminescence emission, excitation, and decay kinetics measurements.

### Acknowledgments

The work is supported by Operational Programme Research, Development and Education financed by European Structural and Investment Funds and the Czech Ministry of Education, Youth and Sports (Project No. SOLID21 CZ.02.1.01/0.0/0.0/16\_019/0000760).

# Fast neutron imaging using carbazole and p-terphenyl scintillator

**S. Kurosawa<sup>1</sup>, A. Yamaji<sup>1</sup>, C. Fujiwara<sup>1</sup>, A. Yoshikawa<sup>1</sup>**

<sup>1</sup>New Industry Creation Hatchery Center (NICHe), Tohoku University, 6-6-10 Aoba, Aramaki, Aoba-ku, Miyagi 980-8579, Japan

<sup>2</sup>Institute for Materials Research (IMR), Tohoku University, 2-1-1 Katahira, Aoba-ku, Sendai, 980-8577, Japan

**E-mail: kurosawa@imr.tohoku.ac.jp**

Organic plastic scintillators are used for detection of particles such as neutrons or muons, and their advantages are generally fast decay (< 10 ns) and low sensitivity for gamma-rays when compared to inorganic scintillators such as Tl:NaI, Ce:Lu<sub>2</sub>SiO<sub>5</sub>, CeBr<sub>3</sub>. Under high gamma-ray dose conditions which are for example in a nuclear fusion reactor, decay time is also an important factor to suppress the pile-up events.

Although plastic scintillators are easier to handle when compared to liquid materials, their melting point is generally lower than that of inorganic materials; the typical softening point is approximately 343 K (i.e. [1]). Radiation measurements at higher temperatures (over 372 K), including neutrons and alpha-rays detection, are required in several fields such as nuclear fusion [2]. Therefore, we have developed novel organic scintillators with fast decay times and high melting temperatures above 372K which would replace inorganic scintillators.

We grew p-terphenyl and carbazole crystals by the self-seeding vertical Bridgman technique which enables to grow the crack-free crystal. As raw materials, p-terphenyl (99.0% up purity, Tokyo Chemical Industry) and carbazole (97.0% purity, Tokyo Chemical Industry) powders were used and loaded into quartz ampoules. Crystal growth was performed under 99.999% purity nitrogen atmosphere in a sealed chamber. To evaluate the light output we measured pulse height spectra of these samples under alpha-rays (<sup>241</sup>Am, 5.5 MeV) and gamma-rays (<sup>137</sup>Cs, 662 keV) excitation with a photomultiplier tube (PMT) (R6231-100MOD Hamamatsu Photonics).

( $\alpha/\gamma$ ) ratios were calculated by the light yields for respective radiation with the same energy. The results are shown in Table 1. Additionally, we grew 2-inch diameter p-terphenyl crystals and assembled pixel scintillation array. In this paper, we show the above results and the imaging test. Moreover, emission intensity for these samples from 10 to 423 K, and the photoluminescence quantum yield was almost constant up to 423 K for the samples.

Table 1 Light yield for p-terphenyl and carbazole compared to GS20 reference scintillator and ( $\alpha/\gamma$ ) ratios

	Light yield [photons /5.5 MeV ( $\alpha$ )]	Light yield [photons /MeV ( $\gamma$ )]	( $\alpha/\gamma$ )
GS20	5,060	4,000	0.23
p- Terphenyl	9,030	18,500	0.09
Carbazole	10,870	13,700	0.14

## References

- [1] Saint-Gobain, “Bc-400 404 408 412 416,” Data Sheet. 2] M. Sasao, et al., “Chapter 9: Fusion product diagnostics,” Fusion Sci. Technol., 53 (2008) 604–639.

## First-principles calculations of electronic properties of scintillating materials

**M.G. Brik<sup>1,2,3</sup>, C.-G. Ma<sup>1</sup>, M. Piasecki<sup>3,4</sup>, A. Suchocki<sup>5</sup>**

<sup>1</sup> *CQUPT-BUL Innovation Institute & College of Sciences, Chongqing University of Posts and Telecommunications, Chongqing, 400065, People's Republic of China*

<sup>2</sup> *Institute of Physics, University of Tartu, W. Ostwald Str. 1, Tartu, 50411, Estonia*

<sup>3</sup> *Department of Theoretical Physics, Jan Długosz University, Armii Krajowej 13/15, PL-42200, Częstochowa, Poland*

<sup>4</sup> *Department of Solid State Physics, Eastern European National University, Voli Ave. 13, Lutsk, 43025, Ukraine*

<sup>5</sup> *Institute of Physics, Polish Academy of Sciences, Al. Lotnikow 32/46, 02-668, Warsaw, Poland*

**E-mail: mikhail.brik@ut.ee**

First-principles calculations of the electronic and optical properties of scintillating crystals are an important and powerful tool for understanding of their performance and design of new materials with improved performance. Crucial characteristics such as electronic bands composition, widths of inter- and intra-band gaps, location of the impurity ions energy levels in the band gap etc can all be calculated using modern computational approaches.

In the present paper we summarize the results of such calculations for a number of doped and neat systems, e.g. trivalent lanthanides in  $\text{YAlO}_3$  crystal [1],  $\text{CdWO}_4$  and  $\text{ZnWO}_4$  [2], neat spinels [3] and neat cubic elpasolites [4]. The calculated results were compared with the experimental (whenever available) data. Systematic analysis of the calculated results across large groups of isostructural compounds allowed to reveal certain correlations between the chemical composition and various physical properties. Combined application of the first-principles calculations with the crystal field analysis for the  $\text{Ce}^{3+}$  or  $\text{Ti}^{3+}$  energy levels allowed to establish complete energy level scheme of studied materials, which contain impurity levels superimposed onto the host's band structure. Such modelling was proved successful for understanding of the emission properties of impurities.

### References

- [1] M.G. Brik, C.-G. Ma, M. Piasecki, A. Suchocki, *Opt. Mater.* 113 (2021) 110843.
- [2] M.G. Brik, V. Nagirnyi, M. Kirm, *Mater. Chem. Phys.* 134 (2012) 1113-1120.
- [3] Y. Wang, W.-B. Chen, F.-Y. Liu, D.-W. Yang, Y. Tian, C.-G. Ma, M.D. Dramićanin, M.G. Brik, *Res. Phys.* 13 (2019) 102180.
- [4] B. Wu, M.-L. Yang, Y.-C. Yan, C.-G. Ma, H.-W. Zhang, M.G. Brik, M.D. Dramićanin, U.V. Valiev, M. Piasecki, *J. Am. Ceram. Soc.* 104 (2021) 1489-1500.

### Acknowledgments

This research was supported by the Chongqing Recruitment Program for 100 Overseas Innovative Talents (Grant No. 2015013), the Program for the Foreign Experts (Grant No. W2017011), Wenfeng High-end Talents Project (Grant No. W2016-01) offered by Chongqing University of Posts and Telecommunications (CQUPT), Estonian Research Council grant PUT PRG111, European Regional Development Fund (TK141) and NCN project 2018/31/B/ST4/00924.

# Radiative and nonradiative recombination in $\beta$ -Ga<sub>2</sub>O<sub>3</sub> scintillator crystals

**A.J. Wojtowicz<sup>1</sup>, M.E. Witkowski<sup>1</sup>, M. Makowski<sup>1</sup>, W. Drozdowski<sup>1</sup>, K. Irmscher<sup>2</sup>,  
R. Schewski<sup>2</sup>, Z. Galazka<sup>2</sup>**

<sup>1</sup>*Institute of Physics, Faculty of Physics, Astronomy and Informatics, Nicolaus Copernicus University in Toruń, ul. Grudziądzka 5, 87-100 Toruń, Poland*

<sup>2</sup>*Leibniz-Institut für Kristallzüchtung, Max-Born-Str. 2, 12489 Berlin, Germany*

**E-mail: andywojt@umk.pl**

Fast and efficient scintillation in a recently rediscovered and fashionable wide bandgap semiconductor  $\beta$ -Ga<sub>2</sub>O<sub>3</sub> ( $\beta$ -gallium sesquioxide) [1,2] could provide an important addition to a range of outstanding features of this material such as a high breakdown electric field, easily achievable primary color emissions and reasonably high free charge carrier concentrations and mobilities under appropriate doping and, in pure crystals, deep UV-transparency [3].

Substantial amount of information about the emission-related centers in  $\beta$ -Ga<sub>2</sub>O<sub>3</sub> has been collected during the last fifty years (see e.g. [4]) including some recent results of sophisticated EPR work on structural defects (vacancies, self-trapped holes), shallow and deep dopant-related donors and acceptors [5]. Some of these centers, targeted in this work, may be responsible for a lower than expected scintillation light yield at ambient temperatures.

We will present results of two-beam experiments on  $\beta$ -Ga<sub>2</sub>O<sub>3</sub> crystals (the IR laser probe and the X-ray pump), originally proposed by Poolton et al. [6]. While the dominant contribution to UV emission in  $\beta$ -Ga<sub>2</sub>O<sub>3</sub> under ionizing excitation is due to the prompt recombination of free electrons and self-trapped holes, the slow component is likely to involve detrapping of electrons from shallow donor traps and deeper acceptor-like traps such as Fe (2+/3+). We also observe some effects that are likely to involve deep donor-like hole-traps such as Ir (3+/4+). These, in turn, may be responsible for lower scintillation light yield at higher temperatures.

## References

- [1] M.R. Lorenz, J.F. Woods and R.J. Gambino, *J. Phys. Chem. Solids*, 28 (1967) 403-404.
- [2] T. Yanagida, G. Okada, T. Kato, D. Nakauchi, S. Yanagida, *Appl. Phys. Express*, 9 (2016) 042601/1-4.
- [3] Z. Galazka, *Semicond. Sci. Technol.* 33 (2018) 113001.
- [4] W.C. Herbert et al, *J. Electrochem. Soc.*, 116 (1969) 1019-1021; G. Blasse and A. Bril, *J. Phys. Chem. Sol.*, 31 (1969) 707-711, S.I. Stepanov et al, *Rev. Adv. Mater. Sci.*, 44 (2016) 63-86.
- [5] C.A. Lenyk et al, *J. Appl. Phys.*, 125 (2019) 045703-8, C.A. Lenyk et al, *J. Appl. Phys.*, 126 (2019) 245701-9.
- [6] N.R.J. Poolton et al, *New J. Phys.*, 8 (2006) 76/1-15.

## Acknowledgments

This research has been financed from the funds of the Polish National Science Centre (NCN) and the German Research Foundation (DFG) in frames of a joint grant (NCN: 2016/23/G/ST5/04048, DFG: GA 2057/2-1).

## Heading for brighter and faster $\beta$ -Ga<sub>2</sub>O<sub>3</sub> scintillator crystals

**W. Drozdowski<sup>1</sup>, M. Makowski<sup>1</sup>, A. Bachiri<sup>1</sup>, M.E. Witkowski<sup>1</sup>, A.J. Wojtowicz<sup>1</sup>,  
K. Irscher<sup>2</sup>, R. Schewski<sup>2</sup>, Z. Galazka<sup>2</sup>**

<sup>1</sup>*Institute of Physics, Faculty of Physics, Astronomy and Informatics, Nicolaus Copernicus University  
in Toruń, ul. Grudziądzka 5, 87-100 Toruń, Poland*

<sup>2</sup>*Leibniz-Institut für Kristallzüchtung, Max-Born-Str. 2, 12489 Berlin, Germany*

**E-mail: wind@fizyka.umk.pl**

Five years after the first report on promising scintillation properties of  $\beta$ -Ga<sub>2</sub>O<sub>3</sub> crystals [1] a strongly increased interest in this field can easily be noticed. Research is carried on at several laboratories, in which diverse growth technologies are applied and various dopants are examined, mostly aimed at enhancement of the basic scintillation parameters, such as light yield, energy resolution and decay time constants [1-7]. Most importantly, at least part of these studies is not based on trials and errors, but focuses on understanding the physics that stands behind the acquired data and observed correlations, providing an important feedback for subsequent growth campaigns.

In this Communication we present the sequel of our research on scintillation properties of Czochralski-grown  $\beta$ -Ga<sub>2</sub>O<sub>3</sub> crystals [6]. Through several new crystals (either pure or doped with Si) with free electron concentrations of  $10^{17} \text{ cm}^{-3} < n < 10^{18} \text{ cm}^{-3}$ , we fill the antecedent gap between lightly conducting crystals ( $n < 10^{17} \text{ cm}^{-3}$ ) with higher yields but slower scintillation decays and highly conducting ones ( $n > 10^{18} \text{ cm}^{-3}$ ) with lower yields but faster decays. The new data extend our knowledge on factors that impact on scintillation characteristics of  $\beta$ -Ga<sub>2</sub>O<sub>3</sub> and let us conjecture on possibilities of its further development.

### References

- [1] T. Yanagida, G. Okada, T. Kato, D. Nakauchi, S. Yanagida, *Applied Physics Express* 9 (2016) 042601/1-4.
- [2] Y. Usui, T. Oya, G. Okada, N. Kawaguchi, T. Yanagida, *Optik* 143 (2017) 150-157.
- [3] N. He, H. Tang, B. Liu, Z. Zhu, Q. Li, C. Guo, M. Gu, J. Xu, J. Liu, M. Xu, L. Chen, X. Ouyang, *Nuclear Instruments and Methods in Physics Research A* 888 (2018) 9-12.
- [4] Y. Usui, D. Nakauchi, N. Kawano, G. Okada, N. Kawaguchi, T. Yanagida, *Journal of Physics and Chemistry of Solids* 117 (2018) 36-41.
- [5] M. Makowski, W. Drozdowski, M.E. Witkowski, A.J. Wojtowicz, K. Irscher, R. Schewski, Z. Galazka, *Optical Materials Express* 9 (2019) 3738-3743.
- [6] Z. Galazka, R. Schewski, K. Irscher, W. Drozdowski, M.E. Witkowski, M. Makowski, A.J. Wojtowicz, I.M. Hanke, M. Pietsch, T. Schulz, D. Klimm, S. Ganschow, A. Dittmar, A. Fiedler, T. Schroeder, M. Bickermann, *Journal of Alloys and Compounds* 818 (2020) 152842/1-7.
- [7] W. Drozdowski, M. Makowski, M.E. Witkowski, A.J. Wojtowicz, R. Schewski, K. Irscher, Z. Galazka, *Optical Materials* 105 (2020) 109856/1-6.

### Acknowledgments

This research has been financed from the funds of the Polish National Science Centre (NCN) and the German Research Foundation (DFG) in frames of a joint grant (NCN: 2016/23/G/ST5/04048, DFG: GA 2057/2-1).



## Timing properties of radioluminescence in nanoparticle ZnS:Ag scintillators

**S. Mann<sup>1,2</sup>, G. J. Sykora<sup>1</sup>**

<sup>1</sup> *ISIS neutron and muon source, Rutherford Appleton Laboratory, Science and Technology Facilities Council, Harwell Oxford, United Kingdom*

<sup>2</sup> *School of Physics, University of Bristol, Bristol, United Kingdom*

**E-mail: sarah.mann@stfc.ac.uk**

Neutron scattering facilities employ a range of highly valuable techniques, including diffraction, spectroscopy and reflectometry to study the structure of matter from atomic to macromolecular scales. These experiments rely on accurate neutron detectors to measure the position and time of arrival of neutrons. Micro-particle ZnS:Ag/<sup>6</sup>Li scintillation based detectors are widely deployed in large scale facilities. These detectors are extensively used because they have excellent gamma discrimination, high thermal neutron detection efficiency, good position resolution, and are relatively affordable.

The main limitation of ZnS:Ag scintillation detectors is that the count-rate capability is inherently limited by the afterglow of the scintillator [1]. Afterglow in ZnS:Ag is caused by electron and hole traps related to defect levels within the band gap. Delayed luminescence is thought to occur when trapped electrons are liberated via thermal stimulation or quantum tunnelling and radiatively recombine with holes. Reducing particle size from micro to nanoscale changes the proportion of volume to surface defects, altering the timing properties of the scintillator.

Nanoparticle ZnS:Ag scintillators are investigated here as a potential low afterglow alternative to the standard micro-particle scintillator. ZnS:Ag and ZnS nanoparticles have been hydrothermally synthesised with varying proportions of zinc and sulphur, creating a number of crystalline defects including sulphur vacancies and zinc interstitials. X-ray diffraction has confirmed that the resultant nanoparticles have cubic crystal structure.

The effect of varied defect structure on the luminescent behaviour of nanoparticle ZnS:Ag will be presented. Photo- and radioluminescence emission wavelengths are shown to shift significantly compared to micro-particles as a result of the altered luminescent pathways. The time-resolved radioluminescence of nanoparticle ZnS:Ag has been measured and the effect of particle size on scintillation decay will be discussed. Exploiting the defect dependent timing properties of luminescence in nanoparticle ZnS:Ag has the potential to create low afterglow scintillators. These could be used to produce detectors that maintain the numerous benefits of current standard ZnS:Ag based detectors while improving count-rate capability.

### References

[1] G. J. Sykora, E. Schooneveld, N. Rhodes, *Nucl. Instr. Meth. A*, 883 (2018) 75-82.

## Sensitization of scintillation in multicomponent polymeric composites

I. Villa<sup>2</sup>, M. Orfano<sup>1</sup>, F. Cova<sup>1</sup>, V. Secchi<sup>1</sup>, C. Colombo<sup>1</sup>, A. Vedda<sup>1</sup>, M. Nikl<sup>2</sup>,  
A. Monguzzi<sup>1</sup>

<sup>1</sup> Dipartimento di Scienza dei Materiali, Università degli studi di Milano-Bicocca, Milano, Italy

<sup>2</sup> Institute of Physics, Academy of Sciences of the Czech Republic, Prague, Czech Republic

E-mail: [angelo.monguzzi@unimib.it](mailto:angelo.monguzzi@unimib.it)

The effective sensitization of scintillation in composite polymeric materials is highly desired in order to enhance the performance of low density scintillators, which have good time response and light yield but low interaction cross section with the ionizing radiation that limits the out luminescence intensity.<sup>1</sup> By including coupling to heavier materials in composite systems, we can enhance the interaction cross section and therefore increase the amount of deposited energy. The global sensitization efficiency of emitter's luminescence is therefore given by the sum of two contributions. The first is the direct transfer of the additional harvested energy from the host matrix. The second one occurs if the heavy systems are luminescent. Under specific energetic resonance conditions, the emitter can be indeed activated by energy transfer from the heavy elements. In this work we investigate a model system where the scintillating dye rhodamine 6G is coupled to heavy luminescent gold quantum clusters aggregates in a transparent polymer matrix of poly(2-hydroxyethyl methacrylate). The sensitization effect is studied as a function of the system composition. We introduce a system of rate equations that allows us to predict the theoretical scintillation sensitization efficiency on the basis of few parameters of the constituent sensitizers and emitter moieties.

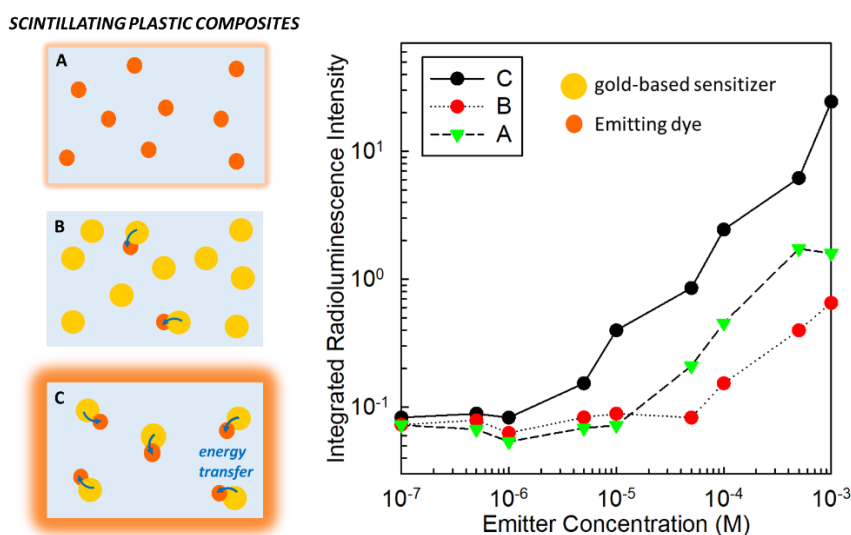


Fig.1. Sensitization of scintillation in multicomponent plastic composites.

### References

- [1] T. J. Hajagos, C. Liu, N. J. Cherepy, Q. Pei, High-Z sensitized plastic scintillators: a review. *Adv. Mater.* 30, 1706956 (2018).

## Organic heterostructured scintillators with a high pulse shape discrimination capability

**N. Galunov<sup>1,2</sup>, I. Khromiuk<sup>1</sup>, N. Karavaeva<sup>1</sup>, A. Krech<sup>1</sup>, Ya. Polupan<sup>1</sup>, O. Tarasenko<sup>1</sup>, S. Khabuseva<sup>3</sup>**

<sup>1</sup>*Institute for Scintillation Materials NAS of Ukraine, 60 Nauky Ave., Kharkiv, 61072, Ukraine*

<sup>2</sup>*V. N. Karazin Kharkiv National University, 4 Svobody Sq., Kharkiv, 61022, Ukraine*

<sup>3</sup>*State Scientific Institution "Institute for Single Crystals" NAS of Ukraine, 60 Nauky Ave., Kharkiv, 61072, Ukraine*

**E-mail: n.galunov@gmail.com**

We have recently developed a new type of scintillator material, namely composite scintillators. It is a non-scintillating gel composition containing grains of organic single crystals. The grains are obtained after directional crystallization of the material by grinding a polycrystalline ingot under a layer of liquid nitrogen. This approach removes technological restrictions on the area of the entrance window of the scintillator, does not require the growth of structurally perfect single crystals and their subsequent mechanical treatment. In contrast to organic single crystals and liquids, these materials are not continuous media but heterostructured ones. The ability of single crystals and liquids to separate signals from radiations with different specific energy losses  $dE/dx$  is well known. Due to the peculiarities of the creation and recombination of triplet-excited ( $T$ ) states in these objects, which is also well studied. Such information on heterostructured scintillation materials, for which the grain size can limit migration of  $T$ -states, is practically absent [1, 2].

We discuss the results of the investigation of the relative light yield and optical transmission of composite scintillators containing *p*-terphenyl grains (both activated and non-activated) or *trans*-stilbene grains. We used the grain fractions from 0.06 to 2.5 mm. Additionally, we investigated the luminescence spectra upon excitation by light into the  $T$ -states absorption region. We studied both single-layer samples (the thickness of the sample practically corresponded to the grain size of the scintillation material) and samples of 5 mm thick. The research results showed that samples with a grain fraction of less than 0.4, 0.6, between 0.06–0.1, and 0.1–0.3 mm have very low relative light output and optical transmission values. We obtained that to separate radiations with different  $dE/dx$  by the shape of the radioluminescence pulse; it is advisable to use grain fractions larger than 0.3 mm. We also discuss the physical processes that can lead to such results.

### References

- [1] N. Galunov, I. Khromiuk, O. Tarasenko Nuclear Inst. Methods, A949 (2020) 456-478. Article number 162870.
- [2] N. Galunov, et al., *Journal of Luminescence*, 226 (2020) 456-478. Article number 117477.

### Acknowledgements

The National Research Foundation of Ukraine supported this work (project No. 2020.01/0133, "Heterostructured organic scintillators with high pulse shape discrimination capability for radioecology problems").

## Scintillation properties for $\text{Cs}_2\text{Hf}(\text{I}, \text{Br})_6$ with red emission for real-time high dose rate monitor

**C. Fujiwara<sup>1</sup>, S. Kodama<sup>2</sup>, S. Kurosawa<sup>3,4</sup>, A. Yamaji<sup>3</sup>, Y. Ohashi<sup>3</sup>, Y. Yokota<sup>1</sup>, K. Kamata<sup>3,5</sup>, H. Sato<sup>3</sup>, S. Toyoda<sup>3</sup>, M. Yoshino<sup>1</sup>, T. Hanada<sup>1</sup>, A. Yoshikawa<sup>1,3,5</sup>.**

<sup>1</sup>Institute for Materials Research (IMR), Tohoku University, 2-1-1 Katahira, Aoba-ku, Sendai, 980-8577, Japan

<sup>2</sup>Graduate School of Science and Engineering, Saitama University, 255 Shimoohkubo, Sakura-ku, Saitama, Saitama 338-8570, Japan

<sup>3</sup>New Industry Creation Hatchery Center (NICHe), Tohoku University, 6-6-10 Aoba, Aramaki, Aoba-ku, Sendai, Miyagi 980-8579, Japan

<sup>4</sup>Faculty of science, Yamagata University, 1-4-12 Kojirakawa-machi, Yamagata, 990-8560, Japan

<sup>5</sup>C&A Corporation, 6-6-40 Aoba, Aramaki, Aoba-ku, Sendai, Miyagi, 980-8577, Japan

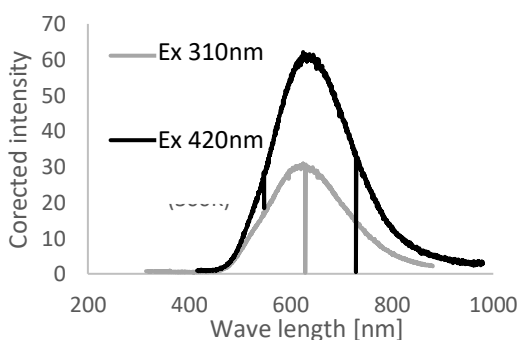
**E-mail: [chihaya.fujiwara@imr.tohoku.ac.jp](mailto:chihaya.fujiwara@imr.tohoku.ac.jp)**

Real-time dose monitors under the high dose-rate condition are required to remove the debris in the Fukushima Daiichi Nuclear Power Plant as the decommissioning step. We have proposed a dose monitor consisting of a scintillator, optical fiber and CCD spectrometer, and scintillation photons are read under lower dose condition with the CCD [1]. Conventional scintillators have an emission region of green or the shorter wavelength bands. Since such bands are overlapped with noise bands under the such high dose rate due to scintillation or Cherenkov photons in the optical fiber, we have developed red/NIR-emission and high light output scintillators like  $\text{Cs}_2\text{HfI}_6$  (CHI) [1]. Here, some anion-complex materials were reported to be higher light output or fast decay time [2]. Thus, scintillation properties for  $\text{Cs}_2\text{Hf}(\text{I}, \text{X})_6$  are shown in this presentation, where X is Br.

$\text{Cs}_2\text{Hf}(\text{I}, \text{X})_6$  crystals were grown by the vertical Bridgman-Stockbarger method. The phase of the obtained crystals were investigated by the powder X-ray diffraction (D8 DISCOVER, Bruker). Photoluminescence (PL) excitation and emission properties were measured with an absolute PL-quantum-yield spectrometer and a CCD spectrometer in the Synchrotron facility. To evaluate the light output, the pulse height spectra were also measured with a Si-avalanche photo-diode (S8664-1010, Hamamatsu K.K.), and the decay times were measured with a photo tube (H11934-300, Hamamatsu KK).

We succeeded in growing  $\text{Cs}_2\text{Hf}(\text{I}, \text{Br})_6$  crystals, and  $\text{Cs}_2\text{HfI}_2\text{Br}_4$ ,  $\text{Cs}_2\text{HfI}_3\text{Br}_3$  and  $\text{Cs}_2\text{HfI}_2\text{Br}_4$  had similar emission wavelengths to  $\text{Cs}_2\text{HfI}_6$  have (around 700nm) as shown in Figure 1 (i.e.  $\text{Cs}_2\text{HfI}_3\text{Br}_3$ ). The Maximum light outputs was approximately 60,000 Photons/MeV for  $\text{Cs}_2\text{HfI}_6$ . To discuss the emission mechanism, we also measure temperature dependence of light intensity from 5K to room temperature. In this paper, we show the above results and discussions.

Fig. 1. Photo-luminescence Emission spectra of  $\text{Cs}_2\text{HfI}_3\text{Br}_3$  excited by 310 and 420-nm photons.



### References

- [1] S. Kodama, S. Kurosawa, A. Yamaji, *Journal of Crystal Growth*, 492 (2018) 1-5, [2] A. V. Gektin et al., *IEEE TNS* 61 262 (2014)

# Energy transfer and NIR luminescence in lanthanoid and transition metal codoped storage phosphors

**S. Tanabe<sup>1</sup>, J. Xu<sup>1</sup>**

<sup>1</sup> Graduate School of Human and Environmental Studies, Kyoto University,  
Sakyo-ku, Kyoto 606-8501, Japan

E-mail: tanabe.setsuhisa.4v@kyoto-u.ac.jp

Persistent phosphor materials at the transparent windows of bio-tissues are expected for *in vivo* imaging without excitation source, which produces various noises such as auto-fluorescence. The ZnGa<sub>2</sub>O<sub>4</sub>:Cr<sup>3+</sup> spinel phosphor[1] is a successful example of persistent luminescence at 700nm, corresponding to the 1st bio-imaging window. Because of lower scattering loss and recently advanced availability of InGaAs photo-detectors, near-infrared (NIR) fluorescence probes have been widely developed with luminescence of Nd<sup>3+</sup>:1.06- $\mu$ m and Er<sup>3+</sup>:1.55- $\mu$ m, where conventional photoluminescence (PL) is working. In contrast to Cr<sup>3+</sup>, Mn<sup>2+</sup>, Ce<sup>3+</sup>, Pr<sup>3+</sup>, and Eu<sup>2+</sup> ions, the photo-ionization mechanism by UV illumination for the electron charging seems unfeasible in the Nd<sup>3+</sup> and Er<sup>3+</sup> ions, which take very stable trivalent state. We have developed garnet-based and perovskite-based persistent phosphors in which Nd<sup>3+</sup>[2], Er<sup>3+</sup>[3], or Ho<sup>3+</sup> [4] ions show very efficient and long NIR persistent luminescence. Photon emission rate and duration of these materials are only slightly lower and shorter than the visible persistent phosphors of Ce<sup>3+</sup>, Cr<sup>3+</sup>-codoped garnets [5] and Cr<sup>3+</sup>-doped perovskite [6] we developed in 2014 and 2015, respectively, the performance of which is almost comparable to the SrAl<sub>2</sub>O<sub>4</sub>: Eu<sup>2+</sup>, Dy<sup>3+</sup> phosphor. These phosphors can be applied to *in vivo* imaging in the 2nd and 3rd bio-imaging windows of high transparency and sensitivity of InGaAs detectors [7].

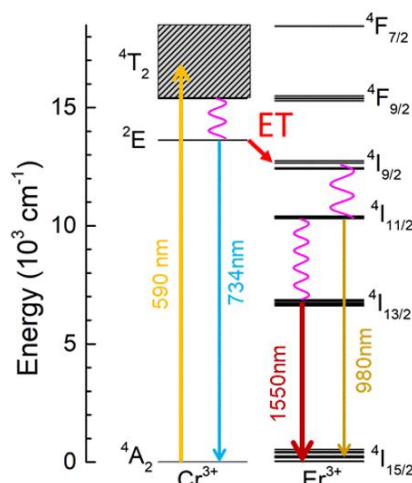


Fig.1. Energy transfer mechanism and observed persistent luminescence transitions in Cr-Er codoped LaAlO<sub>3</sub> perovskite.

## References

- [1] T. Maldiney, A. Bessiere, et al, *Nat. Mater.* 13, (2014) 418-426.
- [2] J. Xu, S. Tanabe, et al, *Appl. Phys. Lett.* 107, (2015) 081903(4p).
- [3] J. Xu, D. Murata, J. Ueda, S. Tanabe, *J. Mater. Chem. C* 4, (2016) 11096-11103.
- [4] J. Xu, D. Murata, Y. Katayama, J. Ueda, S. Tanabe, *J. Mater. Chem. B* 5, (2017) 6385-6393.
- [5] J. Ueda, K. Kuroishi, S. Tanabe, *Appl. Phys. Lett.* 104, (2014) 101904(4p).
- [6] Y. Katayama, H. Kobayashi, S. Tanabe, *Appl. Phys. Express* 8, (2015) 012102(3p).
- [7] J. Xu, S. Tanabe, *J. Lumin.* 205, (2019) 581-620.

## Broadband near-infrared phosphors for light emitting diodes

**S. Mahlik**<sup>1</sup>

<sup>1</sup>*Institute of Experimental Physics, Faculty of Mathematics, Physics and Informatics, University of Gdansk, Wita Stwosza 57, 80-308 Gdansk, Poland*

**E-mail: s.mahlik@ug.edu.pl**

The near-infrared (NIR) light source is desirable for real-time non-destructive examination applications, including food freshness analysis, health monitoring, infrared cameras, agriculture, and bio-applications. [1-4] The light emission spectra of such infrared light sources should be broad as possible for effective performance because of the broad absorption and reflection of light by the organic elements present in foodstuffs and human health in the blue and NIR regions of the electromagnetic spectrum, respectively. With the maturity of blue LED chips, phosphor-converted light-emitted diodes (pc-LEDs) with broadband emission have been recently proposed as a suitable and efficient NIR light source, even in portable devices.[5]

In this paper, the most recently developed broadband near-infrared phosphors and their applications are presented. The most attention is paid to materials activated by Cr<sup>3+</sup> ions as an ideal candidate for producing IR light. Depending on the crystal field strength of the host lattices, it can provide narrowband emission (700 nm) from the spin-forbidden <sup>2</sup>E→<sup>4</sup>A<sub>2</sub> transition or the broadband emission (650–1200 nm) ascribed to the spin-allowed <sup>4</sup>T<sub>2</sub>→<sup>4</sup>A<sub>2</sub> transition. Distortions of the crystal structure or phase transition may cause unanticipated photoluminescent properties. Hence, adjusting the host lattices through a solid solution and high-pressure luminescence method can effectively and systematically tune the crystal field strength and luminescent wavelength.

Finally, broadband near-infrared phosphors based on lanthanide and other transition metal ions are shown and discussed.

### References

- [1] B.M. Nicolai, K. Beullens, E. Bobelyn, A. Peirs, W. Saeys, K.I. Theron, *J. Lammertyn Postharvest Biol. Technol.*, 46 (2007) 99-118.
- [2] Y.H. Chien, Y.L. Chou, S.W. Wang, S.T. Hung, M.C. Liao, Y.J. Chao, C.H. Su, C.S. Yeh *ACS Nano*, 7 (2013) 8516-8528.
- [3] V. Rajendran, M.H. Fang, G. N. D. Guzman, T. Leśniewski, S. Mahlik, M. Grinberg, G. Leniec, S. M. Kaczmarek, Y. S. Lin, K. M. Lu, C. M. Lin, H. Chang, S. F. Hu, R. S. Liu, *ACS Energy Lett.* 3 (2018) 2679–2684.
- [4] M. H. Fang, P. Y. Huang, Z. Bao, N. Majewska, T. Leśniewski, S. Mahlik, M. Grinberg, G. Leniec, S. M. Kaczmarek, C. W. Yang, K. M. Lu, H. S. Sheu, R. S. Liu, *Chem. Mater.* 32 (2020) 2166–2171.
- [5] L. Zhang, S. Zhang, Z. Hao, X. Zhang, G.-H. Pan, Y. Luo, H. Wu, J. Zhang, *J. Mater. Chem. C* 6 (2018) 4967–4976.

### Acknowledgments

This work was supported by the National Science Centre Poland Grant Opus (Nos. 2016/23/B/ST3/03911, 2018/31/B/ST4/00924 and 2019/33/B/ST3/00406) and the National Centre for Research and Development Poland Grant (No. PL-TW/VIII/1/2021).

## Accelerated radiative transitions in impurities due to energy transfer from impurity-bound excitons

N. Vereschagina<sup>1</sup>, M. Danilkin<sup>2</sup>, Yu. Vainer<sup>1,3</sup>, M. Kochiev<sup>2</sup>, S. Ambrozevich<sup>2</sup>, I. Romet<sup>4</sup>,  
D. Spassky<sup>4,5</sup>, A. Selyukov<sup>2</sup>

<sup>1</sup>Moscow Institute of Physics and Technology (State University), 9 Institutskii Per., 141700  
Dolgoprudnyi, Moscow Region, Russia

<sup>2</sup>P.N. Lebedev Physical Institute of the Russian Academy of Sciences, 53 Leninsky Prospect, 119991  
Moscow, Russia

<sup>3</sup>Institute of Spectroscopy of the Russian Academy of Sciences, 5 Fizicheskaya Str., 108840 Troitsk,  
Moscow, Russia

<sup>4</sup>Physics Institute of the University of Tartu, W. Ostwaldi tn. 1, 50411 Tartu, Estonia

<sup>5</sup>Skobeltsyn Institute of Nuclear Physics (SINP MSU), M.V. Lomonosov Moscow State University, 1-2  
Leninskiye Gory, 119991 Moscow, Russia

**E-mail: mihhail.danilkin@ya.ru**

The radiative decay time of an impurity-bound exciton is often very short, much shorter than any atomic radiative decay time for the same radiation frequency [1-3]. This is believed to be due to giant oscillator strength which results from the coherent action of the atoms involved in the exciton. The oscillator strength is proportional to the number of molecular subunits covered by the bound exciton wave function [2]. For the polaronic exciton of a smaller radius, the number of involved subunits is also smaller. Nevertheless, in the latter case, there are other factors that still accelerate radiative transitions even to a greater extent. Namely, a strong local field and mixing of electronic states would essentially increase the density of states and, accordingly, decrease the radiative lifetime.

What happens when an impurity-bound exciton transfers excitation energy to the impurity? In which cases and to which extent the radiative transitions of the impurity can be accelerated by energy transfer from the exciton? We would like to report and discuss the relevant experimental results concerning a very unusual behaviour of the Mn<sup>2+</sup> luminescence in lithium tetraborate (LTB).

The ceramic samples LTB:Sn+Mn and LTB:Cu+Mn, with excitation energy transfer observed previously [4], are compared with LTB:Mn at pulsed (2.3 ps) laser excitation. Excitation at 350 nm provided in-situ frequency doubling at the surface of microcrystals, which helped to access the so-called “prespectral” bands [1] in LTB. We connect these bands with impurity-bound excitons. Such excitation (though accompanied with a slow decay of the Mn<sup>2+</sup> luminescence, excited directly by the 350 nm radiation) resulted in ultrafast radiative transitions at a sub-nanosecond time scale ( $\tau_1 \approx 20\text{-}50$  ps and  $\tau_2 \approx 200$  ps). LTB:Sn+Mn and LTB:Cu+Mn also reveal UV excitation bands (240-300 nm) for Mn<sup>2+</sup>, with energy transfer from another type of exciton created inside the impurity-oxygen complex. The latter excitation does not produce any acceleration of the Mn<sup>2+</sup> luminescence.

### References

- [1] E. Rashba, G. Gurgenishvili, *Sov. Phys. - Solid State*, 4 (1962) 759-760.
- [2] J. Wilkinson, K. Ucer, R. Williams, *Nucl. Instrum. Methods Phys. Res. A*, 537 (2005) 66-70.
- [3] K. Cho, *J. Supercond. Novel Magn.*, 16 (2003) 789-794.
- [4] N. Vereschagina, M. Danilkin, M. Kazaryan, D. Ozol, E. Sheshin, D. Spassky, *Proc. SPIE*, 10614, (2018) 106141F.

## Excitation relaxation via intra- and intercenter transitions of Pr<sup>3+</sup> ion in garnet-type scintillator

A. Vaitkevičius<sup>1</sup>, S. Nargelas<sup>1</sup>, G. Dosovitskiy<sup>2</sup>, M. Korzhik<sup>3</sup>, G. Tamulaitis<sup>1</sup>

<sup>1</sup>*Institute of Photonics and Nanotechnology, Vilnius University, Saulėtekio Ave. 3, Vilnius 10257, Lithuania*

<sup>2</sup>*NRC "Kurchatov Institute" - IREA, Bogorodskiy 3, Moscow, 107076, Russia*

<sup>3</sup>*Institute for Nuclear Problems, Belarusian State University, Bobruiskaya Str. 11, Minsk, 220006, Belarus*

**E-mail: [augustas.vaitkevicius@ff.vu.lt](mailto:augustas.vaitkevicius@ff.vu.lt)**

Efficient and fast scintillating materials are on increasing demand in development of radiation detectors for medical imaging and high-luminosity high-energy physics experiments. Garnet-type single crystals benefit from band gap engineering and serve as a convenient matrix for different rare earth ion activators. Cerium is the most studied and exploited activator. Other activators, like praseodymium have also received some attention. Praseodymium-doped lutetium aluminum garnets (LuAG) have been shown to have good scintillation properties, however, the factors limiting the luminescence response time remain scarcely studied.

In this study, we report on the origin and properties of the key processes of electronic excitation transfer between configurations  $4f^2$  and  $4f^15d^1$  in the Pr<sup>3+</sup> ion used as an activator in LuYAG single crystal. These transitions limit the response kinetics of this scintillating material.

A typical sample of Pr-doped LuYAG single crystal has been investigated. Optical pump and probe technique was exploited. Short light pulses (250 fs) delivered by a Yb: KGW laser equipped with harmonics generators and a parametric amplifier were employed. Photon energy of the pump pulse was tuned to Pr<sup>3+</sup> intracenter absorption bands. The probe beam was equipped with a sapphire plate to generate a white light continuum in the range from 1.3 to 2.7 eV (950–460 nm). The spectrum of the transient absorption as a difference in the optical absorption with and without excitation by the pump pulse was measured as a function of the delay between the pump and probe pulses. The delay was varied by using an optomechanical delay line. To analyse the contributions of different transient absorption components, global analysis has been employed.

The analysis of experimental data on transient absorption shows multiple spectral components. Using global analysis, these components have been attributed to specific states of Pr<sup>3+</sup> ion and the information is used for sketching an updated diagram of the energy levels of the Pr<sup>3+</sup> ion in  $4f^2$  and  $4f^15d^1$  configurations. Analysis of transient absorption kinetics in LuYAG:Pr shows that the rising part of population of the radiative level in Pr<sup>3+</sup> has two components: a fast component (~0.8 ps) due to intraconfigurational relaxation and a slower component (~3 ps) due to interconfigurational relaxation via the level <sup>1</sup>S<sub>0</sub> of  $4f^2$  configuration of Pr<sup>3+</sup> ion. These processes also possibly involve the extended states in the conduction band. The characteristic time of the second, slower, component might be shortened by engineering of the crystal composition to affect the crystal field in the vicinity of Pr<sup>3+</sup> ions. Since the luminescence kinetics depends on the population of the emitting level of the activator ion, a faster excitation transfer would allow for a shorter luminescence rise time and enable improvement of the timing properties of this scintillator.

### Acknowledgments

This research has been carried out in the framework of Crystal Clear Collaboration at CERN and received funding from the European Regional Development Fund under grant agreement with the Research Council of Lithuania (project No. 01.2.2-LMT-K-718-01-0041).



## Relaxation of electronic excitation at cerium ions in GAGG matrix studied using transient absorption technique

**S. Nargelas<sup>1</sup>, A. Vaitkevičius<sup>1</sup>, G. Dosovitskiy<sup>2</sup>, M. Korjik<sup>3</sup>, G. Tamulaitis<sup>1</sup>**

<sup>1</sup>*Institute of Photonics and Nanotechnology, Vilnius University, Sauletekio Ave. 3, Vilnius, Lithuania*

<sup>2</sup>*NRC “Kurchatov Institute” - IREA, Bogorodskiy val 3, Moscow, Russia*

<sup>3</sup>*Institute for Nuclear Problems, Belarusian State University, Bobruiskaya Str. 11, Minsk, Belarus*

**E-mail: saulius.nargelas@ff.vu.lt**

In the last decade, the demand for fast scintillation detectors substantially increases due to their applications in high-luminosity high-energy physics experiments, and high-spatial-resolution medical imaging systems. This demand encourages searching for new scintillating materials with fast luminescence response and re-engineering the scintillators currently in use to improve their timing properties. The corresponding shift of the time range of interest toward the picosecond domain requires the application of novel experimental techniques enabling the investigation of excitation dynamics in scintillators with time resolutions better than 10 ps. The techniques able to monitor the relaxation of excitation induced by sub-picosecond laser pulses become the key tool providing the high time resolution to study fast processes in novel scintillating materials. The transient absorption (TA) technique has already been proven to be a good candidate for such techniques as it was successfully applied to study fast excitation relaxation processes in various scintillators from CsI:Tl to LYSO.

In this research, we report on electronic excitation relaxation processes at cerium ions in GAGG scintillator studied by TA technique in two complementary configurations: i) pump and probe (PP), and ii) pump-repump and probe (PrPP). The latter is an enhanced version of the common pump-probe technique and enables studying the processes of electron relaxation between higher excited levels and radiating level of Ce<sup>3+</sup>, which are obscured by the overlap of contributions of absorption components due to different structural units in PP configuration. Both configurations ensure i) high time resolution which is limited only by the laser pulse duration, ii) selective excitation of different structural units of the crystal, and iii) simultaneous monitoring of time and spectral characteristics of the response, which enables spotting specific features due to the contributions of different structural units and response mechanisms. Numerical modelling was applied to describe the experimental results and estimate the time constants of the electron relaxation from higher excited levels to the radiative level of Ce<sup>3+</sup>.

A set of four GAGG:Ce samples with different levels of Mg co-doping in the range of 0-25 ppm is used in this study. It is demonstrated that the relaxation of electrons from the higher excited levels to the radiating state of Ce<sup>3+</sup> consists of two competing routes: direct intracenter relaxation and the route involving the extended states in the conduction band and affected by trapping and detrapping processes. The analysis of the results enabled us to estimate the time of the net intracenter relaxation from triplet level  $t_{2g}$  down to the emitting level  $5d_1$  of Ce<sup>3+</sup> to be less than a picosecond. The faster response of TA signal was found with increasing content of divalent Mg and interpreted by suppression of the impact of electron trap levels. The influence of the competing relaxation route including trap levels, which could result in slow scintillation response and decreased light yield, was analysed.

### Acknowledgments

This research has been carried out in the framework of Crystal Clear Collaboration at CERN and was supported by the project FARAD (Grant No. 09.3.3-LMT-K-712-01-0013) funded by the European Social Fund via the Lithuanian Research Council.

# Luminescence properties and energy transfer processes in LiSrPO<sub>4</sub>:Pr<sup>3+</sup>, Na<sup>+</sup>, Mg<sup>2+</sup>

**E. Trofimova<sup>1</sup>, V. Pustovarov<sup>1</sup>, S. Omelkov<sup>2</sup>, I. Romet<sup>2</sup>, M. Kirm<sup>2</sup>**

<sup>1</sup>*Institute of Physics and Technology, Ural Federal University, 19 Mira St., Ekaterinburg, 620002 Russia*

<sup>2</sup>*Institute of Physics, University of Tartu, W. Ostwald Str. 1, Tartu, 50411 Estonia*

**E-mail: trofimovaes@urfu.ru**

In this report the luminescence properties and the peculiarities of energy transfer processes are studied in LiSrPO<sub>4</sub> crystalline powder single-doped with Pr<sup>3+</sup> (1 mol.%) ions and double-doped with Pr<sup>3+</sup>/Na<sup>+</sup> or Pr<sup>3+</sup>/Mg<sup>2+</sup> ions (1 mol.% for both dopants). The objects were studied from the viewpoint of their possible application as scintillator materials, using X-ray and UV-vacuum UV excited luminescence and time-resolved pulsed cathodoluminescence (PCL) spectroscopy methods in wide temperature range.

It was found that fast 5d-4f luminescence of Pr<sup>3+</sup> ions in single-doped LiSrPO<sub>4</sub> was strongly affected by defects, most probably caused by charge compensation required for Pr<sup>3+</sup> ions incorporation [1]. Therefore, the luminescence characteristics of LiSrPO<sub>4</sub>:Pr<sup>3+</sup> were compared to those of double-doped objects.

However, the study of double-doped objects found no significant improvement in fast luminescence characteristics brought by introduction of co-dopants. For instance, Figure 1 shows PCL decay kinetics and PCL spectra measured for the objects at room temperature. Nevertheless, the study revealed complex energy transfer processes between activator ions and defects, which might be of interest for further studies of orthophosphate-based potential scintillator materials.

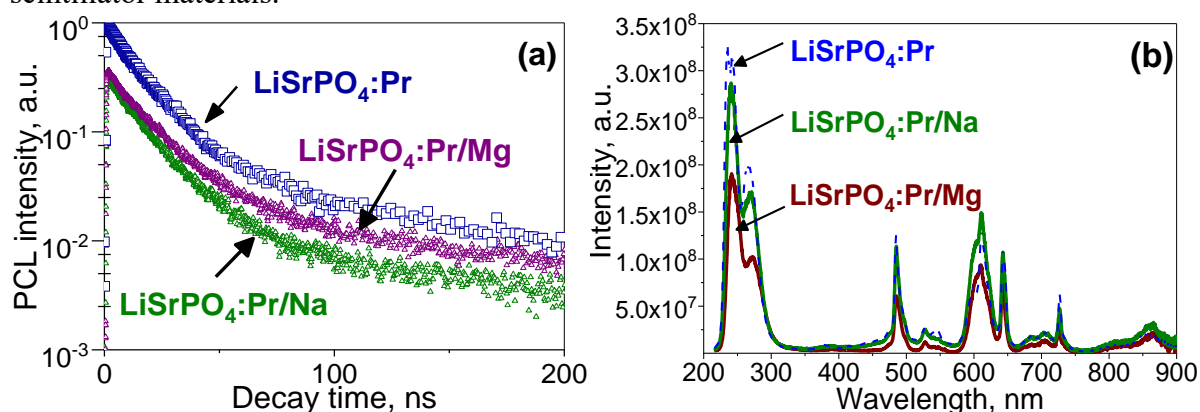


Figure 1. (a) PCL decay kinetics measured for emission at  $\lambda = 265$  nm and (b) PCL spectra of LiSrPO<sub>4</sub>:Pr<sup>3+</sup>/Na<sup>+</sup>, LiSrPO<sub>4</sub>:Pr<sup>3+</sup>/Mg<sup>2+</sup> and LiSrPO<sub>4</sub>:Pr<sup>3+</sup>, T = 295 K

## References

- [1] V. A. Pustovarov et. al, *Radiat. Meas.*, 123 (2019) 39-43.

## Acknowledgments

This work was supported by the Ministry of Science and Higher Education of the Russian Federation (FEUZ-2020-0060), Estonian Research Council (PRG-111, PRG-629) and the European Regional Development Fund.

## A rapid screening method for novel scintillator crystals

**A. Yoshikawa<sup>1,2,3</sup>**

<sup>1</sup>*Institute for Material Research, Tohoku University. Sendai, Miyagi, Japan*

<sup>2</sup>*New Industry Creation Hatchery Center, Tohoku University. Sendai, Miyagi, Japan*

<sup>3</sup>*C&A corporation. Sendai, Miyagi, Japan*

**E-mail: akira.yoshikawa.d8@tohoku.ac.jp**

A number of halide and oxide scintillator materials have been developed in past decades [1-5]. Currently, these materials are widely used in various fields including astronomy, medical imaging, and homeland security. Although halide scintillators, such as Tl:NaI, Tl:CsI, and Ce:LaBr<sub>3</sub>, have high light outputs of more than 30,000 photons/MeV, they are rather hygroscopic that makes their device application comparatively complicated. On the other hand, most of oxide scintillators are well resistant to moisture and humidity.

Since scintillators require a transparent bulk body, it is essential to be able to fabricate a bulk single crystal using melt growth when designing a practical scintillator. Therefore, it is desirable to use a crystal fabrication method based on melt growth.

Here, three methods are introduced as typical examples: (i) the Micro-Pulling Down method, (ii) the Core Heating method, and (iii) the Multi-ampoule Bridgman method.

(i) The "Micro-Pulling Down method" is a crystal growth method that was mostly developed in our laboratory in early 90's. General scheme of the growth system is relatively simple: the melt (oxide, fluoride, metal, etc.) residing in a crucible is transported in downward direction through micro-capillary channel(s) made in the bottom of the crucible. Two driving forces (capillary action and gravity) support delivery of the melt onto liquid/solid growth interface that is formed under the crucible due to properly established temperature gradient. Appropriate configuration of the crucible bottom allows control of the crystal shape (fibers, rods, tubes, plates, etc.) and dimensions of the crystals cross-sections that approximately range from 0.1 to 10 mm. Number of scientifically and industrially important optical crystal fibers were successfully produced using this method [1,2].

(ii) The "Core Heating method" developed in our laboratory is suitable for searching materials in the temperature range above the softening point of iridium [3]. In this method, pellets of the raw material to be melted are prepared and placed together with iridium, and then the iridium is melted by arc flash, the pellets are melted by thermal conduction, and the pellets are cooled together with the iridium to promote melt growth (Fig.1).

(iii) The "Multi-ampoule Bridgman method" is also very effective and useful method. Multiple ampoules are placed in a furnace and melt growth is performed under the same temperature profile [4]. This is one of the best methods for exploring scintillators with high hygroscopicity, such as halides.

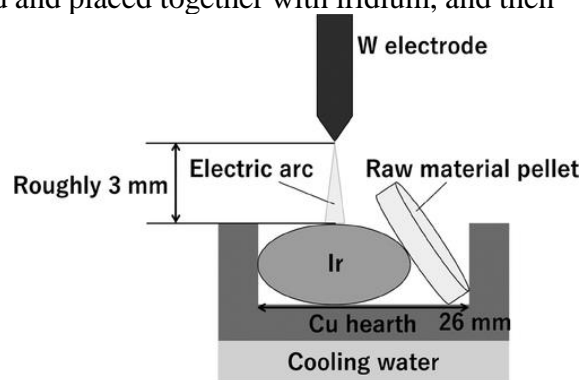


Fig. 1. Schematic of the "Core Heating method".

### References

- [1] A. Yoshikawa, M. Nikl, G. Boulon, T. Fukuda, *Opt. Mater.* 30 (2007) 6.
- [2] A. Yoshikawa, T. Satonaga, K. Kamada, H. Sato, M. Nikl, N. Solovieva, T. Fukuda, *J. Cryst. Growth* 270 (2004) 427.
- [3] Y. Kurashima, S. Kurosawa, R. Murakami, K. Kamada, A. Yoshikawa, et al., *Cryst. Growth Des.* 21, 1(2021) 572.
- [4] A. C. Lindsey, M. Zhuravleva, C. L. Melcher et al., *J. Cryst. Growth* 470 (2017) 20.

## Advances in technologies of bulk crystal growth from non-precious metal crucibles

**O. Sidletskiy<sup>1,2</sup>, Ia. Gerasymov<sup>1</sup>, S. Tkachenko<sup>1</sup>, P. Arhipov<sup>1</sup>, E. Galenin<sup>1</sup>,  
Ya. Boyaryntseva<sup>1</sup>, Yu. Zorenko<sup>2</sup>, K. Lebbou<sup>3</sup>, B. Grynyov<sup>1</sup>**

<sup>1</sup>*Institute for Scintillation Materials NAS of Ukraine 60 Nauky Ave., 61072 Kharkiv, Ukraine*

<sup>2</sup>*Institute of Physics, Kazimierz Wielki University in Bydgoszcz, Powstancow Wielkopolskich str., 2,  
85090 Bydgoszcz, Poland*

<sup>3</sup>*Institute of Light and Matter UMR 5306, University Claude Bernard Lyon 1, CNRS, 69100  
Villeurbanne, France*

**E-mail: sidletskiy@isma.kharkov.ua**

Czochralski and Bridgman techniques are still the basic fabrication methods of complex bulk oxide crystals, including garnet Ce-doped rare-earth (RE)  $\text{RE}_3\text{Al}_5\text{O}_{12}$ , perovskite  $\text{REAlO}_3$ , ortho-  $\text{RE}_2\text{SiO}_5$ , and pyrosilicate  $\text{RE}_2\text{Si}_2\text{O}_7$  scintillators. Because of the high melting points of these compounds, most of the producers use iridium (Ir) crucibles and crystalliser parts in technological processes. The drastic increase of Ir price in the last decade promotes the search for alternative crucible materials and development of crucible-free methods [1] for bulk crystal growth.

This report reviews the recent advances in the growth of scintillating bulk crystals from tungsten (W) and molybdenum (Mo) crucibles in ISMA NAS of Ukraine. High-quality aluminium garnet and perovskite crystals were grown with the Ce, Pr, Sc-doping. The peculiar feature of this technological process is the use of Ar+CO reducing atmosphere, which makes possible to introduce carbon to the crystals. The concentration of carbon was optimized in YAG:Ce,C to achieve the light yield up to 29600 phot/MeV [2]. The impact of carbon-related defects to the scintillation process was discussed [3]. Furthermore,  $(\text{La,Gd})_2\text{Si}_2\text{O}_7$ :Ce pyrosilicate and  $\text{Y}_2\text{SiO}_5$ :Ce orthosilicate were grown first time in Mo and W crucibles by the Czochralski and Bridgman methods, respectively [4].

We also address the recent results on the scaling up of  $\text{Y}_3\text{Al}_5\text{O}_{12}$ :Ce growth technologies, status of works on the enhancement of  $(\text{La,Gd})_2\text{Si}_2\text{O}_7$ :Ce crystals quality, growth of  $\text{RE}_2\text{O}_3$ -based crystals from W crucibles, LPE-grown composite scintillators grown on the bulk single crystalline substrates obtained by the novel fabrication process.

### References

- [1] Y. Kurashima et al. *Cryst. Growth Des.* 21 (2021) 572–578.
- [2] O. Sidletskiy et al. *Cryst. Growth Des.* (2021) DOI: 10.1021/acs.cgd.1c00259.
- [3] J. Zhu et al. *Opt. Mater.* 111 (2021) 110561.
- [4] S. Tkachenko et al. *Cryst. Eng. Comm.* 23 (2021) 360-367.

### Acknowledgments

This work was partially supported by the International Research Project “ScintLab” of CNRS, France, and French-Ukrainian bilateral project “Dnipro”, and Polish National Science Centrum project 2018/31/B/ST8/03390. O. Sidletskiy acknowledges the scholarship of the Polish National Agency for Academic Exchange under the agreement No. PPN/ULM/2020/1/00298/U/00001.

## La codoping strategy for modifying atoms segregation and luminescence and scintillation properties of LuAG:Pr single crystals

**K. Bartosiewicz<sup>1,2</sup>, A. Yamaji<sup>2</sup>, S. Kurosawa<sup>3,4</sup>, A. Yoshikawa<sup>2,3</sup>, T. Zorenko<sup>1</sup>, Yu. Zorenko<sup>1</sup>**

<sup>1</sup>IP, UKW, Powstancow Wielkopolskich 2, 85-090, Bydgoszcz, Poland

<sup>2</sup>IMR, Tohoku University, 2-1-1 Katahira Aoba-ku, Sendai, 9808577, Japan

<sup>3</sup>NICHe, Tohoku University, 6-6-10 Aoba, Aramaki, Aoba-ku, Sendai, 980-8579, Japan

<sup>4</sup>Facility of Science, Yamagata University, 1-4-12, Kojirakawa-machi, Yamagata

**E-mail: karol@ukw.edu.pl**

Pr<sup>3+</sup> activated Lu<sub>3</sub>Al<sub>5</sub>O<sub>12</sub> (LuAG:Pr) single crystal belongs to the family of high performances complex oxides scintillators. Pr<sup>3+</sup> centers in LuAG host offer high quantum efficiency and fast response (~20 ns decay time) in the 310 nm emission band [1]. However, one of the main issues in Pr doped LuAG single crystal grown by the micro-pulling-down ( $\mu$ -PD) method is sustaining the uniform activator distribution in the longitudinal and transverse directions. Such inhomogeneous distribution of the activator in the crystal can significantly reduce luminescence and scintillation performances [2].

The motivation for this research is to study the effects of La codoping in LuAG:Pr on the crystal growth, atoms segregation as well as luminescence and scintillation characteristics. La codoping might improve segregation of Pr ions in  $\mu$ -PD grown LuAG crystal. A larger ionic radius of La<sup>3+</sup> (1.165 Å) than Pr<sup>3+</sup> (1.126 Å) ion, causes that La atoms concentrate mainly at the crystal periphery. This process hamper the location of Pr atoms on the crystal edge, but facilitates their localization towards the crystal core. Consequently, the distribution of Pr atoms might be more homogeneous within the cross-section of the crystal. The scintillation characteristics of LuAG:Pr crystal can be further improved by La codoping. Large La<sup>3+</sup> ions form La<sub>Lu</sub> luminescence centers in LuAG crystal, which can localize and/or bound excitons [3]. Moreover, La<sup>3+</sup> centers can transfer the excitation energy towards Pr<sup>3+</sup> centers due to good spectral overlap of the La<sub>Lu</sub> related emission band (radiation decay of excitons localized and/or bound at La<sup>3+</sup> ions) centered around 275 nm with the 4f $\rightarrow$ 5d<sub>1</sub> absorption band of Pr<sup>3+</sup> [3,4].

The LuAG:Pr,La (La=0, 0.15, 0.3 at. %) crystals were grown from the melt by  $\mu$ -PD method. They were characterized by absorption, cathodoluminescence and photoluminescence (PL) excitation/emission spectra as well as PL decay kinetic measurements. Scintillation properties are studied through light yield value and scintillation decay analysis under excitation by  $\alpha$  particles depending on the La content and La/Pr ratio in the crystals. Moreover, the energy transfer process from La-related exciton center to Pr<sup>3+</sup> ions is investigated.

### References

- [1] J. Pejchal, et al., J. Phys. D: Appl. Phys. 42 (2009) 055117.
- [2] O. Sidletskiy et al. CrystEngComm, (23) 2021, 2633-2643.
- [3] K. Bartosiewicz, et al., J. Lum. 235 (2021) 118013.
- [4] P. Prusa, et al., J. Cryst. Growth 318 (2011) 545-548.

### Acknowledgments

This work was supported by the Japan Society for the Promotion of Science P17379 (JSPS) and Polish NCN project 2016/21/B/ST8/03200 and 2018/31/B/ST8/03390 projects.

## Single crystal growth of garnets by floating zone method in laser furnace

**F. Zajíc<sup>1</sup>, J. Pospíšil<sup>1</sup>, M. Klejch<sup>2</sup>, M. Nikl<sup>3</sup>**

<sup>1</sup>Charles University, Faculty of Mathematics and Physics, Ke Karlovu 5, 121 16 Prague, Czech Republic

<sup>2</sup>CRYTUR, spol. s r.o., Na Lukách 2283, 51101 Turnov, Czech Republic

<sup>3</sup>Institute of Physics, Academy of Sciences of the Czech Republic, Cukrovarnicka 10, 162 00 Prague 6, Czech Republic

**E-mail: jiri.pospisil@mff.cuni.cz**

Single crystals of optical materials are industrially grown mostly by the Czochralski method, while in the laboratory scale new compositions of single crystals are primarily tested and grown using the micro-pulling down method. Both of these methods are so-called crucible methods, which brings few fundamental limitations. Because of very high materials reactivity at temperatures of the melting point of common photonic single crystals, which is often higher than 2000°C materials of the crucible is the main obstacle. Such reactivity leads to the incorporation of the crucible atoms into the crystal lattice of growing single-crystal creating the lattice impurities. Moreover, during the growth process, a very clean protective Ar atmosphere is also needed to avoid degradation of the expensive noble metals crucibles, which, however, leads to oxygen vacancies in the single-crystal lattice of oxides [1]. Both types of lattice imperfections significantly affect their scintillation properties.

We present a innovative way of single crystal growth of garnets by the floating zone method implemented to a modern 5-lasers optical furnace. This method is contactless and crucible-free. Only a small amount of the melted material is trapped by surface tension between the precursor rod and the grown single crystal. This allows the growing of materials of high purity and with very high melting points. The extra advantage of the crucible free floating zone method is the possibility of growth under a pure oxygen atmosphere.

We chose well-known Nd:YAG as testing material for optimization of the growing process by floating zone method. We will describe in detail the method of preparation of precursors and their development with respect to the stability of the growth process and reproducibility of the quality of obtained single crystals. We will focus on the individual parameters of the growth process and finally on the optical properties of the grown single-crystals.

### References

[1] A. Suzuki et al., *Physica Status Solidi C*, 9 (2012) 2251–2254.

### Acknowledgments

This work is part of the research program GACR 21-17731S, which is financed by the Czech Science Foundation. Experiments were performed in the Materials Growth and Measurement Laboratory, which is supported within the program of Czech Research Infrastructures (Project No. 424LM2018096).

## Effects of co-doping on optical and scintillation properties of YAG:Ce,C crystals

**Ia. Gerasymov<sup>1</sup>, O. Sidletskiy<sup>1,2</sup>, Ya. Boyaryntseva<sup>1</sup>, S. Tkachenko<sup>1</sup>, P. Arhipov<sup>1</sup>, E. Galenin<sup>1</sup>, D. Kurtsev<sup>1</sup>, O. Zelenskaya<sup>1</sup>, V. Alekseev<sup>1</sup>, S. Witkiewicz-Lukaszek<sup>2</sup>, T. Zorenko<sup>2</sup>, Yu. Zorenko<sup>2</sup>**

<sup>1</sup>*Institute for Scintillation Materials of National Academy of Science of Ukraine, 60 Nauky ave., 61072 Kharkiv, Ukraine*

<sup>2</sup>*Institute of Physics Kazimierz Wielki at University in Bydgoszcz (UKW), 2 Powstańców Wielkopolskich str., 85-090 Bydgoszcz, Poland*

**E-mail: yarosgerasimov@gmail.com**

Recently, there has been a trend towards an increase of the frequency of particle beams collisions [1] in accelerators, as well as a decrease of the dose load on a patient during PET diagnostics by increasing the scanning speed [2]. All this imposes new requirements on the scintillators speed. Among the variety of scintillation materials, oxide single crystals of rare-earth garnets, activated with cerium, demonstrate rather short decay times of luminescence and the ability to withstand significant dose loads. However, the luminescence associated with recombination on trivalent cerium ions in such matrices, although relatively fast but already insufficient for new applications. One of the ways to influence on the time characteristics of oxide scintillators is co-doping by the elements of the 1<sup>st</sup> or 2<sup>nd</sup> groups of the periodic table. Often, decreasing of the light output is the negative side of the such co-doping. Therefore, it is advisable to reduce the decay times of luminescence in scintillators with a high light output. Not so far in time, it was possible to achieve a high light yield in a seemingly long-studied commercial material - yttrium-aluminum garnet, activated by cerium and carbon, but the luminescence decay time of this material is still quite long [3].

This work presents the results of studies of YAG:Ce,C crystals co-activated with elements of the 1<sup>st</sup> (Li, Na, K) and 2<sup>nd</sup> (Mg, Ca, Sr, Ba) groups in different concentrations, grown in an reduction atmosphere preventing tungsten crucible damage.

### References

- [1] Burkhard Schmidt. The High-Luminosity upgrade of the LHC. Journal of Physics: Conference Series 706 (2016) 022002, p. 1-42.
- [2] P. Lecoq. Pushing the Limits in Time-of-Flight PET Imaging. IEEE TRANSACTIONS ON RADIATION AND PLASMA MEDICAL SCIENCES, VOL. 1, NO. 6, NOVEMBER 2017. P. 473-485.
- [3] O. Sidletskiy et al. Cryst. Growth Des. (2021) DOI: 10.1021/acs.cgd.1c00259.

### Acknowledgments

This work was supported by the National Academy of Science of Ukraine in the frame of “Carbon” project, and Polish National Science Centrum project 2018/31/B/ST8/03390. O. Sidletskiy acknowledges the scholarship of the Polish National Agency for Academic Exchange under the agreement No. PPN/ULM/2020/1/00298/U/00001.

## Growth and characterization of mixed LuYAG:Ce crystals under reducing atmosphere

**D. Kofanov<sup>1</sup>, Ia. Gerasymov<sup>1</sup>, P. Arhipov<sup>1</sup>, S. Tkachenko<sup>1</sup>, D. Kurtsev<sup>1</sup>,  
Ya. Boyaryntseva<sup>1</sup>, O. Zelenskaya<sup>1</sup>, T. Gorbacheva<sup>1</sup>, K. Lebbou<sup>2</sup>, O. Sidletskiy<sup>1,3</sup>**

<sup>1</sup>*Institute for Scintillation Materials NAS of Ukraine, 60 Nauky Ave., 61072 Kharkiv, Ukraine*

<sup>2</sup>*Institute of Light and Matter UMR 5306, University Claude Bernard Lyon 1, CNRS, 69100  
Villeurbanne, France*

<sup>3</sup>*Institute of Physics, Kazimierz Wielki University in Bydgoszcz, Powstancow Wielkopolskich str., 2,  
85090 Bydgoszcz, Poland*

**E-mail: phkofanov@gmail.com**

Garnet-based scintillators are widely used in various fields including scintillation detectors, LED engineering, etc.  $Y_3Al_5O_{12}:Ce$  is one of the most popular composition among them, due to its low cost, possibility to produce large bulks crystals by various methods, for example, by the Czochralski, using W or Mo crucibles [1]. However, typical light yield of manufactured YAG:Ce crystals did not exceed 15000–25000 phot/MeV, while according to the band gap value the theoretical light yield in rare earth garnets should be around 50000–60000 phot/MeV [2].

On practice the comparable light yield values were achieved just in  $Gd_3Al_2Ga_3O_{12}:Ce$  mixed crystals. On the way of the band gap engineering various mixed compositions were proposed based on the cation substitution in rare earth garnets, for example, above-mentioned GAGG:Ce. Another mixed crystals is  $(Lu_{1-x}Y_x)_3Al_5O_{12}$ , which almost doubled its light yield compared to LuAG in the case of Pr activation [3]. Decay time and energy resolution were improved either. Recently, it was shown that YAG:Ce crystals with carbon doping grown under the reducing conditions demonstrate a high light yield of up to ca. 30000 phot/MeV [4]. Therefore, transfer to mixed composition of crystals grown under the same conditions may be promising.

In this study, the impact of Lu addition to the YAG matrix was investigated at growth by Czochralski technique under reducing conditions in Ar+CO atmosphere from W crucible and graphite heat insulation. The series of mixed crystals with the length up to 9 cm and different Lu-Y ratios  $(Lu_{1-x}Y_x)_3Al_5O_{12}:Ce$  were obtained. Optical, luminescent, and scintillation parameters of crystals were studied to evaluate the impact of Lu addition.

### References

- [1] O. Sidletskiy, P. Arhipov, S. Tkachenko, Ia Gerasymov, D. Kurtsev, V. Jarý, R. Kuřcerkova, M. Nikl, K. Lebbou, E. Auffray, *Springer Proceedings in Physics*, 227, (2019), 83–95, 346.
- [2] P. Dorenbos, *Nucl. Instrum. Methods Phys. Res.*, A 486, (2002), 191–207.
- [3] C. Foster, Y. Wu, L. Stand, M. Koschan, C. L. Melcher, *Phys. Status Solidi*, (2018), 1800280.
- [4] O. Sidletskiy, Ia. Gerasymov, Ya. Boyaryntseva, P. Arhipov, S. Tkachenko, O. Zelenskaya, K. Bryleva, K. Belikov, K. Lebbou, C. Dujardin, B. Büchner, B. Grynyov, *Crystal Growth & Design*, (2021), DOI: 10.1021/acs.cgd.1c00259.

### Acknowledgments

This work was partially supported by the International Research Project “ScintLab” of CNRS, France, and French-Ukrainian bilateral project “Dnipro”. O. Sidletskiy acknowledges the scholarship of the Polish National Agency for Academic Exchange under the agreement No. PPN/ULM/2020/1/00298/U/00001.



## Luminescence mechanism and Ce incorporation in LaAP:Ce single crystals

**J. Pejchal<sup>1</sup>, M. Buryi<sup>1</sup>, V. Laguta<sup>1</sup>, V. Babin<sup>1</sup>, F. Hajek<sup>1</sup>, J. Paterek<sup>1</sup>,  
L. Prochazkova-Prouzova<sup>1,2</sup>, L. Havlak<sup>1</sup>, V. Vanecek<sup>1,2</sup>, J. Havlicek<sup>3</sup>, V. Dolezal<sup>3</sup>,  
K. Rubesova<sup>3</sup>, P. Zemenova<sup>1</sup>, R. Kral<sup>1</sup>**

<sup>1</sup> Institute of Physics, Czech Academy of Sciences, Cukrovarnicka 10, 16200 Prague, Czech Republic

<sup>2</sup> Faculty of Nuclear Sciences and Physical Engineering, Brehova 7, 11519 Prague, Czech Republic

<sup>3</sup> University of Chemistry and Technology, Technicka 5, 166 28 Prague, Czech Republic

**E-mail: pejchal@fzu.cz**

Aluminum perovskites represent an important group of promising scintillation materials [1], but due to a difficult crystal growth, not much attention has been paid to them so far. The reported decay time of the Ce and Pr-doped YAlO<sub>3</sub> (YAP) luminescence is as short as 18 ns and 8 ns, respectively, which makes it one of the fastest materials among the Ce and Pr-doped oxide scintillators [2,3]. Furthermore, YAP:Ce shows very small nonproportionality of the scintillation response, which results in its excellent energy resolution.

However, the growth of YAP single crystals is still quite difficult due to a strong tendency of the garnet phase creation. Therefore, we decided to study its analogue LaAlO<sub>3</sub> (LaAP), the growth of which is easier due to the stabilization of the perovskite phase by a large La<sup>3+</sup> cation in the material structure.

Moreover, it seemed that the potential of Ce-doped LaAlO<sub>3</sub> cannot be ruled out yet due to observation of intense blue luminescence [4]. On the other hand, some reports claim that Ce<sup>3+</sup> luminescence is completely absent in this matrix [5]. We decided to study this material in detail to explain the observed discrepancy and underlying phenomena. Crystal growth by the micro-pulling-down method will be reported together with luminescence and scintillation properties. We will demonstrate influence of other aluminate phases created during the crystal growth on the luminescence processes and energy transfer. These phases were also confirmed by observation with scanning electron microscope and correlated cathodoluminescence and X-ray analysis. Electron paramagnetic resonance has shown incorporation of Ce ions in different environments and their clustering, which might be one of the causes of low scintillation efficiency generally observed for this materials system.

### References

- [1] M. Nikl, A. Yoshikawa, *Advanced Optical Materials*, 3 (2015) 463-481.
- [2] M. J. Weber, *Journal of Applied Physics*, 44 (1973) 3205-3208.
- [3] E. Gumanskaya, A. O. Egorycheva, et al., *Optics and Spectroscopy*, 72 (1992) 395-399.
- [4] X. Zeng et al., *Journal of Crystal Growth*, 271 (2004) 319-324.
- [5] E. van der Kolk, J.T.M. de Haas, et al., *Journal of Applied Physics*, 101 (2007) 083703 (1-4).

### Acknowledgments

This work was supported by the Czech Science Foundation (GACR) 18-14789S project.

## Growth and scintillation properties of rare-earth doped SrO and CaO by core heating method

**K. Kamada**<sup>1,2</sup>, **R. Kucerkova**<sup>4</sup>, **M. Nikl**<sup>4</sup>, **S. Ishikawa**<sup>2</sup>, **M. Yoshino**<sup>3</sup>, **R. Murakami**<sup>2,3</sup>,  
**K. J. Kim**<sup>1,2</sup>, **V. Kochurikhin**<sup>2,4</sup>, **A. Yoshikawa**<sup>1,2,3</sup>

<sup>1</sup>New Industry Creation Hatchery Center, Tohoku University, Sendai, Japan,

<sup>2</sup>C&A Corporation, Sendai, Japan,

<sup>3</sup>Institute for Materials Research, Tohoku University, Sendai, Japan,

<sup>4</sup>Institute of Physics AS CR, Czech Republic

E-mail: kamada@imr.tohoku.ac.jp

Inorganic scintillators have been playing a major role in many fields of radiation detection, including astro-particle physics experiment, medical imaging, security, etc. SrO and CaO are interesting host for both phosphor and scintillator materials due to their possible emission by doping of rare earth elements. However SrO and CaO have generally high melting temperatures of 2531°C and 2572°C, respectively, and it is difficult to obtain transparent single crystals. Their boiling point of 3200°C and 2850°C, respectively, are close to their melting point and make trouble due to its evaporation during crystal growth. Recently, we proposed a novel indirect heating growth method using arc plasma and Ir metal melt for materials survey. Arc plasma preferentially heat for metal due to the difference of electrical conductivity. We referred to this indirect heating growth method as the core heating (CH) method[1].

In this study rare earth elements such Tb, Eu, Ce are doped in SrO and CaO. SrO and CaO crystals were grown by the CH method. Figure 1 shows an example photograph of the grown undoped, Ce, Eu and Sm doped CaO crystals. These crystals shows enough transparency and size for luminescence and radiation response measurements. The Eu doped SrO and CaO samples shows orange  $\text{Eu}^{3+}$  4f4f emission peaking at around 590-640. Only Eu doped CaO showed  $\text{Eu}^{2+}$  4f5d emission peaking at around 740 nm. Details of growth procedure, crystal phase, XRC, optical and scintillation properties will be presented.

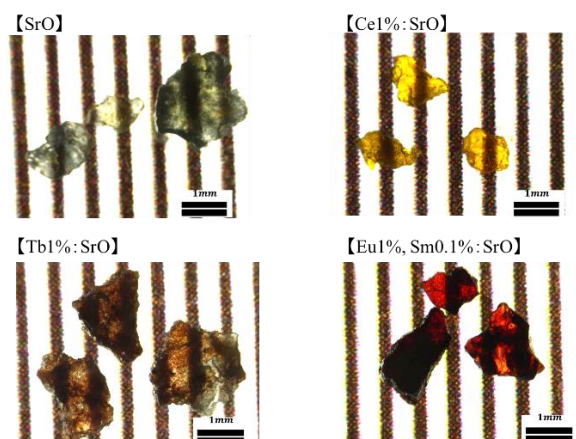


Fig.1 Photographs of the grown SrO crystals

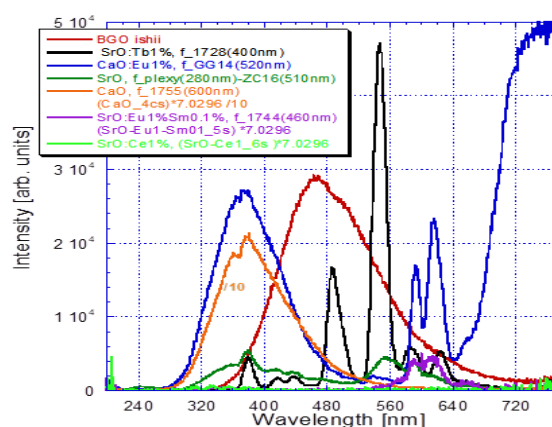


Fig.2 radioluminescence spectra of the grown rare earth doped SrO and CaO.

### References

- [1] K. J. Kim, K. Kamada, Crystals 2020, 10(7), 619.

## **Cs<sub>2</sub>Hf<sub>x</sub>Zr<sub>1-x</sub>Cl<sub>6</sub> mixed crystals, their growth by vertical Bridgman method and characterization of luminescent and scintillation properties**

**R. Král<sup>1</sup>, V. Vaněček<sup>1,2</sup>, J. Páterek<sup>1,2</sup>, M. Buryl<sup>1</sup>, V. Babin<sup>1</sup>, K. Zloužeová<sup>1,3</sup>,  
S. Kodama<sup>4,5</sup>, S. Kurosawa<sup>4,6</sup>, Y. Yokota<sup>4</sup>, A. Yoshikawa<sup>4,6,7</sup>, M. Nikl<sup>1</sup>**

<sup>1</sup>*Institute of Physics, Czech Academy of Sciences, Cukrovarnicka 10, Prague, Czech Republic*

<sup>2</sup>*FNSPE, Czech Technical University in Prague, Brehova 7, Prague, Czech Republic*

<sup>3</sup>*UCT Prague, Technická 5, Prague, 166 28 Czech Republic,*

<sup>4</sup>*IMR, Tohoku University, 2-1-1, Katahira, Aoba-ku, Sendai, Miyagi, 980-8577 Japan*

<sup>5</sup>*Saitama University, 2-5-5 Shimo-Okubo, Sakura-ku, Saitama 338-8570, Japan*

<sup>6</sup>*NICHe, Tohoku University, 6-6-10 Aza-Aoba, Aoba-ku, Sendai, Miyagi, 980-8579 Japan,*

<sup>7</sup>*C&A corporation, 6-6-40 Aza-Aoba, Aramaki, Aoba-ku, Sendai, Miyagi, 980-8579 Japan*

**E-mail: kralr@fzu.cz**

Cesium hafnium chloride (Cs<sub>2</sub>HfCl<sub>6</sub>) has been widely studied for its promising scintillation properties as a new cost effective scintillator for gamma ray spectroscopy. The Cs<sub>2</sub>HfCl<sub>6</sub> has high light yield up to 54,000 ph/MeV, energy resolution of 2.8 % at 662 keV, scintillation response of 4.4 ms (95 % of energy) at 662 keV, moderate density of 3.86 g/cm<sup>3</sup> [1], and low hygroscopicity. [2]. These properties make the Cs<sub>2</sub>HfCl<sub>6</sub> a suitable candidate for new cost-effective radiation detectors. The scintillating mechanism in the undoped Cs<sub>2</sub>HfCl<sub>6</sub> is ascribed to intrinsic luminescence originating in a self-trapped excitons (STE) represented by a V<sub>k</sub> center [3]. The Cs<sub>2</sub>HfCl<sub>6</sub> is formed by cesium chloride (CsCl) and hafnium chloride (HfCl<sub>4</sub>) mixed together in stoichiometric ratio 2:1 congruently melting at ca. 821°C [4]. The Cs<sub>2</sub>HfCl<sub>6</sub> crystallizes in cubic structure with lattice parameters  $a = 10.42 \pm 0.01 \text{ \AA}$  (space group Fm-3m).

In this work we continue in the study of Cs<sub>2</sub>Hf<sub>x</sub>Zr<sub>1-x</sub>Cl<sub>6</sub> (CHZC) crystals formed by mixing Cs<sub>2</sub>HfCl<sub>6</sub> and Cs<sub>2</sub>ZrCl<sub>6</sub> in wide stoichiometry (x=0-1) and growth of the solid solution CHZC by the vertical Bridgman method. The goal is to analyse the influence of the Hf/Zr ratio on the STE intrinsic emission and determine the threshold when the main emission originates in the Hf or Zr emission for possible tunability of the CHZC matrix. Grown CHZC crystals were characterized by measuring their structural, optical, luminescence, and scintillation properties.

### **References**

- [1] A. Burger et al., *Appl. Phys. Lett.*, 107 (2015) 143505.
- [2] S. Lam et al., *J. Cryst. Growth*, 483 (2018)121-124.
- [3] R. Král et al., *J. Phys. Chem. C*, 121 (2017) 12375-12382.
- [4] R. Kral et al., *J. Therm. Anal. Calorim.*, 141 (2020) 1101–1107.

### **Acknowledgments**

The support of Czech Science Foundation by project no. 18-17555Y and partial support by Operational Programme Research, Development and Education financed by European Structural and Investment Funds and the Czech Ministry of Education, Youth and Sports (Project No. SOLID21 CZ.02.1.01/0.0/0.0/16\_019/0000760) is gratefully acknowledged. The authors thank to Mr. A. Bystricky for preparation and purification of starting materials.

## Crystallization of $Y_2O_3$ melt in tungsten crucibles

**E. Galenin<sup>1</sup>, Ia. Gerasymov<sup>1</sup>, O. Sidletskiy<sup>1</sup>, S. Tkachenko<sup>1</sup>,  
D. Kurtsev<sup>1</sup>, A. Shaposhnyk<sup>2</sup>**

<sup>1</sup>*Institute for Scintillation Materials of NAS of Ukraine, 60 Nauky ave., 61072 Kharkiv, Ukraine*

<sup>2</sup>*SSI "Institute for single crystals" NAS of Ukraine, 60 Nauky ave., 61072 Kharkiv, Ukraine*

**E-mail: e.galenin@gmail.com**

Crystals based on the oxides of rare earth elements (RE) are promising for photonics applications [1, 2]. Obtaining of bulk RE oxide crystals is complicated due to their extremely high temperature (>2400 °C) causing a need to use expensive rhenium crucibles.

Recently, the progress was achieved at growing of high temperature crystals of RE silicates and aluminates from tungsten crucibles [3, 4]. Authors claim good quality of obtained crystals and essential decrease of production cost due to substitution of iridium by tungsten as a crucible material.

The goal of this work was to evaluate possibilities of obtaining of  $Y_2O_3$  crystals in tungsten crucibles.

A preliminary sintered  $Y_2O_3$  rods with a density of more than 85% of that in the crystals was were melted in tungsten crucibles with a diameter of 6 mm. The raw materials were inductively heated in tungsten crucibles by controlling the input power. After the melting and crystallization controlled by the external reference  $Y_2O_3$  crystal the ingots were slowly cooled to room temperature. Black ingots of few mm size were obtained, which became cloudy white after annealing in air at 1300 °C. According to the XRD data, the main phase in the ingot is the cubic modification of  $Y_2O_3$  with traces of yttrium carbides. Luminescence and optical measurements of the obtained sample were also investigated.

### References

- [1] P. Loiko et al., IEEE Journal of Selected Topics in Quantum Electronics, vol. 24, no. 5, pp. Art no. 1600713.
- [2] V. Peters, et al. J. of Crys. Growth, V237–239(1), 2002, 879-883.
- [3] S. Tkachenko et al. CrystEngComm, 2021, 23, 360-367.
- [4] O. Sidletskiy et al. Eng. Of Scint. Mat. And Rad. Techn., 2019, V227, ISBN : 978-3-030-21969-7.

### Acknowledgments

This work was supported by the National Academy of Science of Ukraine in the frame of project "Corze", No. 0121U108986.

## Growth and scintillation properties of CsI/CsCl/KCl eutectics for radiation imaging applications

**Y. Takizawa<sup>1</sup>, K. Kamada<sup>2,3</sup>, N. Kutsuzawa<sup>3</sup>, K. J. Kim<sup>2</sup>, M. Yoshino<sup>1</sup>, A. Yamaji<sup>2</sup>,  
S. Kurosawa<sup>2</sup>, Y. Yokota<sup>1</sup>, H. Sato<sup>2</sup>, S. Toyoda<sup>2</sup>,  
Y. Ohashi<sup>2</sup>, T. Hanada<sup>1</sup>, V. Kochurikhin<sup>3</sup>, A. Yoshikawa<sup>1,2,3</sup>**

<sup>1</sup>Institute for Material Research, Tohoku University. Sendai, Miyagi, Japan

<sup>2</sup>New Industry Creation Hatchery Center, Tohoku University. Sendai, Miyagi, Japan

<sup>3</sup>C&A corporation. Sendai, Miyagi, Japan

**E-mail: yui.tacky@imr.tohoku.ac.jp**

Imaging detectors that detect radiation such as X-rays, gamma rays are widely used in applications such as medical imaging, high energy physics, astronomy etc.. Up to now, we have been studying an optical waveguide type high-resolution eutectic scintillator that utilizes the difference between the fibrous eutectic structure and the refractive index of the crystal phase to improve the spatial resolution in radiation imaging[1]. A phase-separated scintillator fiber (PSSF) is composed of a eutectic having multiple crystal phases, and improves the position resolution of the radiation detector by optimizing the combination of the eutectic structure, the scintillator properties of the crystal phases, and the refractive index. As of now, GdAlO<sub>3</sub>/a-Al<sub>2</sub>O<sub>3</sub>[1] and Tl:CsI/CsCl/NaCl [2] have been reported as directionally solidified eutectics (DSE) for use as eutectic components. In this work, we researched a novel ternary eutectic of CsI/CsCl/KCl containing PSSFs of Tl:CsI. CsI/CsCl/KCl ternary eutectics and their PSSFs structures were investigated.

The starting materials were prepared using CsI, CsCl, KCl and TII powders (4N). Tl-doped and non-doped CsI/CsCl/KCl eutectics were grown at the eutectic composition. The starting powders were enclosed in a quartz tube with 3.8 mm inner diameter under high vacuum ( $\sim 10^{-4}$  Pa). Crystal growth was performed by the vertical Bridgman Stockbarger (VB) method.

The Tl doped CsI/CsCl/KCl eutectics were grown by the VB method (Fig.1). Circular samples with 1 mm thickness were cut from the grown crystal. The cut surface was mechanically polished and the eutectic phase structure was observed by back scattered electron image (BEI). The BEI of transverse & vertical cross-section of the eutectic are shown in Fig. 2. Phases were uniformly distributed in the transverse direction and slightly aligned along the growth direction. Here, refractive index of CsI, CsCl and KCl are 1.8, 1.61 and 1.49@550nm, respectively. The CsI scintillator matrix phase can have waveguiding function. CsI/CsCl/KCl have higher density and  $Z_{eff}$  than that of CsI/CsCl/NaCl. Higher sensitivity can be expected. In our presentation, relationship between growth rate, and eutectic structure will be discussed. Details of scintillation properties, emission image map and radiation imaging using the grown eutectic plates will be also reported.

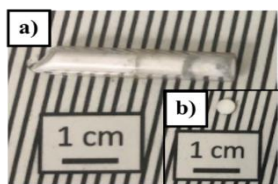


Fig.1 Photographs of the grown eutectics(a) and a wafer sample(b).

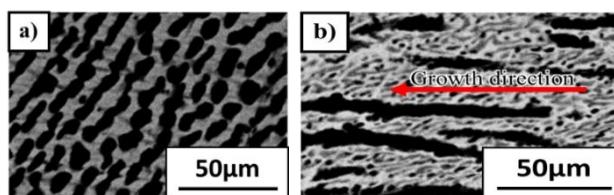


Fig.2 BEI of CsI/CsCl/KCl eutectic on transverse (a) & vertical (b) cross-section.

### References

- [1] K. Kamada et al, IEEE Trans. Nucl. Sci. 65(8) 2036–2040 (2018).
- [2] Y. Takizawa et al., Jpn. J. Appl. Phys. 60, no. SB (2020).

## Melt growth of $Zn_3Ta_2O_8$ crystal by core heating method and its scintillation properties

**R. Yajima<sup>1</sup>, K. Kamada<sup>2,3</sup>, S. Ishikawa<sup>3</sup>, Y. Takizawa<sup>1</sup>, K. J. Kim<sup>2</sup>, M. Yoshino<sup>1</sup>,  
A. Yamaji<sup>2</sup>, S. Kurosawa<sup>2</sup>, Y. Yokota<sup>1</sup>, H. Sato<sup>2</sup>, S. Toyoda<sup>2</sup>, Y. Ohashi<sup>2</sup>,  
T. Hanada<sup>1</sup>, V. Kochurikhin<sup>3</sup>, A. Yoshikawa<sup>1,2,3</sup>**

<sup>1</sup>Institute for Material Research, Tohoku University. Sendai, Miyagi, Japan

<sup>2</sup>New Industry Creation Hatchery Center, Tohoku University. Sendai, Miyagi, Japan

<sup>3</sup>C&A corporation. Sendai, Miyagi, Japan

E-mail: ryuga.yajima@imr.tohoku.ac.jp

Inorganic scintillators have been playing a major role in many fields of radiation detection, including astro-particle physics experiment, medical imaging, security, etc. In these applications heavy and fast scintillator materials are required. Tantalate compounds such  $Mg_4Ta_2O_9$ ,  $Li_3TaO_4$ ,  $YTaO_4$  etc. are attractive host material due to their high density and large  $Z_{eff}$ . Among of them,  $Zn_3Ta_2O_8$  powder showed promising properties such density of  $7.14 \text{ g/cm}^3$  and decay time of  $0.2 \mu\text{s}$  (20%),  $1.1 \mu\text{s}$  (80%)[1]. However melt growth of this compound was not possible due to the high vapor pressure of ZnO[1]. Up to now, we propose a novel indirect heating growth method named core heating (CH) method[2]. It is characterized by high-speed crystal growth and can minimize the evaporation of ZnO during the crystal growth. In this study,  $Zn_3Ta_2O_8$  crystal was grown from the melt by the CH method. Luminescence and scintillation properties were studied.

A stoichiometric mixture of 4N purity ZnO and  $Ta_2O_5$  powders were used as the starting material. Nominally, starting powders were prepared according to the formulas of  $Zn_3Ta_2O_8$ . Crystals were grown by the CH method by using arc plasma furnace (GES-300A)[2]. Mixed powder was compressed into the bottom of a water-cooling copper hearth with 30 mm diameter and 10 mm depth. An iridium pellet with around 25mm diameter was placed on the compressed powder. The iridium pellet was heated and melted by arc plasma from the tungsten electrode. The arc plasma power was increased up to the powder melted. After confirming the expansion of the melt area, the power was reduced down to 0 during 2.5 minutes.

Figure 1 shows an example photograph of the grown  $Zn_3Ta_2O_8$  crystal grown by the Cz method. This crystal shows enough transparency and size for luminescence and scintillation properties measurements. The sample shows expected charge transfer emission from  $TaO^{4-}$  peaking at around 410 nm, respectively. Details of growth procedure, crystal phase, XRC, optical and scintillation properties will be presented.



Fig.1 Photographs of the grown crystal

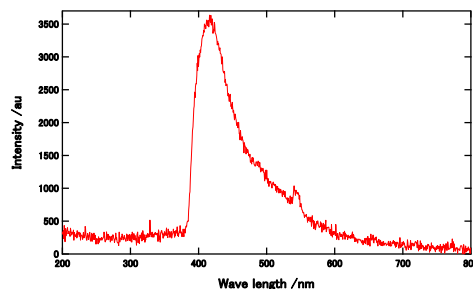


Fig.2 Radioluminescence spectra of the grown crystal

### References

- [1] E. D.Bourret et al. *J. Luminescence* 2020, 202, 332-338.
- [2] K. J. Kim, K. Kamada, *Crystals* 2020, 10(7), 619.

## Optimization of cathodoluminescence efficiency of scintillators for low-energy electron detectors

**O. Lalinský<sup>1</sup>, P. Schauer<sup>1</sup>, M. Kučera<sup>2</sup>**

<sup>1</sup>*Institute of Scientific Instruments of the CAS, Kralovopolska 147, 612 64 Brno, Czech Republic*

<sup>2</sup>*Charles University, Faculty of Mathematics and Physics, 121 16 Prague, Czech Republic*

**E-mail: xodr@isibrno.cz**

Scanning electron microscopy (SEM) imaging of a sample with the primary beam (PB) of energy in the order of keV or less has a number of advantages over a typical PB energy of 10 keV. The most significant advantages are the smaller depth of sample damage and, with the appropriate PB energy, complete elimination of sample charging [1]. This is especially critical for biological and other samples, where conductive coating distorts or even destroys sample information. However, low-energy PB imaging induces a problem in the detection of signal electrons. Whereas secondary electrons are accelerated to high energy, backscattered electrons (BSEs) are usually not accelerated or even negatively biased [2]. Because most of the BSEs have an energy very close to the PB energy [3], a decrease in the PB energy results in a decrease in the energy of the BSEs. This causes a lower cathodoluminescence (CL) scintillator response. In addition, there may be an increase in electron energy losses in the scintillator coating. Therefore, the coating-scintillator system for the detection of low-energy BSEs needs to be optimized.

Scintillators of Y<sub>3</sub>Al<sub>5</sub>O<sub>12</sub>:Ce (YAG:Ce), YAlO<sub>3</sub>:Ce (YAP:Ce), CRY018 and the most recently developed Gd<sub>3</sub>Al<sub>2.3</sub>Ga<sub>2.7</sub>O<sub>12</sub>:Ce (GAGG:Ce) [4] were selected for this study. Al, Sc, Ni and Indium Tin Oxide (ITO) were selected as conductive coatings for the scintillators. The study of the coatings showed that electrons with an energy  $\geq 5$  keV are best detected by a scintillator covered with an Al layer of 25–50 nm. For smaller energies up to 0.8 keV, a 4 nm thin ITO layer was the best choice. For electron energies less than 0.8 keV, it is most advantageous not to cover the scintillator at all in comparison with the studied coatings. In a study of uncoated scintillators, YAG:Ce and GAGG:Ce excelled in slow electron detection. These scintillators with the above-mentioned coating parameters are therefore promising for the detection of slow electrons.

### References

- [1] L. Reimer, *Image Formation in Low-voltage Scanning Electron Microscopy*, SPIE (1993).
- [2] P. Wandrol, *Journal of Microscopy-Oxford*, 227 (2007) 24–29.
- [3] L. Reimer, *Scanning Electron Microscopy: Physics of Image Formation and Microanalysis*, Springer (1998).
- [4] J. Bok, O. Lalinsky, M. Hanus, Z. Onderisinova, J. Kelar, M. Kucera, *Ultramicroscopy*, 163 (2016) 1–5.

### Acknowledgments

The research was supported by the Technology Agency of the Czech Republic (project TN01000008), the Ministry of Industry and Trade of the Czech Republic (project TRIO FV30271); the infrastructure by the Czech Academy of Sciences (project RVO:68081731).

## Growth and properties of multicomponent garnet and perovskite films for low afterglow scintillators

**M. Kucera<sup>1</sup>, M. Rathaiah<sup>1</sup>, M. Nikl<sup>2</sup>, A. Beitlerova<sup>2</sup>, O. Lalinsky<sup>3</sup>**

<sup>1</sup>Charles University, Faculty Math. & Physics, 12116 Prague, Czech Republic

<sup>2</sup>Institute of Physics ASCR, 16200 Prague, Czech Republic

<sup>3</sup>Institute of Scientific Instruments ASCR, 61264 Brno, Czech Republic

**E-mail: miroslav.kucera@mff.cuni.cz**

Scintillation materials with short decay time and low afterglow are crucial in applications where fast response is required, such as high rate imaging techniques, medical applications, or electron-beam inspection systems. Garnet or perovskite films are used as state-of-the-art scintillation screens for X-ray micro-imaging 2D detectors with submicrometer resolution. The single crystalline films for this application are grown by liquid phase epitaxy [1]. This technology is also a suitable method for fast material screening.

In this contribution, a survey of liquid phase epitaxial technology for the growth of high-quality single crystalline films for scintillation application will be presented. We will focus on oxide scintillation films, primarily multicomponent GAGG and GSAG garnets and LuYAP perovskites activated by Ce<sup>3+</sup> or Pr<sup>3+</sup> ions, which meet the requirements for cutting edge scintillators. The scintillation characteristics of these material systems can be significantly improved by intentional co-doping of divalent Mg<sup>2+</sup> or Ca<sup>2+</sup> ions which results in a substantial reduction of afterglow and TSL signals, a reduction in slow components in the scintillation response, and an improvement of the rise time under pulsed high-energy excitation. The emission and scintillation properties of the above materials will be reviewed and discussed.

### References

- [1] M. Kucera, P. Prusa, LPE-grown thin-film scintillators, in: M. Nikl (Ed.) *Nanocomposite, Ceramic, and Thin Film Scintillators*, Pan Stanford Publ., Singapore, 2017, pp. 155-226.

### Acknowledgments

This work was supported by the Grant Agency of the Czech Republic, project no. 21-17731S.



## Raman spectroscopy of single crystalline films of perovskites

**T. Runka<sup>1</sup>, W. Dewo<sup>1</sup>, V. Gorbenko<sup>2</sup>, Y. Syrotych<sup>2,3</sup>, M. Kaczmarek<sup>3</sup>, Yu. Zorenko<sup>2</sup>**

<sup>1</sup>Faculty of Technical Physics, Institute of Materials Research and Quantum Engineering, Poznan University of Technology, Piotrowo 3, 60-965 Poznań, Poland

<sup>2</sup>Institute of Physics, Kazimierz Wielki University in Bydgoszcz, Powstańców Wielkopolskich 2, 85-090 Bydgoszcz, Poland

<sup>3</sup>Mechatronic Department, Kazimierz Wielki University in Bydgoszcz, Kopernika 1, 85-074 Bydgoszcz, Poland

**E-mail: tomasz.runka@put.poznan.pl**

Ce<sup>3+</sup> doped single crystals (SC) of YAlO<sub>3</sub> and LuAlO<sub>3</sub> perovskites (YAP and LuAP) have become known as scintillators for PET tomography since the 1980's. During the last decade single crystalline films (SCFs) analogues of Ce<sup>3+</sup> and Eu<sup>3+</sup> doped YAP and LuAP [1, 2] and Eu<sup>3+</sup> doped TbAlO<sub>3</sub> (TbAP) perovskites [3] were synthesized using liquid-phase epitaxy (LPE) growth method for application as scintillation screens in microtomography devices.

In this report we present Raman microscopy investigations of Ce<sup>3+</sup> doped of LuAP and YAP SCFs [1] as well as Mn<sup>2+</sup> doped TbAP SCFs [3] grown using LPE method onto undoped YAP substrates. In order to record undisturbed Raman spectra of SCF and YAP substrate, the mentioned epitaxial structures were broken and the spectra of particular parts of the cross-section were measured with 1 μm step. The evolution of Raman spectra and Raman maps recorded for TbAP:Mn SCF/YAP SC, LuAP:Ce SCF/YAP SC and YAP:Ce SCF/YAP SC epitaxial structures allow to detect a distinction between SCFs and the substrates.

Furthermore, evolution of Raman spectra allows also identification of the *mechano-optical effects* in the main volume of TbAP and LuAP SCFs in the respective epitaxial structures. Such effects are connected with the presence of the huge mechanical stress on the SCF/substrate interface with typical thickness 5-8 nm due to very large (up to ±2 %) difference in the lattice constants between SCF and substrate [4]. The propagation of such stress on the main volume of SCFs can cause a gradual change in the cation-anion distances resulting in a notable change of the optical spectra of TbAP and LuAP host lattices including any dopants in them. The gradual change in the peak positions of confocal Raman spectra were observed in LuAG:Ce SCF grown onto YAG SC substrates with SCF/SC misfit of 0.7 % [5]. In the present work, we also observed similar changes in the mechano-optical properties of the TbAP:Mn and LuAP:Ce SCFs, starting from SCF/substrate interfaces towards the main volume of mentioned films. The respective dependencies of the Raman spectra changes on the distance between SCF/substrate interface and point of observation are presented as well allowing numerical estimations of the mechanical stress relaxation in SCF volume.

### References

- [1] Yu. Zorenko and V. Gorbenko, Phys. Solid State 51 (2009) 1800.
- [2] Yu. Zorenko, V. Gorbenko, T. Zorenko, K. Paprocki, F. Riva, P.A. Douissard, T. Martin, Ya. Zhydachevskii, A. Suchocki, A. Fedorov. CrystEngComm, 2018, **20**, 937-945.
- [3] Yu. Zorenko, V. Gorbenko, T. Voznyak, M. Batentschuk, A. Osvet, A. Winnacker. Phys. Stat. Sol. (a), 2010 (207) 967.
- [4] A. Markovskiy, V. Gorbenko, T. Zorenko, T. Yokosawa, J. Will, E. Spiecker, M. Batentschuk, J. Elia, A. Fedorov, Yu. Zorenko. CrystEngComm, 2021 (23) 3212.
- [5] W. Dewo, V. Gorbenko, Yu. Zorenko, T. Runka. Optical Materials X, 2019 (3) 100029.

### Acknowledgments

This work was supported by the research Projects of the Polish Ministry of Education and Science 0511/SBAD/2151 and 2018/31/B/ST8/03390.

## Growth and luminescent properties of Bi<sup>3+</sup>, Tb<sup>3+</sup> and Eu<sup>3+</sup> doped Lu<sub>2</sub>O<sub>3</sub> single crystalline films and composites on their base

V. Gorbenko<sup>1</sup>, P. Veber<sup>2</sup>, M. Velázquez<sup>3</sup>, S. Witkiewicz-Lukaszek<sup>1</sup>, T. Zorenko<sup>1</sup>,  
Yu. Zorenko<sup>1</sup>

<sup>1</sup>Institute of Physics, Kazimierz Wielki University in Bydgoszcz, 85-090 Bydgoszcz, Poland

<sup>2</sup>CNRS, Institut Lumière Matière, Univ. Claude Bernard Lyon 1, 69622 Villeurbanne, France

<sup>3</sup>Univ. Grenoble Alpes, CNRS, Grenoble INP, SIMAP, 38000 Grenoble, France

E-mail: zorenko@ukw.edu.pl

The liquid phase epitaxy (LPE) growth method enables development of luminescent materials in the single crystalline film (SCF) forms based on the different oxide compounds [1]. Nowadays, the LPE technology is also used for creation of the advanced composite luminescent materials based on the SCFs and crystal substrates with the same (homoepitaxy) or close crystalline structure (quasi-homoepitaxy) [2, 3].

The Lu<sub>2</sub>O<sub>3</sub> oxide (Lutetia) has enormous potential applications as a host material for solid-state lasers operating at high average powers [4], scintillating screens for visualization of X-ray images with high spatial resolution [5] as well as for other advanced optoelectronic devices. However, its development is limited by the lack of large sized single crystals with high quality due to very high temperature (2450°C) of Lu<sub>2</sub>O<sub>3</sub> melting point. As compared to the traditional melt growth method (Czochralski, MPD, etc.), the LPE method, based on using low-temperature melt-solution, possesses the unique possibility for producing the high-perfection SCFs of different Lu<sub>2</sub>O<sub>3</sub> based materials [5].

This work presents the first attempt in creation of the composite luminescent materials based on the epitaxial structures of Lutetia. The as-grown undoped and Yb<sup>3+</sup> doped Lu<sub>2</sub>O<sub>3</sub> single crystals (SC) [6] were selected as substrates for the epitaxial growth of Bi<sup>3+</sup>, Eu<sup>3+</sup> and Tb<sup>3+</sup> doped Lu<sub>2</sub>O<sub>3</sub> SCFs. The LPE growth of Lu<sub>2</sub>O<sub>3</sub>:Bi and Lu<sub>3</sub>O<sub>3</sub>:Eu SCFs was performed from the overcooled melt-solutions based on the Bi<sub>3</sub>O<sub>3</sub> flux, whereas the Lu<sub>2</sub>O<sub>3</sub>:Tb and Lu<sub>2</sub>O<sub>3</sub>:Eu SCFs were grown using also PbO-B<sub>2</sub>O<sub>3</sub> flux. We have also perform the LPE growth of Lu<sub>2</sub>O<sub>3</sub>:Eu SCF/Lu<sub>2</sub>O<sub>3</sub>:Bi SCF/Lu<sub>2</sub>O<sub>3</sub>:Yb SC and Lu<sub>2</sub>O<sub>3</sub>:Eu SCF/Lu<sub>2</sub>O<sub>3</sub>:Tb SCF/Lu<sub>2</sub>O<sub>3</sub>:Yb SC epitaxial structures and investigated their properties.

The morphology and structural properties of the SCF samples were characterized using electron microscopy and X ray diffraction. The optical properties of SCFs and epitaxial structures on their base were studied using absorption, cathodoluminescence (CL), photoluminescence (PL) and thermoluminescence (TSL) as well as scintillation LY and decay kinetics under  $\alpha$ -particles excitation (for Lu<sub>2</sub>O<sub>3</sub>:Bi SCFs). The CL and PL spectra of Lu<sub>2</sub>O<sub>3</sub>:Bi, Lu<sub>2</sub>O<sub>3</sub>:Eu and Lu<sub>2</sub>O<sub>3</sub>:Tb SCFs show the dominant Bi<sup>3+</sup>, Eu<sup>3+</sup> and Tb<sup>3+</sup> luminescence in the lutetia host, respectively. The PL spectra of Lu<sub>2</sub>O<sub>3</sub>:Bi SCF/Lu<sub>2</sub>O<sub>3</sub>:Yb SC, Lu<sub>2</sub>O<sub>3</sub>:Eu SCF/Lu<sub>2</sub>O<sub>3</sub>:Yb SC and Lu<sub>2</sub>O<sub>3</sub>:Tb SCF/Lu<sub>2</sub>O<sub>3</sub>:Yb SC composites show the presence of Bi<sup>3+</sup>→Yb<sup>3+</sup>, Eu<sup>3+</sup>→Yb<sup>3+</sup> and Tb<sup>3+</sup>→Yb<sup>3+</sup> energy transfer (ET) processes. Most effective ET in lutetia host is observed for Bi<sup>3+</sup>→Yb<sup>3+</sup> pairs. Furthermore, the cascade Bi<sup>3+</sup>→Eu<sup>3+</sup>→Yb<sup>3+</sup> and Bi<sup>3+</sup>→Eu<sup>3+</sup>→Yb<sup>3+</sup> ET processes are observed in the above mentioned three layered epitaxial structures.

The obtained results can be suitable for development of composite scintillating screens for microtomography, laser media as well as for the cathodoluminescence screens with variable color of lighting.

### References

- [1] Nanocomposite, Ceramic, and Thin Film Scintillators, Pan Stanford Publishing Pte. Ltd.; Nov. 11, 2016.
- [2] S. Witkiewicz-Lukaszek, V. Gorbenko, T. Zorenko, O. Sidletskiy, I. Gerasymov, A. Fedorov, A. Yoshikawa, J. M. Mares, M. Nikl, Y. Zorenko. *Crystal Growth and Design* 18 (2018) 1834.
- [3] S. Witkiewicz-Lukaszek, V. Gorbenko, T. Zorenko, K. Paprocki, O. Sidletskiy, A. Fedorov, R. Kucerkova, J. A. Mares, M. Nikl, Yu. Zorenko. *CrystEngComm* 20 (2018) 3994.
- [4] Y. Yin, G. Wang, Z. Jia, W. Mu, X. Fu, J. Zhang and X. Tao, *CrystEngComm*, 22 (2020) 6569.
- [5] F. Riva, T. Martin, P-A. Douissard, C. Dujardin, C. J. Instrum. 11 (2016) C10010.
- [6] Veber, P., Velázquez, M., Jubera, V., Péchev, S., Viraphong, O., *CrystEngComm*, 13(16) (2011) 5220.

### Acknowledgments

The work was performed in the frame of Polish NCN 2016/21/B/ST8/03200 and 2018/31/B/ST8/03390 projects.

## Investigation of scintillating properties of single crystalline film and composite scintillators based on simple and mixed garnets

**J.A. Mares<sup>1</sup>, M. Nikl<sup>1</sup>, R. Kucerkova<sup>1</sup>, A Beitlerova<sup>1</sup>, V. Gorbenko<sup>2</sup>,  
S. Witkiewicz-Lukaszek<sup>2</sup>, T. Zorenko<sup>2</sup>, Yu. Zorenko<sup>2</sup>**

<sup>1</sup> Institute of Physics AS CR, Cukrovarnicka 10, 162 53 Prague 6, Czech Republic

<sup>2</sup> Institute of Physics, Kazimierz Wielki University in Bydgoszcz, Powstańców Wielkopolskich str., 2,  
85090 Bydgoszcz, Poland

**E-mail: amares@amares.cz**

Nowadays, a large variety of efficient oxide scintillators with high light yield are developed as e.g. BGO, YAP:Ce, LYSO:Ce, LuAG:Ce/Pr, Gd<sub>3</sub>Ga<sub>3</sub>Al<sub>2</sub>O<sub>12</sub>:Ce [1,2]. These scintillators are widely used in advanced equipment's as in computed and positron emission tomography, electromagnetic calorimeters and a lot of other ones [2,3]. A special application is high resolution X-ray imaging radiography which allows to imagine small objects of dimensions around 1 μm [4]. This imaging systems uses very either very thin single crystal plates of ≈ 20 μm thickness or also thin epitaxial films of similar thickness can be used. Preparation of such film scintillators is provided using a liquid phase epitaxy (LPE) growth method [3]. This method enables to grow either single crystalline films (SCF) onto inorganic single crystal substrates as are e.g. YAG, LuAG garnets and mixed garnets (Lu,Y,Gd)<sub>3</sub>(Al,Ga)<sub>5</sub>O<sub>12</sub> (either undoped or doped mainly with Ce<sup>3+</sup>, Pr<sup>3+</sup> or Sc<sup>3+</sup> ions [3,5]). Latest achievement of LPE technology resulted in development of "composite" scintillators consisting one or two SCF scintillators grown onto same substrate-scintillators [2].

This work will present either (i) how to measure and investigate scintillating properties of SCF's or composite scintillators using α- and β-particles and γ-rays excitation (spectroscopy) [5] or (ii) a summary of scintillating properties of selected SCF's and composites scintillators. Namely, we consider the following scintillating properties: N<sub>phels</sub> photoelectron and LY light yields, ER energy resolution, LY nonproportionality and scintillation decays [5]. All properties were measured under α- and β-particles and γ-rays excitation.

Here, we will present and summarize the results of the latest investigation of SCF's and composites scintillators based on the Ce<sup>3+</sup> and Pr<sup>3+</sup> doped YAG and LuAG simple garnets or (Lu,Y,Gd)<sub>3</sub>(Al,Ga)<sub>5</sub>O<sub>12</sub> mixed garnets. Differences between processes under α-/and or β-particles or γ-rays excitation will be discussed.

We will perform also the previous studied of scintillation properties of crystals and films suitable for the creation of composite scintillators using LPE growth method.

### References

- [1] M. Nikl, A. Yoshikawa, K. Kamada, K. Nejezchleb, et al. *Prog. Cryst. Growth Character. Mat.* 59 (2013) 47-72.
- [2] S. Witkiewicz-Lukaszek, V. Gorbenko, T. Zorenko, O. Sidletskiy, et al., *Cryst. Growth Des.* 18 (2018) 1834-1842.
- [3] S. Witkiewicz-Lukaszek, V. Gorbenko, T. Zorenko, K. Paprocki, et al., *Cryst. Eng. Comm.* 20 (2018) 3994-4002
- [4] J. Tous, K. Blazek, M. Kucera, M. Nikl, J. A. Mares, *Rad. Meas.*, 47 (2012) 311-314.
- [5] J.A. Mares, S. Witkiewicz-Lukaszek, V. Gorbenko, T. Zorenko, et al., *Opt. Mat.* 96 (2019) 109268(1-10).

## High pressure studies of Ce<sup>3+</sup> luminescence in epitaxial LuAlO<sub>3</sub> single crystalline film

L.-I. Bulyk<sup>1</sup>, A. K. Somakumar<sup>1</sup>, P. Ciepielewski<sup>1</sup>, Yu. Zorenko<sup>2</sup>,  
Ya. Zhydachevskyy<sup>1</sup>, I. Kudrjajtseva<sup>3</sup>, V. Gorbenko<sup>2</sup>, A. Lushchik<sup>3</sup>, M. G. Brik<sup>3</sup>,  
A. Suchocki<sup>1</sup>

<sup>1</sup>*Institute of Physics, Polish Academy of Sciences, Al. Lotnikow 32/46, 02-668, Warsaw, Poland*

<sup>2</sup>*Institute of Physics, Kazimierz Wielki University in Bydgoszcz, Powstańców Wielkopolskich str., 2, 85-090 Bydgoszcz, Poland.*

<sup>3</sup>*Institute of Physics, University of Tartu, W. Ostwaldi 1, 50411 Tartu, Estonia*

**E-mail: suchy@ifpan.edu.pl**

The results of absorption measurements in near-UV region of YAP and LuAP crystals allowed to establish experimentally accurate value of the band-gap for YAlO<sub>3</sub> crystal at room temperature, which is equal to about 7.6 eV, assuming direct type of band-gap. High temperature luminescence efficiency of YAP:Ce, which thermal quenching begins at temperature of about 650 K, locate the energy difference of the lowest excited 5d level of Ce<sup>3+</sup> 1.58 eV below the bottom of conduction band. This value is affected by the temperature change of the band-gap, i.e. at low temperatures the difference between the energy of 5d level and the bottom of conduction band is larger. This conclusion correlates within the limits of error bars with the with estimations of Dorenbos theory and DFT calculations.

Ce<sup>3+</sup> luminescence quenching is not observed in LuAP crystals up to about 900 K. This is a result of larger band-gap of LuAP as compared with YAP.

The calculated downshift of the 3d energy levels of Ce<sup>3+</sup> versus the energy of in free Ce<sup>3+</sup> from Dorenbos theory does not agree with experimental data. The difference can be reconciled if the down shift is calculated relative to the bandgap energy of YAP and LuAP. This approach also allows correlating observed changes of the energies of 3d states under pressure in LuAP, related to the pressure-induced changes of the average cation-anion distances, assuming that the main changes of the bandgap are due to increase of the bottom energy of conduction band.

The other possibility might be related to proposed in Ref. pressure-induced shift of both 4f and 5d manifolds energies. This effect would led to lack or very little dependence of the 4f ↔ 5d transition energies versus pressure. This is somehow in contradiction to the Dorenbos model and also common expectations that 5d states are more influenced by the ligands than 4f.

We suggest that observed change of the pressure coefficients of the 5d→4f Ce<sup>3+</sup> luminescence bands is associated with pressure-induced structural transitions, occurring in the liquid-phase epitaxy grown layers at pressure of about 10 GPa, and at higher pressures in micro-pulling down crystals. We related that difference with certain unintentional dopants present in the micro-pulled down crystals. Similar changes of pressure coefficients of the Raman modes confirms this hypothesis.

Raman experiments also detect presence of so called “soft mode” in LuAP:Ce crystal, which energy diminished with applied pressure. This is also an additional hint supporting hypothesis about pressure-induced phase transitions observed in examined material.

### References

- [1] S. Mahlik, A. Lazarowska, J. Ueda, S. Tanabe and M. Grinberg, Phys. Chem. Chem. Phys., 2016, 18, 6683.

### Acknowledgments

This work was partially supported by the grant 2018/31/B/ST8/03390 of the Polish National Science Center.

## Development of composite scintillators based on the Ce<sup>3+</sup> doped single crystalline films and single crystals of orthosilicate compounds

**V. Gorbenko<sup>1</sup>, O. Sidletskiy<sup>1,2</sup>, S. Witkiewicz-Lukaszek<sup>1</sup>, T. Zorenko<sup>1</sup>,  
J.A. Mares<sup>3</sup>, M. Nikl<sup>3</sup>, A. Beitlerova<sup>3</sup>, R. Kucerkova<sup>3</sup>, Yu. Zorenko<sup>1</sup>**

<sup>1</sup>*Institute of Physics, Kazimierz Wielki University in Bydgoszcz, 85-090 Bydgoszcz, Poland*

<sup>2</sup>*Institute for Scintillation Materials NAS of Ukraine, 6100 Kharkiv, Ukraine*

<sup>3</sup>*Institute of Physics, Academy of Sciences of Czech Republic, 16200 Prague, Czech Republic*

**E-mail: gorbenko@ukw.edu.pl**

The LPE growth technology enables current development of the advanced composite scintillators based on the epitaxial structures of different oxide compounds. Such composite structures containing crystalline films (SCF) and single crystal (SC) substrates can be used for simultaneous registration of the different components of the mixed ionization fluxes due to the different pass-ways of particles and quanta in the film and bulk scintillation materials. Recently, the possibility of the simultaneous registration of  $\alpha$ -particles and  $\gamma$ -quanta by means of separation of the scintillation decay kinetics of the film and crystal parts of composite scintillators based on the epitaxial structures of garnet compounds has been demonstrated in several our works [1-3].

This our work presents the first attempt in creation of the composite detectors for the simultaneous registration of the mixed ionization fluxes, containing  $\alpha$ - and  $\beta$ -particles and  $\gamma$ -quanta, in the form of the epitaxial structures based on SCFs and SCs of Ce<sup>3+</sup> doped (Y,Lu,Gd)<sub>2</sub>SiO<sub>5</sub> orthosilicate compounds. For this reason, we studied the absorption, luminescent and scintillation properties of the SCFs of Ce doped (Lu<sub>1-x</sub>Y<sub>x</sub>)<sub>2</sub>SiO<sub>5</sub>; x=0.1-0.2 (LYSO:Ce) and (Lu<sub>1-x</sub>Gd<sub>x</sub>)<sub>2</sub>SiO<sub>5</sub>; x=1.0-1.25 (LGSO:Ce) orthosilicates, grown onto undoped Y<sub>2</sub>SiO<sub>5</sub> (YSO) and Ce doped Y<sub>2</sub>SiO<sub>5</sub>:Ce (YSO:Ce) and (Lu<sub>0.9</sub>Y<sub>0.1</sub>)<sub>2</sub>SiO<sub>5</sub>:Ce (LYSO:Ce) SC substrates. YSO, YSO:Ce and LYSO:Ce crystals for preparation of substrates were grown by the Czochralski method at ISMA, Kharkiv, Ukraine. The samples of composite scintillators in the form of YSO:Ce SCF/LYSO:Ce SC, LSO:Ce/ LYSO:Ce, LYSO:Ce SCF/ LYSO:Ce SC and LGSO:Ce SCF/LYSO:Ce epitaxial structures were crystallized using the LPE method from a melt-solution based on PbO-B<sub>2</sub>O<sub>3</sub> oxide at Institute of Physics UKW in Bydgoszcz, Poland.

The influence of high-temperature annealing on the scintillation properties of the obtained epitaxial structures was investigated. The possible ways to improve the scintillation properties of the SCF and SC of orthosilicate compounds for their use as components of composite detectors are discussed.

### References

- [1] S. Witkiewicz-Lukaszek, V. Gorbenko, T. Zorenko, O. Sidletskiy, I. Gerasymov, A. Fedorov, A. Yoshikawa, J. M. Mares, M. Nikl, Y. Zorenko. *Crystal Growth and Design* 18 (2018) 1834-1842.
- [2] S. Witkiewicz-Lukaszek, V. Gorbenko, T. Zorenko, K. Paprocki, O. Sidletskiy, A. Fedorov, R. Kucerkova, J. A. Mares, M. Nikl, Yu. Zorenko. *CrystEngComm* 20 (2018) 3994-4002.
- [3] S. Witkiewicz-Lukaszek, V. Gorbenko, T. Zorenko, Y. Syrotych, R. Kucerkova, J. A. Mares, M. Nikl, O. Sidletskiy, A. Fedorov, S. Kurosawa, K. Kamada, A. Yoshikawa, Yu. Zorenko *Materials Science @ Engineering B*. 2021, 264 (114909).

### Acknowledgments

The work was performed in the frame of Polish NCN 2018/31/B/ST8/03390 projects and Czech OP RDE&MEYS Project No. SOLID21 CZ.02.1.01/0.0/0.0/16\_019/0000760.

## Optical and magnetic properties of epitaxially grown GaN:Ge(Si) thin films

**M. Buryi<sup>1</sup>, V. Babin<sup>1</sup>, Z. Remeš<sup>1</sup>, T. Hubáček<sup>1</sup>, V. Jarý<sup>1</sup>**

<sup>1</sup>*Institute of Physics CAS, Cukrovarnicka 10, 162 00 Prague, Czech Republic*

**E-mail: buryi@fzu.cz**

Since the invention of the first blue light emitting diodes (LED) using InGaN/GaN multiple quantum well (MQW) structures, new generations of the LED-based solid-state light sources were designed [1]. Relatively recently, the InGaN/GaN heterostructures have been considered as potentially interesting fast scintillators [2] since they exhibit excellent scintillating performance including subnanosecond scintillation decay time due to exciton emission. Therefore, the InGaN/GaN MQW can be implemented in e.g., time-of-flight positron emission tomography (TOF-PET). The faster the exciton emission is, the higher apparatus sensitivity can be reached and subsequently the coincidence time resolution of the TOF-PET can be improved [3]. On the other hand, the strong drawback of the GaN-based structures is the presence of slow defect-related bands.

To understand the processes occurring in MQW structures, we present the detailed study of MOVPE (Metal Organic Vapour Phase Epitaxy) grown GaN layers doped with Si or Ge. This study includes the measurements of optical absorption, scintillation decay kinetics, luminescence (radio-, photo- and thermally stimulated luminescence, RL, PL and TSL, respectively) as well as magnetic properties (studied by electron paramagnetic resonance, EPR). The representative luminescence spectra are composed of two bands. The narrow and fast band peaking at about 360 nm is ascribed to excitons and the broad and slow band with the maximum at about 570 nm is produced by defects. It has been found that the exciton and defect emission maxima and amplitudes are sensitive to the doping level of Si or Ge. Moreover, the defect band amplitude is sensitive to the intensity of the excitation light evidencing trapping of charge carriers confirmed also by TSL. Interestingly, the effect similar to cyclotron resonance was observed by means of EPR.

Basing on the presented results one may conclude that the addition of Si or Ge can govern the defect-related luminescence improving the exciton-related band.

### References

- [1] S. Nakamura, M. Senoh, S. Nagahama, N. Iwasa, T. Yamada, T. Matsushita, H. Kiyoku, Y. Sugimoto, *Jpn. J. Appl. Phys., Part 2* 35 (1996) L74.
- [2] P. Pittet, G. N. Lu, J. M. Galvan, J. M. Bluet, A. Ismail, J. Y. Giraud, J. Balosso, *Opt. Mater.* 31 (2009) 1421.
- [3] A. Hospodková, M. Nikl, O. Pacherová, J. Oswald, P. Brůža, D. Pánek, B. Foltynski, E. Hulicius, A. Beitlerová, M. Heuken, *Nanotechnology* 25 (2014) 455501.

### Acknowledgments

This work was supported by the Czech Science Foundation project No. 20-05497Y and the Operational Programme Research, Development and Education financed by European Structural and Investment Funds and the Ministry of Education, Youth and Sports of *Czech Republic* under project No. SOLID21 CZ.02.1.01/0.0/0.0/16\_019/0000760.

## Scintillation mechanisms in II-VI semiconductor nanostructures

Z. Meng<sup>1</sup>, B. Mahler<sup>1</sup>, J. Houel<sup>1</sup>, G. Ledoux<sup>1</sup>, F. Kulzer<sup>1</sup>, A. Vasil'ev<sup>2</sup>, C. Dujardin<sup>1</sup>

<sup>1</sup>*Institut Lumière Matière, UMR5306 Université Lyon 1-CNRS, Université de Lyon, 69622  
Villeurbanne cedex, France*

<sup>2</sup>*Skobeltsyn Institute of Nuclear Physics, Lomonosov Moscow State University, 119991 Moscow,  
Russia*

**E-mail: christophe.dujardin@univ-lyon1.fr**

When suitably synthesized, II-VI semiconductor-based nanocrystals are known to show very good optical quantum yields. As direct band gap semiconductors they also exhibit a rather fast excitonic emission in the order of a few tens of ns. In addition, because of their reduced size, multiple excitation generation is favoured, resulting in a significantly faster emission which can be attractive for the scintillation field. Nevertheless, the stopping power for X-ray and gamma-ray requires to handle materials in bulky form or to implement strategies with hybrid materials. As an illustration a CdSe nanoplatelets layer deposited on Lu<sub>2</sub>SiO<sub>5</sub>Ce<sup>3+</sup> single crystal, and the energy sharing has demonstrated a coincidence time resolution improvement [1], a crucial parameter for time of flight positron emission tomography. Nevertheless, the use of CdSe at very high concentration (as well as for other direct band gap semi-conductors) is severely facing the self-absorption issue due to a small Stokes shift, leading to a decrease of the light extraction efficiency. Because a shell is generally required to obtain a good optical quantum yield, one strategy to overcome the self-absorption issue, is to drastically increase the shell thickness, allowing increasing the stopping power of the media while keeping constant the amount of emitting centers and thus the self-absorption. The shell acts in this case as a collector for the ionising radiation and do not contribute to the self-absorption. On the opposite it reduces the confinement effect and may induce defects at large sizes. In addition, Geant4-based Monte Carlo simulations have demonstrated in the frame of X-rays induced photodynamic therapy, that hybrid media including nanoscintillators experience a complex energy deposition mechanism in the nanostructures [2].

Therefore, exploring nanocrystal-based materials in a large variety of morphology and size is of high interest to describe the underlying physics of the energy deposition and relaxation processes under ionizing radiation in nanoscintillators. In this contribution, we present the case of CdSe/CdS based spherical quantum wells, nanoplatelets as core crown, core shell and core crown shell, and discuss the comparison of optical response under intense optical excitation, x-ray excitation as compared to simulations of energy relaxation.

### References

- [1] Turtos, R. M., Gundacker, S., Omelkov, S., Mahler, B., Khan, A. H., Saaring, J., Meng, Z., Vasil'ev, A., Dujardin, C., Kirm, M., Moreels, I., Auffray, E., & Lecoq, P. (2019). On the use of CdSe scintillating nanoplatelets as time taggers for high-energy gamma detection. *Npj 2D Materials and Applications*, 3(1), 37.
- [2] Bulin, A.-L., Vasil'ev, A., Belsky, A., Amans, D., Ledoux, G., & Dujardin, C. (2015). Modelling energy deposition in nanoscintillators to predict the efficiency of the X-ray-induced photodynamic effect. *Nanoscale*, 7(13), 5744–5751.

## **Scintillation properties of advanced nanocomposite materials**

**I. Villa**<sup>1</sup>

<sup>1</sup> *FZU Institute of Physics, Academy of Sciences of the Czech Republic, Prague – Czech Republic*

**E-mail: villa@fzu.cz**

Many radiation detectors work by recording the light pulses produced by the interaction of ionizing radiation with a luminescent material, i.e. the scintillator. Recently, a new class of hybrid nanoscintillators embedded in polymeric matrix has come into the spotlight as alternative to the traditional bulk crystals and plastic scintillators for affordable and reliable detectors for ionizing radiation in medical diagnostics, nuclear control, and high-energy physics. These composites are made up by high-Z elements to stop the ionizing radiation and highly emissive organic dyes to obtain systems presenting high interaction with ionizing radiation, efficient scintillation, fast emission lifetime, and reduction of self-absorption effect. In nanocomposites, the factors affecting the quantum efficiency and timing qualities of the scintillation can be controlled by the choice of composition, dimension, and timing/luminescence performances of the individual components. Especially for medical imaging, these advanced materials are evaluated to reach the long-time desired ultra-high time resolution of 10 ps, crucial for early-stage oncological diagnosis.

I present here the most recent results obtained on two classes of hybrid scintillators. In one case, the nanocomposite is based on crystalline metal-organic frameworks (MOFs) consisting of metal clusters linked by coordinating organic groups.<sup>1</sup> Highly emissive MOF nanocrystals based on zirconium oxo-hydroxy clusters as heavy nodes and scintillating ligands of 9,10 diphenylanthracene have been embedded in a polymeric/elastomer matrix. The peculiarity of nodes-ligands distance in the framework enables the fast sensitization of the dye emission by energy transfer, avoiding the problems typical of multicomponent systems regarding the managing of two complementary components. As a result of prompt sensitization, the prototype nanocomposite devices fabricated show a scintillation response in the tens of picoseconds time scale. In the other case, the composite is fabricated exploiting CsPbBr<sub>3</sub> perovskite scintillating nanocrystals.<sup>2</sup> Embedded in the polymeric host, the high-Z nanocrystals are conjugated to an organic dye with large Stokes shift and fast emission lifetime in the red spectral region. The experiment performed display an effective sensitization of the fast dye emission (~3.4 ns) under ionizing radiation without reabsorption effects. An efficient radioluminescence, comparable to that of commercial-grade inorganic and plastic scintillators, demonstrates the possibility to use CsPbBr<sub>3</sub> perovskite nanocrystals to detect high-energy photons and charged particles with nearly no reabsorption losses for large-size devices.

These findings are of great importance in the search of fast scintillating materials and pave the way to the use of hybrid scintillators nanocomposites in a broad range of applications.

### **References**

- [1] J. Perego et al., *Nature Photonics*, (2021) 1-8.
- [2] M. Gandini et al., *Nature Nanotechnology*, 15(6) (2020) 462-468.



## The role of Cs<sub>4</sub>PbBr<sub>6</sub> phase in the luminescence performance of bright CsPbBr<sub>3</sub> nanocrystals

K. Děcká<sup>1,2</sup>, A. Suchá<sup>1</sup>, J. Král<sup>1</sup>, I. Jakubec<sup>3</sup>, M. Nikl<sup>2</sup>, V. Jarý<sup>2</sup>, V. Babin<sup>2</sup>, V. Čuba<sup>1</sup>,  
E. Mihóková<sup>1,2</sup>

<sup>1</sup>Department of Nuclear Chemistry, Faculty of Nuclear Sciences and Physical Engineering, Czech Technical University in Prague, Břehová 7, 115 19 Prague 1, Czech Republic

<sup>2</sup>Institute of Physics, Czech Academy of Sciences, Cukrovarnická 10, 162 00 Prague 6, Czech Republic

<sup>3</sup>Institute of Inorganic Chemistry, Czech Academy of Sciences, Husinec-Řež č.p. 1001, 250 68 Řež, Czech Republic

E-mail: mihokova@fzu.cz

Nanocrystals of cesium lead halide perovskites CsPbX<sub>3</sub> (X=Cl, Br, I) are currently extensively studied as highly promising material for various applications, in particular for solar cells [1], LEDs [2] or displays [3]. Due to their excellent luminescence properties, such as high quantum efficiency, narrow emission lines and fast decay they also appear as prospective candidates for building up a scintillation detector.

CsPbBr<sub>3</sub> nanocrystals feature bright green luminescence. Similar bright emission was also found in nominally pure Cs<sub>4</sub>PbBr<sub>6</sub> crystals [4,5]. First, it soon triggered a debate on its origin in these crystals. One group of authors supported the idea that it is due to CsPbBr<sub>3</sub> nanoinclusions that are nonetheless present in Cs<sub>4</sub>PbBr<sub>6</sub> crystals [6]. Another group of authors proposed the luminescence is due to point defects in the Cs<sub>4</sub>PbBr<sub>6</sub> structure [7]. Second, depending on the method of synthesis of CsPbBr<sub>3</sub> nanocrystals, the prepared material can, besides the CsPbBr<sub>3</sub> phase, also contain the Cs<sub>4</sub>PbBr<sub>6</sub> phase. Therefore, it is essential to understand how the presence of Cs<sub>4</sub>PbBr<sub>6</sub> phase can affect the luminescence and scintillation performance of CsPbBr<sub>3</sub> nanocrystals.

In this work we intend to contribute to both issues above. We synthesize CsPbBr<sub>3</sub> nanocrystals by two methods. The hot injection method provides high quality, pure CsPbBr<sub>3</sub> nanocrystals, while the supersaturation recrystallization method results in various mixtures of both CsPbBr<sub>3</sub> and Cs<sub>4</sub>PbBr<sub>6</sub> phases. We study the luminescence properties of the samples, namely photoluminescence, radioluminescence, including decay kinetics, with respect to their composition, structure and morphology. We compare and evaluate samples prepared by different methods in view of possible future applications.

### References

- [1] M. Kulbak et al., *Journal of Physical Chemistry Letters* 7 (2016) 167-172.
- [2] Y. H. Song et al., *Nanoscale* 8 (2016) 19523-19526.
- [3] A. Swarnkar et al., *Angewandte Chemie - International Edition* 54 (2015) 15424-15428.
- [4] M. I. Saidaminov et al., *ACS Energy Letters* 1 (2016) 840-845.
- [5] Y. Zhang et al., *ACS Nano* 13 (2019) 2520-2525.
- [6] F. Cao et al., *The Journal of Physical Chemistry C* 125 (2021) 3-19.
- [7] J. H. Cha et al., *ACS Energy Letters* 5 (2020) 2208-2216.

### Acknowledgments

This work was supported by the Czech Science Foundation, Grant No. GA20-06374S.

## **Modification of optical properties of the GaN nanostructures via annealing in various atmospheres**

**V. Jarý<sup>1</sup>, M. Buryi<sup>1</sup>, V. Babin<sup>1</sup>, Z. Remeš<sup>1</sup>, T. Hubáček<sup>1</sup>**

<sup>1</sup>*Institute of Physics CAS, Cukrovarnicka 10, 162 00 Prague, Czech Republic*

**E-mail: jary@fzu.cz**

Gallium nitride is a wide band gap semiconductor with the  $E_g = 3.39$  eV at room temperature and the InGaN/GaN quantum wells (QWs) are widely used in modern light-emitting diodes and lasers as the active region because of their surprisingly high luminous efficacy especially in the blue region of visible spectrum [1,2]. Recently, InGaN/GaN heterostructures have become interesting for scintillating applications as well, mainly due to high excitonic binding energy leading to a sub-nanosecond decay time, high density ( $6.15 \text{ g/cm}^3$ ), high radiation resistance, perfect temperature and chemical stability, feasibility of tuning emission wavelength and the availability of MOVPE (metal-organic vapour phase epitaxy) technology for growing high crystallographic quality layers [3,4]. Therefore, the InGaN/GaN can be implemented in the time-of-flight techniques, e.g., in TOF-PET (positron emission tomography). On the other hand, the strong drawback of the GaN-based structures is the limited thickness of the multiple quantum wells active region which significantly restricts detection efficiency, and the slow defect-related band, origin of which in bulk GaN and InGaN/GaN MQW structures is still under consideration [5,6].

To understand better the processes occurring in the MQW structures we propose the detailed study of Ge- and Si-doped GaN epitaxial layers prepared by MOVPE technology. We will focus on sample characterization by means of absorption spectroscopy, time-resolved luminescence/scintillation spectroscopy and electrically detected magnetic resonance (EDMR). Special attention will be given to photoluminescence excitation and emission spectra, photoluminescence decay curves under various excitations together with their temperature dependences (8 – 800 K temperature range), time-resolved radioluminescence spectra with the time resolution below 100 ps, wavelength-resolved thermally stimulated luminescence and EDMR spectra. Furthermore, the most promising samples will be consequently annealed in various atmospheres (those being  $\text{H}_2$ ,  $\text{N}_2$ ,  $\text{NH}_3$ ) and different temperature regimes. Influence of applied annealing on optical, scintillation and magnetic characteristics of samples under consideration will be investigated thoroughly.

Based on the combination of presented results, we will conclude the effect of Ge and Si-doping in GaN-based heterostructures and annealing in different atmospheres on the properties of defect-related luminescence.

### **References**

- [1] Y. Narukawa et al. *J. Phys. D: Appl. Phys.* 43(35), 2010, 354002.
- [2] S. Nakamura et al. *Jpn. J. Appl. Phys.* 35, 1996, L74.
- [3] V. Jarý et al. *IEEE Transactions on Nuclear Science* 67(6), 2020, 974-977.
- [4] T. Hubáček et al. *CrystEngComm* 21(2), 2019, 356 - 362.
- [5] D. O. Demchenko et al. *Phys. Rev. Lett.* 110, 2013, 087404.
- [6] R. Seitz et al. *J. Cryst. Growth* 189–190, 1998, 546.

### **Acknowledgments**

This work was supported by the Czech Science Foundation project No. 20-05497Y and the Operational Programme Research, Development and Education financed by European Structural and Investment Funds and the Ministry of Education, Youth and Sports of Czech Republic under project No. SOLID21 CZ.02.1.01/0.0/0.0/16\_019/0000760.

## The influence of precursor ratio in the Cd-Zn-S quantum dots synthesis on their morphological and optical properties

**M. Chylii<sup>1</sup>, L. Loghina<sup>1</sup>, A. Kaderavkova<sup>1</sup>, M. Vlcek<sup>1</sup>**

<sup>1</sup> Center of Materials and Nanotechnologies, Faculty of Chemical Technology, University of Pardubice, nam. Cs. legii 565, Pardubice 53002, Czech Republic

**E-mail: Maksym.Chylii@upce.cz**

Presently, chalcogenide semiconductor quantum dots (QDs) have found the application in many areas of science and technology due to their unique optical properties. QDs are used as biological labels [1], components in LEDs and displays [2, 3], photo- and high-energy quanta detectors [4, 5], *etc.* The optical properties of QDs strongly depend on the size- and shape uniformity of QDs which can be reached by synthetic methods.

Here we report a study of the effect of the precursors' ratios within the synthesis of Cd-Zn-S QDs series. In the synthesis of Cd<sub>0.2</sub>Zn<sub>0.8</sub>S QDs (Cd, Zn : S molar ratios = 1 : 0.5; 1 : 1; 1 : 1.5; 1 : 2; 1 : 2.5) and Cd<sub>x</sub>Zn<sub>1-x</sub>S QDs (where x = 0.1; 0.25; 0.5; 0.75; 0.9) the N, N', N' - trisubstituted thiourea (N-phenylmorpholine-4-carbothioamide) as a new and environmentally friendly source of sulphur has been investigated. Increasing the molar ratio of N, N', N' - trisubstituted thiourea to metals in the synthesis of QDs leads to the growth of their sizes and small emission's redshift. However, no significant changes in the elemental ratio in the material were detected. The main effect was observed in photoluminescence decay of Cd<sub>0.2</sub>Zn<sub>0.8</sub>S QDs. With the rising of the sulphur molar ratio, the average decay time reduced from 11 to 0.1 ns which can be caused by sulphur surface passivation and the numbers of surface defects reductions of Cd<sub>0.2</sub>Zn<sub>0.8</sub>S QDs.

In the case of decreasing the Zn to Cd ratio in Cd<sub>x</sub>Zn<sub>1-x</sub>S QDs, the maximum of the emission was shifted to the red region of the spectrum, and an increase in the size of QDs was observed. Based on the XRD data, a gradual transition from a cubic to a hexagonal crystal structure was detected. Through the changing of crystal structure grows the number of defects into Cd<sub>x</sub>Zn<sub>1-x</sub>S QDs, which leads to the significant transformation of photoluminescence decay curves. The average decay time was reduced from 5.9 to 0.1 ns with the increase of the Cd content in Cd<sub>x</sub>Zn<sub>1-x</sub>S QDs from 10 to 90%, respectively.

In conclusion, obtained Cd-Zn-S QDs possess the narrow photoluminescence signal (FWHM < 31 nm), high quantum yield (up to 70 %), fast decay time, and well size uniformity which make them promising materials for high-sensitive sensors and LEDs production.

### References

- [1] O. Adegoke, M.W. Seo, T. Kato, et al., *J. Mater. Chem. B*, 4 (2016) 1489–1498.
- [2] T. Lee, D. Hahm, K. Kim, et al., *Small*, 15 (2019) 1905162.
- [3] H. Kang, S. Kim, J.H. Oh, et al., *Adv. Opt. Mater.*, 6 (2018) 1701239.
- [4] H.X. Chuo, T.Y. Wang, W.G. Zhang, *J. Alloys Compd.*, 606 (2014) 231–235.
- [5] C. Liu, Z. Li, T.J. Hajagos, et al., *ACS Nano*, 11 (2017) 6422–6430.

### Acknowledgments

Authors appreciate the financial support from the project “High-sensitive and low-density materials based on polymeric nanocomposites” - NANOMAT (No. CZ.02.1.01/0.0/0.0/17\_048/0007376) and grant LM2018103 from the Ministry of Education, Youth and Sports of the Czech Republic.

## Radio- and photo- luminescence of ZnO nanoparticles with different morphologies and functionalization

**R. Crapanzano<sup>1</sup>, I. Villa<sup>1,†</sup>, S. Mostoni<sup>1,2</sup>, M. D'Arienzo<sup>1,2</sup>, B. Di Credico<sup>1,2</sup>, M. Fasoli<sup>1</sup>, R. Lorenzi<sup>1</sup>, R. Scotti<sup>1,2</sup>, A. Vedda<sup>1</sup>**

<sup>1</sup>Department of Materials Science, University of Milano - Bicocca, Via Cozzi 55, 20125, Milano, IT

<sup>2</sup>INSTM, University of Milano - Bicocca, Via Cozzi 55, 20125 Milano, IT

<sup>†</sup>Now at FZU Institute of Physics of the Czech Academy of Science, Cukrovarnicka 10/112, 16200 Prague, CZ

E-mail: Maksym.Chylii@upce.cz

ZnO is a wide band gap semiconductor ( $E_g = 3.37$  eV) with a large excitonic binding energy (60 meV) [1], that is mostly applied in optoelectronics, photonics, sensing, catalysis, and nanomedicine [2,3]. ZnO biocompatibility together with the anti-inflammatory and anti-cancer activities paved the way for medical applications [4]. ZnO-based optical devices exploit its near-UV excitonic emission, stable even at room temperature, and its VIS defect-related bands. However, the identification of the defects responsible for ZnO luminescence is controversial [2].

This work explores the role of different excitations, from optical sources to ionizing radiation, on the luminescence of ZnO nanoparticles (NPs) including the effects of different morphologies (by changing NPs synthetic approach and thus their size and surface chemistry). The luminescence of NPs functionalized by porphyrin was also investigated.

The optical properties of isolated ZnO NPs of 5 and 22 nm diameter, synthesized by hot injection method, were investigated by both radio- (RL) and photoluminescence (PL) and compared to those of ZnO NPs of 5 nm diameter, synthesized by sol-gel process and grown onto silica NPs with both spherical and rod-like shape. The spectral analysis of the luminescence features discloses the presence of one UV excitonic peak at 3.27 eV and four VIS defect-related components (at 1.83, 2.29, 2.68, and 3.05 eV) whose relative intensities vary with the excitation energies and the material parameters, unveiling the possibility of engineering ZnO luminescence by tuning synthesis conditions and size.

ZnO NPs grown onto spherical silica surface were functionalized with different porphyrin content (from 0.1 wt% to 1 wt%). The PL analysis reveals that non-radiative energy transfer is absent, while a weak radiative one occurs. Differently, porphyrin emission is hugely enhanced under X-rays irradiation thanks to the augmented energy deposition, caused by the NPs close proximity. Hence, functionalized ZnO NPs are interesting platforms for anti-cancer therapies and imaging that exploit ionizing radiation.

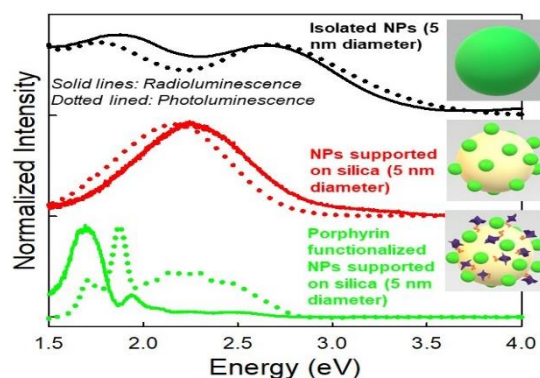


Figure 1: Normalized radio- and photoluminescence (excitation energy 3.7 eV) of ZnO NPs. Insets: Sketches of studied ZnO NPs.

### References

- [1] Ü. Özgür, et al, *J. Appl. Phys.* 2005, 98, 1-103.
- [2] R. Crapanzano, et al, *Nanomaterials* 2020, 10, 1-19.
- [3] M. D'Arienzo, et al, *J. Phys. Chem. C* 2019, 123, 21651-21661.
- [4] P. K. Mishra, et al, *Drug Discov. Today* 2017, 22, 1825-1834.

## **Electron and hole trapping in wide band-gap oxide scintillation crystals**

**V. Laguta<sup>1</sup>, M. Buryi<sup>1</sup>, M. Nikl<sup>1</sup>**

<sup>1</sup> *Institute of Physics AS CR, Cukrovarnicka 10, 16253 Prague, Czech Republic*

**E-mail: laguta@fau.cz**

Charge carriers trapping phenomenon and related lattice defects in solid states are important tasks of the physics of luminescence and scintillation materials. These tasks are especially actual for scintillating materials which are widely used as a convertor transforming the energy of ionizing radiation photons or high-energy particles into UV/visible light. Dielectric or semiconductor wide band-gap oxide materials of high degree of structural perfection are the most suitable for such a purpose. They must accomplish the fast and efficient transformation of energy of incoming photons/particles in a number of electron-hole pairs collected in the conduction and valence bands, respectively, and their radiative recombination at suitable luminescence centers. However, before the radiative recombination, the migrating electrons and holes (eventually created excitons) can be trapped at a lattice defect or even selftrapped leading potentially to marked decrease in the scintillation performance. Therefore, monitoring of electron/hole trapping states in a scintillator material and revealing the nature of corresponding lattice defects is of crucial importance for further optimization of this entire family of scintillators.

It is the aim of this report to present selected results of Electron Paramagnetic Resonance and Thermally Stimulated Luminescence study of various trapped-electron and trapped-hole centers which participate in the processes of charge carriers transfer and capture in the family of practically important complex oxide single crystal scintillators based on yttrium/lutetium garnets [1,2] and yttrium/lutetium pyrosilicates and oxyorthosilicates [3]. Particular attention is paid to the most natural defects inevitably present or created by radiation in oxide materials, such as self-trapped electron and hole states (small and bond small polarons), anion and cation vacancies (F<sup>+</sup> color centers). Current understanding of the nature of charge trapping states, mechanisms of their creation and their role in scintillation mechanism in oxide luminescence and scintillation materials will be discussed.

### **References**

- [1] V. Laguta, M. Buryi, J. Pejchal, V. Babin, M. Nikl, *Phys. Rev. Appl.* 10 (2018), 034058.
- [2] V. Laguta, M. Buryi, P. Arhipov, et al., *Phys. Rev. B* 101 (2020), 024106.
- [3] V. Laguta, M. Buryi, Y. Wu, G. Ren, M. Nikl, *Phys. Rev. Appl.* 13 (2020) 044060.

### **Acknowledgments**

This work was supported by the Czech Science Foundation under project No. 20-12885S.

## Detection of uncatchable oxygen interstitials in neutron-irradiated corundum crystals

**A. Lushchik<sup>1</sup>, V. Seeman<sup>1</sup>, E. Shablonin<sup>1</sup>, E. Vasil'chenko<sup>1</sup>, E.A. Kotomin<sup>2</sup>,  
V.N. Kuzovkov<sup>2</sup>, A.I. Popov<sup>2</sup>**

<sup>1</sup>*Institute of Physics, University of Tartu, W. Ostwald Str. 1, 50411 Tartu, Estonia*

<sup>2</sup>*Institute of Solid State Physics, University of Latvia, Kengaraga 8, Riga LV-1063, Latvia*

**E-mail: [aleksandr.lushchik@ut.ee](mailto:aleksandr.lushchik@ut.ee)**

Sufficient tolerance to harsh radiation environment is an important requirement that limits the range of wide-gap materials suitable for technological applications. Along with the use of corundum as laser media, dosimeters, scintillators and various components in fission-based nuclear energetics,  $\alpha$ -Al<sub>2</sub>O<sub>3</sub> single crystals and polycrystalline transparent ceramics are in the short list of promising optical window materials for projected D-T fusion devices.

By the modern concept, material radiation resistance mainly depends on the accumulation of stable lattice defect, primary interstitial-vacancy Frenkel pairs and their aggregates. Under fast neutron irradiation, primary structural defects are solely formed via the displacement (collision, impact) mechanism – elastic collisions of incident neutrons with material nuclei. Although Frenkel defects containing oxygen-vacancy ( $F^+$  and  $F$  centers – one or two electrons trapped by a vacancy) were thoroughly studied, the complementary defect – a single oxygen interstitial still remained the most hidden primary defect in wide-gap metal oxides

Using the EPR method, for the first time we have succeeded to reveal a single oxygen interstitial in irradiated corundum single crystals ( $6.9 \times 10^{19} \text{ n/cm}^2$ ). This interstitial does not contain any other imperfect/defect in its close vicinity and forms a chemical bonding with a regular oxygen ion. The EPR-determined structure of this single interstitial – a superoxide ion  $O_2^-$  that occupies one regular oxygen site along  $a$  axis and is stabilized by a trapped hole – is in line with the results of advanced DFT calculations (see also [1]).

Additional information on the origin/structure of point defects could be obtained by studying the radiation damage recovery via a consequent comparative thermal annealing (under the same conditions) of the EPR signals and induced optical absorption [1, 2]. In particular, a tentative absorption band (elementary Gaussian peaked at 5.6 eV) connected with the  $O_2^-$  defect (related with a charged interstitial  $O$ ) has been revealed in a neutron-irradiated  $\alpha$ -Al<sub>2</sub>O<sub>3</sub>. Note that just interstitials are the mobile component determining the mutual recombination of interstitial-vacancy Frenkel pairs. Applying a new theoretical analysis of the optical absorption annealing kinetics, we have demonstrated for the first time the co-existence of two interstitial types – neutral  $O$  atoms and negatively charged  $O^-$  ions (absorption bands at 6.5 eV and 5.6 eV, respectively) and have obtained their diffusion parameters, necessary for the prediction of secondary defect-induced reactions and defect stability.

### References

- [1] V. Seeman, A. Lushchik, E. Shablonin et al., *Sci. Reports* 10 (2020) 15852.
- [2] E. Shablonin, A.I. Popov, G. Prieditis et al., *J. Nucl. Mater.* 543 (2021).

### Acknowledgments

This work has been carried out within the framework of the EUROfusion Consortium and has received funding from the Euratom research and training programme 2014-2018 and 2019-2020 under grant agreement No. 633053. The views and opinions expressed herein do not necessarily reflect those of the European Commission.

## Fine structure of 4f-5d absorption spectra of MeF<sub>2</sub>-Yb<sup>3+</sup> in the vacuum ultraviolet region under synchrotron excitation

**E. Radzhabov<sup>1</sup>, R. Shendrik<sup>1</sup>, V. Pankratov<sup>2</sup>, K. Cherenenko<sup>3</sup>**

<sup>1</sup> Institute of Geochemistry SB RAS, Favorskii St. 1a, 664033 Irkutsk, Russian Federation

<sup>2</sup> Institute of Solid State Physics, University of Latvia, 8 Kengaraga iela, LV-1063 Riga, Latvia

<sup>3</sup> MAX IV Laboratory, Lund University, PO BOX 118, SE-221 00 Lund, Sweden

E-mail: eradzh@igc.irk.ru

The absorption (excitation) spectra of 4f – 5d interconfiguration transitions of trivalent lanthanide ions at low temperatures exhibit a fine structure that is more pronounced in low-energy bands [1-3]. At room temperature, the structure of the bands disappeared, leaving wide absorption bands [1].

In this work, we studied the 4f-5d absorption (excitation) spectra of Yb<sup>3+</sup> ions in alkaline-earth fluoride crystals with a resolution of 0.01 nm. The crystals were grown in the Institute of Geochemistry SB RAS. Spectra were measured at 7 K on the photoluminescence endstation *FINESTLUMI* of the FinEstBeAMS undulator beamline at 1.5 GeV storage ring of MAX IV synchrotron facility (Lund, Sweden) [4].

In alkaline-earth fluoride crystals with a double activation of Yb<sup>3+</sup>-Er<sup>3+</sup> ions, broad excitation bands of 4f-5d transitions of Er<sup>3+</sup> ions emitting in the green and red spectral regions were observed in the vacuum ultraviolet region of 8-11 eV. Against the background of the excitation spectrum, we found narrow spectral holes, which can be compared with lines of 4f-5d transitions in Yb<sup>3+</sup> ions. The observed spectral hole lines in the excitation spectrum can be converted to the absorption lines of Yb<sup>3+</sup> ions.

Two groups of lines are observed in the absorption spectrum of MeF<sub>2</sub>-0.1%Er-0.1%Yb. The halfwidth of some lines is near 0.005 eV (~40 cm<sup>-1</sup>). The energy range 8.5–9.3 eV refers to the first absorption band of Yb<sup>3+</sup> 4f-5d(e<sub>g</sub>), and transitions above 9.5 eV belong to the second band of 4f-5d(t<sub>2g</sub>). The shift of the spectrum toward high energies in the row of CaF<sub>2</sub>-SrF<sub>2</sub>-BaF<sub>2</sub> is due to a decrease in the crystal field strength and, accordingly, a decrease in the 5d (t<sub>2g</sub>-e<sub>g</sub>) splitting in this series. The positions of the absorption lines in CaF<sub>2</sub>-0.1Yb-0.1Er are in good agreement with the lines in the spectrum of CaF<sub>2</sub>-0.05 Yb<sup>3+</sup> [2], with the exception that the lines of 4f-5d transitions we measured with higher spectral resolution.

The small width of the absorption lines of the 4f-5d transitions of Yb<sup>3+</sup> in all alkaline-earth fluorides confirms the assumption [3] about the strong screening of 5d states by the states of 5p<sup>6</sup>, 6s<sup>2</sup> shells.

### References

- [1] Schlesinger, M., Szczurek, T., *Physical Review*, B 8 (1973) 2367- 2368.
- [2] Szczurek, T., Schlesinger, M., In *Proc. Rare Earths Spectrosc. Symp.*, (1985) 309-330.
- [3] Schlesinger, M., Szczurek, T., Wade, M. K., Drake, G. W. F., *Physical Review B*, 18 (1978) 6388-6390.
- [4] Pankratov, V., Kotlov, A., *Nuclear Instruments and Methods in Physics Research Section B: Beam Interactions with Materials and Atoms*, 474 (2020) 35-40.

## Gadolinium-aluminum-gallium garnet single crystals with partial substitution of gallium with aluminum and their optical characterization

**E. Zabelina<sup>1</sup>, N. Kozlova<sup>1</sup>, V. Kasimova<sup>1</sup>, D. Spassky<sup>2,3</sup>, O. Buzanov<sup>4</sup>, P. Lagov<sup>1,5</sup>, Y. Pavlov<sup>5</sup>, T. Kulevoy<sup>6</sup>, V. Stolbunov<sup>6</sup>**

<sup>1</sup> National University of Science and Technology MISiS, Moscow, Russia

<sup>2</sup>Skobeltsyn Institute of Nuclear Physics, Moscow State University, Moscow, Russia

<sup>3</sup>Institute of Physics, University of Tartu, Estonia

<sup>4</sup>FOMOS-MATERIALS, Moscow, Russia

<sup>5</sup>A.N. Frumkin Institute of Physical Chemistry and Electrochemistry Russian Academy of Sciences (IPCE RAS), Moscow, Russia

<sup>6</sup>Institute of Theoretical and Experimental Physics (ITEP), Moscow, Russia

**E-mail: zabelina.ev@misis.ru**

Garnet crystals with cubic symmetry  $\text{Gd}_3\text{Al}_2\text{Ga}_3\text{O}_{12}:\text{Ce}$  (GAGG:Ce) are high potential scintillation crystals with remarkable properties [1]. Garnet structure contains 160 elements in unit cell and one of the specific types of defects in garnets is antisite defect [2], which significantly influence on their physical properties [2, 3]. The nature of the defect structure and the mechanism of defect formation in GAGG:Ce is not clear yet. To get insight into the origin of GAGG:Ce defect structure, it is necessary to study the undoped crystal matrix in initial state. Here we present the results of our studies of the effect of the partial substitution of gallium with aluminum in gadolinium-aluminum-gallium garnet single crystals on its optical properties for the crystals in initial state and after proton irradiation.

Crystals of the charge composition  $\text{Gd}_3\text{Al}_x\text{Ga}_{5-x}\text{O}_{12}$  ( $x=1, 2, 3$ ) were grown in FOMOS-MATERIALS. Samples were investigated in initial state and after proton irradiation, performed at linear accelerator I-2 at the Center of Collective Use «Kamiks» of ITEP. Spectral dependences of absorption and refractive coefficients were measured using «Cary-5000» spectrophotometer with «UMA» accessory. Luminescence properties were studied using specialized set-up for VUV luminescence spectroscopy. The modification of optical band gap was determined by the Tauc method from the transmission spectra as well as by analysis of excitation spectra of  $\text{Gd}^{3+}$  luminescence. The dependence of optical properties on proton irradiation is shown for the samples with different composition. The origin of irradiation-induced defect centers is analysed.

### References

- [1] K. Kamada. *IEEE NSS/MIC*. 2011. P. 1927 – 1929.
- [2] E. V. Zharikov. *Proc. of the USSR Ac. of Sc. Inorg. mat.* 1984. V. 20. No. 6. P. 984-991.
- [3] K. Kamada. *Optical Materials*. 2014. V. 36. № 12. P. 1942–1945.

### Acknowledgments

The research was supported by Russian Foundation for Basic Research №20-02-00688.



## Band gap engineering of $\text{RAIO}_3$ (R = Y, La, Gd, Yb, Lu) perovskites

**Yu. Hizhnyi<sup>1,2</sup>, S.G. Nedilko<sup>1</sup>, Ya. Zhydachevskyy<sup>2,3</sup>, I. Kudrjajtseva<sup>4</sup>, V. Pankratov<sup>5</sup>,  
V. Stasiv<sup>2</sup>, L. Vasylechko<sup>3</sup>, A. Lushchik<sup>4</sup>, M. Berkowski<sup>2</sup>, A. Suchocki<sup>2</sup>**

<sup>1</sup>Taras Shevchenko National University of Kyiv, 64/13 Volodymyrska st., Kyiv 01033, Ukraine

<sup>2</sup>Institute of Physics, Polish Academy of Sciences, Al. Lotników 32/46, Warsaw 02-668, Poland

<sup>3</sup>Lviv Polytechnic National University, 12 Bandera, Lviv 79013, Ukraine

<sup>4</sup>Institute of Physics, University of Tartu, W. Ostwaldi 1, Tartu 50411, Estonia

<sup>5</sup>Institute of Solid State Physics, University of Latvia, 8 Kengaraga st., Riga LV-1063, Latvia

**E-mail: hizhnyi@univ.kiev.ua**

The “band-gap engineering” approach has been recognized as a powerful tool for tuning charge trapping properties of oxide compounds [1, 2]. The main idea of this approach is that cationic substitution in oxide crystal may change its band gap and, consequently, the energy levels of defects states can change their depth with respect to the band edges. The band-gap engineering effect has been experimentally evidenced for several classes of oxide compounds. However specific electronic-level mechanisms which govern this effect in a particular crystal still remain unknown. The present work reveals such mechanisms in the case of  $\text{RAIO}_3$  perovskite crystals and solid solutions with various cations R = Y, La, Gd, Yb and Lu.

The DFT-based theoretical calculations with use of the Plane-Wave Pseudopotential method were carried out in order to establish the electronic band structures of  $\text{RAIO}_3$  crystals and qualitatively estimate the trends in the band-gap energies of with various R cations (R = Y, La, Gd, Yb and Lu). Results obtained in the calculations are compared with corresponding experimental data which can provide estimation of the band-gap energies of studied compounds. Experiments on the optical absorption in the VUV-UV range, luminescence spectroscopy under synchrotron radiation excitation, thermally stimulated luminescence (TSL) in 300 - 500 °C temperature range are carried out for the specially grown set of  $\text{RAIO}_3$  single crystals and solid solutions.

The energy positions of the most common defects, namely cationic and/or oxygen native vacancies, iso- and aliovalent substitutions and their combinations in  $\text{RAIO}_3$  crystals and solid solutions with R = Y, La, and Lu are calculated within the super-cell approach. The mechanism of the temperature shift of TSL glow peaks of  $(\text{Y,Gd,La})\text{AlO}_3:\text{Mn}^{4+}$  microcrystalline phosphors is explained using the obtained computational results. The origin of traps, which form the TSL glow peaks of  $\text{YAlO}_3$  crystals above room temperature, are also discussed.

### References

- [1] I.V. Vrubel, et al., *Crystal Growth and Design*, 17 (2017) 1863-1869.
- [2] M. Fasoli, et al. *Physical Review B*, 84 (2011) 081102(R).

### Acknowledgments

The work was supported by the Polish National Science Centre (project no. 2018/31/B/ST8/00774), by the NATO SPS Project G5647, and by the National Research Foundation of Ukraine (grant 2020.01/0248).

## Influence of irradiation with fast electron beam on energy transport in praseodymium-ion doped phosphates

S.A. Kiselev<sup>1</sup>, V.A. Pustovarov<sup>1</sup>

<sup>1</sup>Ural Federal University, Mira st., 19, Ekaterinburg, Russian Federation, 620002

E-mail: s.a.kiselev@urfu.ru

Investigation of new scintillating materials pay a lot of attention to rare earth-doped inorganic compound due to potential variety of their applications in different spheres, such as detecting systems, medical tomography, nuclear physics, etc. Their properties are partly produced by presence of fast interconfigurational  $5d - 4f$  optical transitions. In comparison with widely used impurity  $Ce^{3+}$  ions, praseodymium emission is located in higher energy region and has shorter lifetime (20-30 ns instead of 30-60) [1]. Emission transitions  $5d - 4f$  of  $Pr^{3+}$  appear when strong enough crystal field moves the lowest  $4f^15d^1$  excited state lower than  $^1S_0$  state.

This paper reports the spectroscopic properties of praseodymium-doped phosphates,  $KLuP_2O_7$ ,  $Sr_9Sc(PO_4)_7$ ,  $K_3Lu(PO_4)_2$  doped with  $Pr^{3+}$  ions. Spectra of photoluminescence (PL) upon selective UV-VUV photon excitation and PL excitation spectra were measured. Recordings of luminescence spectra were done with pure samples and after irradiating with fast electrons ( $E = 10$  MeV) using the UELR-10-10C2 linear electron accelerator in Ural Federal University. The absorbed dose varied in the range of 150-300 kGy.

Results of non-irradiated spectroscopy measurements of studied samples were previously published in [2-4]. Irradiation of spectroscopic objects with 10 MeV electrons influence on the distribution of energy inside the material. The new ratio of emission levels is observed, the effectiveness of energy transport changes.

One of studied samples –  $K_3Lu(PO_4)_2:Pr^{3+}$  (1%) demonstrates two channels of emission in 200-800 nm region: dominant interconfigurational  $5d - 4f$  bands in 250-350 nm and defect-related luminescence with peaks in 450-600 nm. Pure sample has “ $d - f$  / defect-related” ratio 5.0, two unequal peaks at 260 and 290 nm, and defect-related emission appears as wide complex band. After irradiation redistribution of interconfigurational transitions is observed.  $5d - 4f$  emission is presented as one wide band with maximum at 275 nm. The second, but not less important change is about luminescence ratio. Interconfigurational transitions became more dominant and exceed defect-related emission in 9.1 times. Thus, it can be concluded that irradiation changes the energy distribution and transport inside crystal lattice.

### References

- [1] K.V. Ivanovskikh, Q. Shi, M. Bettinelli, V.A. Pustovarov, *Opt. Mater.* 79 (2018) 108-114.
- [2] V.A. Pustovarov, K.V. Ivanovskikh, S.A. Kiselev, E.S. Trofimova, S. Omelkov, M. Bettinelli, *Opt. Mater.* 108 (2020) 110234.
- [3] K.V. Ivanovskikh, V.A. Pustovarov, S. Omelkov, M. Kirm, F. Piccinelli, M. Bettinelli, *J. of Lumin.* 230 (2021) 117749.
- [4] M. Trevisani, K. Ivanovskikh, F. Piccinelli, M. Bettinelli, *J. of Chemical Sciences* 152 (2014) 2-6.

### Acknowledgments

The work was partially supported by the Ministry of Science and Higher Education of the Russian Federation (through the basic part of the government mandate, project No. FEUZ-2020-0060).

## Gamma-ray-induced positron annihilation lifetime spectroscopy for characterization of imperfections in scintillator crystals

**M. Kitaura<sup>1</sup>, Y. Taira<sup>2,3</sup>, S. Watanabe<sup>4</sup>**

<sup>1</sup>*Faculty of Science, Yamagata University, Yamagata 990-8560, Japan.*

<sup>2</sup>*UVSOR synchrotron facility, Institute for Molecular Science, Okazaki 444-8585, Japan.*

<sup>3</sup>*The Graduate University for Advanced Studies, Okazaki 444-8585, Japan.*

<sup>4</sup>*Institute of Innovative Research, Tokyo Institute of Technology, Tokyo 152-8550, Japan*

**E-mail: [kitaura@sci.kj.yamagata-u.ac.jp](mailto:kitaura@sci.kj.yamagata-u.ac.jp)**

Lattice imperfections greatly affect scintillation properties of solids. Characterization of such imperfections in crystals gives us a clue to find excellent scintillators and to improve their scintillation properties. In most of scintillators, luminescence spectroscopy have been adopted as a first choice to obtain the information on imperfections. The information is restrictive to clarify the origins of imperfections. Experimental techniques based on different methodology are needed for the characterization of lattice imperfections in scintillators.

The effect of impurity-codoping on scintillation properties in various scintillators has been studied so far. It was reported that Mg codoping in Ce-doped  $\text{Gd}_3\text{Al}_2\text{Ga}_3\text{O}_{12}$  (Ce:GAGG) caused weakening of phosphorescence [1]. This phenomenon was connected to the suppression of Al/Ga vacancies by charge compensation due to Mg codoping [2]. In order to clarify the existence of Al/Ga vacancies in Ce:GAGG, we performed Gamma-induced positron annihilation lifetime spectroscopy (GiPALS) experiment [3], which is a unique method to probe the existence of cation vacancies by ultrashort laser-Thomson-scattered gamma-ray pulses as a positron source [4]. Comparison of GiPALS spectra between Ce:GAGG and Ce,Mg:GAGG crystals revealed that the vacancy-related component is drastically weakened by Mg codoping. Clearly, Mg codoping reduces Al/Ga vacancies in Ce,Mg:GAGG.

Evaluation of crystallinity among various crystal growth methods is also significant to obtain scintillator crystals of high quality. GiPAL was useful for this purpose. Comparison of GiPALS spectra between Ce:GAGG crystals grown by Czochralski (Cz) and micro-pulling down (m-PD) methods revealed that positron annihilation lifetimes are different between Cz and m-PD grown crystals. Especially, the lifetime of the main component was between those at the bulk and monovacancy states. This feature suggests that m-PD grown crystals have negatively-charged spaces smaller than monovacancies. From the analysis of single crystal XRD data, it turned out that m-PD grown crystals have large isotropic displacement parameters, compared to Cz grown crystals. Since the isotropic displacement parameter reflects lattice disorder in crystal, the crystallinity of Cz grown crystals is better than that of m-PD grown crystals. Details are in investigation using scanning transmittance electron microscope (STEM).

### References

- [1] M. Kitaura *et al.*, Appl. Phys. Express 9, 072602 (2016).
- [2] M. Kitaura *et al.*, Appl. Phys. Lett. 113, 041906 (2018).
- [3] K. Fujimori *et al.*, Appl. Phys. Express 13, 085505 (2020).
- [4] Y. Taira *et al.*, Rev. Sci. Instrum. 84, 053305 (2014).

### Acknowledgments

This work was supported by JSPS KAKENHI grant (No. 19K04997) and Joint Research by Institute for Molecular Science (IMS) (IMS program No. 211).

## Detailed analysis of self-trapped hole $V_k$ center mobility in binary and complex halides as a function of lattice parameters

**A. I. Popov<sup>1</sup>, E.A. Kotomin<sup>1</sup>**

<sup>1</sup>*Institute of Solid State Physics, University of Latvia, 8 Kengaraga, LV-1063, Riga, Latvia*

**E-mail: [popov@latnet.lv](mailto:popov@latnet.lv)**

The self-trapped hole (STH) polarons (called also as  $V_k$  centres) where a hole is shared by two nearest halogens,  $X_2^-$ , are very common color centers created in alkali halides and alkaline-earth halides under all kinds of irradiation (UV light, electrons, gamma rays, neutrons, heavy swift ions). The hole polarons start to migrate and recombine above certain critical temperatures. Their thermally induced decay has been observed by different experimental techniques (optical absorption, EPR, thermostimulated luminescence and etc) in almost all alkali halides, as well as in some other metal halides and more complex halides, such as perovskite halides, ammonium halides, halide sodalites etc [1].

In this report, we review and analyse the self-trapped hole center migration temperatures for a whole series of alkali and alkaline-earth halides, and also for  $MgF_2$ ,  $CdF_2$ ,  $SrI_2$ ,  $CaI_2$ , fluoroperovskites such as  $KMgF_3$ ,  $RbMgF_3$ ,  $BaLiF_3$  etc, fluorohalides such  $BaFBr$ ,  $BaFI$ ,  $PbFCl$  and etc as a function of halogen-halogen distance in a regular crystalline lattice as well as of halogen-halogen distance in isolated molecular ions. We will also report new results on TSL of  $ScF_3$ . Finally, we will discuss a similar situation in some other metal halides, such as  $CeF_3$  or  $PbF_2$ , where  $V_k$  have not been observed.

### References

[1] A.I. Popov, E.A. Kotomin, J. Maier. *Solid State Ionics*, 302 (2017) 3-6.

### Acknowledgments

This work was supported by the National Research Program under the topic "High-Energy Physics and Accelerator Technologies" (Agreement No: VPP-IZM-CERN-2020/1-0002).

The research was performed in the Institute of Solid State Physics, University of Latvia ISSP UL. ISSP UL as the Center of Excellence is supported through the Framework Program for European universities Union Horizon 2020, H2020-WIDESPREAD-01–2016–2017-TeamingPhase2 under Grant Agreement No. 739508, CAMART2 project.

## Interconfigurational $4f^15d \rightarrow 4f$ radiative transitions of $\text{Pr}^{3+}$ ions doped in $\text{Li}_6\text{Y}(\text{BO}_3)_3$ single crystals

**V. Nagirnyi<sup>1</sup>, I. Romet<sup>1</sup>, É. Tichy-Rács<sup>2</sup>, E. Feldbach<sup>2</sup>, K. Lengyel<sup>2</sup>, G. Corradi<sup>2</sup>, K. Chernenko<sup>3</sup>, M. Kirm<sup>2</sup>, L. Kovács<sup>2</sup>**

<sup>1</sup> *Institute of Physics, University of Tartu, W. Ostwald Str. 1, 50411 Tartu, Estonia*

<sup>2</sup> *Wigner Research Centre for Physics, Konkoly-Thege M. út 29-33, H-1121, Budapest, Hungary*

<sup>3</sup> *MAX IV Laboratory, Lund University, P.O. Box 118, 22100 Lund, Sweden*

**E-mail: vitali.nagirnoi@ut.ee**

Many scintillator applications set high demands on the yield or temporal response of luminescence, sometimes requiring superior values for both characteristics. In rare cases only can an intrinsic luminescence (e.g., excitonic emission) partly meet these demands, while most practical applications rely on the emission of impurity dopants. In view of recent developments based on time-of-flight methods in the fields of medical diagnostics or high-energy physics increasing attention is paid to the interconfigurational  $4f^15d \rightarrow 4f^2$  radiative transitions of praseodymium ions having an inherent fast decay time of  $\sim 10$ - $30$  ns, though possessing a relatively low yield of luminescence occurring in the UV region. Lithium yttrium borate ( $\text{Li}_6\text{Y}(\text{BO}_3)_3$ , LYB) may be considered as a perspective host for  $\text{Pr}^{3+}$  ions due to its wide bandgap (7.44 eV) and convenient crystalline lattice isostructural to all  $\text{Li}_6\text{RE}(\text{BO}_3)_3$  materials offering the same unique site for Y and arbitrarily high concentrations of the rare-earth (RE) dopant [1]. Praseodymium doped LYB single crystals have not been studied yet. Only preliminary data on room-temperature emission features of LYB:Pr powders have been published earlier [2].

We present the results of a time-resolved spectroscopic study of the  $\text{Pr}^{3+} 4f^15d \rightarrow 4f^2$  emission in Czochralski grown  $\text{Li}_6\text{Y}(\text{BO}_3)_3:\text{Pr}$  single crystals under excitation by UV-VUV photons, synchrotron radiation and a pulsed electron beam. The study was also combined with a thermoluminescence analysis in order to clarify the role of  $\text{Pr}^{3+}$  ions in the recombination of charge carriers created in crystals irradiated by X-rays and 10-keV electrons.

A series of  $\text{Pr}^{3+} 4f^15d^1 \rightarrow 4f^2$  emission bands peaking at 4.77, 4.51 and 4.2 eV and possessing a short decay time of 9 ns were found in LYB:Pr at low temperatures. The energy separations between these bands allows to relate them to the transitions from the lowest  $4f^15d^1$  state to the  $^3\text{H}_4$ ,  $^3\text{H}_5$ ,  $^3\text{H}_6$  states of the ground state multiplet, respectively. These emissions can be excited in the 5.1, 5.6 eV, 6.15 and 6.65 eV bands due to the transitions to the  $4f^15d^1$  multiplet situated below the highest  $4f^1\text{S}_0$  state. For that reason, no cascade or 4f-4f emissions is observed under UV excitation. An efficient energy transfer from the host to  $\text{Pr}^{3+}$  ions takes place at low temperatures, however, the  $4f^15d^1 \rightarrow 4f^2$  emission is strongly quenched at room temperatures and therefore is not suitable for radiation detector applications. Neither participate  $\text{Pr}^{3+}$  ions in the thermally induced electron-hole recombination processes in heated irradiated crystals. The energy structure of the electronic states of  $\text{Pr}^{3+}$  centres in LYB:Pr crystals and their relative position with respect to the host and defect electronic states will be discussed.

### References

- [1] R. Yavetskiy et al. *Opt. Mater.* 30 (2007) 119–121.
- [2] S.A. Kiselev, V.A. Pustovarov. *AIP Conference Proceedings* 2174 (2019) 020120.

## Spectroscopic studies of Bi<sup>3+</sup> - doped Ca<sub>3</sub>Ga<sub>2</sub>Ge<sub>3</sub>O<sub>12</sub> garnet

**V. Tsiumra<sup>1,2</sup>, A. Krasnikov<sup>3</sup>, L. Vasylechko<sup>4</sup>, S. Zazubovich<sup>3</sup>, L. Wachnicki<sup>1</sup>,  
Ya. Zhydachevsky<sup>1,4</sup>, A. Suchocki<sup>1</sup>**

<sup>1</sup> Institute of Physics, Polish AS, Al. Lotników 32/46, 02-668 Warsaw, Poland

<sup>2</sup> Ivan Franko National University of Lviv, 107 Tarnavskoho str., 79017 Lviv, Ukraine

<sup>3</sup> Institute of Physics, University of Tartu, W. Ostwaldi 1, 50411 Tartu, Estonia

<sup>4</sup> Lviv Polytechnic National University, Bandera 12, 79013 Lviv, Ukraine

**E-mail: tsiumra@ifpan.edu.pl**

Bismuth-doped materials are intensively studied due to their possible application as UV- and visible light-emitting phosphors, quantum-cutting materials to enhance the silicon solar cells efficiency, and scintillators. The possible application of such materials, owing to the presence of broad and intense absorption bands in the ultraviolet spectral region, intense broad visible Bi<sup>3+</sup> - related emission bands, and an effective energy transfer from the Bi<sup>3+</sup> - related excited states to the RE<sup>3+</sup> ions, giving rise to an intense visible emission from the RE<sup>3+</sup> ions, are still intensively studied.

Recently, materials without rare earth, known as rare-earth-free compounds, attracted attention as the possible replacement of the well-known WLEDs phosphors due to low price in production. In this work, the Ca<sub>3</sub>Ga<sub>2</sub>Ge<sub>3</sub>O<sub>12</sub> garnet was chosen as one of such materials. The low melting point at 1370 °C and the broad defect-related absorption and luminescence bands make this material an ideal candidate to be studied as the phosphor for WLEDs. The luminescence origin of Bi<sup>3+</sup> - doped Ca<sub>3</sub>Ga<sub>2</sub>Ge<sub>3</sub>O<sub>12</sub> garnets was never investigated before.

In this work, the Ca<sub>3</sub>Ga<sub>2</sub>Ge<sub>3</sub>O<sub>12</sub> garnets, pure and Bi<sup>3+</sup> - doped, were carefully studied in a wide temperature range (4.2 – 500 K) by the steady-state and time-resolved luminescence spectroscopy methods. The obtained results allow clarifying the origin of the luminescence centers in these materials. In particular, no exciton-like luminescence has been observed in the undoped Ca<sub>3</sub>Ga<sub>2</sub>Ge<sub>3</sub>O<sub>12</sub> garnet. The main luminescence band peaked at 2.74 eV with excitation around 5.04 eV and in the band-to-band absorption region appears due to charge-transfer transitions from oxygen O<sup>2-</sup> levels at the top of the VB to the ground state of intrinsic defects.

In contrast, the luminescence spectrum of Bi<sup>3+</sup> - doped Ca<sub>3</sub>Ga<sub>2</sub>Ge<sub>3</sub>O<sub>12</sub> consists of at least four ultraviolet (UV) emission bands and the visible (VIS) emission. The four UV emission bands located around 3.9 eV and 3.06 eV arise from the triplet relaxed excited states (RES) of Bi<sup>3+</sup> ions having different nearest surroundings, i.e., these bands correspond to the <sup>3</sup>P<sub>1,0</sub> → <sup>1</sup>S<sub>0</sub> transitions of a free Bi<sup>3+</sup> ion. The corresponding triplet RES are characterized by large spin-orbit splitting energies (in the range from 56 to 100 meV). However, much larger Stokes shift and full width at half maximum (FWHM) of the visible (2.41 eV) emission band and especially the extremely small spin-orbit splitting energy (1.4 meV) of the corresponding triplet excited state are characteristic for the luminescence of the exciton-like origin. Therefore, the 2.41 eV emission was suggested to arise from an exciton localized around a Bi<sup>3+</sup> ion.

The broad absorption band around 4.4 eV arises from the electron transitions from the ground state to the lowest-energy triplet excited state of a Bi<sup>3+</sup> ion in the Ca<sub>3</sub>Ga<sub>2</sub>Ge<sub>3</sub>O<sub>12</sub> host, corresponding to the <sup>1</sup>S<sub>0</sub> → <sup>3</sup>P<sub>1</sub> transitions of a free Bi<sup>3+</sup> ion. It is interesting to note that the triplet emissions of both the Bi<sup>3+</sup> ion and the exciton localized around the Bi<sup>3+</sup> ion coexist in the Ca<sub>3</sub>Ga<sub>2</sub>Ge<sub>3</sub>O<sub>12</sub>:Bi garnet and are excited in the same absorption band. The Bi<sup>3+</sup> centers in Ca<sub>3</sub>Ga<sub>2</sub>Ge<sub>3</sub>O<sub>12</sub> can contain different excess positive charge compensating defects in the nearest surroundings of a Bi<sup>3+</sup> ion.

The appearance under excitation in the ultraviolet Bi<sup>3+</sup> - related absorption region, besides the ultraviolet and visible Bi<sup>3+</sup> - related emissions, also of the red emission of Mn<sup>4+</sup> indicates that the Ca<sub>3</sub>Ga<sub>2</sub>Ge<sub>3</sub>O<sub>12</sub>:Bi<sup>3+</sup>, Mn<sup>4+</sup> phosphors could be applied in white LEDs as well.

## Luminescence and thermal behavior of $\text{La}_2\text{MgTiO}_6$ - $\text{Ba}_2\text{MgWO}_6$ solid solution

**D. Stefańska<sup>1</sup>, T.H.Q. Vu<sup>1</sup>, P. J. Dereń<sup>1</sup>**

<sup>1</sup>*Trzebiatowski Institute of Low Temperature and Structure Research PAS, Wrocław, 50-422, Poland*

**E-mail: [d.stefanska@intibs.pl](mailto:d.stefanska@intibs.pl)**

Double perovskites with general formula  $\text{A}_2\text{BB}'\text{O}_6$  is a large group of materials. Due to their excellent performance such as good chemical stability, high emission intensity, and thermal stability they provide growing interest. Double perovskites are very promising as ceramic and scintillating materials, they can be used as a luminescent thermometer or for LED lighting. These materials crystallize in a different crystallographic structure such as cubic, tetragonal, monoclinic, and orthorhombic depending on the charge and ionic radii.

$\text{Ba}_2\text{MgWO}_6$  (BMW) crystallized in cubic structure with a space group  $Fm\bar{3}m$ , while  $\text{La}_2\text{MgTiO}_6$  (LMT) in orthorhombic  $Pbnm$  one. Investigated samples were obtained by co-precipitation method, the purity of prepared samples was confirmed by X-ray diffraction. Both compounds exhibit broad host emission assigned to  $\text{WO}_6$  and  $\text{TiO}_6$  groups located in the blue-green spectral range. However, for the samples doped with  $\text{Eu}^{3+}$  strong energy transfer from host to dopant ions occurred. BMW: $\text{Eu}^{3+}$  presents unusual emission with only one strong line attributed to magnetic dipole transition, while in LTM: $\text{Eu}^{3+}$  electric dipole one dominant. A series of samples  $x$  LMT -  $(1-x)$  BMW were  $x= 1, 0.9, 0.67, 0.5, 0.3, 0$  solid-solution pure and doped with 1% of  $\text{Eu}^{3+}$  were obtained and investigated in details. The changes of position and shape of emission bands in the LMT-BMW series were analyzed. Only for BMW  $\text{Eu}^{3+}$  ions occupies high  $\text{O}_h$  symmetry sites, while in the LMT-BMW solution they prefer  $\text{C}_i$  position of  $\text{La}^{3+}$  ions. Temperature-dependent emission spectra under the 266 nm excitation line will be discussed with the ability for non-contact luminescent thermometry.

### **Acknowledgments**

This study was supported by "The National Science Centre" under Grant No. 2017/25/B/ST5/02670, which is gratefully acknowledged.

## The broadband IR emission from Cr<sup>3+</sup> ions in Magnetoplumbite

**N. Majewska<sup>1</sup>, T. Leśniewski<sup>1</sup>, S. Mahlik<sup>1</sup>, V. Rajendran<sup>2</sup>, M.-H. Fang<sup>2</sup>, W.-T. Huang<sup>2</sup>,  
G. Leniec<sup>3</sup>, S. M. Kaczmarek<sup>3</sup>, R.-S. Liu<sup>2</sup>**

<sup>1</sup>*Institute of Experimental Physics, Faculty of Mathematic, Physics, and Informatics, Gdańsk University, Wita Stwosza 57, 80-308 Gdańsk, Poland*

<sup>2</sup>*Department of Chemistry, National Taiwan University, Taipei 106, Taiwan*

<sup>3</sup>*Institute of Physics, Department of Mechanical Engineering and Mechatronics, West Pomeranian University of Technology Szczecin, al. Piastow 48, 70-311 Szczecin, Poland*

**E-mail: natalia.majewska@phdstud.ug.edu.pl**

The Cr<sup>3+</sup>-activated luminescent materials have recently become a research hotspot worldwide due to potential biological applications.<sup>[1, 2]</sup> Recently, Cr<sup>3+</sup>-activated luminescent materials that can produce either sharp-line or broadband spectra have become a promising candidate in phosphor-converted IR light-emitting diodes (pc-IR LEDs). It found application in the food's freshness, quality, and composition analysis.<sup>[3]</sup> One of the promising materials for NIR sources are magnetoplumbites activated by Cr<sup>3+</sup> ions. These materials are characterized by efficient NIR luminescence in 650–950 nm range. The emission spectra show two different emission types, a narrow line emission around 690 nm and broad emission in longer wavelengths extending from 650 to 950 nm, coming from two different crystallographic sites denoted by Cr1 and Cr2, respectively. Surprisingly, the broadband Cr2 emission at 650–950 nm is not related to the <sup>4</sup>T<sub>2</sub>→<sup>4</sup>A<sub>2</sub> transition. Namely, the time resolve spectroscopy shows that the decay time of Cr2 emission is in ms range at room temperature, which shows that this luminescence certainly is not the spin-allowed <sup>4</sup>T<sub>2</sub>→<sup>4</sup>A<sub>2</sub> transition. Additionally, the high-pressure induce shift of Cr2 emission towards lower energies with the rate around – 1.5 cm<sup>-1</sup>/kbar, is a strong indicator that Cr2 emission cannot be accounted to the <sup>4</sup>T<sub>2</sub>→<sup>4</sup>A<sub>2</sub>, which would shift towards shorter wavelengths, typically at a much stronger rate. The direction and magnitude of the pressure shift is in good agreement with the typical pressure shift rate of the <sup>2</sup>E→<sup>4</sup>A<sub>2</sub> transition, which suggest that we deal with spin forbidden <sup>2</sup>E→<sup>4</sup>A<sub>2</sub> transition of Cr<sup>3+</sup> or Cr<sup>3+</sup> pairs.

### References

- [1] K. Van Den Eeckhout, D. Poelman and P. F. Smet, *Materials*, 2013, 6, 2789–2818.
- [2] M. Back, J. Ueda, M. G. Brik, T. Lesniewski, M. Grinberg, S. Tanabe, *ACS Applied Materials and Interfaces* 10 (2018) 41512–41524.
- [3] S. Mahlik, M. Grinberg, G. Leniec, S. M. Kaczmarek, Y.-S. Lin, K.-M. Lu, C.-M. Lin, H. Chang, S.-F. Hu, R.-S. Liu, *ACS Energy Lett.* 2018, 3, 2679–2684.

### Acknowledgments

This work was financially supported by the National Science Center Poland Grant Opus (Nos. 2016/23/B/ST3/03911 and No. 2019/33/B/ST3/00406), and the National Center for Research and Development Poland Grant (No. PL-TW/V/1/2018).



## **Time-resolved luminescence spectroscopy in studies of ultrafast processes in wide gap materials using advanced light sources**

**M. Kirm**<sup>1</sup>

<sup>1</sup>*Institute of Physics, University of Tartu, W. Ostwald Str 1, 50411 Tartu, Estonia*

**E-mail: marco.kirm@ut.ee**

Ultrafast scintillators with a superior temporal resolution are needed in different applications: in high-energy physics to prevent pile-up effects at high event rates as well as in time-of-flight positron emission tomography to improve the resolution in diagnostic images in medicine. In order to develop such materials extensive knowledge is needed on their electronic band structure verified with experimental spectroscopic data in a wide energy range. Time-resolved luminescence spectroscopy is an indispensable tool in studies of wide gap scintillators, in particular, the peculiarities of relaxation processes of electronic excitations and their time evolution. In order to study ultrafast processes, experimental facilities with sub-nanosecond time resolution are needed. At MAX IV Lab (Lund, Sweden), such luminescence setups have been successfully implemented permanently at FinEstBeAMS [1] and as a mobile endstation at the FemtoMAX beamlines, where the instrumental response function as short as 160 ps in a single bunch mode [2] and 28 ps [3], respectively, were achieved. Based on the results obtained at these setups by time-resolved luminescence methods, in my presentation the relaxation processes of electronic excitations in novel hexafluorogermanate scintillators (pure and doped) leading to the ultrafast cross- and intraband luminescence with sub-nanosecond lifetime will be discussed. Also examples of study cases of other advanced wide gap materials for scintillation and optical applications will be elucidated.

### **References**

- [1] V. Pankratov, R. Pärna, M. Kirm, *et al.*, *Radiation Measurements* 121 (2019), 91–98.
- [2] I. Kamenskikh, E. Tishchenko, M. Kirm, *et al.*, *Symmetry* 12 (2020) 914.
- [3] R.M. Turtos, S. Gundacker, S. Omelkov, *et al.*, *npj 2D Materials and Applications* 3 (2019) 37.

### **Acknowledgments**

The synchrotron radiation research at MAX IV Lab leading to this result has been supported by the project CALIPSOplus under the Grant Agreement 730872 from the EU Framework Programme for Research and Innovation HORIZON 2020. This research was also supported by the ERDF fundings in Estonia granted to the Centre of Excellence TK141 “Advanced materials and high-technology devices for sustainable energetics, sensorics and nanoelectronics (HiTechDevices)” (grant no. 2014-2020.4.01.15-0011) and Estonian Research Council grant PRG-629. The FinEstBeAMS beamline operation costs were partially supported within the MAX-TEENUS project (grant no. 2014-2020.4.01.20-0278 by the ERDF funding in Estonia granted to University of Tartu.

## Emission properties of rare earth doped materials under high power excitation

**W. Strek<sup>1</sup>, R. Tomala<sup>1</sup>, M. Chaika<sup>1</sup>, M. Stefanski<sup>1</sup>**

<sup>1</sup>*Institute of Low Temperature and Structure Research, Polish Academy of Sciences, Okolna 2, 50-422 Wrocław, Poland*

**E-mail: w.strek@intibs.pl**

The excitation of RE-doped materials by high power excitation density leads to generation of bright broadband white emission<sup>1</sup>. As recent reports demonstrated that the emission in visible range is accompanied by emission in NIR range<sup>2,3</sup>. The resonant excitation of RE ions results in intense luminescence assigned to f-f transition. The relation between f-f transitions and broadband emission has been investigated as a function of RE concentration, excitation wavelength and excitation power density.

The intensity of broadband white emission was characterized by excitation density threshold. It increased exponentially with excitation power. It was observed decreasing of f-f transitions with simultaneous increasing broadband white emission. Besides, the efficient photocurrent co-occurs with appearance of white emission was investigated. It increased exponentially with excitation power density. The mechanism of white light emission was discussed in terms of multiphoton ionization leading to creation of (RE<sup>2+</sup>, RE<sup>3+</sup>) ionic pairs and the intervalence charge transfer (IVCT) responsible for broadband emission transitions. The possibilities of application of white light emission for optoelectronic devices are presented.

### References

- [1] Strek, W.; Tomala, R.; Marciniak, L.; Lukaszewicz, M.; Cichy, B.; Stefanski, M.; Hreniak, D.; Kedzierski, A.; Krosnicki, M.; Seijo, L. Broadband Anti-Stokes White Emission of Sr<sub>2</sub>CeO<sub>4</sub> Nanocrystals Induced by Laser Irradiation. *Phys. Chem. Chem. Phys.* 2016, 18 (40), 27921–27927.
- [2] Tomala, R.; Strek, W. Emission Properties of Nd<sup>3+</sup>:Y<sub>2</sub>Si<sub>2</sub>O<sub>7</sub> Nanocrystals under High Excitation Power Density. *Opt. Mater.* 2019, 96.
- [3] Chaika, M.; Tomala, R.; Strek, W. Laser Induced Broadband Vis and NIR Emission from Yb:YAG Nanopowders. *J. Alloys Compd.* 2021, 865, 158957.

### Acknowledgments

This work was financed from the National Science Centre Poland within the OPUS 19 (NCN 2020/37/B/ST5/02399) grant.

## Time-resolved luminescence and VUV excitation spectroscopy of GGAG:Ce single crystals

V. Pankratova<sup>1</sup>, A.P. Kozlova<sup>2</sup>, O.A. Buzanov<sup>3</sup>, K. Chernenko<sup>4</sup>, K. Klementiev<sup>4</sup>,  
A. Šarakovskis<sup>1</sup>, V. Pankratov<sup>1</sup>

<sup>1</sup>*Institute of Solid State Physics, University of Latvia, 8 Kengaraga iela, LV-1063 Riga, Latvia*

<sup>2</sup>*National University of Science and Technology "MISiS", Leninsky Pr. 4, 119049 Moscow, Russia*

<sup>3</sup>*OJSC "Fomos-Materials" Co., Buzheninova street 16, 107023 Moscow, Russia*

<sup>4</sup>*MAX IV Laboratory, Lund University, PO BOX 118, SE-221 00 Lund, Sweden*

**E-mail: vladimirs.pankratovs@cfi.lu.lv**

In the last decade it was demonstrated that the crystals of  $\text{Gd}_3\text{Ga}_3\text{Al}_2\text{O}_{12}:\text{Ce}^{3+}$  (or GGAG:Ce) reveal a huge interest for application as a scintillator. Due to the superior scintillation properties GGAG:Ce crystals are perspective materials in high-energy physics as well as in medical applications in emission tomography, in particular in TOF PET.

In the current research cerium doped GGAG single crystals as well as GGAG:Ce single crystals co-doped by divalent ( $\text{Mg}^{2+}$ ,  $\text{Ca}^{2+}$ ) and tetravalent ( $\text{Zr}^{4+}$ ,  $\text{Ti}^{4+}$ ) ions have been studied by means of the time-resolved luminescence as well as the excitation luminescence spectroscopy. Time-resolved luminescence experiments have been carried out under a tuneable laser excitation in order to obtain luminescence characteristics under excitations in  $\text{Ce}^{3+}$ ,  $\text{Gd}^{3+}$  and excitonic absorption bands. The influence of the co-dopant ions on the  $\text{Ce}^{3+}$  luminescence decay kinetics is elucidated [1]. The fastest luminescence decay was observed for the  $\text{Mg}^{2+}$  co-doped crystals under any excitation below bandgap energy indicating the perturbation of  $\text{Mg}^{2+}$  ions on the 5d states of  $\text{Ce}^{3+}$  emission centers.

Synchrotron radiation from 1.5 GeV storage ring of MAX IV synchrotron was utilized for the luminescence excitation in vacuum ultraviolet (VUV) and soft X-ray (XUV) energy range (4.5 to 800 eV). The experiments have been carried out on the photoluminescence endstation [2, 3] of the FinEstBeAMS beamline [4]. The influence of the co-dopant ions on the transitions in the excitonic spectral range was revealed examining the luminescence emission and excitation spectra of both  $\text{Gd}^{3+}$  and  $\text{Ce}^{3+}$  ions in all single crystals studied. Special attention was paid to the analysis of  $\text{Ce}^{3+}$  excitation spectra in VUV and XUV spectral range where multiplication of electronic excitation (MEE) processes occur [5]. It was demonstrated that GGAG:Ce single crystals co-doped by  $\text{Mg}^{2+}$  ions as well as the crystal annealed in vacuum reveal the most efficient excitation of  $\text{Ce}^{3+}$  emission in VUV-XUV excitation range. The role of intrinsic defects in MEE processes in the co-doped as well as in the annealed GGAG:Ce single crystals is discussed.

### References

- [1] V. Pankratova, A.P. Kozlova, O.A. Buzanov, et al., Scientific Reports 10 (2020) 20388.
- [2] V. Pankratov, R. Pärna, M. Kirm, et al., Radiation Measurements, 121 (2019) 91-98.
- [3] V. Pankratov and A. Kotlov, Nucl. Inst. Meth. Phys. Research B, 474 (2020) 35-40.
- [4] R. Pärna, R. Sankari, E. Kukk, et al., Nucl. Inst. Meth. Phys. Research A, 859 (2017) 83-89.
- [5] A.P. Kozlova, V.M. Kasimova, O.A. Buzanov, Results in Physics 16 (2020) 103002.

### Acknowledgments

This work was supported by the Latvian Science Council grant No. LZP 2020/2-0074 and National Research Program under the topic "High-Energy Physics and Accelerator Technologies".

## Structural and optical studies of novel, cerium-tungstate double perovskites doped with rare-earth ions

**D. Włodarczyk<sup>1</sup>, M. J. Chrunik<sup>2</sup>, M. Amilusik<sup>3</sup>, K. M. Kosyl<sup>1</sup>, M. Strankowski<sup>4</sup>,  
V. Tsiurma<sup>1</sup>, T. Giela<sup>5</sup>, M. Zając<sup>5</sup>, A. Grochot<sup>1</sup>, K. Jabłońska<sup>1</sup>, A. Reszka<sup>1</sup>,  
P. Iwanowski<sup>1</sup>, H. Przybylińska<sup>1</sup>, M. Boćkowski<sup>3</sup>, A. Suchocki<sup>1</sup>**

<sup>1</sup>*Institute of Physics PAS, Lotnikow Av. 32/46, 02-668, Warsaw, Poland*

<sup>2</sup>*Military University of Technology, Gen. Sylwestra Kaliskiego 2, 00-908, Warsaw, Poland*

<sup>3</sup>*Institute of High Pressure PAS, Sokolowska 29/37, 01-142, Warsaw, Poland*

<sup>4</sup>*Gdansk University of Technology, G. Narutowicza 11/12, 80-233, Gdansk, Poland*

<sup>5</sup>*SOLARIS NSRC, Jagiellonian University, Czerwone Maki 98, 30-392, Cracow, Poland*

**E-mail: wloдар@ifpan.edu.pl**

Double perovskites are rock-salt type minerals named after the resemblance to typical,  $ABX_3$  perovskite structures having one simple exception in mind - the fact that the unit cell size is two times larger than normal. A-site cations are mostly considered to be divalent, alkaline metals (Ca, Sr, Ba). B are suitable combinations of rare-earth (i.e. Ce, Pr, Yb) or d-block type metals (like W, Mn, Zn). X can vary depending on chemical flexibility – these atoms could be oxygen or related to halides, nitrides and even sulfides. In this case it would be  $O^{2-}$  building clusters ordered in such a fashion that they will share corner arrangement of both  $BO_6$  and  $B'O_6$  units creating general  $A_2BB'O_6$  formula. Since those types of compounds were constantly investigated since early 1950's they have found their way in many research fields and applications such as optoelectronics, superconductors, catalysts, dielectrics, piezoelectrics, various temperature sensors, electrodes, and components to form well-developed fuel or solar cells... Broad literature review [1] alongside with own experimental studies, regarding popular  $BaWO_4$  scintillator [2], inspired researchers to an original approach in order to form a new compound amongst aforementioned family of materials. Thus, a novel cerium-tungstate double perovskite was created, based on solid state reaction, inert atmosphere and high pressure technologies, in hopes of finding new, efficient NUV-NIR downconverter. (High and low) Temperature and pressure stability was checked in terms of possible phase transitions or eventual decomposition of these newly created materials. Techniques like powder XRD, XPS, XAS, EPR, Raman and FTIR spectroscopies or even DSC with TG were involved to thoroughly describe any behavioral changes (polymorphism) and possible charge transfer in both doped and undoped materials. After checking these compounds in pristine conditions, rare-earth dopants, such as Pr & Yb, were chosen to optimize the content in order to establish proper energy-transfer. To achieve this absorption, excitation and emission spectra were taken and decay kinetics are planned to be collected in order to verify whether or not these materials are indeed stable enough to carry out tasks assigned to them (downconverters, temperature sensors) without any unwanted effects or abrupt decomposition.

### References

- [1] S. Vasala, M. Karppinen, *Prog. Solid State Chem.* 2015, 43 (1-2), pp 1-36.
- [2] D. Włodarczyk et al., *Inorg. Chem.* 2019, 58 (9), pp. 5617-5629.

### Acknowledgments

These studies were financed by Polish National Science Center from Preludium 17 Edition project in Material Sciences - reg. no. 2019/33/N/ST5/02317.

## Luminescence properties of GAGG:Ce scintillator under intense laser irradiation

**D. Spassky<sup>1,2</sup>, A. Vasil'ev<sup>1</sup>, N. Krutyak<sup>2,3</sup>, O. Buzanov<sup>4</sup>, N. Kozlova<sup>5</sup>, E. Zabelina<sup>5</sup>,  
A. Belsky<sup>6</sup>, N. Fedorov<sup>6</sup>, P. Martin<sup>6</sup>**

<sup>1</sup>Skobeltsyn Institute of Nuclear Physics, Moscow State University, Moscow, Russia

<sup>2</sup>Institute of Physics, University of Tartu, Estonia

<sup>3</sup>Physics Department, M.V. Lomonosov Moscow State University, Moscow, Russia

<sup>4</sup>Fomos-Materials, Moscow, Russia

<sup>5</sup>National University of Science and Technology MISiS, Moscow, Russia

<sup>6</sup>CELIA, Université de Bordeaux, CNRS, CEA, 33405 Talence, France

**E-mail: spas@srd.sinp.msu.ru**

Gd<sub>3</sub>Al<sub>2</sub>Ga<sub>3</sub>O<sub>12</sub>:Ce<sup>3+</sup> (GAGG:Ce) scintillator is a high-density chemically stable compound with high scintillation yield (~60000 ph/MeV), which is used in medicine and high-energy physics [1]. The scintillation of GAGG:Ce is due to 5d–4f Ce<sup>3+</sup> transitions, which give rise to emission band peaking at ~550 nm. When a scintillator absorbs high-energy particle it converts its energy into electronic excitations whose spatial distribution depend on the particles type and energy as well as stopping power of scintillator. High concentration of excitations in the local volume usually occurs in the end of the particle's tracks and results in the effect of non-proportional response to the energy of the ionizing particles [2]. The effect is due to the interaction of electronic excitations in case of their high density and it can be studied using intense laser sources. Here we present the study of the interaction of electronic excitations in GAGG:Ce under intense laser irradiation. The single crystals of GAGG:Ce were grown by the Czochralski method. The experiments were performed using Ti:sapphire laser system at the CELIA laser center. The luminescence was excited using the 4<sup>th</sup> harmonic (6.2 eV) of laser radiation with the pulse energy up to 100 nJ that allowed to reach the initial concentration of electrons and holes up to 10<sup>22</sup> pairs/cm<sup>3</sup>. The density of excitations was controlled by (i) the translation of the focusing lens and (ii) by the variation of laser beam energy. The time windows were used to separate the influence of density effects on the “fast” emission with characteristic for Ce<sup>3+</sup> decay times of tens of ns and delayed “slow” emission of Ce<sup>3+</sup> with decay times up to several μs. The emission intensity and decay characteristics of Ce<sup>3+</sup> emission strongly depend on the excitation density. In particular, emission intensity measured in the fast time window decreases with the excitation density while opposite dependence is observed in the slow time windows. The observed effect is ascribed to the interaction of electronic excitations and peculiarities of energy transfer from matrix to emitting centers under high density excitation.

### References

- [1] P. Lecoq, *Nucl. Instr. and Meth. in Phys. Res.*, A 809 (2016) 130.
- [2] A.N. Vasil'ev, A.V. Gektin, *IEEE T NUCL SCI*, 61 (2014) 235.

### Acknowledgments

The measurements at CELIA were performed within the project CNRS-CELIA002573. This project has received funding from the European Union's Horizon 2020 research and innovation programme under grant agreement no 654148 Laserlab-Europe. The research was supported by Russian Foundation for Basic Research №20-02-00688.

## Pressure induced blue luminescence in CsPbBr<sub>3</sub> single crystals

**L.-I. Bulyk<sup>1,2</sup>, Ya. Chornodolsky<sup>2</sup>, T. Demkiv<sup>2</sup>, R. Gamernyk<sup>2</sup>,  
V. Vistovsky<sup>2</sup>, A. Suchocki<sup>1</sup>, A. Voloshinovskii<sup>2</sup>**

<sup>1</sup>*Institute of Physics, Polish Academy of Sciences, Al. Lotnikow 32/46, 02-668, Warsaw, Poland*

<sup>2</sup>*Ivan Franko National University of Lviv, 8 Kyryla I Mefodiya Str., Lviv, Ukraine*

**E-mail: bulyk@ifpan.edu.pl**

The use of hydrostatic pressure to study of single crystals provides new opportunities to elucidate the nature of luminescent processes, phase transformations, defect formation processes, and so on. Such phenomena have been a subject of many research in perovskite crystals, which have provided new data on the dynamics of changes in their crystallographic and electronic structure. The results of previous studies can be summarized as follows. When the hydrostatic pressure increases to  $\sim 1.3$  GPa, the interatomic distances of Pb-Br bonds in the PbBr<sub>6</sub> octahedron change, which leads to a shift of the near-edge luminescence to the long-wavelength region [1]. With a further pressure increase the tilt of the octahedra occurs, which leads to an increase of the energy bandgap and, accordingly, to the shift of the edge luminescence in the short-wavelength region of the spectrum. At pressures greater than 3-4 GPa, the transition of crystal to the amorphous phase occurs, which is accompanied by a decrease of the luminescence intensity.

Our studies of the single crystal luminescence at hydrostatic pressure in argon pressure transmitting medium reveal somewhat different regularities. At pressures of about 1.3 GPa, as in previous experiments, the near-edge luminescence band peaked at about 528 nm (at T = 300 K, P = 0.0 GPa) undergoes the expected shift to the low energy region. At higher pressures the near-edge luminescence begins to disappear transforming into a wide non-structured band in the range of 500–800 nm. In the same pressure range (P > 1 GPa) an unexpected narrowband luminescence in the range of 400–500 nm appears, which can be attributed to the emission of CsPbBr<sub>3</sub> nanoparticles. The luminescence bands peaked at 416, 444 and 460 nm are typical for the emission of nanoparticles with a thickness of 1, 2 and 3 perovskite unit cells [2]. After the pressure release the luminescent properties of the crystal return to those which were before the pressure application. The possible mechanisms of formation and localization of CsPbBr<sub>3</sub> nanoparticles in single crystals due to hydrostatic compression are discussed in this paper.

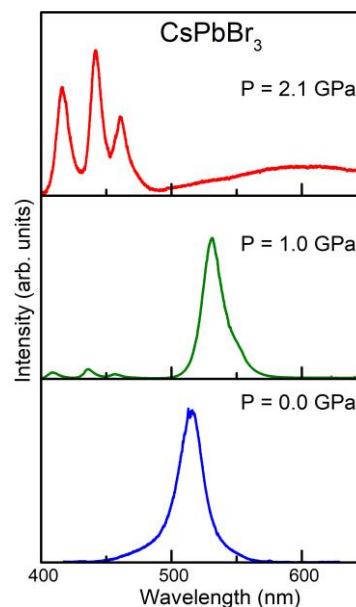


Fig.1. Emission of CsPbBr<sub>3</sub> single crystals under hydrostatic pressure.

### References

- [1] L. Zhang, Q. Zeng, K. Wang, J. Phys. Chem. Lett. 8 (2017) 3752–3758.
- [2] Y. Bekenstein, B. Koscher, S. Eaton, P. Yang, A. Alivisatos, J. Am. Chem. Soc. 137 (2015) 16008–16011.

## Relaxation of anion and cation electronic excitations in hexafluorogermanates

**J. Saaring<sup>1</sup>, S. Omelkov<sup>1</sup>, E. Feldbach<sup>1</sup>, V. Nagirnyi<sup>1</sup>, I. Romet<sup>1</sup>, O. Rebane<sup>1</sup>,  
A. Vanetsev<sup>1</sup>, M. Kirm<sup>1</sup>**

<sup>1</sup>*Institute of Physics, University of Tartu, W. Ostwald Str. 1, 50411 Tartu, Estonia*

**E-mail: juhan.saaring@ut.ee**

Research and development of inorganic scintillator materials are driven by specific needs of demanding applications [1]. Short decay time of emissions, leading to high time resolution, is one of the parameters sought in materials to be used in ionizing radiation detector applications such as, e.g., high-energy physics and time-of-flight positron emission tomography. Cross-luminescence (CL) arises from an intrinsic radiative recombination of core holes with valence electrons, resulting in fast emission with sub-ns decay time [2]. It can help improving the time resolution of future detectors based on scintillation. Although intrinsically fast, CL has a relatively low light yield and is emitted mostly in the VUV-UV spectral region, making its detection more complicated. New attention to the CL materials is due to the development of novel silicon-photomultipliers (SiPMs) with increased sensitivity in UV-VUV (13% photon detection efficiency-PDE at 220 nm). This could be significantly improved by shifting resulting emissions to the longer wavelengths, where the PDE of SiPMs peaks at 50% (~ 450 nm).

For this purpose, powder samples of  $K_2GeF_6$  and  $BaGeF_6$  were synthesized via co-precipitation from concentrated HF solutions and nearly phase pure polycrystalline particles were obtained. According to band structure calculations (AFLOW [3]), both ternary compounds host complex valence band structures due to the sub-bands of the Ge 4s,4p states, potentially resulting in CL transitions between the core (K 3p) and valence band (F 2p, Ge 4s,4p) states as well as intraband luminescence (IBL) between the valence sub-bands. The samples were investigated by means of cathodoluminescence and time-resolved luminescence spectroscopy under synchrotron radiation excitation at 7 K (FinEstBeAMS, MAX IV, Lund, Sweden).

Various intrinsic emissions were investigated. A luminescence band at 510 nm with the decay time in the  $\mu s$  range is assigned to the decay of self-trapped excitons (STE) in  $K_2GeF_6$ . From the recorded excitation spectrum of STE emission, the band gap value is estimated to ~ 11 eV, which exceeds the fitted gap value 9.25 eV from AFLOW. Fast emission bands with decay times in ~ 300-500 ps range extend from VUV to visible (155 – 500 nm) and are assigned to cross- and intraband luminescence transitions between the valence sub-bands. Fast emissions are shifted towards longer wavelengths and overlap well with the sensitivity of novel SiPMs. The creation of cation excitons in  $K_2GeF_6$  starts at 18.1 eV. Their non-radiative decay results in the formation of holes in the Ge valence band leading to the appearance of fast IBL at energies below the CL excitation onset (K 3p) at 20 eV. Based on the electronic band structure from AFLOW and results of time-resolved luminescence spectroscopy, the relaxation processes of cation and anion electronic excitations occurring in ternary hexafluorogermanates will be discussed. A potential of the studied compounds for scintillation applications will be evaluated.

### References

- [1] C. Dujardin, et al., IEEE Trans. Nucl. Sci., 65 (2018) 1977–1997.
- [2] V.N. Makhov, Physica Scripta, 89 (2014) 044010.
- [3] O. Isayev, et al., Nature Communications, 8 (2017) 15679.

# Theory and a novel approach to optically stimulated luminescence in complex systems

**A. Mandowski**<sup>1</sup>

<sup>1</sup>*Department of Experimental and Applied Physics, Jan Długoż University  
ul. Armii Krajowej 13/15, 42-200 Częstochowa, Poland*

**E-mail: a.mandowski@ujd.edu.pl**

Thermoluminescence (TL) and optically stimulated luminescence (OSL) are typically used in dosimetry of ionizing radiation and luminescence dating of archaeological and geological samples. Both phenomena are related to defects of crystalline structure of wide band gap dielectric materials. The OSL method has become very popular since the 90s of the last century because of the easier and faster method of measurement. An OSL reader is a fully optical device not requiring heating elements and precise temperature control. The OSL technique is suitable for all types of dosimetry measurements.

Nevertheless, this method also has significant drawbacks. First of all, the number of potential OSL materials (detectors) is much smaller than the number of TL sensitive materials [1]. Contrary to the TL measurement, the OSL decay curve does not allow to determine any parameters of traps and recombination centres relating to the emission of the luminescence. For this reason, some researchers say about the "featureless" OSL decay [2]. The analysis of the OSL decay is usually limited to the simplest and unrealistic first order case.

A real OSL detector contains at least several trap levels and many types of recombination centres (RCs). Moreover, the recombination mechanisms are different – localized and delocalized [3]. Some of them are non-radiative. During a typical CW-OSL readout all of these traps/RCs and processes may be involved. Hence, the question arises: what effective values could be really measured in OSL? Is the popular approach based on deconvolution of CW-OSL decay into several exponential decays justified? Is it rational?

This lecture presents some analytical and numerical examples revealing usefulness or uselessness of these popular concepts. A novel theoretical approach is suggested based on effective parameters of trap system for both recombination mechanisms. It is shown that some novel OSL measurement methods allow to obtain more valuable information on the fundamental processes occurring in the detectors. Appropriate modification of the stimulation vs time profile expands the measurement capabilities.

## References

- [1] E. G. Yuhihara, S. W. S. McKeever, *Optically Stimulated Luminescence: Fundamentals and Applications*, Wiley (2011).
- [2] R. Chen, V. Pagonis, *J. Phys. D: Appl. Phys.* 41 (2008) 035102.
- [3] A. Mandowski, *Radiat. Prot. Dosimetry*, 119 (2006) 23-28.

## Acknowledgments

This work was supported by the National Science in Poland (2018/31/B/ST10/03966).



## The still unexplained mechanism of the UV emission of Al<sub>2</sub>O<sub>3</sub>:C: what do we know and how do we move forward?

**E. G. Yukihara<sup>1</sup>, O. Pakari<sup>1</sup>, J. Christensen<sup>1</sup>, L. Bossin<sup>1</sup>**

<sup>1</sup>Department of Radiation Safety and Security, Paul Scherrer Institute, Villigen PSI, Switzerland

**E-mail: eduardo.yukihara@psi.ch**

The optically stimulated luminescence (OSL) material Al<sub>2</sub>O<sub>3</sub>:C remains one of the most used detectors in dosimetry, with applications in various fields such as personal, medical, environmental and space dosimetry. It has long been known that the main OSL emission band is the blue emission band, centered at 420 nm. It is attributed to F-centers and yields a lifetime of 35 ms [1]. A weaker OSL emission band, observed in the UV (335 nm), has been attributed to F<sup>+</sup>-centers and is associated with a lifetime < 7 ns [2]. The ratio between these two emission bands was shown to be dependent on the ionization density of the radiation and, therefore, on the linear energy transfer (LET) of the radiation [2]. This phenomenon was proposed for LET measurements of clinical proton beams [3].

The mechanism for the UV emission, however, remains unclear and there are many unexplained phenomena associated with it. Step-annealing data of the OSL signal of both blue and UV emission bands suggest that both emissions are related to similar trapping centers with similar thermal stabilities and, therefore, the charges related to both emissions should be the same (e.g., electrons). Nevertheless, the UV emission band increase with time after irradiation, whereas the blue emission does not. Furthermore, to explain both blue and UV emission by invoking electron recombination would require the existence of stable F<sup>2+</sup> centers (bare oxygen vacancies) in the crystal, which are not believed to be stable. Explaining the UV emission by hole recombination cannot explain the fact that the thermal stability of both blue and emission OSL signals are similar.

In this presentation we will summarize what is known about the blue and UV emission bands of Al<sub>2</sub>O<sub>3</sub>:C, how they can be separately measured, how they can be useful for LET measurements, and what the current issues are. We will also discuss possible ideas to move forward in this investigation and briefly introduce a few recent results that shine new light into this problem.

### References

- [1] B. G. Markey, L. E. Colyott, S. W. S. McKeever, *Radiat. Meas.*, 24 (1995) 457-463
- [2] E. G. Yuki
- [3] G. O. Sawakuchi, N. Sahoo, P. B. R. Gasparian, M. G. Rodriguez, L. Archambault, U. Titt, E. G. Yuki

### Acknowledgments

This project was partly supported by the Swiss Nuclear Safety Inspectorate (Contract CTR00491).

## Infrared-stimulated luminescence of garnets

**P. Bilski<sup>1</sup>, A. Mrozi<sup>1</sup>, W. Gieszczyk<sup>1</sup>, M. Kłosowski<sup>1</sup>, Yu. Zorenko<sup>2</sup>,  
K. Kamada<sup>3</sup>, A. Yoshikawa<sup>3</sup>, O. Sidletskiy<sup>4</sup>**

<sup>1</sup>*Institute of Nuclear Physics, Polish Academy of Sciences, Kraków, Poland*

<sup>2</sup>*Institute of Physics, Kazimierz Wielki University, Bydgoszcz, Poland*

<sup>3</sup>*Institute for Material Research, Tohoku University, Sendai, Japan*

<sup>4</sup>*Institute for Scintillation Materials, National Academy of Sciences of Ukraine, Kharkiv, Ukraine*

**E-mail: pawel.bilski@ifj.edu.pl**

Optically stimulated luminescence (OSL) is nowadays widely applied in radiation dosimetry. Oppositely to scintillation and thermoluminescence, there are so far only two materials successfully used in commercial OSL dosimetry systems: Al<sub>2</sub>O<sub>3</sub>:C and BeO. In both these materials luminescence is emitted mostly in the UV range, while stimulation is performed with blue or green light.

In the present work we studied luminescence of Ce-doped garnets under stimulation with the light of another wavelength: infrared (IR, 870 nm). The IR stimulation is commonly applied in luminescence dating with feldspars. The samples under study were: yttrium-aluminium garnets (YAG), mixed gadolinium aluminium-gallium garnets (GAGG), and lutetium-aluminium garnets (LuAG). All crystals were grown with the Czochralski method.

We found that all of the tested samples exhibited a strong IRSL signal. The emission spectrum was peaked between 500 nm and 600 nm, what is typical for the luminescence of Ce in garnets. The most sensitive were some versions of YAG and GAGG crystals. The intensity of their IRSL signal suggests the possibility of their application in radiation dosimetry. We studied also relations between TL and IRSL, which enabled to determine trapping sites responsible for IRSL. From a practical point of view, the most perspective appears to be YAG:Ce, as its IRSL seems to be related to the TL peak at nearly 200°C, which suggests good stability of the signal (fig. 1).

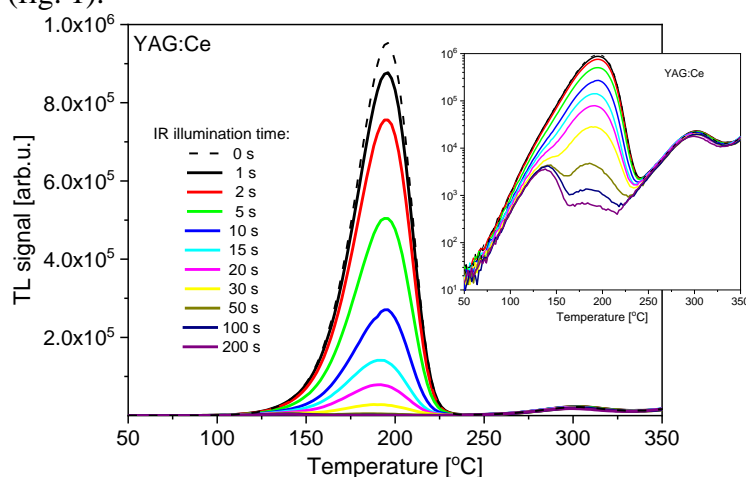


Fig. 1. Influence of IR illumination on TL glow-curve of YAG:Ce.

### Acknowledgments

This work was performed in the frame of Polish NCN UMO-2018/31/B/ST8/03390 project.

## Green-emitting polystyrene scintillators for plastic scintillation dosimetry

**Ł. Kaplon**<sup>1,3</sup>, **G. Moskal**<sup>2,3</sup>

<sup>1</sup> Department of Experimental Particle Physics and Applications, Faculty of Physics, Astronomy and Applied Computer Science of the Jagiellonian University, ul. Lojasiewicza 11, 30-348 Krakow, Poland

<sup>2</sup> Department of Chemical Technology, Faculty of Chemistry of the Jagiellonian University, ul. Gronostajowa 2, 30-387 Krakow, Poland

<sup>3</sup> Total-Body Jagiellonian-PET Laboratory, Jagiellonian University, ul. Lojasiewicza 11, 30-348 Krakow, Poland

**E-mail: lukasz.kaplon@uj.edu.pl**

Plastic scintillators are used in many applications connected with medical devices, for example in time-of-flight positron emission tomography [1], long-axial field of view positron emission tomography scanners [2] and in plastic scintillation dosimetry [3].

Scintillators absorb ionizing radiation and convert its energy into visible light via fluorescence. Purpose of this research is to find optimal fluorescent dyes combination dissolved in polystyrene matrix. Polymer scintillators were synthesized from styrene monomer in bulk radical polymerization [4]. Polystyrene was selected as a base of scintillators due to its water equivalent needed in dosimetry.

In this research one the best fluorescent compound emitting ultraviolet light is combined with a few fluorescent dyes shifting scintillators emission to green light [5]. Emission maxima of manufactured polystyrene scintillators are in green region of visible light (480 – 550 nm) and are close to maximum quantum efficiency of light detectors used in plastic scintillation dosimetry. Light output of scintillators as a measure of gamma radiation conversion into green light will be presented. High light output and matching emission spectra of scintillator with quantum efficiency of light detector is needed to obtain good signal-to-noise ratio in scintillation detectors [6].

Green-emitting plastic scintillators have several advantages over blue-emitting scintillators. Firstly, green light is less attenuated by polystyrene matrix and yellow compounds resulting from radiation damage. Secondly, the longer the wavelength of scintillators light, the smaller portion of Cerenkov light is emitted in this green bandwidth in plastic dosimeter and subtraction of this stem signal is easier. Thirdly, green light around 500 nm is the least attenuated in plastic optical fibers usually glued to plastic scintillators forming scintillation dosimeter.

Results of this work can be used in a reconfigurable three-dimensional detector matrix for measuring the spatial distribution of gamma radiation dose for applications in the preparation of individual patient treatment plans in oncology centers.

### References

- [1] S. Niedźwiecki et al., *Acta Phys. Pol. B*, 48 (2017) 1567-1576.
- [2] P. Moskal, E. Stepień, *PET Clin*, 15 (2020) 439-452.
- [3] L. Beaulieu, S. Beddar, *Phys. Med. Biol.*, 61 (2016) R305-R343.
- [4] Ł. Kaplon et al., *Bio-Algorithms and Med-Systems*, 10 (2014) 27-31.
- [5] Ł. Kaplon, *Acta Phys. Pol. B*, 51 (2020) 225-230.
- [6] A. Wiczonek et al., *PLoS ONE*, 12 (2017) e0186728 1-16.

# Photoluminescence and radioluminescence properties of hafnium oxide-based metal organic framework (MOF)

**M. Orfano<sup>1</sup>, J. Perego<sup>1</sup>, F. Cova<sup>1</sup>, C. Dujardin<sup>2</sup>, A. Comotti<sup>1</sup>, P. E. Sozzani<sup>1</sup>, A. Vedda<sup>1</sup>, A. Monguzzi<sup>1</sup>**

<sup>1</sup> Dipartimento di Scienza dei Materiali, Università degli Studi Milano-Bicocca, Milano, Italy

<sup>2</sup> Institut Lumière Matière, Université Claude Bernard Lyon1, Lyon, France

E-mail: m.orfano2@campus.unimib.it

Porous scintillators are currently investigated for the development of high-sensitivity detectors of radioactive gases based on time-coincidence techniques. According to the fast scintillation response and outstanding compositional tunability,<sup>1</sup> highly porous and fluorescent metal-organic frameworks (MOFs) nanocrystals can be considered as scintillating building blocks for the fabrication of the porous detectors required. We show here the photoluminescence and radioluminescence properties of newly developed hafnium-based nanocrystals (Hf-MOF). The results obtained highlight their fast emission properties, with a fluorescence lifetime lower than 5 ns particularly suitable for time-coincidence based detection techniques, and an excellent fluorescence quantum yield of ~40%. The successful inclusion of an heavy element such as hafnium allows to double the radioluminescence yield of polymeric nanocomposite scintillators based on Hf-MOFs, thus outperforming the reference systems based on lighter zirconium ions.<sup>2</sup> These findings and the huge porosity degree achievable in these materials strongly support their possible use for the fabrication of technologically appealing sensors for the detection of natural and anthropogenic radioactive gases at ultralow concentrations.

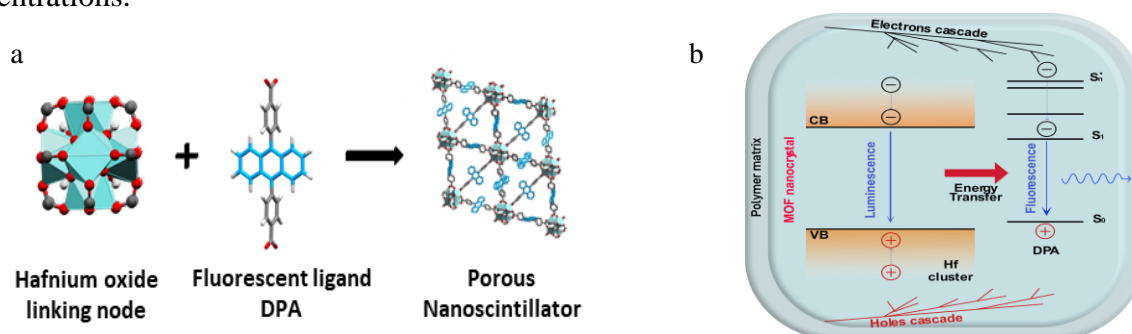


**Fig. 1.** (a) molecular structure of the MOF building blocks. Hafnium oxide clusters frame fluorescent DPA ligands in a crystalline structure. (b) Photo-physics of the scintillation process. Free charges are generated by interaction of the ionizing radiation with the polymer and MOF nanocrystals. They recombine generating emissive singlets on the DPA molecules, where the fluorescence can be detected by a photon counter. The resonance between the X-ray-activated luminescence of the clusters and the DPA absorption enables the sensitization of ligand singlets by radiative and non-radiative energy transfer from excited clusters

## References

- [1] F. P. Doty, C. A. Bauer et al. Scintillating metal-organic frameworks: a new class of radiation detection materials, *Adv. Mater.*, 21, 95–101 (2009).
- [2] J. Perego, I. Villa et al. Composite fast scintillators based on high-Z fluorescent metal-organic framework nanocrystals, *Nature Photonics*, 10.1038/s41566-021-00769-z, (2021).

## Acknowledgments

This work was supported by the SPARTE project (EU funded project from Horizon 2020 research and innovation program under grant agreement No. 899293).

## Characterization of BSO and mixed BGSO crystals for future dual-readout calorimetry

**R. Cala<sup>1,2</sup>, N. Kratochwil<sup>1,3</sup>, L. Martinazzoli<sup>1,2</sup>, M. T. Lucchini<sup>4</sup>, S. Gundacker<sup>5</sup>,  
E. Galenin<sup>6</sup>, O. Sidletskiy<sup>6,7</sup>, M. Nikl<sup>8</sup>, E. Auffray<sup>1</sup>**

<sup>1</sup>European Organization for Nuclear Research, Geneva, Switzerland

<sup>2</sup>Università degli Studi di Milano-Bicocca, Milan, Italy

<sup>3</sup>University of Vienna, Vienna, Austria

<sup>4</sup>Princeton University, NJ, United States

<sup>5</sup>PMI ExMI RWTH Aachen University, Aachen, Germany

<sup>6</sup>Institute for Scintillation Materials NAS of Ukraine, 60 Nauky Ave., Kharkiv, Ukraine

<sup>7</sup>Institute of Physics, Kazimierz Wielki University in Bydgoszcz, Bydgoszcz, Poland

<sup>8</sup>Institute of Physics of the Czech Academy of Sciences, Prague, Czech Republic

**E-mail: roberto.cala@cern.ch**

Bismuth Germanate (BGO) is a well known high density scintillating material widely used in many applications such as high energy physics and medical imaging. The possibility to exploit the Cherenkov emission in addition to scintillation emission of BGO has recently triggered new interest to use such material in Time-of-Flight Positron Emission Tomography scanners [1] and for dual readout calorimetry at future collider experiments.

Bismuth Silicate (BSO) features properties similar to BGO in terms of stopping power and Cherenkov photon yield with a lower scintillation light output but faster effective decay time. This makes BSO more attractive than BGO for some applications which require good timing performances and operation in high rate environments. Mixed crystals such as BGSO make it possible to optimize decay time and light yield [2, 3] based on the detector needs.

We performed a characterization campaign of the optical and scintillation properties of two sets of  $\text{Bi}_4(\text{Ge}_x\text{Si}_{1-x})_3\text{O}_{12}$  ( $x$  varying from 0 to 1) mixed crystals grown with two different methods. The samples were characterized in terms of optical transmission, light output and energy resolution, scintillation kinetics upon X-ray excitation and coincidence time resolution (CTR). A coincidence time resolution of  $259 \pm 8$  ps FWHM was measured for a  $6 \times 6 \times 1$  mm<sup>3</sup> sized plate with  $x = 0.5$  coupled to a  $6 \times 6$  mm<sup>2</sup> SiPM from Broadcom, while better CTR of  $208 \pm 2$  ps was measured for a  $2 \times 2 \times 3$  mm<sup>3</sup> size sample ( $x = 0.4$ ) coupled to a  $4 \times 4$  mm<sup>2</sup> SiPM.

In addition we demonstrated the possibility to efficiently separate the Cherenkov and scintillation light contribution using a time correlated single photon counting setup and placing optical filters between the crystal and the stop detector. Such a technique could be exploited in a crystal-based dual readout calorimeter to improve the energy resolution for hadronic showers and jets [4].

### References

- [1] Kratochwil et al 2020, Phys. Med. Biol. 65 115004.
- [2] Ishii et al 2002, Optical Materials 19 201-212.
- [3] Galenin et al 2015, Functional Materials 22 No.4 p423-428.
- [4] Lucchini et al 2020 JINST 15 P11005.

### Acknowledgments

This work was performed in the framework of the Crystal Clear Collaboration.

## **Mechanisms of radiochromic response in polymer gel dosimeters**

**J. Marek<sup>1</sup>, M. Maryński<sup>1</sup>**

<sup>1</sup>*Faculty of Applied Physics and Mathematics, Institute of Nanotechnology and Materials Engineering,  
Gdańsk University of Technology, Narutowicza 11/12 Gdańsk, Poland*

**E-mail: [marek.maryanski@pg.edu.pl](mailto:marek.maryanski@pg.edu.pl)**

Polymer gel dosimeters are soft-tissue-equivalent gels in which radiation induces free-radical chain polymerization of acrylic monomers to form either nanoparticles that scatter visible light or oligomeric color centers, depending on formulation. The latter is a reversible process and allows for multiple usage of the dosimeter. Both change the spectrum of transmitted light and both lend themselves to high-definition three-dimensional readout by computed transmission laser tomography. Both the nanoparticles and the color centers are trapped in the gel network, forming stable 3D images of dose distributions. Applications to radiosurgery and radiotherapy dosimetry and patient-specific quality assurance have been amply demonstrated in both radiosurgery and radiotherapy, including photons, protons and various brachytherapy sources. In proton therapy, polymer gel formulations have been developed that are LET-independent, hence do not exhibit response quenching in the Bragg peak region. Still other formulations have enhanced response in proportion to LET. The author's recent results show the feasibility of a formulation in which there exists an optical signature of LET such that a single exposure of a gel phantom records 3D distributions of both dose and LET. Each can be digitized by properly configured optical CT.

Mechanisms of radiochromic response in polymer gel dosimeters include the full spectrum of energy transfer processes that also have their relevant analogues in biological tissues: 1) free-radical products of water radiolysis, 2) direct electronic excitations in acrylic monomers and subsequent bond dissociation, 3) direct ionization of acrylic monomers. All three lead to the initiation of free-radical chain polymerization of the monomers whose concentration in the gel is typically between 0.1M and 1M and whose average nearest-neighbor distance is on the order of 1nm. Relative contributions from these three pathways of polymerization initiation as well as kinetics of polymerization and termination is subject to fine control by the chemical composition of the gel.

The other aspect of radiochromic response in polymer gel dosimeters is dose- and/or LET-dependent absorption spectrum of visible light. Both Mie scattering on polymerized nanoparticles and absorption spectra of color centers are sensitive to their immediate molecular environment which again is a function of chemical composition of the gel and the protocol of its preparation and as such is subject to fine control. This is the subject of the author's current work.

## **Luminescence dosimetry in proton therapy**

**P. Olko<sup>1</sup>, P. Bilski<sup>1</sup>, J. Gajewski<sup>1</sup>, M. Kłosowski<sup>1</sup>, B. Marczevska<sup>1</sup>**

<sup>1</sup>*Institute of Nuclear Physics PAN, Radzikowskiego 152, 31-342 Kraków, Poland*

**E-mail: pawel.olko@ifj.edu.pl**

Protons with energies from about 60 MeV to 250 MeV are useful for cancer treatment because of the phenomenon of the Bragg peak i.e. increasing of energy deposition at the end of protons path in tissue. The proton energy can be selected in such a way that the particles range slightly exceeds the position of the tumor, which keeps save healthy tissues laying deeper. Therefore, a big advantage of protons is that the unwanted doses to healthy organs are largely reduced as compared to high energy X-rays used in conventional radiotherapy. Progress in proton radiotherapy is closely related to the latest developments in the acceleration techniques, methods of beam delivery, dosimetry, quality control and diagnostics. One of the most significant innovations was the introduction of Pencil Beam Scanning (PBS) technology, which eliminated patient specific collimators and compensators and allowed for irradiations with excellent dose distribution. However, PBS technique is very demanding for dosimetry and Quality Assurance (QA).

At the Institute of Nuclear Physics Polish Academy of Sciences (IFJ PAN) regular patient treatment with PBS technique started in November 2016. Several methods and techniques were developed and applied at IFJ PAN to support clinical dosimetry and QA. Pairs of MTS-7 and MTS-6 LiF:Mg,Ti thermoluminescence (TL) detectors were applied for investigation of scattered neutron doses in anthropomorphic phantoms [1]. MTS-N (LiF:Mg,Ti) powder was used for the test mailed dosimetry audit of the PBS beam. TL foils based on MCP-N (LiF:Mg,Cu,P) and dedicated TL readers were developed and applied for in-phantom two dimensional (2D) dosimetry [2]. Similar development but based on flexible sheets made of a polymer (PDMS) with the embedded LiF:Mg,Cu,P or LiMgPO<sub>4</sub> grains and the self-developed 2D OSL setup, was applied for direct measurements of 3D dose distributions of the proton beam [3]. A real-time dosimetry system PORTOS with home grown LiMgPO<sub>4</sub> crystal was developed to measure not only the beam structure with a millisecond resolution and also the integrated dose [4]. TL/OSL detector signal is practically independent on dose rate, which becomes important for very-high dose rate (FLASH) proton therapy. However, more research is needed to reduce the major disadvantage of luminescence dosimeters i.e. the energy (LET) dependence, especially for low energy protons.

### **References**

- [1] A. Wochnik et al, *Phys. Med. Biol.* 66 (2021) 035012.
- [2] P. Olko et al *Radiat. Prot. Dosim.*, 118 (2006) 213.
- [3] M. Sadel et al, *Radiat. Meas.*, 133 (2020) 106293 and *Radiat. Meas.*, 133 (2020) 106255.
- [4] B. Marczevska et al *Radiat. Meas.* 136 (2020) 106408.

### **Acknowledgments**

The study was partially supported by the EU Horizon 2020 project INSPIRE Grant Agreement 730983

## Development of red-emitting oxide scintillator for decommissioning Fukushima Daiichi Nuclear Power Plant

**S. Ishizawa<sup>1</sup>, S. Kurosawa<sup>1,2</sup>, Y. Kurashima<sup>1</sup>, A. Yamaji<sup>1,2</sup>, S. Ishikawa<sup>1,3</sup>, C. Fujiwara<sup>1</sup>,  
A. Yoshikawa<sup>1,2,3</sup>, H. Tanaka<sup>4</sup>**

<sup>1</sup>Institute of Materials Research, Tohoku University, 2-1-1 Katahira, Sendai, Miyagi, Japan

<sup>2</sup>New Industry Creation Hatchery Center, Tohoku University, 6-6-10 Aoba, Sendai, Miyagi, Japan

<sup>3</sup>C&A Corporation, 6-6-40, Aoba, Aramaki, Aoba-ku, Sendai, Japan

<sup>4</sup>Institute for Integrated Radiation and Nuclear Science, Kyoto University, Kumatori, Osaka, Japan

**E-mail: ishizawa@imr.tohoku.ac.jp**

Decommissioning of the Fukushima Daiichi Nuclear Power Plant (1F) should be operated with safety, and the distribution of high-dose radioactive debris (more than 10 Sv/h) in the reactor must be revealed. In such high-dose-rate, the conventional semiconductor components of photosensors and electric circuits can be damaged due to ionizing radiation. Therefore, a real-time remote radiation monitoring system has been proposed with scintillator and long silica optical fiber [1].

In such high-dose-rate, the fiber itself is emitting below 600 nm mainly due to Cherenkov or scintillation photon originating from the defect in the fiber, so that a red-emitting scintillator is required. Cs<sub>2</sub>HfI<sub>6</sub> (CHI) has an emission wavelength of 700 nm and high light output of 64,000 photons/MeV [2]. However, CHI has a severely hygroscopic nature, and the package is required for CHI; We cannot apply to alpha-particle detection such as <sup>238</sup>Pu and <sup>239</sup>Pu.

We proposed Yb-doped La<sub>2</sub>Hf<sub>2</sub>O<sub>7</sub> (Yb:LHO) as a red-emitting oxide scintillator with no hygroscopic nature, grown by Core Heating (CH) Method [3]. Figure 1 shows radioluminescence spectra for Yb:LHO and Cr:α-Al<sub>2</sub>O<sub>3</sub> as a typical red-emitting scintillator, excited by X-rays. The peak wavelengths of Yb:LHO and Cr:α-Al<sub>2</sub>O<sub>3</sub> were 974 and 692 nm, respectively. We successfully confirmed Yb:LHO had a peak wavelength of more than 600 nm.

The emission spectra were measured at several dose-rate condition for Yb:LHO irradiated with gamma rays from a <sup>60</sup>Co source with an activity of ~100 TBq at the Gamma-ray Irradiation Facility in Institute for Integrated Radiation and Nuclear Science, Kyoto University. The effective air dose rates in this setup were the same level as the that of inside of the 1F. In this report, we show the result of the above experiments.

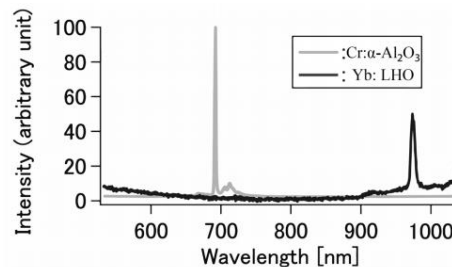


Fig. 1 Radioluminescence spectra for Yb:LHO and Cr:α-Al<sub>2</sub>O<sub>3</sub> excited by X-rays.

### References

- [1] C. Ito et al., ICONE22-31110, V006T13A021 (2014).
- [2] S. Kodama et al., Appl. Phys. Express, 13 (2020) 4.
- [3] Y. Kurashima et al., Cryst. Growth Des., 21 (2021) 572–578.



## UV detector based on polycrystalline CVD diamonds

**K.Fabisiak<sup>1</sup>, K.Paprocki<sup>1</sup>, S.Łoś<sup>2</sup>, M. Szybowicz<sup>3</sup>, J. Winiński<sup>4</sup>**

<sup>1</sup>*Institute of Physics, Kazimierz Wielki University, Powstańców Wielkopolskich 2, 85-064 Bydgoszcz, Poland*

<sup>2</sup>*Institute of Mathematics and Physics, UTP University of Science and Technology, Profesora Sylwestra Kaliskiego 7, 85-796 Bydgoszcz, Poland*

<sup>3</sup>*Faculty of Materials Engineering and Technical Physics, Institute of Materials Research and Quantum Engineering, Poznań University of Technology, Piotrowo 3, 61-138 Poznań, Poland*

<sup>4</sup>*Oncology Center, Medical Physics Department, ul. Romanowskiej 2, 85796 Bydgoszcz, Poland*

**E-mail: [kfab@ukw.edu.pl](mailto:kfab@ukw.edu.pl)**

Due to remarkable physical properties CVD diamond is considered as material for the fabrication of novel radiation detectors. In fact, they have several properties which make them suitable for detector fabrication: radiation hardness, chemical resistance, high thermal conductivity, high resistivity, high carrier mobility and a large energy bandgap (5.5 eV). The latter makes them insensitive to visible radiation and allows low noise measurements without any cooling. Thermally stimulated luminescence (TL), cathodoluminescence (CL), X-ray diffraction (XRD) and Raman spectroscopy of CVD diamond films grown on silicon substrates have been studied in order to obtain information on defects created during the growth, which induce the levels within the gap. TL between 300 K and 670 K, and CL from 200 nm to 1200 nm have been measured.

TL spectra of CVD diamond layers have been registered after they exposure to UV radiation in the wavelength below 260 nm. The glow curves show a peak located around 510 K with different intensities, depending on the sample thickness, associated with a trap of energy, equal to 0.52 eV and with attempt-to-escape-time of the order of  $10^3\text{s}^{-1}$ . In the CL spectra the broad bands were observed at  $428\pm 1$  nm ( $2.815\pm 0.001$  eV) and  $603\pm 1$  nm ( $2.056\pm 0.004$  eV). The TL and CL results were correlated with diamond quality estimated from Raman spectroscopy measurements and preferential ordering of crystallites in the layers estimated from XRD measurements.

### References

- [1] Chen, M.; Jian, X.; Sun, F.; Hu, B.; Liu, X. Development of diamond-coated drills and their cutting performance. *J. Mater. Process. Technol.* 2002, 129, 81–85.
- [2] Sein, H.; Ahmed, W.; Rego, C. Application of diamond coatings onto small dental tools. *Diam. Relat. Mater.* 2002, 11, 731–735.
- [3] Paprocki, K.; Fabisiak, K.; Łoś, S.; Winnicki, J.; Malinowski, P.; Fabisiak, R.; Franków, W. Morphological, cathodoluminescence and thermoluminescence studies of defects in diamond films grown by HF CVD technique. *Opt. Mater.* 2020, 99, 109506.

## Investigation of the UV emission mechanism in Al<sub>2</sub>O<sub>3</sub>:C using pulsed OSL and photo-transfer experiments

O. V. Pakari<sup>1</sup>, L. Bossin<sup>1</sup>, J. B. Christensen<sup>1</sup>, E.G. Yukihiro<sup>1</sup>

<sup>1</sup>Department of Radiation Safety and Security, Paul Scherrer Institut 5232 Villigen PSI, Switzerland

E-mail: Oskari.pakari@psi.ch

Al<sub>2</sub>O<sub>3</sub>:C is a versatile and well-studied material used in the field of radiation detection, notably for its favorable optically stimulated luminescence (OSL) properties. As such, the OSL of Al<sub>2</sub>O<sub>3</sub>:C has found practical application in personnel, space, and medical dosimetry, among others. The efficacy of Al<sub>2</sub>O<sub>3</sub>:C as a dosimeter is believed to stem from both an abundance of defect traps as well as a high concentration of luminescent recombination centers. The main recombination centers have been correlated with the emissions of excited F and F<sup>+</sup>-centers. With a lifetime of 35 ms, an excited F-center gives the characteristic blue emission at 420 nm [1]. Conversely, excited F<sup>+</sup>-center emissions with a lifetime of < 7 ns are hypothesized to be responsible for the UV emission around 340 nm [2]. Using pulsed OSL (POSL) methods, one can exploit the difference in decay time of the respective excited states and thus measure their relative contribution. Despite a long history, the exact luminescence mechanisms of the UV component have remained elusive. In particular, the time dependence of the UV emission, Linear Energy Transfer, and dose effects have difficulties being reconciled with previously proposed models, e.g. [3]. In this work, we present new evidence regarding the UV emission mechanism obtained using POSL and photo-transfer experiments. Using a range of samples of Al<sub>2</sub>O<sub>3</sub>:C with apparently differing deep trap structure (as revealed by photo-transfer), we show new correlations between the deep trap structure and the UV and blue emission bands. These correlations call into question the currently hypotheses regarding the UV emission and present new evidence that could ultimately serve to constrain models for the OSL emission mechanism of Al<sub>2</sub>O<sub>3</sub>:C.

### References

- [1] K. H. Lee, and J. H. Crawford, Luminescence of the F center in sapphire, *Physical Review B*, V. 19, No. 6, 1979-03.
- [2] S. W. S. McKeever *et al.*, Characterisation of Al<sub>2</sub>O<sub>3</sub> for Use in Thermally and Optically Stimulated Luminescence Dosimetry, *Radiation Protection Dosimetry*, V. 84, No. 1, 1999-08.
- [3] E.G. Yukihiro *et al.*, Effect of high-dose irradiation on the optically stimulated luminescence of Al<sub>2</sub>O<sub>3</sub>:C, *Radiation Measurements*, V. 38, No. 3. 2004-06.

### Acknowledgments

This work was supported by a Swiss National Science Foundation SPARK grant (project number CRSK-2\_196453). The Risø TL/OSL-DA-20 reader (DTU Nutech, Denmark) was acquired with partial support from the Swiss National Science Foundation (R'Equip project 206021\_177028).

## Improving linear energy transfer measurements using automated OSL readers

**J.B. Christensen<sup>1</sup>, O.V. Pakari<sup>1</sup>, L. Bossin<sup>1</sup>, E.G. Yukihara<sup>1</sup>**

<sup>1</sup>Paul Scherrer Institute, Forschungsstrasse 111, 5232 Villigen PSI, Switzerland

**E-mail: jeppe.christensen@psi.ch**

Particle therapy centres worldwide increasingly rely on the relative biological effectiveness (RBE) of protons and heavier ions to optimize treatment plans. The RBE is typically predicted through the linear energy transfer (LET) computed by means of Monte Carlo methods as LET measurements remain a challenge if possible at all. Hence, there is a need for a point-like (or 2D) detector capable of measuring both the LET and the dose to validate complex treatment plans. Moreover, as the interest for applying ultra-high dose rates (FLASH) in clinical fields also increases, the ideal LET detector would also be dose rate independent.

Different optically stimulated luminescence detectors (OSLDs) have been proposed as candidates for such simultaneous dose and LET measurements. Particularly Al<sub>2</sub>O<sub>3</sub>:C exhibits attractive properties for said measurements due to two emission bands which can be related to the dose and the LET given proper calibrations [1]. The material was in addition recently demonstrated to be dose rate independent in proton beams up to 150 kGy/s [2] and as such applicable to FLASH dosimetry. One emission band is centred in the blue region (~ 420 nm) with a long 35 ms lifetime and the other in the UV region (~ 330 nm) with a fast lifetime on the nanosecond timescale, which allows the two bands to be separated using pulsed OSL. The ratio of the two emission bands correlates well with the LET. In this work we use OSL powder mixed with a binder and cast to a < 100 µm thickness polymer sheet, which allows for a versatile OSLD film that can be used both as point like or 2D dosimeter. Furthermore, we discuss how batch-to-batch variations of the OSLD sheets and different OSLD sizes affect the luminescence response and thus the derived dose and LET. The transmission of the UV emission band through the polymer sheet is particularly prone to variations, which is crucial to the LET measurement, as the transmission of the blue emission band is less sensitive to variations.

We demonstrate how automated low-LET irradiations of each OSLD can be used as reference to correct both the blue and UV emission bands for OSLD size and material differences. The standard deviation of the quantity of interest for five OSLDs irradiated under the same conditions is, after application of automated corrections, of the order of 1.5 %. Given the dose rate independency and excellent reproducibility for dose and LET measurements, the Al<sub>2</sub>O<sub>3</sub>:C OSLDs are suitable for both ultra-high dose rate and LET measurements in proton beams.

### References

- [5] D. A. Granville, N. Sahoo, G. O. Sawakuchi, *Phys. Med. Biol.* 59 (2014) 4295-4310.
- [6] J. B. Christensen, E. G. Yukihara et al, *Phys. Med. Biol.* 66 (2021) 085003.

### Acknowledgments

This work was partially funded by the Swiss Federal Nuclear Safety Inspectorate ENSI (Contract no. CTR00491). The Risø TL/OSL-DA-20 reader (DTU Nutech, Denmark) was acquired with partial support from the Swiss National Science Foundation (R'Equip project 206021\_177028).

## **The purposes, principles and common techniques used in radiation**

**J. Winięcki<sup>1,2</sup>**

<sup>1</sup>*Department of Oncology and Brachytherapy, Collegium Medicum in Bydgoszcz, Nicolaus Copernicus  
University in Toruń, Poland*

<sup>2</sup>*Medical Physics Department, Oncology Center in Bydgoszcz, Poland*

**E-mail: [j.winięcki@cm.umk.pl](mailto:j.winięcki@cm.umk.pl)**

Radiotherapy is perhaps one of the most sophisticated methods used by modern oncology. Ionizing radiation, discovered at the turn of the nineteenth and twentieth centuries, initially tamed, though not immediately understood, quickly found its use in the fight against a terrible disease, which is cancer. Nowadays, millions of people are gaining a second life every year thanks to remarkable advances in the physics of radiation, particularly in the field of interaction of ionizing radiation with a living matter.

The aim of this speech is to present the honourable group of outstanding scientists, participants of the LUMDETR 2021 conference, the purposes, principles and common techniques used in modern radiotherapy.

The cause of the success of radiotherapy will be elucidated, consisting in a much greater sensitivity of cancer cells to the harmful effects of ionizing radiation compared to normal cells. To achieve the clinical goal, a specific amount of radiation must be delivered to the tumor area. On the other side the dose absorbed by the surrounding healthy tissues should also be minimized to minimize the risk of complications. The final distribution of the dose in the patient's body is the result of the use of sophisticated tools for the production of radiation and the skillful modification of beam parameters by medical physicists working in radiotherapy. Before starting therapy, it should be verified whether the planned dose distribution can actually be achieved. Measurement methods used in clinical dosimetry must take into account the specific clinical conditions existing in the treatment room, these methods must be non-invasive and, very importantly, must not interfere with the course of therapy. The most important techniques used in radiotherapy will be discussed, with an indication of the typical difficulties occurring during their implementation.

Dosimetry techniques used in laboratory and industrial settings often do not match clinical conditions. The development of radiotherapy requires the construction of new measurement tools to verify the absorbed dose. Scientists and designers should understand the rules of radiation therapy in order to make these tools more effective.

### **References**

- [1] Winięcki, J., 2020. Physical Sciences Reviews 0.
- [2] Bajek, A., Tylkowski, B. (Eds.), 2021. Medical Physics. De Gruyter.

## **What is plan quality in radiotherapy?**

**T. Piotrowski**<sup>1,2</sup>

<sup>1</sup> *Department of Electroradiology, Poznan University of Medical Sciences, Poznan, Poland*

<sup>2</sup> *Department of Medical Physics, Greater Poland Cancer Centre, Poznan, Poland*

**E-mail: [tomasz.piotrowski@icloud.com](mailto:tomasz.piotrowski@icloud.com)**

Plan quality is commonly assessed by evaluating the dose distribution calculated by the treatment planning system. Evaluating the 3D dose distribution is not easy, however; it is hard to fully evaluate its spatial characteristics and we still lack the knowledge for personalising the prediction of the clinical outcome based on individual patient characteristics. Additionally, the calculated dose distribution is not exactly the dose delivered to the patient due to uncertainties in the dose calculation and the treatment delivery, including variations in the patient set-up and anatomy. Consequently, plan quality also depends on the robustness and complexity of the treatment plan.

## Basic characteristics of dose distributions of photons beam for radiotherapeutic applications using YAG:Ce crystal detectors

**S. Witkiewicz-Lukaszek<sup>1</sup>, J. Winięcki<sup>2</sup>, P. Michalska<sup>2</sup>, S. Nizhankovskiy<sup>3</sup>, Yu. Zorenko<sup>1</sup>**

<sup>1</sup>*Institute of Physics, Kazimierz Wielki University, Pow. Wielkopolskich 2, Bydgoszcz, 85090, Poland*

<sup>2</sup>*Oncology Center, Medical Physics Department, Romanowskiej 2, Bydgoszcz, 85796, Poland*

<sup>3</sup>*Institute for Single Crystals, National Academy of Sciences of Ukraine, av. Nauki 60, 61178 Kharkiv, Ukraine*

**E-mail: s-witkiewicz@wp.pl**

The primary goal of therapy is this optimizing the radiation properties so that a sufficiently large dose of radiation is delivered to tumor while minimizing the irradiation of healthy tissues. The use of an electron beam for radiotherapeutic applications requires that that the spatial distribution of the delivered dose (profile) is uniform in the irradiated volume object and as small as possible outside of it. In fact, however, due to the impacts, it is not possible to achieve this profile. It is therefore defined parameter referred to as flatness [1].

Thermoluminescence dosimetry (TLD) is a versatile tool for the assessment of dose from ionising radiation. Ce<sup>3+</sup> doped Y<sub>3</sub>Al<sub>5</sub>O<sub>12</sub>:Ce garnet (YAG:Ce) with a  $\rho = 4.5 \text{ g/cm}^3$ ;  $Z_{\text{eff}} = 35$  was recently emerged as a possible alternative material in radiotherapy applications due to its excellent radiation stability, high yield ( $\sim 21 \text{ Ph/KeV}$ ), acceptable decay time (70 ns) [3] and good position of main TSL peak around 280 K (Fig.1). Furthermore, the new types of composite TLD detectors based on the YAG:Ce single crystal and single crystalline films of Ce<sup>3+</sup> doped Lu<sub>3</sub>Al<sub>5</sub>O<sub>12</sub> garnet (LuAG:Ce) were developed using the LPE growth method for simultaneous registration of the different components of ionization radiation [2].

In the current work we have used the three sets YAG:Ce TSL detectors, prepared with the same Czochralski grown crystal, as tool for the investigation of the uniformity of ionising radiation dose (Fig.1). The presented in Fig.1a results shown that intensity of TSL peaks strongly decrease from the centrum of target to their boundary. This means that the intensity of the TSL curves is influenced not only by the dose but also by the energy of radiation. A special wedge was used to maintain dose uniformity (Fig.1b). The application of such wedges results in much closer intensity peaks of TL curves of detectors placed in the different parts of target.

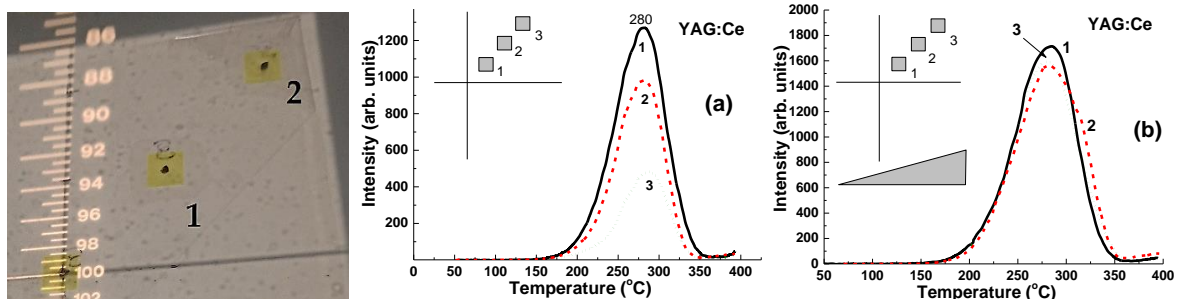


Fig.1. The location of the YAG:Ce crystal detectors on a 15x15 cm field target (left) and TL glow curves of three YAG:Ce crystal detectors' irradiated by X ray (a) and irradiated across wedge (b) (right).

### References

- [1] E. Oponowicz, *Medyczne akceleratory elektronów*, Warszawa 2014.
- [2] S. Witkiewicz-Lukaszek, V. Gorbenko, A. Mrozik, P. Bilski, e. a. *Rad. Measur.*128 (2019) 106.
- [3] L. Chen, S. O'Keeffe, S. Chen, P. Woulfe, e. a. *J. Lightwave Technology* 37 (2019) 4741.

## Time-resolved fluorescence study of bacterial spores treated by hydrogen peroxide vapour for monitoring decontamination process

**O. Rebane<sup>1,2</sup>, S. Babichenko<sup>2</sup>, K. Chernenko<sup>3</sup>, V. Nagirnyi<sup>1</sup>, I. Romet<sup>1</sup>, M. Kirm<sup>1</sup>**

<sup>1</sup>*Institute of Physics, University of Tartu, W. Ostwald Str. 1, 50411 Tartu, Estonia*

<sup>2</sup>*LDI Innovation OÜ, Sära Str. 7, 75312 Peetri, Estonia*

<sup>3</sup>*MAX IV Laboratory, Lund University, P.O. Box 118, SE-22100 Lund, Sweden*

**E-mail: ott.rebane@ut.ee**

The fluorescence of bacterial spores has been used to design a novel luminescent detector intended for real-time monitoring of the efficiency of vaporised hydrogen peroxide decontamination procedure [1]. Here, we study the underlying physical phenomena behind this detector principle using a time-resolved luminescence spectroscopy and discuss the feasibility of the implementation of time-resolved fluorescence technique as a next iteration in the detector development for decontamination monitoring.

The efficiency of pathogen decontamination procedures is often monitored by their impact on an anthrax-simulating spore-forming bacterium species *Bacillus atrophaeus*. In the present research, the spores of *Bacillus atrophaeus* were exterminated by using vaporized hydrogen peroxide (VHP; 600 ppm for 20 min). The VHP-deceased spore samples were compared with the untreated viable spore samples by using time-resolved fluorescence spectroscopy. The study was performed under UV (275 nm) and VUV (190 nm) excitation at room temperature and the time-resolved fluorescence spectra in the UV-Vis range were analysed. The study was carried out with synchrotron radiation with a time-resolution of ~160 ps at the FinEstBeAMS beamline at the MAX IV Lab. The comparison of the fluorescence decay curves of the VHP treated and viable spores revealed that for the VHP-treated spores there is a significant intensity reduction for all 3 exponential decay components analysed, while the relevant decay times for the deceased spores become longer. Both observations can be a manifestation of the reduced energy transfer between the 3 fluorescent amino acids (Phe – Tyr – Trp) involved in the spore fluorescence process. This effect indicates that the time-resolved detection mode can be applied in the detector design for monitoring decontamination process in real time. The experimental findings, including changes in emission and excitation spectra together with the underlying biophysical processes responsible for fluorescence will be discussed in our contribution.

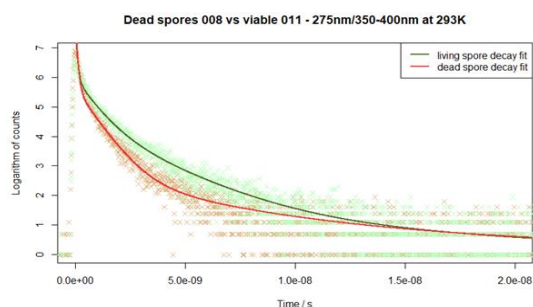


Figure 2. A comparison of decay curves of 350-400 nm fluorescence for spores treated by H<sub>2</sub>O<sub>2</sub> vapor (red line) and viable spores (dark green line).

### References

- [1] O. Rebane, P. Wilska, I. Sobolev, L. Poryvkina, L. M. Kirm, H. Hakkarainen, S. Babichenko (2021), *Proceedings of the Estonian Academy of Sciences*, 70 (2021), 51-61

## **LiMgPO<sub>4</sub>:RE – review of the results of 7-years investigations on new dosimetric crystals**

**W. Gieszczyk<sup>1</sup>, P. Bilski<sup>1</sup>, B. Marczevska<sup>1</sup>, M. Kłosowski<sup>1</sup>**

<sup>1</sup>*The Henryk Niewodniczański Institute of Nuclear Physics Polish Academy of Sciences (IFJ PAN),  
Radzikowskiego 152, PL31342 Krakow, Poland*

**E-mail: Wojciech.Gieszczyk@ifj.edu.pl**

Lithium magnesium phosphate (LiMgPO<sub>4</sub>, LMP) is a relatively new and very promising luminescent material that nowadays undergoes extensive studies. It has attracted huge attention of scientific society because it is characterized by a very high sensitivity to ionizing radiation, comparable or even higher than that of LiF:Mg,Ti (a commonly used standard material for TL radiation dosimetry) or Al<sub>2</sub>O<sub>3</sub>:C and BeO (the only materials commercially available for OSL measurements). Among the possible dopants, rare-earth (RE) elements are considered as the most suitable for the needs of radiation measurements applications due to their 4f-4f electronic transitions that give a narrow luminescence emission over the well-defined spectral range. It is also worth mentioning that, in most cases, the LMP material is investigated in form of powders or cold-pressed and sintered pellets. However, the group of scientists from the IFJ PAN, Krakow, is probably the only research group in the world that studies this material in form of melt-grown crystals. Since 2014, the LMP crystals are obtained in our crystal growth facility using a novel micro-pulling-down ( $\mu$ -PD) method and the influence of various crystal growth conditions on luminescent and dosimetric properties of the obtained crystals is continuously investigated. In this work, a review of results obtained over 7-years investigations of the LMP compound by the research group from IFJ PAN in Krakow will be presented. A crystal growth technology, luminescent properties investigations and possible new areas of applications, will be discussed as well. Comparison of the LMP performance in different physical forms (i.e. powders, crystals, foils) [1] under the different modes of stimulation [2], as well as the application in various fields of radiation dosimetry (over both low and high dose ranges) [3], the efficiencies for different radiation qualities (photons, protons, alpha particles, neutrons) [4] and the applications for real-time measurements [5], will be the topics covered by this presentation. It is important to note that the obtained results suggest that the LiMgPO<sub>4</sub> compound may be considered as promising material for routine applications in luminescent radiation dosimetry.

### **References**

- [1] D. Kulig, W. Gieszczyk, B. Marczevska, P. Bilski, M. Kłosowski, A.L.M.C. Malthez. *Radiation Measurements* 106 (2017), 94-99.
- [2] A. Sas-Bieniarz, B. Marczevska, M. Kłosowski, P. Bilski, W. Gieszczyk. *Journal of Luminescence* 218 (2020), 116839.
- [3] D. Kulig, W. Gieszczyk, P. Bilski, B. Marczevska, M. Kłosowski. *Radiation Measurements* 85 (2016), 88-92.
- [4] W. Gieszczyk, P. Bilski, M. Kłosowski, T. Nowak, L. Malinowski. *Radiation Measurements* 113 (2018), 14-19.
- [5] A. Sas-Bieniarz, B. Marczevska, P. Bilski, W. Gieszczyk, M. Kłosowski. *Radiation Measurements* 136 (2020), 106408.



# Trapping and recombination mechanisms in YAP:Mn<sup>2+</sup> crystals as promising TL/OSL detectors

Ya. Zhydachevskyy<sup>1,2</sup>

<sup>1</sup> *Institute of Physics, Polish Academy of Sciences, Warsaw, Poland*

<sup>2</sup> *Lviv Polytechnic National University, Lviv, Ukraine*

**E-mail: zhydach@ifpan.edu.pl**

Mn<sup>2+</sup>-doped YAlO<sub>3</sub> (YAP) is known as a perspective high-Z material applicable for thermoluminescent (TL) or optically stimulated luminescent (OSL) dosimetry of ionizing radiation (see [1] and references therein). In particular, the green-color emission from Mn<sub>Y</sub><sup>2+</sup> ions occurring at the main TL peak at about 200 °C can be used for this purpose. This TL signal fades strongly at daylight (bleaching effect), therefore optical stimulation with visible light can be used for its readout [2].

The TL and OSL properties of YAP:Mn<sup>2+</sup> crystals will be shortly reviewed, demonstrating the prospects and benefits of this material for radiation dosimetry.

In addition, recent experimental results obtained using EPR, optical absorption, photoluminescence, and thermally stimulated luminescence techniques will be analyzed in more details. The aim of the studies was to get a better insight into the recharging processes of Mn<sup>2+</sup> ions, occurring at and above room temperature. As a result, a general model of trapping and recombination mechanisms responsible for thermoluminescence of YAP:Mn crystals above room temperature is proposed [3]. The role of Mn<sub>Y</sub><sup>2+</sup> centers themselves, defect-related electron and hole traps intrinsic to YAP lattice (including the electron trap at 1.7 eV depth responsible for the dosimetric TL peak at about 200 °C), as well as deeper (≥2.0 eV) dopant-related electron and hole traps like Mn<sub>Al</sub><sup>4+</sup> and Cr<sub>Al</sub><sup>3+</sup> centers, will be discussed.

## References

- [1] Ya. Zhydachevskii et al., Energy response of the TL detectors based on YAlO<sub>3</sub>:Mn crystals, *Radiat. Meas.* 90 (2016) 262-264.
- [2] Ya. Zhydachevskii et al., Time-resolved OSL studies of YAlO<sub>3</sub>:Mn<sup>2+</sup> crystals, *Radiat. Meas.* 94 (2016) 18-22.
- [3] H. Przybylińska, Ya. Zhydachevskyy, A. Grochot et al., EPR studies of Mn<sup>2+</sup> ions and trapping mechanisms in thermally stimulated luminescence of YAlO<sub>3</sub>:Mn crystals, *to be published*.

## Acknowledgments

The work was supported by the Polish National Science Centre (project no. 2018/31/B/ST8/00774), by the NATO SPS Project G5647, and by the Ministry of Education and Science of Ukraine (project DB/Kinetyka).

## 2D OSL dosimetry based on LiMgPO<sub>4</sub> powder embedded into the flat sheet silicone foils

**M. Sadel<sup>1</sup>, J. Gajewski<sup>1</sup>, J. Swakoń<sup>1</sup>, P. Bilski<sup>1</sup>, U. Sowa<sup>1</sup>, T. Kajdrowicz<sup>1</sup>, A. Pedracka<sup>1</sup>, T. Horwacik<sup>1</sup>, M. Kłosowski<sup>1</sup>**

<sup>1</sup>*Institute of Nuclear Physics Polish Academy of Sciences, PL-31342 Krakow, Poland*

**E-mail: [michal.sadel@ifj.edu.pl](mailto:michal.sadel@ifj.edu.pl)**

In modern radiotherapy techniques (RT), such as proton therapy, the necessary doses to a treated volume (tumour), are delivered using complex and high-resolution treatment plans, in order to optimize curative effects and lowering side effects. Therefore, there is an unmet need to provide precise and accurate dosimetry, using techniques which enable more than one dimensional direction measurement e.g. two-dimensional (2D) dosimetry.

One of the new and promising approach to the 2D dosimetry, based on optically-stimulated luminescence (OSL) phenomena. By using the prototype 2D OSL dosimeters in the form of flat and flexible sheets made of a polymer, with the embedded OSL material in the form of powder (LiMgPO<sub>4</sub>, LMP), and self-developed optical imaging setup, consisting of an illuminating light source and high-sensitive CCD camera, a real 2D proton dose distribution has been verified [1,2].

Present work concerning a step forward into the future clinical applications of the recently developed 2D OSL technology, and focusing on investigating the possibility of using 2D LMP OSL silicone foils, to verify the real proton depth dose distribution of the eyeball phantom. To achieve that, during a specially prepared experiment, 2D OSL signals captured from a stack of 40 prototype circular silicone 2D LMP foils attached to PMMA holders behind a hemispherical phantom, were analysed after proton irradiation using a dedicated patient irregular collimator and 58.8 MeV modulated proton beam. The reconstructed three-dimensional (3D) dose distribution obtained from the stack of silicone foils, was later compared with the clinical proton treatment plan, prepared for the same proton beam parameters, using the Eclipse Ocular Proton Planning system (by Varian Medical Systems). The ability to register a delivered spatial proton radiation dose distribution in a quick and easy read-out procedure (based on OSL phenomena), makes the new system one of a state-of-the-art tool in the dosimetry area.

### References

- [1] M. Sadel, et al., *Radiat. Meas*, 133 (2020) 106255.
- [2] M. Sadel, et al., *Radiat. Meas*, 133 (2020) 106293.

### Acknowledgments

This work was supported by the Homing program of the Foundation for Polish Science co-financed by the European Union under the European Regional Development Fund *in Poland* (Homing/2017-4/38).

## Thermoluminescence of beta irradiated $\text{CaAl}_2\text{O}_4:\text{Eu}^{2+}$ , $\text{Dy}^{3+}$ synthesized by combustion method: thermal quenching and thermal cleaning studies

**R. Ruiz-Torres<sup>1</sup>, P. Salas-Castillo<sup>2</sup>, N. J. Zúniga-Rivera<sup>2</sup>, M. Barboza-Flores<sup>3</sup>,  
G. Chernov<sup>4</sup>, V. Chernov<sup>3</sup>**

<sup>1</sup>*Departamento de Física, Posgrado en Nanotecnología, Universidad de Sonora, Hermosillo, Sonora, 83000, México*

<sup>2</sup>*Departamento de Nanotecnología, Centro de Física Aplicada y Tecnología Avanzada, UNAM, Juriquilla, Qro, Mexico*

<sup>3</sup>*Departamento de Investigación en Física, Universidad de Sonora, Hermosillo, Sonora, 83000, México*

<sup>4</sup>*Innovación y Servicios en Nanotecnología S.A. de C.V, Campo Bello 14, Hermosillo, Sonora, 83106 México*

**E-mail: rodolfo.r.t@hotmail.com**

Monocalcium aluminate ( $\text{CaAl}_2\text{O}_4$ ) doped with  $\text{Eu}^{2+}$  is a phosphor that produces phosphorescence in the blue light (440 nm). It has been attracting a great deal of attention because of its wide applications in energy-efficient illumination systems and information displays.  $\text{CaAl}_2\text{O}_4$  codoped with  $\text{Eu}^{2+}$  and  $\text{Dy}^{3+}$  exhibits a very strong and long lasting persistence luminescence that could have many applications in the fields of lighted emergency signs, night-vision signage, in vivo bioimaging, dosimetry and optical data storage.

Nanosized  $\text{CaAl}_2\text{O}_4:\text{Eu}^{2+},\text{Dy}^{3+}$  phosphor was prepared by combustion synthesis method using urea as fuel and boric acid as flux. The synthesized powder was annealed under a carbon atmosphere at 1150 °C for 6 h. The photoluminescence, thermoluminescence (TL) and long persistence luminescence properties of this phosphor were presented by us in [1].

There are a number of TL phosphors (anion-defective  $\text{Al}_2\text{O}_3$ , diamond, quartz, long persistence strontium aluminate), for which the thermal quenching (TQ) of TL emission disturbs a TL glow curve and leads to the decrease of both the TL peak maximum and its area with the increasing of the heating rate.

The purpose of this work is twofold; to study the TQ effect on TL of  $\text{CaAl}_2\text{O}_4:\text{Eu}^{2+},\text{Dy}^{3+}$  and to evaluate the kinetics parameters of “un-quenched” TL peaks. The series of TL glow curves recorded with heating rates from 0.1 to 10 K/s were processed using the method described in [2]. The evaluated TQ parameters, the activation energy of non-radiative transitions and the ratio between the non-radiative and radiative decay rate were found to be 0.52 eV and  $8.9 \times 10^6$ . The structure of the “un-quenched” glow curves was determined by a simultaneous deconvolution of a set of curves recorded after preliminary heating to various temperatures from 40 to 124 °C with the temperature step of 4 °C.

### References

- [1] R. Ruiz-Torres et al., *Optical Materials* 101 (2020) 109763.
- [2] V. Chernov et al., *Physica Status Solidi A*, 209 (2012) 1779–1785.

### Acknowledgments

We acknowledge the partial financial supports from CONACYT, through grant No. 0222610 and CONACYT student scholarship (RRT) and CONACYT posdoctoral financial support (NJZR).

# Luminescent properties of Ba<sub>2</sub>MgWO<sub>6</sub> polycrystals and ceramics doped with the Eu<sup>3+</sup> ions

**K. Lemanski<sup>1</sup>, N. Miniajluk-Gawel<sup>1</sup>, B. Bondzior<sup>1</sup>, P. J. Dereń<sup>1</sup>**

<sup>1</sup> Institute of Low Temperatures and Structure Researches, Polish Academy of Sciences, 50-422 Wrocław, Poland

E-mail: K.Lemanski@intibs.pl

Ba<sub>2</sub>MgWO<sub>6</sub> (BMW) crystal is a double perovskite-type compound, which possesses a cubic structure with an Fm-3m space group [1]. Doped rare earth or metal transition ions are situated at the sites with high point symmetry, where the electrical dipole transitions are forbidden.

Luminescent properties of the BMW crystalline powders and ceramics doped with the Eu<sup>3+</sup> ions were investigated. For the Eu<sup>3+</sup> ions, the dominant emission peak is the magnetic dipole transition of <sup>5</sup>D<sub>0</sub> → <sup>7</sup>F<sub>1</sub>. Calculated asymmetry factor R is low, which confirms the unique high symmetry structure of this compound. The luminescence of the WO<sub>6</sub> groups in the broad visible region was observed under UV as well as the X-ray excitation sources. Investigated compounds have the potential to be used as a scintillator, to detect high energy ionizing radiation.

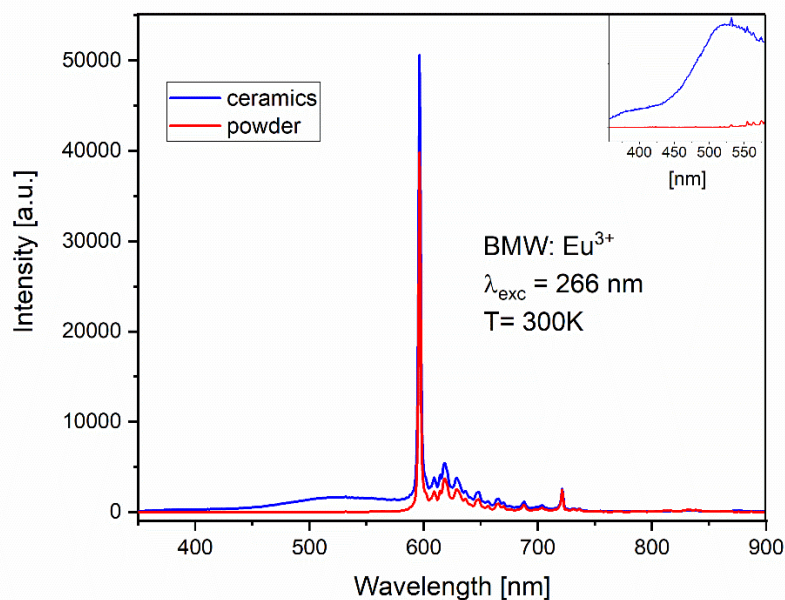


Fig. 1. The emission spectra of the Ba<sub>2</sub>MgWO<sub>6</sub>:Eu<sup>3+</sup> powder and ceramics.

## References

[7] T. H. Q. Vu, B. Bondzior, D. Stefańska, N. Miniajluk, P. J. Dereń, *Materials*, 13 (2020) 1614.

## Acknowledgments

This study was supported by "The National Science Centre" under Grant No. 2017/25/B/ST5/02670, which is gratefully acknowledged.

## Electron traps in Lu<sub>2</sub>O<sub>3</sub>:Hf from density functional calculations

**A. Shyichuk<sup>1</sup>, E. Zych<sup>1</sup>**

<sup>1</sup>*Faculty of Chemistry, University of Wrocław, 14 F. Joliot-Curie 50-383 Wrocław, Poland*

**E-mail: andrii.shyichuk@chem.uni.wroc.pl**

A series of materials based on cubic Lu<sub>2</sub>O<sub>3</sub> exhibit capability of trapping excited charge carriers in metastable excited states formed by dopants (transition metal cations) or defects (oxygen vacancies). Density functional theory (DFT) calculations with advanced meta-generalized gradient approximation (meta-GGA, mGGA) functional were used to analyze electron trapping in cubic Lu<sub>2</sub>O<sub>3</sub> doped with Hf. Individual dopant ions, as well as nearest-neighbor dopant ion pairs were considered. The effects of interstitial anions such as O<sup>2-</sup> and Cl<sup>-</sup> were analyzed. In most of the studied cases the additional electron charge is localized at the dopant site. However, only rarely the dopant states locate significantly below conduction band to assume electron trapping. Mostly, the electron is localized at the dopant in Lu site of C<sub>3i</sub> local symmetry ( $\text{Hf}_{\text{Lu-C}_{3i}}^{\times}$ ) with moderate trap depth of 0.8-0.9 eV. Several special cases corresponding to deeper (1.1-1.4 eV) traps also exist. Unambiguous deep traps (1.5-1.8 eV) correspond to systems with Hf dopant in the cationic void, accompanied with two interstitial oxygens.

### **Acknowledgments**

This work was supported by the National Science Centre (NCN Poland) under grant nr 2017/26/D/ST3/00599. Kevin F. Garrity from the National Institute of Standards and Technology, NIST, is acknowledged for the provided Lu<sup>3+</sup> pseudopotential. Wrocław Centre for Networking and Supercomputing is acknowledged for the provided computing power (grant no. 300). Open-source software was used: Quantum Espresso (<https://www.quantum-espresso.org>), Elk ([elk.sourceforge.net](http://elk.sourceforge.net)), Vesta, Inkscape ([inkscape.org](http://inkscape.org)), Python ([python.org](http://python.org)), Scipy ([scipy.org](http://scipy.org)), ImageMagick (<https://imagemagick.org/>).

## **Natural radiation dosimetry applications: dating ancient bronze statue by luminescence**

**M. Martini<sup>1</sup>, A. Galli<sup>1</sup>**

<sup>1</sup>*Department of Materials Science, University of Milano-Bicocca, Milano, Italy*

**E-mail: [m.martini@unimib.it](mailto:m.martini@unimib.it)**

Luminescence dosimetry has been successfully applied in dating ancient ceramics, in archaeology and in architectural history, as well as in sediment dating, exploiting the delayed luminescence properties of minerals, mainly quartz, both Thermally and Optically Stimulated, TL and OSL respectively. A particular application is the study of clay-cores found inside ancient bronze statues, where the direct dating of the metal is impossible, and the measurement of the clay-core luminescence allows an indirect dating. A number of this application to important bronze statue will be reported, evidencing the complex dosimetry as well as the difficulties in reducing the statistical uncertainties, deriving from the attenuation of the gamma irradiation coming from the exterior of the statues in the centuries and from the composition of the clay-core itself, largely different in the various monuments. Studies on important Roman and Greek bronze statues will be shown, like the St. Peter statue in Vatican and the famous “Lupa Capitolina”, symbol of ancient Rome.

# New challenges and problems in the field of luminescence dating

**A. Chruścińska**<sup>1</sup>

<sup>1</sup>*Institute of Physics, Faculty of Physics, Astronomy and Informatics, Nicolaus Copernicus University, Grudziadzka 5/7, 87-100 Torun, Poland*

**E-mail: alicja@fizyka.umk.pl**

Luminescence dating uses the measurement of the dose accumulated in minerals in the investigation of objects such as geological sediments and archaeological ceramics to determine their age. Analogous measurement for objects of a known age can be used to determine a retrospective dose, e.g. in studies of the effects of nuclear disasters. While everything is done to avoid the latter, it is worth being well prepared for such events. One can say that luminescence dating is constant training in case of such undesirable circumstances. The more accurately we can determine the age, the more accurately we can determine the retrospective dose.

After years of establishing the OSL dating method, several most essential problems need still to be solved. One of them is determining the time range of the reliable application of the method using the so-called fast OSL component in quartz [1, 2]. Another is increasing the dating range by using quartz OSL components with a good dose response over a much wider dose range than the fast component [3, 4]. Both challenges require OSL measurement methods that will allow for effective separation of individual OSL components. Similar needs are met by another recently intensively developed field of OSL application of minerals (especially feldspar and quartz) - thermochronometry, which allows reconstructing the thermal history of rocks close related to the course of land shaping. This application of the OSL requires the precise determination of thermal parameters of traps, which are the source of the signal used. One can estimate these parameters accurately when the investigated OSL signal is not complex and originates exclusively from the traps of interest.

After characterizing the current dating challenges, the presentation will focus on the OSL measurement method, which offers an opportunity for more selective measurements of individual OSL components. The thermally modulated OSL (TM-OSL) measurement exploits the dynamic dependence of the trap optical-cross section on temperature for the energy of photons used for stimulation lower than the optical trap depth. The physical basis of this method and the results of its application to quartz dating will be discussed.

## References

- [1] A. Timar-Gabor et al., *Radiation Measurements* 81 (2015) 150-156.
- [2] X.L. Wang, J. Peng, G. Adamiec, *Quaternary Geochronology*, 62 (2021) 101144.
- [3] C. Ankjærgaard, *Quaternary Geochronology*, 51(2019) 99-109.
- [4] G. Faershtein et al., *Radiation Measurements* 119 (2018) 102–111.
- [5] E.G. Yukihara, *Radiation Measurements*, 120 (2018) 274-280.
- [6] A. Chruścińska, N. Kijek, *Journal of Luminescence*, 174 (2016) 42-48.

## Acknowledgments

This work was supported by the National Science Centre, Poland, no. 2018/31/B/ST10/03917.

# Temperature assisted OSL measurements of display glass from mobile phones for retrospective dosimetry

**M. Discher<sup>1</sup>, H. Kim<sup>2</sup>, M. C. Kim<sup>2</sup>, J. Lee<sup>2</sup>**

<sup>1</sup>Paris-Lodron-University of Salzburg, Department of Geography and Geology, Hellbrunner Str 34, 5020 Salzburg, Austria

<sup>2</sup>Korea Atomic Energy Research Institute, Radiation Safety Management Division, Yuseong, Daejeon, Republic of Korea

**E-mail: michael.discher@sbg.ac.at**

Investigations of retrospective dosimetry have shown that components of mobile phones, i.e. glasses, are suitable as emergency dosimeters in case of radiological incidents. For physical dosimetry, glasses can be read out using optically stimulated luminescence (OSL), thermoluminescence (TL) and phototransferred thermoluminescence (PTTL) methods to determine the absorbed dose [1-7]. This paper deals with a feasibility study of display glass (category A) from modern mobile phones that are measured by temperature assisted optically stimulated luminescence (TA-OSL). For optical stimulation violet (VSL, 405 nm), blue (BSL, 458 nm) and infrared (IR, 850 nm) LEDs were used and three developed protocols (TA-VSL, TA-BSL and TA-IRSL) were tested [4-5]. The aim was to systematically investigate the luminescence properties, compare the results and to develop a robust measurement protocol for the usage as an emergency dosimeter after an incident with ionizing radiation.

First, the native signals were measured to calculate the zero dose signal. Next, the reproducibility and dose response of the luminescence signals were analysed. Finally, the signal stability was tested after the storage of irradiated samples at room temperature. The new protocols are tested using irradiation trials including realistic usage of the phone. In general, the developed protocols indicate usability, however, further research is needed to optimize the potential of a new protocol for physical retrospective dosimetry.

## References

- [1] C. Bassinet, W. Le Bris, *Radiat. Meas.*, 136 (2020), p. 106384.
- [2] J.R. Chandler, S. Sholom, S.W.S. McKeever, H.L. Hall, *J. Appl. Phys.*, 126 (2019), p. 074901.
- [3] M. Discher, E. Bortolin, C. Woda, *Radiat. Meas.*, 89 (2016), pp. 44 – 51.
- [4] M. Discher, H. Kim, J. Lee, *Nucl. Engine. and Technol.*, (2021), under review.
- [5] H. Kim, M. Discher, M. C. Kim, C. Woda, J. Lee, *Radiat. Meas.*, (2021), under review.
- [6] S.W.S. McKeever, R. Minniti, S. Sholom, *Radiat. Meas.*, 106 (2017), pp. 423 – 430.
- [7] S. Sholom, S.W.S. McKeever, J.R. Chandler, *Radiat. Meas.*, 136 (2020), p. 106382.

## Acknowledgments

The study was mainly carried out under the National Long- & Intermediate-Term Project of Nuclear Energy Development of Ministry of Science and ICT, Republic of Korea (No.2017M2A8A4015255) and the Nuclear Safety Research Program through the Korea Foundation of Nuclear Safety (KoFONS) (No.1803014). The scientific cooperation is partially conducted in the framework of EPU (Eurasia-Pacific UNINET) network and partially funded by funds of the Federal Ministry of Education, Science and Research (BMBWF) Austria (project periods: 2020/2021).



## Common medicines as emergency dosimeters

**A. Mrozi<sup>1</sup>, P. Bilski<sup>1</sup>**

<sup>1</sup>*Institute of Nuclear Physics Polish Academy of Sciences Radzikowskiego 152 31-342 Kraków, Poland*

**E-mail: [anna.mrozi@ifj.edu.pl](mailto:anna.mrozi@ifj.edu.pl)**

Along with the civilization changes, there is a growing awareness of risks due to the effects of improper use of radioactive sources. Accidental dosimetry is a developing area due to the need for radiological safety assurance of society and estimation of the potential doses in the case of a radiation incident.

While progress has been made in the application of thermoluminescence (TL) and optically stimulated luminescence (OSL) techniques to components of mobile phones and other electronic devices, their suitability in real emergencies can be put into question, e.g. due to requiring destroying of often valuable items of persons, as well as time-consuming sample preparation. For that reason, other, more suitable materials are still sought to be personal dosimeter during a radiological accident. This work aimed to investigate the OSL properties of materials likely to be found in personal carried-on bags, like commercial pharmaceuticals (placed in bags and protected from sunlight exposure).

Several over-the-counter medicines (containing ibuprofen, paracetamol, or acetylsalicylic acid) were investigated for the occurrence of the optically stimulated luminescence phenomenon. It was found that all of them exhibit strong luminescence signals following exposure to ionizing radiation. Its intensity increases linearly with the absorbed dose. The highest sensitivity was shown by the popular painkillers based on ibuprofen and paracetamol. The intensity of their luminescence signal was found to enable measurement of doses well below 1 Gy, which is sufficient for application in emergency dosimetry. The measurements of such properties as reproducibility, dose-response, fading, and influence of tablets coating were also performed.

Pharmaceuticals are free of all disadvantages of other emergency dosimeters: their composition is standardized, sampling is immediate, the unit value is usually negligible. We expect our results to be a starting point for broader investigations of various medicines, which might provide a perfect tool for emergency dosimetry.

### References

- [1] N. A. Kazakis, N. Tsirliganis, G. Kitis, *App. Radiat. and Isotopes*. 91 (2014) 79-91.

## Dose recovery test using a TA-OSL protocol of display glass for accident dosimetry

**H. Kim<sup>1</sup>, M. Discher<sup>2</sup>, M. C. Kim<sup>1,3</sup>, J. Lee<sup>1</sup>, I. Chang<sup>1</sup>, S. K. Lee<sup>1</sup>, J.-L. Kim<sup>1</sup>**

<sup>1</sup>*Korea Atomic Energy Research Institute, Radiation Safety Management Division, 989-111 Daedeok-daero, Yuseong, Daejeon, 34057, Republic of Korea*

<sup>2</sup>*Paris-Lodron-University of Salzburg, Department of Geography and Geology, Hellbrunner Str 34, 5020 Salzburg, Austria*

<sup>3</sup>*Hanyang University, 222, Wangsimni-ro, Seongdong-gu, Seoul, 04763, Republic of Korea*

**E-mail: kht84@kaeri.re.kr**

A display glass in a mobile phone has been widely studied as a luminescence material for accident dosimetry. The pre-bleached thermoluminescence (TL) protocol showed successful dose reconstructions in several inter-laboratory comparisons [1-3]. Recent studies are striving to develop advanced measurement protocols such as phototransferred TL (PTTL) [4, 5] and temperature assisted optically stimulated luminescence (TA-OSL) [6, 7] to utilize more stable charges in high temperature traps. An investigation of the TA-OSL protocol of a display glass at different elevated temperatures demonstrated that it is possible to measure trap charges above 300 °C while achieving an acceptable minimal detectable dose (MDD). Although the previous study presented the optical stability of the protocol using several light sources under lab conditions, the TA-OSL signals can be relatively sensitive to external lights compared with the pre-bleached TL signals. Therefore, in the present study, a dose recovery test was designed with a real usage of mobile phone after an exposure.

The purpose of the experiment is to evaluate the effect of realistic light sources such as sunlight, fluorescence light, and backlight unit on a dose estimation using the TA-OSL of glass samples in a mobile phone. Fresh glass samples (Category A) and intact mobile phones were prepared for the experiment. Different doses (un-irradiated, low, medium and high dose level) were selected and the samples were irradiated in a standard radiation field of a Cs-137 source at Korea Atomic Energy Research Institute (KAERI). After the irradiations, a part of the samples was exposed to sunlight and fluorescence light with the display turned on and the other remaining part was stored in the dark as a control group. Measurements were carried out after a few days after the irradiations. The estimated doses were compared to the reference doses and to the results of the pre-bleached TL protocol. As a result, the feasibility of the TA-OSL protocol was verified depending on the mobile phone usage, environmental bleaching impact and signal readings at different elevated temperatures.

### References

- [1] E. Ainsbury, et al., *Internat. Jour. Of Radiat. Bio.* 93 (2017), p. 99-109.
- [2] C. Rojas-Palma, et al., *Jour. of Radio. Prot.* 40 (2020), p. 1286-1298.
- [3] M. Discher, et al., *Radiat. Meas.* 142 (2021), p. 106544.
- [4] S.W.S McKeever, et al., *Radiat. Meas.* 106 (2017), p. 423-430.
- [5] M. Discher, et al., *Radiat. Meas.* 132 (2021), p. 106261.
- [6] H. Kim, et al., *Radiat. Meas.* (2021), under review.
- [7] M. Discher, et al., *Nucl. Engine. and Technol.* (2021), under review.

# Influence of sintering parameters on spectroscopic properties of BMW:Eu<sup>3+</sup> ceramic materials

**N. Miniajluk-Gawel<sup>1</sup>, K. Lemański<sup>1</sup>, P. J. Dereń<sup>1</sup>**

<sup>1</sup>INTiBS, Polish Academy of Science, Wrocław, 50-422, Poland

E-mail: n.miniajluk@intibs.pl

Polycrystalline ceramics is a rapidly developing branch of science, due to the huge needs both in the field of lighting and laser technology. Ceramic materials have numerous properties that exceed the currently used phosphors. Nevertheless, in the field of optics, only a few ceramic matrices are known: Y<sub>3</sub>Al<sub>5</sub>O<sub>12</sub> with Nd<sup>3+</sup> and Ce<sup>3+</sup> and spinel MgAl<sub>2</sub>O<sub>4</sub>. Therefore, new materials are being searched for, among which the ideal candidate is double perovskites with the formula Ba<sub>2</sub>MgWO<sub>6</sub> (BMW). There are four reports in the literature concerning polycrystalline ceramics based on BMW [1-4]. There is no information about BMW: Eu<sup>3+</sup> ceramic materials. Therefore the results presented here are innovative and not yet studied.

BMW: Eu<sup>3+</sup> powders were obtained by the solid-state method. Next, pellets with a diameter of 5 mm were formed and sintered by an alternative method to plasma sintering (SPS), with the difference that a continuous current flow was used, which allowed the use of high pressure. The sintering conditions were optimized by selecting the appropriate pressure (1-8 GPa), temperature (700-1350 °C) and sintering time (1-3 min), while maintaining a constant temperature increase rate. The last stage of the process was machining and polishing. The structural and spectroscopic analysis of the obtained ceramic was performed. Dense double perovskite ceramics with cubic structure was obtained. The obtained spectroscopic results prove (Fig. 1) that the sintering parameters influence the spectroscopic properties of the obtained materials and that BMW: Eu<sup>3+</sup> can be used as a UV detector of ionizing radiation.

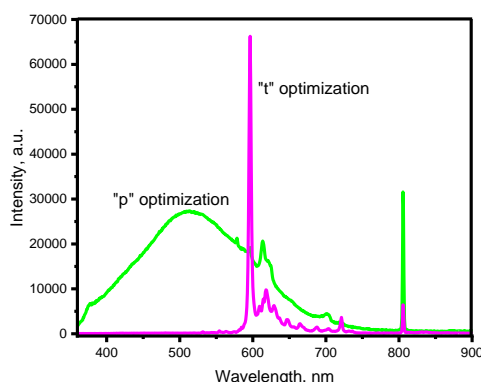


Fig. 1. Emission spectra of BMW:Eu<sup>3+</sup> under 266 nm excitation at 300K.

## References

- [8] Y. Wang, J. Lv, J. Wang, F. Shi, Z. M. Qi, *Ceram. Int.* 47 (2021) 17784-17788.
- [9] Y. C. Chen, Y. N. Wang, R. Y. Syu, *J. Mater. Sci. Mater.* 27 (2016) 4259-4264.
- [10] C. M. Lapa, J. B. Vasconcelos, E. J. P. Santos, Y. P. Yadava, *Proc. – Electrochem. Soc.* 3 (2004) 325-330.
- [11] N. Miniajluk, R. Boulesteix, P. J. Dereń, *Ceram. Int.* 46 (2020) 7602-7608.

## Acknowledgments

This study was supported by "The National Science Centre" under Grant No. 2017/25/B/ST5/02670, which is gratefully acknowledged.

## New phosphors for high temperature thermometry

L. Chepyga<sup>1</sup>, A. Osvet<sup>1</sup>, Yu. Zorenko<sup>2</sup>, A. Winnacker<sup>1</sup>, C. Brabec<sup>1</sup>, M. Batentschuk<sup>1</sup>

<sup>1</sup> Institute of Materials for Electronics and Energy Technology (i-MEET), Friedrich-Alexander-Universität Erlangen-Nürnberg, Martensstraße 7, 91058 Erlangen, Germany

<sup>2</sup> Institute of Physics, Kazimierz Wielki University in Bydgoszcz, 85090 Bydgoszcz, Poland

E-mail: miroslav.batentschuk@ww.uni-erlangen.de

Contactless high-temperature thermometry with luminescent materials has been an important research area over the last 20 years. Phosphor thermometry is an alternative method of measuring temperature from temperature-dependent aspects of the luminescence, such as intensity in different spectral regions, and decay time [1]. Thermographic phosphors have been widely investigated and could be employed for temperature measurement in gas turbines and engines, as well as for temperature analyses on gaseous flows [2]. Due to the need of getting efficient thermographic phosphors, with high chemical stability, high luminescence yield and desirable lifetime of the luminescence an improvement of their optical properties must be achieved.

The commonly used thermographic phosphors for high temperature applications are based on the combination of rare-earth ion centers in crystalline hosts. For instance, YAG doped with rare earth (RE<sup>3+</sup>) ions [3], especially YAG:Dy, and some other garnets [5] are one of the most widely used materials in phosphor thermometry. Likewise, yttrium orthosilicate (Y<sub>2</sub>SiO<sub>5</sub>) offers good chemical and thermal stability, a high melting point (~2070 °C) and has recently been used as a thermal barrier coating ceramic. It can be applied as a host crystal for laser materials as well as a host for scintillators and phosphors [4].

The goal of this work is an overview of methods the further improvement and development of new thermographic phosphors for high temperature measurements, mainly with garnet structure. The rare earth Dy<sup>3+</sup> was chosen as an activator ion for investigations as its temperature dependent <sup>4</sup>I<sub>15/2</sub>-<sup>6</sup>H<sub>15/2</sub> transition located in the blue spectral region of 458 nm, which is less affected by black body radiation at high temperatures. It was found that the luminescence properties of the dopant ion are strongly influenced by the crystal structure and bond nature of its local environment. Powder and single crystalline films were analysed, as well as different co-doping and flux compositions.

### References

- [1] S. W. Allison, G. T. Gillies, Rev. Sci. Instrum. 68, (1997) 2615–50.
- [2] M. Lawrence, H. Zhao, L. Ganippa, Optics Express, 21 (10), (2013) 12260–12281.
- [3] D. A. Rothamer, J. Jordan, Appl. Phys. B Laser Opt. 106 (2), (2012) 435–444.
- [4] C. Deka; B. H. T. Chai; Y. Shimony; X. X. Zhang; E. Munin; M. Bass, Appl. Phys. Lett. (1992) 61, 2141–2143.
- [5] Chepyga L. M., Osvet, A., Levchuk I., Ali A., Zorenko Y., Gorbenko V., Zorenko T., Fedorov A., Brabec C. J., Batentschuk M., *J. Lumin.* 202, (2018) 13-19.

## Light guides based on lanthanide-doped borate glass

M. Grüne<sup>1</sup>, B. Ahrens<sup>1,2</sup>, P. Nolte<sup>2</sup>, S. Schweizer<sup>1,2</sup>

<sup>1</sup>Faculty of Electrical Engineering, South Westphalia University of Applied Sciences, Soest, Germany

<sup>2</sup>Fraunhofer Application Center for Inorganic Phosphors, Branch Lab of Fraunhofer Institute for Microstructure of Materials and Systems IMWS, Soest, Germany

E-mail: stefan.schweizer@imws.fraunhofer.de

Luminescent borate glasses represent an interesting alternative as light-converter for LED and medical applications [1]. They provide a high transparency, a wide glass-forming range, a good chemical stability, and a good solubility for lanthanide ions [2]. Optical activation of the glass with lanthanide ions such as dysprosium, europium, or terbium leads to an intense luminescence in the visible spectral range upon blue and ultraviolet excitation [3]. However, the low optical absorption coefficients of the lanthanide ions result in a poor luminescence yield. Here, luminescent light guides represent a promising alternative to accumulate the generated light and to enable an increased light output.

In this work, the luminance of lanthanide-doped glass light guides is investigated under laser diode excitation in the blue and ultraviolet spectral range. Light guides of different lengths and different lanthanide doping are studied. To complement the experiments, ray-tracing simulations are performed. Absorption, photoluminescence quantum efficiency, as well as photoluminescence emission spectra of the corresponding lanthanide-doped borate glass serve as input data for the simulations. In addition, the effects of different lengths and geometry (cuboid / cylinder) as well as the effect of surface roughness are studied. The output face is investigated in detail as it is an important factor. Also, the improvement of the light guiding properties by applying a reflecting coating such as aluminium to the side faces is investigated. The combination of aluminium-coated side faces and a rough output face promises a significant increase in luminance.

### References

- [1] K. Mariselvam, and R. Arun Kumar, Universal Journal of Chemistry 4 (2016) 55-64.
- [2] M. Bengisu, Journal of Materials Science 51 (2016) 2199-2242.
- [3] A. C. Rimbach, F. Steudel, B. Ahrens, and S. Schweizer, J. Non-Cryst. Solids 499 (2018) 380-386.

## Composite color converters based on $\text{Tb}_{1.5}\text{Gd}_{1.5}\text{Al}_5\text{O}_{12}:\text{Ce}$ single crystalline films and $\text{Y}_3\text{Al}_5\text{O}_{12}:\text{Ce}$ crystal substrates

**A. Markovskiy<sup>1,2</sup>, V. Gorbenko<sup>1</sup>, S. Nizhankovskiy<sup>3</sup>, T. Zorenko<sup>1</sup>, A. Fedorov<sup>3</sup>,  
Yu. Zorenko<sup>1</sup>**

<sup>1</sup>*Institute of Physics, Kazimierz Wielki University in Bydgoszcz, Bydgoszcz, Poland*

<sup>2</sup>*Mechantronic Department, Kazimierz Wielki University in Bydgoszcz, Bydgoszcz, Poland*

<sup>3</sup>*Institute for Single Crystals, National Academy of Sciences of Ukraine, Kharkiv, Ukraine*

**E-mail: a.mark@ukw.edu.pl**

In the last years, the so-called Planar-Chip-Level Conversion (PCLC) design, where the phosphor is free-standing and separated from the LED chip, became accepted predominantly for the production of high power white LEDs (WLED) under near UV and blue LED excitation [1]. In 1996 YAG:Ce was discovered as an efficient photoconverter (PC) of WLED and still is the most widely applied phosphor, despite relatively low rates in conversion properties.

This work is dedicated to development of new type of composite phosphor converters based on the LPE grown single crystalline film (SCF) of  $\text{Tb}_{1.5}\text{Gd}_{1.5}\text{Al}_5\text{O}_{12}:\text{Ce}$  garnet (TbGdAG:Ce) and  $\text{Y}_3\text{Al}_5\text{O}_{12}:\text{Ce}$  single crystal (SC) substrate. The emission spectrum of  $\text{Ce}^{3+}$  ions in TbGdAG:Ce SCF is significantly red-shifted in comparison with YAG:Ce substrate due to the increase of crystal field strength in the dodecahedral sites of the garnet lattice where the Ce ions are localized [2,3].

In this study, the structural, luminescent, and photoconversion properties of novel composite color converters, including color coordinates, color rendering index (CRI), luminous efficacy were studied by varying  $\text{Ce}^{3+}$  concentration in the 0.1-0.25 % range in YAG:Ce substrates and thicknesses of TbGdAG:Ce SCFs in the 12-48  $\mu\text{m}$  range. The combination of different YAG:Ce substrates with various TbGdAG:Ce SCFs enables tuning the white light tons from cold white/ daylight white (correlated color temperature (CCT) > 6000 K) to neutral white (6000 K > CCT > 3300 K). The theoretical white light color coordinates on the chromaticity diagram were almost achieved for TbGdAG:Ce SCF/YAG:Ce (0.5 mm) SC converters with a SCF thickness between 19 and 25  $\mu\text{m}$  under 465 nm LED excitation, with corresponding CRI values in the 79-74 range.

Finely, developed TbGdAG:Ce SCF/YAG:Ce SC composite converters are responsible to produce white light when directly combined with commercially available LEDs and allows for resolving the problem of a high color temperature or low color rendering index of conventional YAG:Ce based WLEDs.

### References

- [1] N. Wei et al Appl. Phys. Lett. 101 (2012) 061902.
- [2] A. Markovskiy et al. J. Alloys Compd. 849 (2020) 155808.
- [3] J. Chen et al. Opt. Mater. Express 9 (2019) 3333.

### Acknowledgments

The work was performed in the frame of Polish NCN 2017/25/B/ST8/02932 project.

# **Ba<sub>2</sub>MgWO<sub>6</sub>:Er<sup>3+</sup> as a novel bifunctional double perovskites for white-light emitting phosphor and low-temperature optical thermometer**

**T. H. Q. Vu<sup>1</sup>, D. Stefańska<sup>1</sup>, P. J. Dereń<sup>1</sup>**

<sup>1</sup>*Department of Optical Spectroscopy, Institute of Low Temperature and Structure Research, Polish Academy of Sciences, Okólna 2, 50-422 Wrocław, Poland*

**E-mail: p.deren@intibs.pl**

Due to the fast growth of science and technology, exploring multifunctional materials with high performance is critical and urgent. Double perovskites compounds are promising materials due to their diverse applicability in many fields. Tungstate double perovskite exhibit simultaneous emissions of the host (blue emission) and the dopant, erbium ions is chosen to embed into Ba<sub>2</sub>MgWO<sub>6</sub> because its emission located in the green and red region which can combine with the blue of the host to create white-light. The optical thermometer is one of the most intensively studied topics in the last decade because it is superior to the conventional temperature sensor in terms of high accuracy, and is capable of working in harsh conditions such as biological fluids, strong electromagnetic fields, high pressure/temperature environment. In this study, Er<sup>3+</sup> concentration was regulated to develop a new efficient phosphor and the possibility of sensing temperature was investigated. The samples were synthesized by the co-precipitation method. The crystal structure and morphology characteristics of the samples were investigated by powder X-ray diffraction and scanning electron microscope measurements, respectively. The emitted light of the sample doped with 0.5 % Er<sup>3+</sup> exhibits the CIE coordinates (0.3025,0.3531) close to the standard of white light (0.3333, 0.3333). The more Er<sup>3+</sup>, the more yellowish the emitted light is. The highest emission intensity was obtained for the sample doped with 4 % of Er<sup>3+</sup>. The dependence of emission spectra of Ba<sub>2</sub>MgWO<sub>6</sub>: 4 % Er<sup>3+</sup> in a function of temperature was analyzed in the range of 77 – 273 K. Furthermore, the highest sensitivity based on the ratio of <sup>4</sup>I<sub>11/2</sub> → <sup>4</sup>I<sub>15/2</sub> and the host emission was found to be 2.25 %/K at 77 K, and the temperature uncertainty was 0.18 K. These findings strongly indicate that this compound can be applied as a bifunctional material for white light-emitting phosphor and low-temperature optical thermometer.

## **Acknowledgments**

This study was supported by “The National Science Centre” under Grant No. 2017/25/B/ST5/02670, which is gratefully acknowledged.

# Poster presentations



## Site-selective luminescence of solid solutions based on silicate-tungstates doped with $\text{Eu}^{3+}$ ions

V.A. Pustovarov<sup>1</sup>, A.A. Vasin<sup>2</sup>, M.G. Zuev<sup>1,2</sup>

<sup>1</sup> Institute of Physics and Technology, Ural Federal University, 19 Mira st., Ekaterinburg, 620002, Russia

<sup>2</sup> Institute of Solid State Chemistry, Ural Branch of the RAS, 620990, Ekaterinburg, Russia

E-mail: v.a.pustovarov@urfu.ru

Materials based on silicates and tungstates doped with rare-earth ions are of wide interest in the study of new effective phosphors with high-intensity luminescence in vision spectral range. Luminescent properties of such materials can be adjusted, tuned and improved with efficient energy transfer between host lattice rare earth ion (sensitizer) and activator. In principle, europium ions can be in crystal hosts simultaneously in the form  $\text{Eu}^{3+}$  and  $\text{Eu}^{2+}$  states that lead to formation of oxygen vacancies. In addition, europium ions can occupy nonequivalent crystallographic positions in a lattice, forming the various optical centers. Apatite-structure silicates are known as effective matrixes for activation by their RE-ions. Due to high luminescence intensity and chemical stability up to 1000 °C these materials can be used as active laser media and red light-emitting for white light-emitting diode [1-3].

In this work solid solution based on silicate-tungstates  $\text{Ca}_2\text{La}_{6.8}\text{Eu}_{1.2}\text{Si}_{5.6}\text{W}_{0.4}\text{O}_{26.4}$  doped with europium and undoped  $\text{Ca}_8\text{Eu}_2\text{Si}_3\text{W}_3\text{O}_{26}$  powders with the crystal structure of silicate apatites were synthesized by the high temperature solid phase method (see in details [3]) and certified by the XRD method. Studies of europium-ion spectroscopic features by means of PL spectroscopy and X-ray excited luminescence in temperature range of 90-295 K were carried out. In the first type of samples, the europium ion partially replaces the lanthanum ion as an impurity ion. In the second type of samples, the europium ion is an ion of the host matrix. In  $\text{Ca}_2\text{La}_{6.8}\text{Eu}_{1.2}\text{Si}_{5.6}\text{W}_{0.4}\text{O}_{26.4}$  only luminescence is observed, which is characterized by a set of  $^5\text{D}_0 \rightarrow ^7\text{F}_j$  intraconfigurational transitions for  $\text{Eu}^{3+}$  ion. Host luminescence, defect-related luminescence and  $\text{Eu}^{2+}$  impurity emission are not observed in studied spectral region. In contrast, in  $\text{Ca}_8\text{Eu}_2\text{Si}_3\text{W}_3\text{O}_{26}$  both the  $^5\text{D}_0 \rightarrow ^7\text{F}_j$  intraconfigurational transitions for  $\text{Eu}^{3+}$  ion and wide 430 nm emission band corresponding to host STE emission are observed. As for other apatite crystals, the  $\text{Eu}^{3+}$  ion can occupy two nonequivalent crystallographic positions.

### References

- [1] M.G. Zuev, A.M. Karpov, A.S. Shkvarin, *Solid State Chem.*, 184 (2011) 52-58.
- [2] T. Jansen, T. Jüstel, M. Kirm, H. Mägi, V. Nagirnyi, E. Töldsepp, S. Vielhauer, N.M. Khaidukov, V.N. Makhov, *J. of Lumin.*, 186 (2017) 205-211.
- [3] A.A. Vasin, M.G. Zuev, I.D. Popov, I.V. Baklanova, D.G. Kellerman, E.V. Zabolotskaya, Ju.G. Zajnuln, N.I. Kadyrov, *Russian Journal of Phys. Chemistry A*, 94 (2020) 2467–2473.

### Acknowledgments

The work was partially supported by the Ministry of Science and Higher Education of the Russian Federation (through the basic part of the government mandate, project No. FEUZ-2020-0060) and RFBR (project No. 20-03-00851) and was performed as part of a State Task (No. 0397-2019-0002) for the Institute of Solid State Chemistry (Ural Branch of the RAS).

## Scattering of hot charge carriers in solid solutions of dielectric crystals with substitutional disorder

A. Belsky<sup>1</sup>, E.V. Tishchenko<sup>2</sup>, A.N. Vasil'ev<sup>3</sup>

<sup>1</sup>*CELIA, Université de Bordeaux, CNRS, CEA, 33405 Talence, France*

<sup>2</sup>*Faculty of Physics, Lomonosov Moscow State University, Leninskie Gory 1-2, 119991 Moscow, Russia*

<sup>3</sup>*Skobel'syn Institute of Nuclear Physics, Lomonosov Moscow State University, Leninskie Gory, 1-2, 119991 Moscow, Russia*

**E-mail: [ev.tishchenko@physics.msu.ru](mailto:ev.tishchenko@physics.msu.ru)**

Mixed crystals in the form of substitutional solid solutions are promising scintillation materials for applications in high-energy physics, nuclear medicine, etc. Indeed, in recent years it has been demonstrated that solid solutions of scintillation materials in a large number of cases have a higher quantum yield, better energy resolution and faster luminescence with less afterglow compared to pure substances [1-3].

This behavior is associated with a significant change in the dynamics of electronic excitations at the thermalization stage, when hot charge carriers start to lose their energy, undergoing inelastic scattering by phonons. The kinetic energy of charge carriers at this stage of relaxation does not exceed the band gap and occurs to be about several eV for typical scintillators. At these energies, the conduction band and the valence band of a dielectric crystal have a complex structure, characterized by the presence of a large number of branches of the dispersion law. In this regard, estimations of the efficiency of scattering of electronic excitations by phonons, made in the simplified approximation of one parabolic branch of the dispersion law, seem to be far from reality.

In addition, in solid solutions with substitutional disorder, this scattering mechanism is supplemented by scattering of charge carriers by spatial fluctuations of potential. However, the efficiency of this scattering in the Born approximation in the model of a single parabolic branch band [4] turns out to be insufficient to explain the reduction in the thermalization length and an increase in the efficiency of carrier recombination in solid solutions of scintillation crystals.

In this work, the elastic (on potential fluctuations) and inelastic (on phonons) scattering of hot charge carriers in the approximation of multiple parabolic branches of the dispersion law are considered. The processes of migration and recombination of charge carriers in this approximation and their influence on the observed optical properties of substitutional solid solutions are investigated. It is shown that presence of several branches of the dispersion law in the conduction band of dielectric crystal accelerates the relaxation of electronic excitations and leads to a decrease in the thermalization length, thus resulting in the increase of the recombination efficiency.

### References

- [1] A. Belsky, A. Gektin, A. Vasil'ev, IEEE Transactions on Nuclear Science, 61 (2013) 262-270.
- [2] O. Sidletskiy, Physica status solidi (a), 215 (2018) 1701034.
- [3] O. Sidletskiy, A. Gektin, A. Belsky, Physica status solidi (a), 211 (2014) 2384-2387.
- [4] A. Belsky, A. Gektin, A. Vasil'ev, Physica status solidi (b), 257 (2020) 1900535.

### Acknowledgments

This work is supported by the Russian Science Foundation under grant 21-12-00219.

## Scintillation yield of Czochralski-grown $\beta$ -Ga<sub>2</sub>O<sub>3</sub> and $\beta$ -Ga<sub>2</sub>O<sub>3</sub>:Si crystals

**A. Bachiri<sup>1</sup>, M. Makowski<sup>1</sup>, W. Drozdowski<sup>1</sup>, M.E. Witkowski<sup>1</sup>, A.J. Wojtowicz<sup>1</sup>,  
K. Irmscher<sup>2</sup>, R. Schewski<sup>2</sup>, Z. Galazka<sup>2</sup>**

<sup>1</sup>*Institute of Physics, Faculty of Physics, Astronomy and Informatics, Nicolaus Copernicus University in Toruń, ul. Grudziądzka 5, 87-100 Toruń, Poland*

<sup>2</sup>*Leibniz-Institut für Kristallzüchtung, Max-Born-Str. 2, 12489 Berlin, Germany*

**E-mail: abdellah@doktorant.umk.pl**

Semiconductor scintillators are clearly gaining popularity, as they define a new and promising class of materials in the current scintillator industry, which is dominated by inorganic insulators. Semiconducting gallium oxide, with a density of 5.96 g/cm<sup>3</sup> and a band gap of 4.85 eV, has recently been identified as a potential material for fast detection of nuclear radiation. To study scintillation properties of  $\beta$ -Ga<sub>2</sub>O<sub>3</sub>, Czochralski-grown bulk single crystals have been used, both undoped and intentionally doped with different elements [1,2]. The research has shown that the scintillation light yield, energy resolution, and scintillation mean decay time are strongly correlated with the free electron concentration [1,3,4].

This Communication relates to our investigations on optimizing the values of scintillation yield and energy resolution of  $\beta$ -Ga<sub>2</sub>O<sub>3</sub>. The studied crystals, either pure or singly-doped with Si, have been grown by the Czochralski method at Leibniz-Institute für Kristallzüchtung (IKZ), Berlin [1,2]. A new set of crystals, both  $\beta$ -Ga<sub>2</sub>O<sub>3</sub> and  $\beta$ -Ga<sub>2</sub>O<sub>3</sub>:Si, reveals higher scintillation yields as compared with those reported so far. The present results confirm that further improvement of scintillation properties of  $\beta$ -Ga<sub>2</sub>O<sub>3</sub> might still be possible.

### References

- [1] Z. Galazka, R. Schewski, K. Irmscher, W. Drozdowski, M.E. Witkowski, M. Makowski, A.J. Wojtowicz, I.M. Hanke, M. Pietsch, T. Schulz, D. Klimm, S. Ganschow, A. Dittmar, A. Fiedler, T. Schroeder, M. Bickermann, *Journal of Alloys and Compounds* 818 (2020) 152842/1-7.
- [2] Z. Galazka, K. Irmscher, R. Schewski, I.M. Hanke, M. Pietsch, S. Ganschow, D. Klimm, A. Dittmar, A. Fiedler, T. Schroeder, M. Bickermann, *Journal of Crystal Growth* 529 (2020) 125297/1-8.
- [3] T. Yanagida, G. Okada, T. Kato, D. Nakauchi, S. Yanagida, *Applied Physics Express* 9 (2016) 042601/1-4.
- [4] W. Drozdowski, M. Makowski, M.E. Witkowski, A.J. Wojtowicz, R. Schewski, K. Irmscher, Z. Galazka, *Optical Materials* 105 (2020) 109856/1-6.

### Acknowledgments

This research has been financed from the funds of the Polish National Science Centre (NCN) and the German Research Foundation (DFG) in frames of a joint grant (NCN: 2016/23/G/ST5/04048, DFG: GA 2057/2-1).

## Developing UV emitters based on undoped ZnAl<sub>2</sub>O<sub>4</sub> nanofibers

**I. Romet<sup>1</sup>, R. E. Rojas-Hernandez<sup>2</sup>, F. Rubio-Marcos<sup>3,4</sup>, I. Hussainova<sup>2</sup>,  
J. F. Fernandez<sup>3</sup>, S. Omelkov<sup>1</sup>, E. Feldbach<sup>1</sup>, V. Nagirnyi<sup>1</sup>**

<sup>1</sup>*Institute of Physics, University of Tartu, W. Ostwald Str. 1, 50411 Tartu, Estonia*

<sup>2</sup>*Department of Mechanical and Industrial Engineering, Tallinn University of Technology, Ehitajate 5, 19180 Tallinn, Estonia*

<sup>3</sup>*Electroceramic Department, Instituto de Cerámica y Vidrio, CSIC, Kelsen 5, 28049, Madrid, Spain*

<sup>4</sup>*Escuela Politécnica Superior. Universidad Antonio de Nebrija. C/Pirineos, 55, 28040, Madrid, Spain*

**E-mail: ivo.romet@ut.ee**

The interest towards deep-UV (180–280 nm) phosphors has recently tremendously grown in view of potential utilization in tri-band based white LEDs for bio-chemical and medical applications. The conventional LED materials have a series of disadvantages in such applications, related to their poor thermal and short chemical stability, laborious synthesis routes, and incorporation of harmful elements which are also environmentally unfriendly. Another limitation is imposed by the necessity to minimize the use of rare-earth elements due to their availability affected by the scarcity of natural resources and rising price. As a consequence, the development of rare-earth free phosphors UV emitters an important challenge.

Here, we present the results of the synthesis, characterization, and spectroscopic studies of undoped ZnAl<sub>2</sub>O<sub>4</sub> fibers produced by a cost-efficient sol-gel route. The crystalline structure of the material was characterized by the XRD and Raman techniques, the local structure of the ZnAl<sub>2</sub>O<sub>4</sub> nanofibers was studied by examining the X-ray absorption near-edge structure (XANES) and extended X-ray absorption fine-structure (EXAFS). Time-resolved spectroscopy studies were carried out in the energy range 1.5–11 eV at the laboratory setups in Tartu, Estonia and in the range 4.5–45 eV at the FinEstBeAMS beamline of the synchrotron radiation facility at MAX IV Lab, Lund, Sweden [1]. Cathodoluminescence investigation of the samples was performed under pulsed excitation by 10-keV or 120 keV electrons in a wide temperature range of 4.2–400 K [2,3].

The ZnAl<sub>2</sub>O<sub>4</sub> undoped nanofibers are shown to exhibit a strong UV emission band peaking 233 nm (5.32 eV). It has a very characteristic excitation spectrum implying its excitonic nature. The intensity of this bright emission can be efficiently controlled by tuning the ratio of the Zn and Al constituents, whereas it has been found that the change of the Zn:Al ratio does not alter the normal spinel structure of the fibers. The origin of the 233 nm emission will be discussed on the basis of the structure-property relationships in the material in order to reveal its connection to the controlled crystal defects such as vacancies or anti-sites defects.

### References

- [1] R. Pärna, R. Sankari, E. Kukk, E. Nömmiste, M. Valden, M. Lastusaari, K. Kooser, K. Kokko, M. Hirsimäki, S. Urpelainen, P. Turunen, A. Kivimäki, V. Pankratov, L. Reisberg, F. Hennies, H. Tarawneh, R. Nyholm, M. Huttula, *Nucl. Instrum. Methods Phys. Res. A* 859 (2017) 83–89.
- [2] E. Feldbach, A. Kotlov, I. Kudryavtseva, P. Liblik, A. Lushchik, A. Maaros, I. Martinson, V. Nagirnyi, E. Vasil'chenko, *NIM B* 250 (2006) 159.
- [3] S.I. Omelkov, V. Nagirnyi, A.N. Vasil'ev, M. Kirm, *J. Lumin.* 176 (2016) 309–317.

## Time-resolved luminescence spectroscopy of rare-earth doped SrMoO<sub>4</sub> single crystals

V. Pankratova<sup>1</sup>, E.E. Dunaeva<sup>2</sup>, A.P. Kozlova<sup>3</sup>, R. Shendrik<sup>4</sup>, V. Pankratov<sup>1</sup>

<sup>1</sup>*Institute of Solid State Physics, University of Latvia, 8 Kengaraga iela, LV-1063 Riga, Latvia*

<sup>2</sup>*Prokhorov General Physics Institute, Russian Academy of Sciences, Vavilov Str.38, Moscow, Russia*

<sup>3</sup>*National University of Science and Technology «MISiS», Leninsky Pr. 4, 119049, Moscow, Russia*

<sup>4</sup>*Vinogradov Institute of Geochemistry, SB RAS, 1a Favorskii Street, 664033, Irkutsk, Russia*

**E-mail: vpank@latnet.lv**

Molybdates MMoO<sub>4</sub> (where M = Ca, Sr, Pb, Cd) have attracted considerable interest in view of various features, mainly related to catalysis and colour pigments but as well including fluorescent and scintillating materials. In particular, CaMoO<sub>4</sub> is known for its fluorescence ranging from blue to green emission, depending on specific doping and crystallinity. In this work, we report results for rare-earth (RE) doped SrMoO<sub>4</sub> single crystals because their optical and luminescence properties are poorly studied so far comparing with other molybdates.

The Czochralski method with a special growth and weight control PC program was used to obtain optically homogeneous SrMoO<sub>4</sub> single crystals doped with different concentrations of RE elements. Time-resolved luminescence characteristics as well as their temperature dependencies (in 10-300 K range) of undoped and RE (Eu or Pr) doped single crystals have been measured and under *tunable* laser excitations [1] varying excitation wavelength in UV spectral range down to 210 nm. The detailed analysis of observed time-resolved luminescence properties of intrinsic and RE emissions will be presented. The mechanism of energy transfer processes from host lattice to RE elements and RE charge compensation will be elucidated and discussed.

### References

- [1] V. Pankratova, A.P. Kozlova, O.A. Buzanov, K. Chernenko, R. Shendrik, A. Sarakovskis, V. Pankratov, Scientific Reports 10 (2020) 20388.

### Acknowledgments

This work was supported by the Latvian Council of Science grant (LZP 2020/2-0074).

## Crystal growth, scintillation property, and pulse shape discrimination of Ca(Br, I)<sub>2</sub> scintillators

**M. Yoshino<sup>1</sup>, K. Kamada<sup>2,3</sup>, K. J. Kim<sup>2</sup>, T. Iida<sup>4</sup>, K. Mizukoshi<sup>5</sup>, T. Miyazaki<sup>6</sup>,  
A. Yoshikawa<sup>1,2,3</sup>**

<sup>1</sup>Tohoku University, Institute for Materials Research, Sendai, 980-8577, Japan

<sup>2</sup>Tohoku University, New Industry Creation Hatchery Center, Sendai, 980-8579, Japan

<sup>3</sup>C&A Corporation, Sendai, 980-0811, Japan

<sup>4</sup>University of Tsukuba, Tsukuba, 305-8571, Japan

<sup>5</sup>Kobe University, Department of Physics, Kobe, 657-8501, Japan

<sup>6</sup>Tohoku University, Graduate School of Engineering, Sendai, 657-8501, Japan

**E-mail: yoshino.masao@imr.tohoku.ac.jp**

Inorganic scintillators have been used in areas of fundamental physics. In double beta decay experiments,  $0\nu\beta\beta$  is very rare signal, and its half-life is longer than  $10^{26}$  years, so low radioactivity and high energy resolution are needed to separate the mono-energetic signal from the other background. Pulse shape discrimination performance (PSD) of the scintillator is also highly important for rejecting the background events. Our recent study reported the growth of CaI<sub>2</sub> scintillator with a high optical yield of 107,000 photons/MeV and a good energy resolution of 3.2% FWHM at 662 keV [1]. Good pulse shape discrimination performance was also reported [2]. In this study, CaI<sub>2</sub>, CaBr<sub>0.7</sub>I<sub>1.3</sub>, 2% Eu doped CaBr<sub>0.7</sub>I<sub>1.3</sub> single crystals were grown by the vertical Bridgman-Stockbarger (VB) method (Fig. 1). The diameter of grown CaI<sub>2</sub> and CaBr<sub>0.7</sub>I<sub>1.3</sub>:Eu crystals is 2-inch, and that of CaBr<sub>0.7</sub>I<sub>1.3</sub> crystal is 1-inch. We measured the scintillation properties of the grown crystals (Fig. 2). The PSD performance was evaluated using <sup>137</sup>Cs and <sup>241</sup>Am as gamma and alpha RI sources (Fig. 3). The best value of F-measure between alpha and gamma was found to be 0.987, 0.980, and 0.982 for CaI<sub>2</sub>, CaBr<sub>0.7</sub>I<sub>1.3</sub>, CaBr<sub>0.7</sub>I<sub>1.3</sub>:Eu in the energy range above 100 keV by simple ratio analysis. A comparison of PSD analysis method, including machine learning, will also be presented.

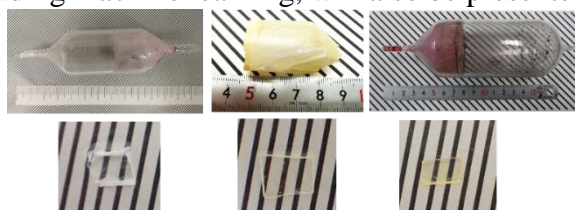


Fig. 1 Photographs of grown crystals.

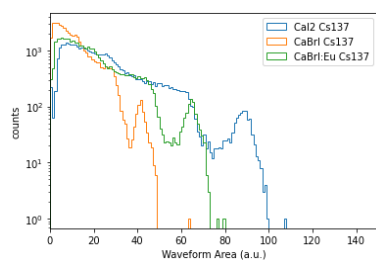


Fig. 2 Histogram of the waveform

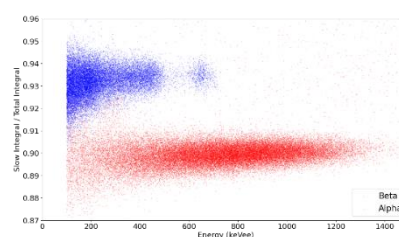


Fig. 3 2D-plot of energy versus PSD performance for

### References

- [1] K. Kamada et al., Single crystal growth and scintillation properties of Ca(Cl, Br, I)<sub>2</sub> single crystal, *Ceram Int.* 43 (2017) S423–S427.
- [2] T. Iida et al., High-light-yield calcium iodide (CaI<sub>2</sub>) scintillator for astroparticle physics, *Nucl Instruments Methods Phys Res A.* 958 (2020) 162629.

## Purification, growth and optical properties of large ${}^6\text{Li}_2\text{MoO}_4$ for scintillating bolometer

M. Velazquez<sup>1</sup>, P. Veber<sup>2</sup>, V. Motto-Ros<sup>2</sup>, **C. Dujardin<sup>2</sup>**,  
 A. Ahmine<sup>1</sup>, T. Duffar<sup>1</sup>, C. Stelian<sup>2</sup>, P. de Marcillac<sup>3</sup>, A. Giuliani<sup>3,4</sup>, S. Marnieros<sup>3</sup>,  
 C. Nones<sup>5</sup>, V. Novati<sup>3</sup>, E. Olivieri<sup>3</sup>, D. V. Poda<sup>3,6</sup>, I. Villa<sup>7</sup>, A. S. Zolotarova<sup>5</sup>, T. Redon<sup>3</sup>

<sup>1</sup>Univ. Grenoble Alpes, CNRS, Grenoble INP, SIMAP, 38000 Grenoble, France

<sup>2</sup>Université Lyon, Université Claude Bernard Lyon 1, CNRS, ILM UMR 5306, France

<sup>3</sup>CSNSM, Univ. Paris-Sud, CNRS/IN2P3, Université Paris-Saclay, 91405 Orsay, France

<sup>4</sup>DISAT, Università dell'Insubria, 22100 Como, Italy

<sup>5</sup>IRFU, CEA, Université Paris-Saclay, F-91191 Gif-sur-Yvette, France

<sup>6</sup>Institute for Nuclear Research, 03028 Kyiv, Ukraine

<sup>7</sup>Department of Material Science, University of Milano-Bicocca, Milano, Italy

**E-mail: christophe.dujardin@univ-lyon1.fr**

Because of their high resolution and low detection thresholds, cryogenic bolometer combining the analysis of heat and scintillating signals (CBHS) under ionizing radiation are very promising for rare event search at the edge of the current astro-particle physics (dark matter, neutrinoless double beta decay). The double readout generally operates in the 10mK temperature range, and the scintillation signal is one of the key aspects in the large-scale experiments. The required ultra-low radioactive background is also very challenging.

In this frame the consortium has achieved to grow  $\text{Li}_2\text{MoO}_4$  crystal weighting from 0.4 to 1 kg using the Czochralski method. The method has been optimized by the mean of multiphysic and numerical modelling. Initial powders of  $\text{Li}_2\text{CO}_3$  and  $\text{MoO}_3$  have been purified through hydrogen carbonation and ammoniac in aqueous solution. The characterisations of the crystals show promising properties in terms of radiopurity, optical transmission, scintillation yield and thermal properties. Scintillation spectra obtained at 10K exhibit an emission band peaking at 558nm where the absorption coefficient is about 8x the radius of the crystal. The 2D thermoluminescence map (T,  $\square$ ) does not show the thermoluminescence signal at 58K, generally assigned to the point defect  $\text{Zn}_{\text{Li}}+\text{V}_{\text{Li}}$ . These crystal demonstrate the lowest know contamination regarding W and Zn, and the scintillation yield is one of the higher observed (in the order of 1300 photons/MeV).

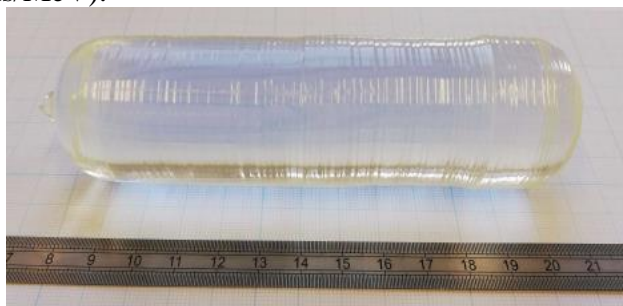


Figure 1. A crystal of 420g of  ${}^6\text{Li}_2\text{MoO}_4$  obtained by the Czochralski method.

### Acknowledgement

This work is part of the CLYMENE project funded by the Agence Nationale de la Recherche (ANR, France; ANR-16-CE08-0018)

## Fabrication of ${}^6\text{LiBr}$ and $\text{BaBr}_2$ based eutectic scintillator and its radiation response

**K. Kamada<sup>1,2</sup>, Y. Takizawa<sup>3</sup>, R. Yajima<sup>3</sup>, M. Yoshino<sup>3</sup>, K. J. Kim<sup>3</sup>,  
V. Kochurikhin<sup>2</sup>, A. Yoshikawa<sup>1,2,3</sup>**

<sup>1</sup>New Industry Creation Hatchery Center, Tohoku University. Sendai, Miyagi, Japan

<sup>2</sup>C&A corporation. Sendai, Miyagi, Japan

<sup>3</sup>Institute for Material Research, Tohoku University. Sendai, Miyagi, Japan

E-mail: kei.kamada.c6@tohoku.ac.jp

The demand for neutron detection has increased for medical imaging, security, astrophysics, and well-logging applications. Neutron detection relies on the distinction between gamma and neutron rays, thus a detector must have high sensitivity to neutron rays and low sensitivity to gamma rays. The scintillators for neutron detection require a large  ${}^6\text{Li}$  density to achieve high neutron detection efficiency. Up to now, our group reported  ${}^6\text{Li}$  containing eutectic scintillator such as  $\text{LiF/LiGdF}_4$ [7,8],  $\text{LiSrI}_3/\text{LiI}$ [9]  $\text{BaCl}_2/\text{LiF}$  [10]. This study aimed to develop a novel  $\text{LiBr/BaBr}_2$  based neutron scintillator with a high Li concentration. The eutectic point of  $\text{LiBr/BaBr}_2$  has been previously reported, and  $\text{Eu}^{2+}$  was added as an activator for  $\text{BaBr}_2$ . The crystal growth and scintillation properties of the Eu-doped  $\text{LiBr/BaBr}_2$  eutectic were evaluated.

Enriched  ${}^6\text{LiBr}$ ,  $\text{BaBr}_2$ , and  $\text{EuBr}_3$  powders (4N purity) were mixed according to a eutectic composition of  $\text{EuBr}_3:{}^6\text{LiBr}:\text{BaBr}_2 = 0.00234:0.766:0.231766$ . Crystal growth was performed via the vertical-Bridgman Stockbarger (VB) method in a quartz ampoule with an inner diameter of 4 mm. The mixed powder was placed in the quartz ampoule in under vacuum ( $\sim 10^{-1}$  Pa) to eliminate water and oxygen. The ample was heated over the melting point and pulled down at seed of 0.2 mm/min.

The Eu 1mdoped  ${}^6\text{LiBr/BaBr}_2$  eutectic was grown by the VB method. Circular samples with 1 mm thickness were cut from the grown crystal(Fig.1-left). The cut surface was mechanically polished and the eutectic phase structure was observed by BEI (Fig. 1-right). As results of BEI and powder XRD analysis, existence of  $\text{BaBr}_2$  and  $\text{LiBr}$  phases were confirmed. Expected  $\text{Eu}^{2+} 4f5d$  emission was observed at 400 nm from the  $\text{Eu}:\text{BaBr}_2$  phase under x-ray excitation. Details of eutectic structure, scintillation properties and neutron responses will be also reported.

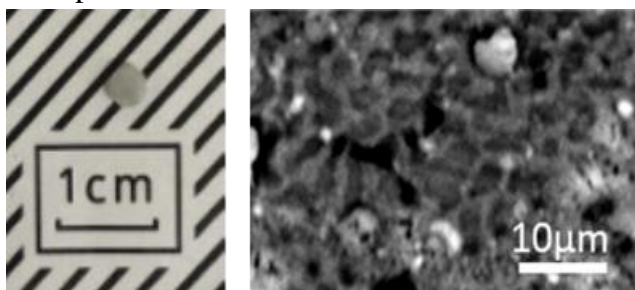


Fig.1 Photographs of the grown eutectics wafer and its BEI.

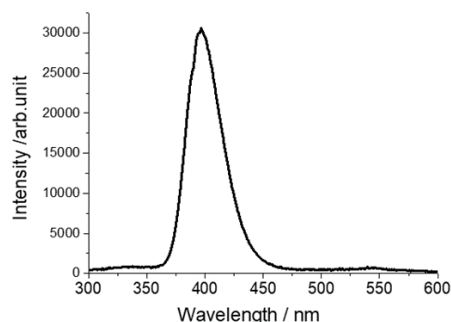


Fig.2 Radioluminescence spectrum of the eutectic under x-ray excitation

### References

- [1] K. Hishinuma, et al.2014. In Key Engineering Materials (Vol. 616, pp. 96-103).
- [2] K. Kamada, et al. 2017. Optical Materials, 68, pp.70-74.
- [3] K. Kamada, et al. 2015. Optical Materials, 50, pp.76-80.



## Growth and scintillation properties of Ce:LaBr<sub>3</sub>/LiBr eutectics

**Y. Takizawa<sup>1</sup>, K. Kamada<sup>2,3</sup>, R. Yajima<sup>1</sup>, K. J. Kim<sup>2</sup>, M. Yoshino<sup>1</sup>, A. Yamaji<sup>2</sup>,  
S. Kurosawa<sup>2</sup>, Y. Yokota<sup>1</sup>, H. Sato<sup>2</sup>, S. Toyoda<sup>2</sup>, Y. Ohashi<sup>2</sup>, T. Hanada<sup>1</sup>,  
V. Kochurikhin<sup>3</sup>, A. Yoshikawa<sup>1,2,3</sup>**

<sup>1</sup>Institute for Material Research, Tohoku University. Sendai, Miyagi, Japan

<sup>2</sup>New Industry Creation Hatchery Center, Tohoku University. Sendai, Miyagi, Japan

<sup>3</sup>C&A corporation. Sendai, Miyagi, Japan

**E-mail: yui.tacky@imr.tohoku.ac.jp**

Recently, scintillator for thermal neutron detection have been developed due to diminishing resources of <sup>3</sup>He gas. Instead of <sup>3</sup>He gas, inorganic scintillators containing <sup>6</sup>Li have been developed due to its high neutron capture cross section. Most recently, eutectic scintillator for neutron detection consisting of <sup>6</sup>Li based neutron-capturing phases and an luminescent phases has been reported. LiF/CaF<sub>2</sub>, LiF/LiGdF<sub>4</sub>, LiF/ CaF<sub>2</sub>/LiBaF<sub>3</sub> and LiSrI<sub>3</sub>/LiI [1-3] are reported as eutectic scintillators containing high concentrations of Li. In addition, Ce activated halide single crystal scintillators for neutron detection and gamma-ray have been reported. Ce:LaBr<sub>3</sub> scintillator has attracted attention due to its high light yield of over 73,000 photons/MeV and fast decay time around 20 ns. In this study, Ce:LaBr<sub>3</sub>/LiBr eutectic is fabricated by the vertical Bridgman (VB) method. Ce:LaBr<sub>3</sub> was selected as scintillator phase to obtain enough scintillation light and fast decay time. Investigations of their crystal phase were per-formed. Luminescence and scintillation properties were also evaluated.

The starting materials were prepared using CeBr<sub>3</sub>, LaBr<sub>3</sub> and <sup>6</sup>Li enriched (95%) LiBr powders with 99.99% purity. Ce:LaBr<sub>3</sub>/LiBr were grown at the eutectic composition of 25 mol% Ce:LaBr<sub>3</sub> and 75 mol% LiBr. Mixed powders were set in the quartz ample after baking process at 100°C under high vacuum (~10<sup>-4</sup> Pa) to eliminate water and oxygen. The ample was heated over its melting point and pulled down at seed of 0.2 mm/min.

The Ce 1mol% doped LaBr<sub>3</sub>/LiBr eutectic was grown by the VB method (Fig.1). Circular samples with 1 mm thickness were cut from the grown crystal. The cut surface was mechanically polished and the eutectic phase structure was observed by BEI (Fig. 2). As results of BEI and powder XRD analysis, existence of LaBr<sub>3</sub> and LiBr phases were confirmed. Expected Ce<sup>3+</sup> 4f5d emission was observed at 340-450 nm range from the Ce:LaBr<sub>3</sub> phase. Details of eutectic structure, scintillation properties and neutron responses will be also reported.

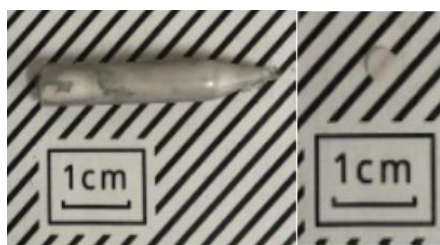


Fig.1 Photographs of the grown eutectics and a wafer sample.

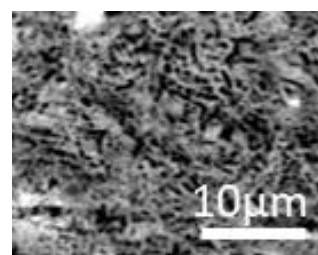


Fig.2 BEI of the grown eutectic.

### References

- [1] K. Kamada et al, J. Phys. Conference Series, 619 (2015) 012036.
- [2] K. Kamada et al, Opt. Mater.41 (2015) 41-45.
- [3] K. Hishinuma et al, Key Engineering Materials, 616 (2014) 96-103.

## New types of composite scintillators based on the single crystalline films and crystals of $\text{Gd}_3\text{Al}_{5-x}\text{Ga}_x\text{O}_{12}:\text{Ce}$ garnets

**Y. Syrotych<sup>1</sup>, S. Witkiewich-Lukaszek<sup>1</sup>, V. Gorbenko<sup>1</sup>, T. Zorenko<sup>1</sup>, R. Kucerkova<sup>2</sup>, J.A. Mares<sup>2</sup>, M. Nikl<sup>2</sup>, O. Sidletskiy<sup>1,3</sup>, K. Kamada<sup>4</sup>, A. Yoshikawa<sup>4</sup>, Yu. Zorenko<sup>1</sup>**

<sup>1</sup>*Institute of Physics, Kazimierz Wielki University in Bydgoszcz, 85090 Bydgoszcz, Poland*

<sup>2</sup>*Institute of Physics, Academy of Sciences of Czech Republic, 16200 Prague, Czech Republic*

<sup>3</sup>*Institute for Scintillation Materials, NAS of Ukraine, 61001 Kharkiv, Ukraine*

<sup>4</sup>*Institute for Materials Research, Tohoku University, Sendai 980-8577, Japan*

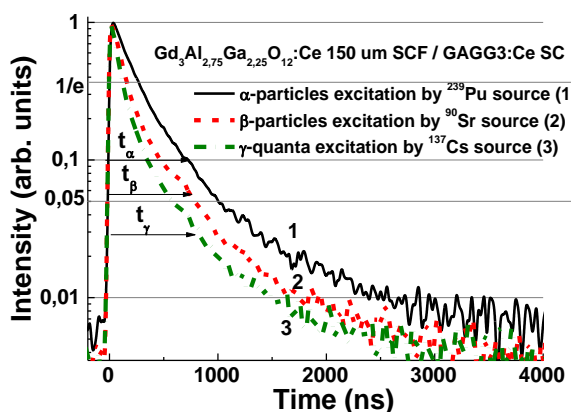
E-mail: syr@ukw.edu.pl

Nowadays the liquid epitaxy (LPE) growth method is a versatile technique for producing advanced composite scintillators of “phoswich-type” (*phosphor sandwich*) for registration of the different components of ionizing radiation with various penetrating depths. Such composite scintillators present the epitaxial structures, including one or two single-crystalline films (SCFs) intended for registration of low penetrating  $\alpha$ - and  $\beta$ -particles, and bulk single crystal (SC) substrates for registration of high penetrating radiation (X or  $\gamma$  rays).

This work presents the results of creation of novel types of composite scintillators based on the  $\text{Ce}^{3+}$  doped  $\text{Gd}_3\text{Al}_{3.25-2.75}\text{Ga}_{1.75-2.25}\text{O}_{12}$  SCFs grown by the LPE method using  $\text{PbO-B}_2\text{O}_3$  flux onto substrates prepared from commercial  $\text{Gd}_3\text{Al}_{2.3}\text{Ga}_{2.7}\text{O}_{12}:\text{Ce}$  (GAGG2.7:Ce) and  $\text{Gd}_3\text{Al}_2\text{Ga}_3\text{O}_{12}:\text{Ce}$  (GAGG3:Ce) SCs. The set of the mentioned SCFs with thicknesses in the 13-150  $\mu\text{m}$  range was grown in the Institute of Physics UKW, Poland onto the mentioned GAGG2.7:Ce and GAGG3:Ce substrates (produced in IMR Tohoku University, Japan) with a relatively small (up to 0.37-0.59 %) misfit between the SCF and substrate lattices. The scintillation properties of the respective epitaxial structures (pulse height spectra, light yield (LY) and decay kinetics) were investigated under excitation by  $\alpha$ -( $^{239}\text{Pu}$ ) and  $\beta$ -( $^{90}\text{Sr}+^{90}\text{Y}$ ) particles and  $\gamma$ -quantum ( $^{137}\text{Cs}$ ) sources.

Under  $\alpha$ -particle excitation by  $\text{Pu}^{239}$  the LY of  $\text{Al}_{3.25-2.75}\text{Ga}_{1.75-2.25}\text{O}_{12}:\text{Ce}$  SCFs is larger than the LY of reference YAG:Ce SCF, but by 1.4-2 times less than that in their SC analogues due to the influence of  $\text{Pb}^{2+}$  flux related dopant [1]. Meanwhile, these types of SCF scintillators under  $\alpha$ -particle excitation possess relatively fast scintillation responses with decay times in the  $t_{1/e}=270-320$  ns and  $t_{0.05}=1010-1170$  ns ranges.

*Such a scintillation decay response is faster in the 0.1-3  $\mu\text{s}$  range than that in the GAGG2.7:Ce SC substrate but slower in comparison with GAGG3:Ce SC substrate under  $\beta$ - and  $\gamma$ -excitation (Figure). For this reason, the epitaxial structures based on the  $\text{Gd}_3\text{Al}_{2.75}\text{Ga}_{2.25}\text{O}_{12}:\text{Ce}$  SCFs, grown onto the respective GAGG2.7:Ce and GAGG3:Ce SC substrates, can be used as composite scintillators for simultaneous registration of  $\alpha$ -,  $\beta$ -particles and  $\gamma$ -quanta. The best time separation of the scintillation response is achieved for  $\text{Gd}_3\text{Al}_{2.75}\text{Ga}_{2.25}\text{O}_{12}:\text{Ce}$  SCF/GAGG3:Ce SC composite scintillator (Figure) with  $t_\alpha/t_\beta=1.25-1.55$ ,  $t_\alpha/t_\gamma=1.65-2.2$  and  $t_\beta/t_\gamma=1.15-1.4$  ratios in the whole 0-3  $\mu\text{s}$  time range.*



### References

[1] Y. Zorenko, V. Gorbenko, T. Zorenko, A. Twardak, P. Bilski; e. a. *pps RRL*, 9 (2015) 489.

**Acknowledgements:** The work was supported by Polish NCN 2018/31/B/ST8/03390, Czech OP RDE&MEYS SOLID21 CZ.02.1.01/0.0/0.0/ 16\_019/ 0000760 project and Japanese 2018SV11 ICC-IMR Tohoku University project. O. Sidletskiy acknowledges the scholarship of the Polish National Agency for Academic Exchange under the agreement No. PPN/U LM/2020/1/00298/U/00001.

# Luminescent properties of YAG:Ce and TbAG:Ce nanopowder thin films in polycarbonate (PC) and polystyrene (PS) matrices

**P. Popielarski<sup>1</sup>, S. Witkiewicz-Lukaszek<sup>1</sup>, V. Gorbenko<sup>1</sup>, T. Zorenko<sup>1</sup>,  
P. Bolek<sup>2</sup>, J. Zeler<sup>2</sup>, E. Zych<sup>2</sup>, Yu. Zorenko<sup>1</sup>**

<sup>1</sup>*Institute of Physics, Kazimierz Wielki University in Bydgoszcz, 85-090, Poland*

<sup>2</sup>*Faculty of Chemistry, University of Wrocław, 50-383 Wrocław, Poland*

**E-mail: pawelpop@ukw.edu.pl**

Y<sub>3</sub>Al<sub>5</sub>O<sub>12</sub> (YAG) and Tb<sub>3</sub>Al<sub>5</sub>O<sub>12</sub> (TbAG garnet hosts are used as excellent objects to study the luminescence of different dopants and energy transfer processes in the simple and concentrated rare-earth based garnets mainly due to the application of these materials in the powder, ceramic, crystal and single crystalline film (SCF) forms as converters for white LEDs [1-3]. In addition, YAG:Ce and TbAG:Ce SCF and nanopowder (NP) films are exploited nowadays also for the production of cathodoluminescent and scintillation screens with a thickness in the μm / sub μm range [4, 5] and photovoltaic devices as well.

This work is devoted to the preparation and investigation of the luminescent properties of thin films, containing nanoparticles (NPs) of YAG:Ce and TbAG:Ce garnet, embedded in two organic matrixes. The YAG:Ce and TbAG:Ce NPs were prepared by Pechini [4] and combustion synthesis [5], respectively. Polycarbonate (PC) and Polystyrene (PS) materials were dissolved in chloroform. Then, YAG:Ce and TbAG:Ce NPs were added to the solutions in a concentration of 1%. Finally, YAG:Ce and TbAG:Ce thin films with thickness of about 200 nm were prepared using the spin-coating method onto glass substrates.

The structure and morphology of NP films are studied using optical and scanning electron microscopy. The optical properties of PS and PC matrixes with YAG:Ce and TbAG:Ce NPs were characterized by absorption, cathodoluminescence (CL) and photoluminescence (PL) spectra and PL decay kinetics in comparison with YAG:Ce and TbAG:Ce SCF counterparts. CL and PL spectra of the thin films based YAG:Ce and TbAG:Ce NPs, embedded in PC and PS matrixes, show the dominant yellow-orange Ce<sup>3+</sup> emission in the garnet structures without presence of any other secondary phases and antisite and vacancy type defects. For this reason, the properties of YAG:Ce and TbAG:Ce NP films were very close to their SCF counterparts [4, 5].

We have also found that application of PC and PS materials provide more uniform structural and optical NP film properties in comparison with the analogues prepared using ZnO based binder [5] and for this reason are more suitable for production high-quality NP films.

## References

- [1] M. Batentschuk, A. Osvet, G. Schierning, A. Klier, J. Schneider, A. Winnacker, *Radiat. Meas.* 38 (2004) 539.
- [2] K. Bartosiewicz, A. Markovskiy, T. Zorenko, A. Yoshikawa, S. Kurosawa, A. Yamaji, Y. Zorenko, *Phys. Status Solidi RRL*, 14 (2020) 2000327.
- [3] A. Markovskiy, V. Gorbenko, T. Zorenko, T. Yokosawa, J. Will, E. Spiecker, M. Batentschuk, J. Elia, A. Fedorov, Yu. Zorenko. *CrystEngComm*, 23 (2021) 3212.
- [4] Yu. Zorenko, E. Zych, A. Voloshinovskii. *Optical Materials*, 31 (2009) 1845.
- [5] P. Bolek, J. Zeler, V. Gorbenko, T. Zorenko, P. Popielarski, K. Bartosiewicz, A. Osvet, M. Batentschuk, E. Zych, Y. Zorenko, *Phys. Status Solidi B*, 257 (2020) 1900495.

## Acknowledgments

The work was performed in the frame of Polish NCN 2019/33/B/ST3/00406 project.

## Analysis of TL signals from SCF/SC composite detectors (LuAG:Ce/YAG) for distinguishing radiation field components

**A. Mrozik<sup>1</sup>, P.Bilski<sup>1</sup>, W.Gieszczyk<sup>1</sup>, M.Kłosowski<sup>1</sup>, Yu.Zorenko<sup>2</sup>,  
S. Witkiewicz-Łukaszek<sup>2</sup>, V. Gorbenko<sup>2</sup>, T.Zorenko<sup>2</sup>**

<sup>1</sup>*Institute of Nuclear Physics Polish Academy of Sciences Radzikowskiego 152 31-342 Kraków, Poland*

<sup>2</sup>*Institute of Physics, Kazimierz Wielki University in Bydgoszcz Powstańców Wielkopolskich Str., 2,  
85090, Bydgoszcz, Poland*

**E-mail: [anna.mrozik@ifj.edu.pl](mailto:anna.mrozik@ifj.edu.pl)**

Composite scintillators of phoswich-type (phosphor sandwich) are frequently being developed for registration of different components of ionizing radiation field, characterized by various penetration depths, e.g. heavy charged particles and gamma-rays [1]. One of the important methods for manufacturing such detectors is liquid phase epitaxy (LPE), which enables growing single-crystalline films (SCF) with thickness from a few  $\mu\text{m}$  up to about 100  $\mu\text{m}$ , onto thick crystal substrates [2]. The separation of the signals originating from both parts of a composite scintillator is based mostly on differences in scintillation decay kinetics [3]. Recently it was proposed to use composite SCF detectors also in passive thermoluminescence (TL) measurements [4]. In this case, the separation of signals (which originate from various types of radiation absorbed in SCF or SC) may be based on differences in temperature peak position (i.e. shape of a TL glow-curve) or wavelengths of luminescence emission produced in the SCF and the substrate. The aim of the present work was to study in quantitative manner feasibility of such an approach.

The investigations were performed using Ce-doped lutetium garnets (LuAG) grown (with LPE method) on undoped yttrium aluminum garnet (YAG) crystals. The samples of the composite detectors with different thickness layers were irradiated with  $\alpha$ ,  $\beta$  particles and X-rays, and their TL glow-curves were registered. The conducted research enabled to determine accurately the differences between TL signals from SCF and substrate depending, on the type of radiation. The precise quantification of the signal contribution from the layer or substrate was possible by using the developed formulas. To verify the correctness of the proposed method, mixed field irradiations were performed. The mixed field tests confirmed the possibility of using the TL method to separate the signals from the SCF and the substrate depending on the type of radiation. The obtained results suggest, that the combination of specially selected materials in the composite detector is suitable for the separation of signals from mixed fields by using the TL method.

### References

- [1] K. Yasuda, S. Usuda, and G. Gunji, *IEEE Trans. Nucl. Sci.*, 47(4) (2000) 1337-1340.
- [2] Thomas F. Kuech (edited by), *Handbook of Crystal Growth. Thin Films and Epitaxy: Basic techniques and materials, process and technology.* Elsevier. 2015.
- [3] Zorenko Yu., Novosad S., Pashkovskii M., Lyskovich A., Savitskii V., Batenchuk M., Nazar I., Gorbenko V., *J. Appl. Spectrosc.*, 52 (1990) 645-649.
- [4] S. Witkiewicz-Lukaszek, V. Gorbenko, T. Zorenko, Yu. Zorenko, W.Gieszczyk, A.Mrozik, P.Bilski, *Radiat. Meas.*, 128 (2019) 106-124.

### Acknowledgments

This work was performed in the frame of Polish NCN UMO-2018/31/B/ST8/03390 project.

# Ce<sup>3+</sup> to Ce<sup>4+</sup> recharge in Ce doped Y<sub>3-x</sub>Ca<sub>x</sub>Al<sub>5-x</sub>Si<sub>x</sub>O<sub>12</sub> and Y<sub>3</sub>Al<sub>5-2y</sub>Mg<sub>y</sub>Si<sub>y</sub>O<sub>12</sub> single crystalline films: EPR and optical studies

V. Gorbenko<sup>1</sup>, V. Laguta<sup>2\*</sup>, M. Buryi<sup>2</sup>, T. Zorenko<sup>1</sup>, Yu. Zorenko<sup>1</sup>

<sup>1</sup>Institute of Physics, Kazimierz Wielki University in Bydgoszcz, 85090 Bydgoszcz, Poland

<sup>2</sup>Institute of Physics, Academy of Sciences of Czech Republic, 16200 Prague, Czech Republic

E-mail: zorenko@ukw.edu.pl

The work is dedicated to the investigation of the Ce<sup>3+</sup> to Ce<sup>4+</sup> recharge processes and local surrounding of different Ce<sup>3+</sup> centers in mixed yttrium aluminum garnets using EPR and optical spectroscopy. For this purpose, two sets of Y<sub>3-x</sub>Ca<sub>x</sub>Al<sub>5-x-y</sub>Si<sub>y</sub>O<sub>12</sub>:Ce and Y<sub>3</sub>Al<sub>5-x-y</sub>Mg<sub>x</sub>Si<sub>x</sub>O<sub>12</sub>:Ce single crystalline films (SCFs) with Ca<sup>2+</sup> or Mg<sup>2+</sup> and Si<sup>4+</sup> content in the x=0-0.2 and y=0-0.5 ranges, respectively, were grown by the liquid phase epitaxy method onto Y<sub>3</sub>Al<sub>5</sub>O<sub>12</sub> (YAG) substrates from melt-solution based on the PbO-B<sub>2</sub>O<sub>3</sub> flux. The absorption and luminescent properties of mentioned SCFs were also investigated and compared with the reference YAG:Ce SCF.

Absorption spectra and EPR measurements of these two types of SCFs confirm the Ce<sup>3+</sup> to Ce<sup>4+</sup> recharge occurring at the excess of Ca<sup>2+</sup> or Mg<sup>2+</sup> ions (Table). Allowing Si<sup>4+</sup> ions in the equimolar to Ca<sup>2+</sup> and Mg<sup>2+</sup> content leads to the partial Ce<sup>4+</sup>→Ce<sup>3+</sup> recharge. However, the main part of cerium ions still remains in Ce<sup>4+</sup> state (Table). That means that the Ca and Si concentration in Y<sub>3-x</sub>Ca<sub>x</sub>Al<sub>5-x</sub>Si<sub>x</sub>O<sub>12</sub>:Ce and Y<sub>3</sub>Al<sub>5-2y</sub>Mg<sub>y</sub>Si<sub>y</sub>O<sub>12</sub>:Ce SCFs is not equal: the Ca<sup>2+</sup> and Mg<sup>2+</sup> content is somewhat larger than Si<sup>4+</sup> ones and the Ca<sup>2+</sup>/Mg<sup>2+</sup> excess is compensated by the Ce<sup>4+</sup> ions formation. Meanwhile, after annealing of SCFs in reducing (N<sub>2</sub>+H<sub>2</sub>) atmosphere at T>1000°C, more extended Ce<sup>4+</sup>→Ce<sup>3+</sup> recharge occurs. Such annealing results in the change of the relative concentration of Ce<sup>4+</sup> and Ce<sup>3+</sup> centers in the SCFs due the creation of the oxygen vacancies. Finally, SCFs annealed at 1300°C possess the scintillation light yield about 30-40% in comparison with reference YAG:Ce SCF and the scintillation/photoluminescence decay kinetics are much closer to those in YAG:Ce counterpart.

We have presupposed also the formation of several types of Ce<sup>3+</sup> centers in the Y<sub>3-x</sub>Ca<sub>x</sub>Al<sub>5-y</sub>Si<sub>y</sub>O<sub>12</sub>:Ce and Y<sub>3</sub>Al<sub>5-2y</sub>Mg<sub>y</sub>Si<sub>y</sub>O<sub>12</sub>:Ce SCFs. These centers possess various local surroundings due to substitution by the Ce<sup>3+</sup> ions of the different types of cations (correspondingly Y<sup>3+</sup> and Ca<sup>2+</sup>) in the dodecahedral positions of garnet host and are characterized by the differing luminescent and radio-spectroscopic behaviors.

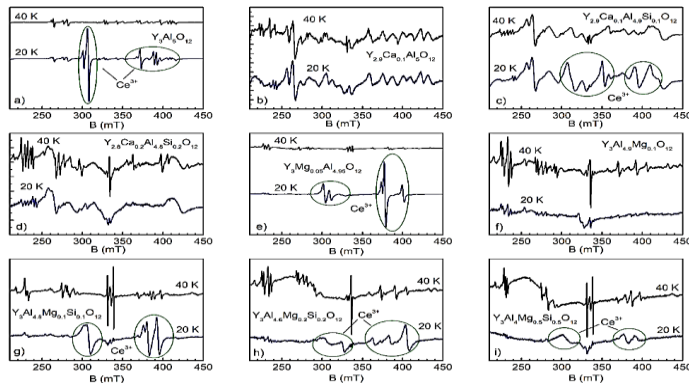


Fig.1. EPR spectra in SCFs.

SCF content	Ce <sup>3+</sup> content
Y <sub>3</sub> Al <sub>5</sub> O <sub>12</sub>	1
Y <sub>2.9</sub> Ca <sub>0.1</sub> Al <sub>5</sub> O <sub>12</sub>	0
Y <sub>2.9</sub> Ca <sub>0.1</sub> Al <sub>4.9</sub> Si <sub>0.1</sub> O <sub>12</sub>	0.049
Y <sub>2.8</sub> Ca <sub>0.2</sub> Al <sub>4.8</sub> Si <sub>0.2</sub> O <sub>12</sub>	0
Y <sub>3</sub> Al <sub>4.95</sub> Mg <sub>0.05</sub> O <sub>12</sub>	0.073
Y <sub>3</sub> Al <sub>4.9</sub> Mg <sub>0.1</sub> O <sub>12</sub>	0
Y <sub>3</sub> Al <sub>4.8</sub> Mg <sub>0.1</sub> Si <sub>0.1</sub> O <sub>12</sub>	0.027
Y <sub>3</sub> Al <sub>4.6</sub> Mg <sub>0.2</sub> Si <sub>0.2</sub> O <sub>12</sub>	0.022
Y <sub>3</sub> Al <sub>4</sub> Mg <sub>0.5</sub> Si <sub>0.5</sub> O <sub>12</sub>	0.016

Table.1. Ce<sup>3+</sup> content in SCFs under study normalized to that in Y<sub>3</sub>Al<sub>5</sub>O<sub>12</sub>

**Acknowledgement.** The work was performed in the frame of Polish NCN 2019/33/B/ST3/00406 project and the Czech Science Foundation under project No. 20-12885S.

# Three-layered composite scintillator based on the YAG and LuAG garnets for simultaneous registration of $\alpha$ -, $\beta$ -particles and $\gamma$ -quanta

**S. Witkiewicz-Lukaszek<sup>1</sup>, V. Gorbenko<sup>1</sup>, T. Zorenko<sup>1</sup>, J. A. Mares<sup>2</sup>, R. Kucerkova<sup>2</sup>, M. Nikl<sup>2</sup>, Yu. Zorenko<sup>1</sup>**

<sup>1</sup>Institute of Physics, Kazimierz Wielki University, Pow. Wielkopolskich 2, Bydgoszcz, 85090, Poland

<sup>2</sup>Institute of Physics, AS Czech Republic, 6253 Prague, Czech Republic

E-mail: sanwit@ukw.edu.pl

The work presents our last achievements in the development of triple composite scintillators based on the single crystalline films (SCF) and single crystals (SC) of garnet compounds for application as scintillating materials for radiation monitoring of mixed ionization fluxes.

The samples of the three-layered epitaxial structures of garnets were grown using the Liquid Phase Epitaxy (LPE) method from a flux based on PbO-B<sub>2</sub>O<sub>3</sub> fluxes. The combination of compounds inside of composite scintillators were selected based on the properties of the SCFs and SCs of Ce<sup>3+</sup>, Pr<sup>3+</sup> and Sc<sup>3+</sup> doped LuAG and YAG garnets. Namely, the two promising composition were selected: YAG:Ce SCF / LuAG:Pr SCF / LuAG:Sc SC and LuAG:Ce SCF / LuAG: Pr SCF / LuAG: Ce SC, which later were grown step-by-step using LPE method.

For the characterization of the luminescent and scintillation properties of SCF and bulk crystal parts of composite scintillators, the absorption spectra, CL spectra and scintillation decay kinetics under  $\alpha$ - and  $\beta$ - particles and  $\gamma$ -quanta excitation were applied. We show the possibility of the simultaneous registration of these types of radiation by the way of separation of the scintillation decay kinetics of SCF and crystal parts of such composite scintillators (Fig.1a).

The best separation of signals coming from the two films and bulk parts of composite scintillators at the registration of the  $\alpha$ - and  $\beta$ - particles and  $\gamma$ -quanta is observed for YAG:Ce SCF / LuAG:Pr SCF / LuAG:Sc SC composition (Fig.1 a). Such type of composite scintillator is also characterised by high LY of their film and bulk crystal parts and suitable Figure of Merit (FOM) ratios under simultaneous registration of mentioned types of radiation (Fig.1b).

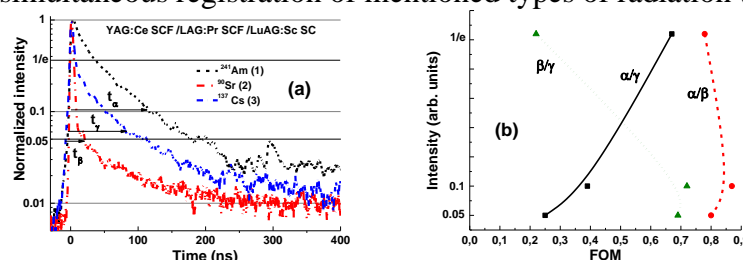


Fig.1. (a) - separation of the scintillation decay curves of YAG: Ce SCF / LuAG: Pr SCF / LuAG:Sc SC under excitation by  $\alpha$ - (<sup>241</sup>Am) and  $\beta$ - (<sup>90</sup>Sr) particles and  $\gamma$ -quanta (<sup>123</sup>Cs). (b) – decay of scintillation intensity and FOM values under registration of mentioned types of radiation.

## References

- [1] S. Witkiewicz-Lukaszek, e. a. *IEEE Transactions on Nuclear Science* 65 (2018) 2114 – 2119.
- [2] S. Witkiewicz-Lukaszek, e. a. *Optical Materials* 84 (2018) 593-599.
- [3] J.A. Mares, S. Witkiewicz-Lukaszek, e. a. *Optical Materials* 96 (2019) 109268.
- [4] S. Witkiewicz-Lukaszek, e. a. *CrystEngComm* 22 (2020) 3713-3724.

## Acknowledgments

The work was performed in the framework of Polish NCN 2018/31/B/ST8/03390 project and partially from the Operational Programme Research, Development and Education financed by European Structural and Investment Funds and the Czech Ministry of Education, Youth and Sports (Project No. SOLID21 CZ.02.1.01/0.0/0.0/16\_019/ 0000760).

## Scintillation time profiles of Czochralski-grown $\beta$ -Ga<sub>2</sub>O<sub>3</sub> and $\beta$ -Ga<sub>2</sub>O<sub>3</sub>:Si crystals

**M. Makowski<sup>1</sup>, M.E. Witkowski<sup>1</sup>, A. Bachiri<sup>1</sup>, W. Drozdowski<sup>1</sup>, A.J. Wojtowicz<sup>1</sup>,  
K. Irscher<sup>2</sup>, R. Schewski<sup>2</sup>, Z. Galazka<sup>2</sup>**

<sup>1</sup>*Institute of Physics, Faculty of Physics, Astronomy and Informatics, Nicolaus Copernicus University  
in Toruń, ul. Grudziądzka 5, 87-100 Toruń, Poland*

<sup>2</sup>*Leibniz-Institut für Kristallzüchtung, Max-Born-Str. 2, 12489 Berlin, Germany*

**E-mail: mimak@doktorant.umk.pl**

$\beta$ -Ga<sub>2</sub>O<sub>3</sub>, a wide bandgap oxide semiconductor, is one of the most promising materials proposed over the last few years for high power electronics and UV optoelectronics. As a result, this compound has become an interesting candidate for a semiconducting scintillator, currently undergoing extensive studies. We have also contributed to broadening of the knowledge about its scintillation properties with a number of scientific papers [1-3], reporting our research on pure and doped gallium oxide single crystals grown by the Czochralski method at the Leibniz-Institut für Kristallzüchtung (IKZ), Berlin [4,5].

In this Communication, we present scintillation time profiles of a brand new series of  $\beta$ -Ga<sub>2</sub>O<sub>3</sub> and  $\beta$ -Ga<sub>2</sub>O<sub>3</sub>:Si samples with free electron densities between 1016 cm<sup>-3</sup> and 1018 cm<sup>-3</sup>, which have already proven to be the most promising in order to obtain fast and efficient scintillation [3]. We also update our approach to their analysis, which now takes into account that the observed curve is, in fact, distorted by an apparatus response, and thus it needs to be deconvolved. This approach outputs clear decay profiles originating from the samples, which greatly improves the credibility of data analyzed in this way.

### References

- [1] W. Drozdowski, M. Makowski, M.E. Witkowski, A.J. Wojtowicz, Z. Galazka, K. Irscher, R. Schewski, *Radiation Measurements*, 121 (2019) 49-53.
- [2] M. Makowski, W. Drozdowski, M.E. Witkowski, A.J. Wojtowicz, K. Irscher, R. Schewski, Z. Galazka, *Optical Materials Express*, 9 (2019) 3738-3743.
- [3] W. Drozdowski, M. Makowski, M.E. Witkowski, A. Wojtowicz, R. Schewski, K. Irscher, Z. Galazka, *Optical Materials*, 105 (2020) 109856/1-6.
- [4] Z. Galazka, R. Schewski, K. Irscher, W. Drozdowski, M.E. Witkowski, M. Makowski, A.J. Wojtowicz, I.M. Hanke, M. Pietsch, Tobias Schulz, D. Klimm, S. Ganschow, A. Dittmar, A. Fiedler, T. Schroeder, M. Bickermann, *Journal of Alloys and Compounds*, 818 (2020) 152842/1-7.
- [5] Z. Galazka, K. Irscher, R. Schewski, I. M. Hanke, M. Pietsch, S. Ganschow, D. Klimm, A. Dittmar, A. Fiedler, T. Schroeder, M. Bickermann, *Journal of Crystal Growth*, 529 (2020) 125297/1-8.

### Acknowledgments

This research has been financed from the funds of the Polish National Science Centre (NCN) and the German Research Foundation (DFG) in frames of a joint grant (NCN: 2016/23/G/ST5/04048, DFG: GA 2057/2-1).

## Raman and luminescent spectroscopy of TbAG:Mn garnet single crystalline film phosphor

**W. Dewo<sup>1</sup>, V. Gorbenko<sup>2</sup>, A. Markovskiy<sup>2,3</sup>, Yu. Zorenko<sup>2</sup>, T. Runka<sup>1</sup>**

<sup>1</sup>*Faculty of Materials Engineering and Technical Physics, Poznan University of Technology, Piotrowo 3, 60-965 Poznan, Poland*

<sup>2</sup>*Institute of Physics, Kazimierz Wielki University, Weyssenhoffa 11, 85-090 Bydgoszcz, Poland*

<sup>3</sup>*Mechantronic Department, Kazimierz Wielki University in Bydgoszcz, Kopernik, 1, 85-074 Bydgoszcz, Poland*

**E-mail: wioletta.z.dewo@doctorate.put.poznan.pl**

Tb<sub>3</sub>Al<sub>5</sub>O<sub>12</sub> (TbAG) garnet is widely considered as a useful hosts for creation of white LED converters, laser crystals, computer memory, thermal barrier coatings, optical lenses and microwave optical elements [1-3]. Recently, the single crystalline films (SCF) of TbAG doped with Ce<sup>3+</sup> ions and co-doped Mn<sup>2+</sup> ions, grown using the liquid phase epitaxy (LPE) method, were considered for application as luminescent converters for blue LEDs [3-6].

In this paper we present first time Raman spectroscopy and high resolution luminescence investigation of the Mn<sup>2+</sup> doped TbAG SCF, grown onto Y<sub>3</sub>Al<sub>5</sub>O<sub>12</sub> garnet (YAG) substrate using melt-solution based on the PbO-B<sub>2</sub>O<sub>3</sub> flux [3]. The measurements were performed in the confocal regime as well as on the cross-section of the TbAG:Mn/YAG epitaxial structures starting from YAG substrate towards top of film across SCF/substrate interface.

The Raman and high resolution luminescence spectra shows clear distinction between TbAG SCF and the YAG substrate. Furthermore, the evolution of Raman spectra allows also identification of the *mechanic-optical effects* in the main volume of TbAG epitaxial structure connected with large mechanical stress on the SCF/substrate border with thickness of about 5-8 nm due to difference in the lattice constants of TbAG and YAG garnets been equal of 0.53 % [4]. The relaxation of such stress can cause a change in the cation-anion distances in the main volume of SCFs resulting in a notable variation of the Raman spectra of TbAG lattice as well as the luminescence of the different dopants in this host.

We observed also respective changes in confocal Raman spectra, starting from SCF/substrate interfaces towards the main volume of SCF, reflecting the mechanic-optical properties of the TbAG:Mn/YAG epitaxial structure. The dependences of the shape of Raman and luminescent spectra on the distance between SCF/substate interface are presented. Such dependences allow assessment of the mechanical stress relaxation in the main volume of SCF.

### References

- [1] K. Papagelis, S. Ves, *J. Phys. Chem. Solids*, 64 (2003) 599.
- [2] K. Papagelis, J. Arvanitidis, S. Ves, G. A. Kourouklis, *Phys. Stat. Sol. (b)*, 235(2003) 348.
- [3] Y. Zorenko, V. Gorbenko, T. Voznyak, M. Batentschuk, e. a., *J. Lumin.*, 130 (2010) 380.
- [4] A. Markovskiy, V. Gorbenko, T. Zorenko, Yu. Zorenko, e. a. *Cryst. Eng. Comm.*, 23 (2021) 3212.
- [5] S. Kuck, S. Hartung, S. Hurling, K. Peterman, G. Huber, *Phys. Rev. B* 57 (1998) 2203.
- [6] K Wisniewski, Yu. Zorenko, V. Gorbenko, T. Zorenko, e. a. *J. Phys. Conf. Ser.*, 249 (2010) 0120.

### Acknowledgments

The work has been supported by the research Project of the Polish Ministry of Education and Science 0511/SBAD/2151 and Polish NCN 2017/25/B/ST8/02932 project.



## Polymer nanocomposites with embedded CsPbBr<sub>3</sub> nanoparticles

M. Dendebera<sup>1</sup>, A. Zaichenko<sup>2</sup>, N. Mitina<sup>2</sup>, Ya. Chornodolskyy<sup>1</sup> T. Demkiv<sup>1</sup>,  
V. Mykhaylyk<sup>3</sup>, V. Vistovskyy<sup>1</sup>, A. Voloshinovskii<sup>1</sup>

<sup>1</sup>Ivan Franko National University of Lviv, 8 Kyryla i Mefodiya str., 79005, Lviv, Ukraine.

<sup>2</sup>Lviv Polytechnic National University 12, S. Bandera St., 79013 Lviv, Ukraine

<sup>3</sup>Diamond Light Source, Harwell Campus, Didcot, OX11 0DE, UK

**E-mail: anatoliy.voloshinovskii@lnu.edu.ua**

The prospect of improving spatial resolution with PET in TOF mode using picosecond time-resolved scintillators has stimulated the search for materials with fast luminescence decay time constant. One of the possible approaches to improve the operation speed and increase the luminescence intensity is to use the scintillation materials at low temperatures. In particular in real devices the scintillators operating at the temperature of liquid nitrogen can be developed easier than operating at the temperature of liquid helium. Such approach was proposed with halide perovskite crystals. At room temperature CsPbBr<sub>3</sub> crystals reveal <500 ph/MeV light yield while at liquid helium temperature this value reaches about 50,000 ph/MeV [1]. Even better parameters can be expected for scintillators based on CsPbBr<sub>3</sub> nanoparticles. The colloidal solution of CsPbBr<sub>3</sub> nanoparticles at room temperature shows a light yield of 20,000 ph/MeV [2]. Hence, one might expect higher scintillation efficiency values for nanoparticle composites at low temperatures.

The polystyrene composites loaded with CsPbBr<sub>3</sub> nanoparticles were prepared in order to determine the features of the scintillation mechanism in nanoparticles at low temperatures. CsPbBr<sub>3</sub> nanoparticles with an average size of 12 nm were added to the polystyrene dissolved in toluene. The samples were obtained in the form of polymer disks with a thickness of 0.1–1 mm and concentration of nanoparticles 0.04, 4, 9, 20, 40 wt.%. The luminescence intensity and the decay kinetics were studied under pulsed excitation of 405 nm laser diode with half-width pulse duration of 400 ps and a pulsed X-ray source with an anode voltage of 40 kV and a pulse duration of 1 ns. In contrast to single crystals, the near band edge luminescence of nanoparticles embedded in polymer matrix, which is explained by direct-band transitions and indirect-band transitions from the Rashba valleys shows no clear doublet structure that is characteristic feature of single crystals [3]. The near band edge luminescence, which can be attributed to exciton emission is observed in the luminescence spectra of nanoparticles at room temperature and T = 77 K. The luminescence intensity under X-ray excitation of composites with 0.1 mm thickness increases by 6 times at cooling from room temperature to 77 K. The luminescence intensity of samples with 1 mm thickness is higher than that for 0.1 mm composite, but on cooling the intensity increases by ca. 4 times. Such differences of the increasing rate of luminescence intensity under X-ray excitation is likely to be due to reabsorption of intrinsic luminescence. The luminescence decay time constant of polystyrene composites at T = 77K is estimated to be less than 0.8 ns.

### References

- [1] V. Mykhaylyk, H. Kraus, V.B. Kapustianyk et al., *Sci. Rep.*, 10 (2020) 8601.
- [2] Y Zhang et al., R. Sun, X. Ou et al., *ACS Nano.*, 13 (2019) 2520–2525.
- [3] M. Dendebera, Y. Chornodolskyy, R. Gamernyk et al., *J. Lumin.*, 225 (2020) 117346.

## Temperature behavior of the near band edge luminescence in CsPbBr<sub>3</sub> single crystals, microcrystals and nanoparticles

M. Dendebera<sup>1</sup>, T. Malyi<sup>1</sup>, A. Zhyshkovich<sup>1</sup>, Ya. Chornodolskyy<sup>1</sup>, A. Pushak<sup>2</sup>, R. Gamernyk<sup>1</sup>, O. Antonyak<sup>1</sup>, T. Demkiv<sup>1</sup>, V. Vistovskyy<sup>1</sup>, A. Voloshinovskii<sup>1</sup>

<sup>1</sup>Ivan Franko National University of Lviv, 8 Kyryla i Mefodiya str., 79005, Lviv, Ukraine.

<sup>2</sup>Ukrainian Academy of Printing, Pidgolosko Street, 19, 79020 Lviv, Ukraine

E-mail: [vitaliy.vistovskyy@lnu.edu.ua](mailto:vitaliy.vistovskyy@lnu.edu.ua)

Despite a certain research effort, the peculiarities of the intrinsic luminescence of halide perovskite single crystals continue to be discussed. First of all, it concerns the nature of narrow emission bands at the edge of intrinsic absorption (near band edge luminescence) and a wide non-elementary emission band with a significant Stokes shift. For APbBr<sub>3</sub> crystals (A = Cs, MA, FA), the near band edge luminescence is represented by a doublet structure, which has recently [1] been interpreted as direct-band exciton transition (high-energy peak A) and indirect-band transition from the Rashba valleys (low-energy peak B). Broadband luminescence (C) is attributed to the luminescence of defects, excitons localized on defects or even self-trapped excitons [2]. Luminescence of nanoparticle ensemble, which is represented by a relatively narrow band associated with exciton luminescence, looks somewhat simpler. We suppose that the key to understanding the nature of the emission band might be the study of temperature dependence of the A and B band positions. Consequently, the temperature dependence of the A (534 nm at T = 14 K) and B band positions (542 nm, T = 14 K) in CsPbBr<sub>3</sub> single crystals and in CsPbBr<sub>3</sub> microcrystals dispersed in the KBr matrix and in ensemble of nanoparticles with an average size of 12 nm was studied.

The A band peak position in CsPbBr<sub>3</sub> single crystals shifts to higher energy region at temperature increase in the range of 10 – 300 K. This behavior is consistent with the determining influence of lattice thermal expansion on the position of A peak. The B emission peak position shows the same trend on heating, but at T > 100 K it is shifted towards lower energies, because of the energy of Rashba valleys decreases at temperature increase. In CsPbBr<sub>3</sub> particles (lateral dimensions about 600 nm, thickness about 20 nm) embedded in KBr matrix the A and B emission bands characteristic of single crystals are observed, but the energy shift of B peak toward lower energies is less pronounced at temperature increase. For the ensemble of CsPbBr<sub>3</sub> nanoparticle only one luminescence band is observed, which can be identified as A band by the temperature behavior of the peak position. These results allow us to conclude that in single crystals near band edge luminescence is due to direct-band emission transitions and transitions from Rashba valleys, while in nanoparticles the exciton luminescence is the dominant emission through direct-band transitions.

### References

- [1] J.A. Steele, P. Puech, B. Monserrat, B. Wu, R.X. Yang, T. Kirchartz, H. Yuan, G. Fleury, D. Giovanni, E. Fron, M. Keshavarz, E. Debroye, G. Zhou, T.C. Sum, A. Walsh, J. Hofkens, M.B.J. Roeffaers, *ACS Energy Lett.*, 4 (2019) 2205–2212.
- [2] M. Dendebera, Y. Chornodolskyy, R. Gamernyk, O. Antonyak, I. Pashuk, S. Myagkota, I. Gnilitzkyi, V. Pankratov, V. Vistovskyy, V. Mykhaylyk, M. Grinberg, A. Voloshinovskii, *J. Lumin.*, 225 (2020) 117346.

## Synthesis and characterization 2D CdTe nanoplatelets for PV application

**A. Akhmetova<sup>1</sup>, A. Kainarbay<sup>1</sup>, T. Nurakhmetov<sup>1</sup>, D. Daurenbekov<sup>1</sup>, Z. Salikhodzha<sup>1</sup>,  
B. Yussupbekova<sup>1</sup>**

<sup>1</sup>L.N. Gumilyov Eurasian National University, 010000, 2 Satpayeva str., Nur Sultan, Kazakhstan

**E-mail: aizhan.s.akhmetova@yandex.kz**

Colloidal 2D semiconductor nanoplates (NPL) are two-dimensional quantum structures with a planar geometry. For NPLs, it is possible to obtain a large transverse size, which can vary from tens to hundreds of nanometers with the small thickness, depending on the synthetic protocol [1]. Quantum confinement effect in nanoscale thickness leads to restrict the movement of charge carriers in the NFL. Such structures are well suited for studying new photophysical properties, such as extremely narrow photoluminescence linewidth, gigantic oscillator strengths, and large nonlinear absorption cross section. Studying the synthesis of NPL is important because it provides a chemical understanding of the kinetics of nucleation and growth of nanostructures and will provide new knowledge useful for understanding the growth mechanism. It is known from the literature that control of the shape of semiconductor nanocrystals can be achieved by controlling the reaction conditions, such as the reaction temperature, the reaction time [2] and the reactivity of the precursor. Although there are comprehensive studies on the colloidal synthesis of CdTe [3-5], there are only a few reports on the form-controlled synthesis of NPL CdTe due to the limited selection of the tellurium precursor, determination of the optimal precursor, and synthesis conditions for obtaining the large NPLs needed for PV applications.

In this study, NPL CdTe samples were synthesized by organometallic synthesis methods. The best conditions for obtaining the required nanostructures are determined. The influence of the synthesis conditions was investigated by optical spectroscopy methods. The purity and crystallinity of the phases are characterized by X-ray diffraction analysis. Morphological features are studied by scanning electron microscopy (SEM, TEM). In addition, NPL CdTe samples were also characterized by FT-IR Raman spectroscopy. The effect of the ligand on the PV properties of CdTe NPL has been studied. The current-voltage characteristics of the INP CdTe samples were measured using complex equipment based on the SolAAA solar simulator, the Keitley 2440 picoammeter.

### References

- [1] V. Smelov, et al., *Optics and Spectroscopy*, 8 (2020) 1226–1229.
- [2] F. Wang, et al., *Australian Journal of Chemistry*, 74 (2020) 179-185.
- [3] S. Pedetti, et al., *Chem. Mater*, 25 (2013) 2455–2462.
- [4] S. Ithurria, et al., *Nature Materials*, 10 (2011) 936–941.
- [5] H. Sun, et al., *ACS Nano*, 12(2018) 12393–12400.

## Micro-powder phosphors based on the Ce<sup>3+</sup> and Mn<sup>2+</sup> doped Ca<sub>2</sub>YMgScSi<sub>3</sub>O<sub>12</sub> silicate garnet for WLED application

**A. Shakhno<sup>1</sup>, S. Witkiewicz-Lukaszek<sup>1</sup>, V. Gorbenko<sup>1</sup>, K. Paprocki<sup>1</sup>, T. Zorenko<sup>1</sup>, Yu. Zorenko<sup>1</sup>**

<sup>1</sup>*Institute of Physics, Kazimierz Wielki University in Bydgoszcz, 85090 Bydgoszcz, Poland*

**E-mail: shakhno@ukw.edu.pl**

Nowadays, development of white LEDs (WLEDs) is one of the promising areas in artificial lighting technology due to their remarkable properties such as long life, high efficiency and environmental friendliness compared to incandescent bulbs. Currently, the most common WLED construction is the combination of a blue LED chip and yellow light-emitting YAG:Ce photoconverters (pc) [1]. Although YAG:Ce garnet has already good thermal stability of luminescence at high temperatures, an alternative is still being sought today due to the lack of red-light emission, especially for headlights. Ce<sup>3+</sup> doped Ca<sub>3</sub>Sc<sub>2</sub>Si<sub>3</sub>O<sub>12</sub>:Ce garnet (CSSG:Ce) is a relatively new phosphor that meets these requirements [1, 2]. However, this phosphor is characterized by the lack of components in the red spectral range. By substituting cations, for example with Y<sup>3+</sup> and Mg<sup>2+</sup> ions, the emission spectrum can be adapted to the requirements [3].

In this work, Y<sup>3+</sup>-Mg<sup>2+</sup> pair alloying in CSSG:Ce silicate phosphor in equimolar content of 1.0 formula units was applied to achieve a better redshift of the Ce<sup>3+</sup> emission. The Mn<sup>2+</sup> co-doping was used also for additional increasing the contribution of the red component in the emission spectrum of CaYMgScSi<sub>3</sub>O<sub>12</sub>:Ce phosphor (CYMSSG:Ce,Mn). It is presupposed that the localization of Mn<sup>2+</sup> ions both in dodecahedral sites of Ca<sup>2+</sup> cation and octahedral sites of Sc<sup>3+</sup> cations promote generation of yellow and red emission, respectively [4]. A significant substitution of Mn<sup>2+</sup> for Sc<sup>3+</sup> can be achieved by balancing the difference in charge by introducing a trivalent rare-earth ion such as Ce<sup>3+</sup> to replace Ca<sup>2+</sup> [4].

The micro-powders (MPs) of CYMSSG:Ce, CYMSSG:Mn and CYMSSG:Ce,Mn garnets were obtained by solid-state synthesis with adding B<sub>2</sub>O<sub>3</sub> flux. The thermal treatment of MP was performed in the air atmosphere at 1350°C. We have also investigated the structural and morphological properties of Ce<sup>3+</sup> and Mn<sup>2+</sup> doped CYMSSGM MPs using X-ray diffraction and electron microscopy. The luminescent properties of MP samples were characterized also by cathodoluminescence (CL) and photoluminescence (PL). The luminescent properties of Ce<sup>3+</sup>-Mn<sup>2+</sup> doped Ca<sub>2</sub>YMgScSi<sub>3</sub>O<sub>12</sub> MPs were compared with the reference Ca<sub>3</sub>Sc<sub>2</sub>Si<sub>3</sub>O<sub>12</sub>:Ce MPs as well as with properties of Ce<sup>3+</sup> and Mn<sup>2+</sup> doped single crystalline film counterparts [5].

We have observed corresponding tendencies in variations of the spectroscopic properties of CYMSSG:Ce,Mn garnet in comparison with CYMSSG:Ce due to arrangement of Ce<sup>3+</sup> and Mn<sup>2+</sup> ions in Ca<sup>2+</sup> and Y<sup>3+</sup> dodecahedral sites as well as Mn<sup>2+</sup> ions in Mg<sup>2+</sup> and Sc<sup>3+</sup> octahedral position, promoting for the development of WLED converters. Furthermore, the prototypes of white LED have been fabricated using coating the CYMSSG:Ce,Mn MPs in epoxy resin onto the 450 nm blue LED for demonstration of the application possibility of the developed garnet phosphor. The fabricated devices with suitable light characteristics demonstrate that the CYMSSG:Ce,Mn phosphor is promising for production of warm WLED light sources.

### References

- [1] Y. Shimomura, T. Kurushima, M. Shigeiwa, N. Kijima, J. Electrochem. Soc. 155 (2008) J45.
- [2] I. Levchuk, A. Osvet, C.J. Brabec, M. Batentschuk, A. Shakhno, T. Zorenko, Yu. Zorenko, Optical Materials 107 (2020) 109978.
- [3] N. Khaidukov, Yu. Zorenko, T. Zorenko, M. Batentschuk, e. a. pss RRL, 11 (2017) 170001.
- [4] Y. Liu, X. Zhang, Z. Hao, Y. Luo, X.J. Wang and J. Zhang, J. Mater. Chem., 21 (2011) 16379.
- [5] V. Gorbenko, T. Zorenko, S. Witkiewicz, K. Paprocki, A. Iskalyeva, A.M. Kaczmarek, R. Van Deun, M.N. Khaidukov, M. Batentschuk, Y. Zorenko, Journal of Luminescence 199 (2018) 245.

**Acknowledgments.** The work was performed in the frame of Polish NCN 2017/25/B/ST8/02932 project.

## Ce<sup>3+</sup> doped Al<sub>2</sub>O<sub>3</sub>-YAG eutectics as converters for WLED application

A. Shakhno<sup>1,2</sup>, T. Zorenko<sup>1</sup>, A. Markovskiy, O. Vovk<sup>3</sup>, S. Nizhankovskiy<sup>3</sup>, Yu. Siryk<sup>3</sup>,  
M. Cieszko<sup>2</sup>, Z. Szczepański<sup>2</sup>, Yu. Zorenko<sup>1</sup>

<sup>1</sup> Institute of Physics, Kazimierz Wielki University in Bydgoszcz, 85090 Bydgoszcz, Poland

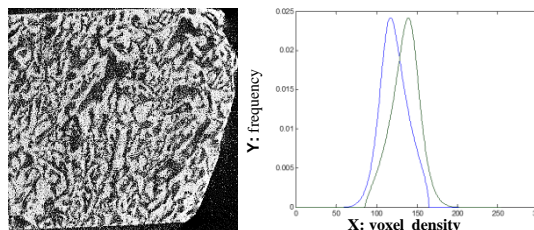
<sup>2</sup> Mechatronic Department, Kazimierz Wielki University in Bydgoszcz, 85-074 Bydgoszcz, Poland

<sup>3</sup> Institute for Single Crystals, National Academy of Sciences of Ukraine, 61178 Kharkiv, Ukraine

E-mail: tzorenko@ukw.edu.pl

Currently, the most known type of white emitting diodes (WLED) is a combination of blue LED chip and powder yellow-emitting YAG:Ce phosphor-converters (pc). However, the lack of red-emitting components in YAG:Ce pc hinders the realization of warm white light. Due to thermal stability of the Ce<sup>3+</sup> emission, heavy Ce<sup>3+</sup> doped YAG-Al<sub>2</sub>O<sub>3</sub> eutectics have been considered as one of the prospective materials for pc for high-power warm WLEDs [1, 2].

Initial charge for Ce doped (4 mole %) YAG-Al<sub>2</sub>O<sub>3</sub> eutectics was prepared using a mixture of Y<sub>2</sub>O<sub>3</sub>, Al<sub>2</sub>O<sub>3</sub>, CeO<sub>2</sub> oxides, pressed in tablets, which were pre-annealed in air at 1200°C. Eutectic crystallization was performed by the horizontal directional crystallization method in Mo crucibles with 240x75x35mm<sup>3</sup> size similar to the YAG:Ce crystal growth procedure. The samples for study were cut from the parts of crystal grown with the same speed. The structural properties of these samples were characterized by X ray microtomography with the 0.5 μm resolution (SkyScan 1272), optical (Keyence VHX-7000) and electronic microscopy (JEOL KSM-6400) and X ray diffractions (XRD); when the optical properties were characterized by the cathode- and photoluminescence (CL and PL). The photoconversion properties of Ce doped YAG-Al<sub>2</sub>O<sub>3</sub> eutectics were studied under 450 nm blue LED excitation. The luminescent and photoconversion properties of Ce-doped Al<sub>2</sub>O<sub>3</sub>-YAG eutectics were compared with the reference YAG:Ce phosphors [3].



The XRD pattern and microtomography of the samples show a Al<sub>2</sub>O<sub>3</sub>-YAG:Ce eutectic structure containing main garnet and sapphire phases in the ratio of 46.6/53.4 % (Figure). The CL emission spectra, as well as PL emission and excitation spectra of the eutectic samples show the Ce<sup>3+</sup> emission band in the visible range, peaked at 552 nm with a decay time of 72 ns, and excitation bands peaked at 343 and 459 nm, corresponding to the 4f-5d transitions of Ce<sup>3+</sup> ions in the YAG:Ce garnet phase. The PL spectra of these samples show also the emission band in the UV range, peaked at 392 nm with a decay time of 40 ns, and excitation bands peaked 240 and 308 nm, respectively, corresponding to Al<sub>2</sub>O<sub>3</sub>:Ce phase. Presence of small (less than 1%) YAP:Ce perovskite phase was also tested in the PL emission/excitation spectra of the eutectic samples. Furthermore, the effective energy transfer processes are observed between Ce<sup>3+</sup> ions in Al<sub>2</sub>O<sub>3</sub> and perovskite phases and garnet phase under high-energy excitation and excitation in the corresponding UV bands.

We have also tested the prototypes of WLEDs, prepared using blue 450 nm LED chip and Ce doped Al<sub>2</sub>O<sub>3</sub>-YAG eutectic pc with the 0.5-1 mm thickness. The results of the tests are encouraging. The emission spectrum for these WLED covers the visible range from 460 to 820 nm with warmer light in comparison with the standard pc YAG:Ce [4]. The as-fabricated prototypes demonstrate also that application of Ce-doped Al<sub>2</sub>O<sub>3</sub>-YAG pc is very promising and can be used for indoor/outdoor lighting systems. For this reason, the future development of these eutectics with different morphology and their spectroscopic investigation can open rich perspectives for designing the novel generations of garnet phosphors for warm WLED convertors.

### References

- [1] Q. Sai, Z. Zhao, C. Xia, X. Xu, F. Wu, J. Di, L. Wang, *Optical Materials* 35 (2013) 2155–2159.
- [2] X. Shen, H. Chen, J. Lin, Y. Li, H. Lin, J. Chen, C. Chen, *IEEE Access* 7 (2019) 118679–118689.
- [3] S. Arjoca, D. Inomata, Y. Matsushita, K. Shimamura, *CrystEngComm* 18 (2016) 4799–4806.
- [4] N. Wei, T. Lu, F. Li, W. Zhang, B. Ma, Z. Lu, J. Qi, *Appl. Phys. Lett.* 101 (2012) 061902.

**Acknowledgments.** The work was performed in the frames of Polish NCN 2017/25/B/ST8/02932 project and Ukrainian № 0117U007370 project.

## Engineering of YAG:Ce to improve its scintillation properties

**O. Zapadlík<sup>1,2</sup>, M. Nikl<sup>2</sup>, J. Polák<sup>1</sup>, J. Houžvička<sup>1</sup>**

<sup>1</sup>CRYTUR, spol. s r.o., Na Lukách 2283, Turnov, 511 01, Czech Republic

<sup>2</sup>Institute of Physics of the Academy of Sciences of the Czech Republic, Cukrovarnicka 10, Prague, 162 53, Czech Republic

**E-mail: Ondrej.Zapadlik@crytur.cz**

Nowadays, both the academic and industrial laboratories are focusing on the development and optimization of scintillation materials to fulfil increasingly demanding requirements of high energy physics (HEP) experiments. Given the large volume of scintillators needed for HEP applications, in addition to high radiation hardness, fast scintillation response and reasonable light yield, the price is a factor of critical importance.

Single crystal of  $\text{Y}_3\text{Al}_5\text{O}_{12}:\text{Ce}$  (YAG:Ce) is well known traditional scintillator [1] which has been applied in different areas of research in nuclear and particle physics and in industry as well. It is a radiation hard, non-hygroscopic and chemically and mechanically stable inorganic scintillator with maximum emission wavelength around 550 nm.

Crytur company is a major producer of YAG:Ce with a mass production capability to grow and deliver high quality crystals in a flexible shapes. To reach low price, Crytur is capable to grow large YAG:Ce single crystals with diameter up to 5-inch with high light yield up to 35 000 ph/MeV. The major drawback of this scintillator, however, consists in its timing characteristics. Standard YAG:Ce growth by Czochralski method (CZ) shows the dominant scintillation decay time nearly two times longer compared to the lifetime of the  $\text{Ce}^{3+}$  luminescent center itself (60 ns), which disables its use for the applications requiring faster timing.

In this paper we study technological limits in the industrial scale growth of YAG:Ce by Czochralski method in a hydrogen-reducing atmosphere to speed-up its scintillation response using heavy codoping by magnesium [2]. In this way we stabilize the  $\text{Ce}^{4+}$  center which reduces the delayed radiative recombination at  $\text{Ce}^{3+}$  centers and consequently suppresses slow scintillation components. Moreover, the created Ce-Mg pairs contribute to scintillation response with faster-than-photoluminescence lifetime components due to decreased barrier for quenching in such pairs [3]. We study the trade-off between the acceleration of scintillation decay and decrease of light yield. With this approach we have developed new commercially available second generation of fast YAG:Ce (YFAG:Ce) scintillator. We will present correlated experiments to characterize luminescence and scintillation properties focusing on light yield, scintillation decay incl. its rise time, and afterglow, and their dependence on magnesium content in the crystals.

YAG:Ce crystal with significantly improved decay parameters can be achieved.

### References

- [1] M. Moszynski, et al, Nucl. Instrum. Methods Phys. Res. A 345 (1994) 461
- [2] A. Nagura, et al, Jp. J. Appl. Physics 54 (2015) 04DH17.
- [3] V. Babin, et al, J. Lumin. 215 (2019) 116608.

## Electronic properties of Mn-related defects in YAlO<sub>3</sub> perovskite crystal

**Yu. Hizhnyi<sup>1,2</sup>, Ya. Zhydachevskyy<sup>2,3</sup>, S.G. Nedilko<sup>1</sup>, H. Przybylińska<sup>2</sup>, M. Berkowski<sup>2</sup>, A. Suchocki<sup>2</sup>**

<sup>1</sup>Taras Shevchenko National University of Kyiv, 64/13 Volodymyrska st., Kyiv, Ukraine

<sup>2</sup>Institute of Physics, Polish Academy of Sciences, Al. Lotników 32/46, Warsaw 02-668, Poland

<sup>3</sup>Lviv Polytechnic National University, 12 Bandera, Lviv 79013, Ukraine

**E-mail: hizhnyi@univ.kiev.ua**

The crystals of yttrium orthoaluminate (YAlO<sub>3</sub>), called also yttrium aluminum perovskite (YAP), is widely known as a host material for solid-state lasers and scintillators. Manganese-doped YAP became of particular interest after its application potential has been shown as well for holographic recording and optical data storage [1] as for dosimetry of ionizing radiation using the thermally (TSL) or optically stimulated (OSL) luminescence [2]. Manganese ions in YAlO<sub>3</sub>:Mn crystals can be present in the form of Mn<sup>4+</sup> ions in octahedral coordination (Al<sup>3+</sup> sites) as well as Mn<sup>2+</sup> ions in strongly distorted dodecahedral coordination (Y<sup>3+</sup> sites). Despite a large volume of accumulated experimental data on optical and TSL properties of YAlO<sub>3</sub>:Mn, YAlO<sub>3</sub>:Mn,Si and YAlO<sub>3</sub>:Mn,Hf crystals the mechanisms of charge transfer processes in Mn-doped YAlO<sub>3</sub> require further clarification.

The report presents a systematic computational study of the electronic structure of a wide set of point defects related to Mn substitutions in YAlO<sub>3</sub> perovskite crystal. The calculations are carried out using the DFT-based Plane-Wave Pseudopotential method. Geometry-optimized spin-polarized calculations with GGA-PBE exchange-correlation functional were applied to (2x2x2) super-cells of YAlO<sub>3</sub> in which various defects and defect combinations like Mn<sub>Al</sub>, Mn<sub>Y</sub>, Mn<sub>Al</sub> + Mn<sub>Y</sub>, Mn<sub>Al</sub> + Hf<sub>Y</sub>, Mn<sub>Y</sub> + Si<sub>Al</sub>, Mn<sub>Y</sub> + V<sub>O</sub> and Mn<sub>Y</sub> + V<sub>O</sub> + V<sub>Al</sub> were considered. The partial densities of states, spatial distributions of the electronic charges, energy depths of the defect levels with respect to the band edges are calculated. Results of the calculations are analysed against existing experimental data on ESR, TSL, optical absorption and photoluminescence of YAlO<sub>3</sub>:Mn crystals.

The obtained computational results have been discussed in the context of possible role of Mn ions in charge trapping processes in YAlO<sub>3</sub> perovskite crystal. The discussion is related to, in particular, the nature of charge carriers traps which determine the TSL glow curves of YAlO<sub>3</sub>:Mn crystals, the possible charge states of Mn dopants in YAlO<sub>3</sub> host, and the main peculiarities of trapping and recombination processes in YAlO<sub>3</sub>:Mn<sup>2+</sup> materials.

### References

- [1] G.B. Loutts, M. Warren, L. Taylor, et al. Phys. Rev. B 57 (1998) 3706-3709.
- [2] Ya. Zhydachevskii, A. Luchechko, D. Maraba, et al. Radiat. Meas. 94 (2016) 18-22.

### Acknowledgments

The work was supported by the Polish National Science Centre (project no. 2018/31/B/ST8/00774), by the NATO SPS Project G5647, and by the National Research Foundation of Ukraine (grant 2020.01/0248).

## Comparative study on the influence of swift heavy ions on structural and luminescent properties of several important optical and scintillator materials

V. Pankratov<sup>1</sup>, V.A. Skuratov<sup>2</sup>, V. Pankratova<sup>1</sup>, A.P. Kozlova<sup>3</sup>, O.A. Buzanov<sup>4</sup>,  
A.I. Popov<sup>1</sup>

<sup>1</sup> Institute of Solid State Physics, University of Latvia, 8 Kengaraga iela, LV-1063 Riga, Latvia

<sup>2</sup> Joint Institute for Nuclear Research, Joliot-Curie 6, 141980, Dubna, Moscow Region, Russia.

<sup>3</sup> National University of Science and Technology "MISIS", Leninsky Pr. 4, 119049 Moscow, Russia

<sup>4</sup> OJSC "Fomos-Materials" Co., Buzheninova street 16, 107023 Moscow, Russia

E-mail: viktorija.pankratova@cfi.lu.lv

Research and development of scintillating materials and novel ionizing radiation detecting devices for particle physics, neutron research and medical imaging - are in the priority list of many European research centres including CERN.

In the current research radiation damages in the following single crystals relevant for nuclear and high-energy applications have been studied: Gd<sub>3</sub>Ga<sub>2</sub>Al<sub>3</sub>O<sub>12</sub> (GGAG), Y<sub>3</sub>Al<sub>5</sub>O<sub>12</sub> (YAG), Tb<sub>3</sub>Gd<sub>5</sub>O<sub>12</sub> (TGG), MgAl<sub>2</sub>O<sub>4</sub>, PbWO<sub>4</sub> and PbF<sub>2</sub>. These crystals were irradiated by 156 MeV Xe ions with several different fluences in the range  $6.6 \times 10^{10}$ - $2 \times 10^{12} \text{cm}^{-2}$ .

The induced damages (radiation defects) in all samples studied have been characterized by means of optical spectroscopy, Raman spectroscopy and luminescence spectroscopy techniques. The dependence of the radiation damage of irradiated crystals on the fluence of incident ions is established, which, however, is different for different materials. The origin of radiation damage, which has its own characteristics in each specific material, will be discussed.

### Acknowledgments

This work was supported by the Latvian Science Council Grant No. LZP 2020/2-0074 and National Research Program under the topic "High-Energy Physics and Accelerator Technologies".



## Synthesis and properties of luminescent glass-ceramics composed of vanadate-borate glass filled with vanadate nanoparticles

**O. Chukova<sup>1</sup>, S.A. Nedilko<sup>1</sup>, S.G. Nedilko<sup>1</sup>, T. Voitenko<sup>1</sup>, M. Androulidaki<sup>2</sup>, E. Stratakis<sup>2</sup>**

<sup>1</sup>Taras Shevchenko National University of Kyiv, Volodymyrska Str., 64/13, Kyiv 01601, Ukraine

<sup>2</sup>Institute of Electronic Structure & Laser (FORTH), Heraklion 711 10 Crete, Greece

**E-mail: chukova@univ.kiev.ua**

Luminescent oxide composite materials, such as activated oxide glass ceramics, are promising for high energy applications as they are usually characterized by high thermal and mechanical stabilities. In a case of activation of glass materials with luminescent nanoparticles, luminescent efficiency of the latter may be decreased due their interaction with a glass matrix. There is a possibility to prevent loses of luminescent characteristics of nanoparticles with their incorporation in such matrices using variations of their compositions. In the present work borate-vanadate glass matrices were incorporated with vanadate nanoparticles. The similar compositions of the both components were chosen with the aim to achieve the best interaction between glass matrix and activating crystalline nanoparticles.

Vanadate-borate glass composites were synthesized by melt quenching procedure from calculated amounts of vanadium  $V_2O_5$  and  $HBO_2$ . The concentration of vanadate component is varied from 3 to 40 mass%. The reagents were grinded, mixed and placed in porcelain crucibles, then melted 2 hours in the air at 700 C in electric muffle furnace. After melting, the samples were quickly quenched using non-magnet metal plates. Some of the samples were doped by the luminescent vanadate  $La_{1-x}Eu_xVO_4$  nanoparticles synthesized by sol-gel method.

Phase compositions of the synthesized samples were determined using X-ray diffractometer Shimatzu 2000 ( $Cu_{K\alpha}$ -radiation with a Ni filter). Microstructure of the samples was studied with a scanning electron microscope (SEM) JEOL JSM-7000F. Reflectance spectroscopy of the samples was performed using Perkin Elmer Lambda 950 spectrometer. Luminescence spectra excited with 325 nm laser were registered using ACTONi (500) monochromator with slit on 50 micron and liquid  $N_2$  - cooled CCD camera.

It was found that decrease of the  $V_2O_5$  vanadium oxide content from 40 to 4% in the glass matrix leads to the increase of intensity of reflection and to the shift of the reflection spectra edge from 560 nm to 480 nm for the  $B_2O_3-V_2O_5$ . Dependencies of band gap energy values on of the components concentration were studied using Kubelko-Munk transformations.

Luminescence properties of the synthesized samples were investigated. Spectra of the doped with vanadate nanoparticles composites contain narrow spectral lines in the 580 -720 nm spectral range, those should be ascribed to well-known f-f electron transitions in the  $Eu^{3+}$  ions. Intensity of this emission depends on the method of luminescent nanoparticles incorporation to the glass. Influence of the synthesis conditions and optimal ratios of the components those allow obtaining of samples promising for practical applications as luminescent detecting materials have been discussed.

### Acknowledgments

This work was supported by the Ministry of Education and Science of Ukraine and by the Horizon Europe research and innovation program within transnational access activity under grant agreement No 654360.

## Scintillation and charge trapping properties of Cs<sub>2</sub>HfCl<sub>6</sub> and Cs<sub>2</sub>ZrCl<sub>6</sub> single crystals in a wide temperature range

**S.S. Nagorny<sup>1,2</sup>, V. Babin<sup>3</sup>, M. Buryi<sup>3</sup>, R. Kandel<sup>2,4</sup>, R. Ligthart<sup>5</sup>, V.B. Mikhailik<sup>6</sup>, V.V. Nahorna<sup>2,4</sup>, S. Nisi<sup>7</sup>, V. Vaněček<sup>3,8</sup>, L. Prouzová Prochazková<sup>3,8</sup>, P. Wang<sup>2,4</sup>**

<sup>1</sup>*Department of Physics, Engineering Physics and Astronomy, Queen's University Kingston, ON, K7L 3N6, Canada.*

<sup>2</sup>*Arthur B. McDonald Canadian Astroparticle Physics Research Institute, Department of Physics, Engineering Physics and Astronomy, Queen's University, Kingston ON K7L 3N6, Canada.*

<sup>3</sup>*Institute of Physics of the Czech Academy of Sciences, Cukrovarnicka 10/112, 16200 Prague, Czech Republic.*

<sup>4</sup>*Chemistry Department, Queen's University Kingston, ON, K7L 3N6, Canada.*

<sup>5</sup>*Utrecht University, Heidelberglaan 8, 3584 CS Utrecht, Netherlands.*

<sup>6</sup>*Diamond Light Source, Harwell Campus, Didcot, OX11 0DE, UK.*

<sup>7</sup>*INFN - Laboratori Nazionali del Gran Sasso, Assergi, AQ, I-67100, Italy.*

<sup>8</sup>*Czech Technical University in Prague, Faculty of Nuclear Sciences and Physical Engineering, Břehová 7, 115 19 Czech Republic.*

**E-mail: sn65@queensu.ca**

Nowadays there is significant interest in Cs<sub>2</sub>HfCl<sub>6</sub> (CHC) scintillating crystals and CHC-family materials because of their outstanding scintillating properties demonstrated in recent measurements - a high light yield (in the range of 30,000-70,000 photons/MeV), perfect linearity of the scintillating response down to low energies (of about 20 keV), excellent energy resolution (< 3.5% at 662 keV in the best configuration), a high quenching factor for alpha particles QF = (0.3-0.5), and an excellent statistical pulse shape discrimination ability.

In framework of this study, Cs<sub>2</sub>HfCl<sub>6</sub> (CHC) and Cs<sub>2</sub>ZrCl<sub>6</sub> (CZC) single crystals were grown by vertical Bridgman method from as-received and purified raw materials. The materials at each stage of the crystal production chain have been characterized by mass-spectrometry technique, thus providing a clear view of impurities re-distribution through a purification and growth processes. Luminescence and charge trapping properties were studied in the CHC and CZC crystals by the correlated measurements of electron paramagnetic resonance (EPR), radioluminescence (RL) and thermally stimulated luminescence (TSL) techniques in a wide temperature range 10-300K.

Moreover, scintillation characteristics of CHC and CZC crystals were studied over the temperature range of 9-295 K in optical cryostat under irradiation of alpha particles. Scintillation decay curves for signal from both crystals were fitted by three components. The CHC crystal demonstrated light yield of 31,000 and 40,000 ph/MeV at room temperature and 9 K, respectively. While, the CZC crystal demonstrated the light yield of 42,000 and 50,000 ph/MeV at room temperature and 9 K under alpha particle irradiation, respectively. The temperature dependence of the scintillation light output for both crystals exhibit unusual s-shaped character with the drop at around 100 K (75 K for CZC) that correlates well with the decrease of the Vk(a) hole trapping center (pseudo molecular ion), EPR signal evidencing de-trapping of the holes trapped at the Vk(a) center in these crystals. Therefore, the Vk(a) center was assumed to be the part of the self-trapped exciton (STE) which participates in the emission above 100 K becoming "frozen" below 100 K. Further discussion on the defect structure of Cs<sub>2</sub>HfCl<sub>6</sub> and Cs<sub>2</sub>ZrCl<sub>6</sub> scintillating crystals are presented.

Furthermore, future perspectives of the use of Cs<sub>2</sub>HfCl<sub>6</sub> and Cs<sub>2</sub>ZrCl<sub>6</sub> scintillating crystals as highly sensitive detectors to search for rare nuclear processes are also discussed.

## **New type of ultra-high (<3%) energy resolution gamma spectrometry using traditional scintillators**

**V.Gayshan<sup>2</sup>, A.Gektin<sup>1</sup>, P.Steinmeyer<sup>3</sup>, V.Suzdal<sup>1</sup>**

<sup>1</sup>*Amcrys Ltd, Kharkov, Ukraine*

<sup>2</sup>*ScintiTech, Inc, Shirley, MA USA*

<sup>3</sup>*Radiation Safety Associates, Inc, Hebron, CT, USA*

**E-mail: [vgayshan@scintitech.com](mailto:vgayshan@scintitech.com)**

The results of the first phase of development of an ultra-high energy resolution acquisition system, "Eagle Eye," are presented. The goal of this phase was to modify an existing commercial multichannel analyzer (MCA) to utilize an Eagle Eye type of spectrum acquisition; to conduct measurements of Cs137, Ba133, Co60 isotopes with NaI(Tl), CsI(Na), CsI(Tl), SrI<sub>2</sub>(Eu) and LBC crystals; and to validate the results. Also, spectra from different types of damaged crystals (hydration, mechanical damage, or otherwise non-optimal light collection) were studied with the goal of using Eagle Eye-equipped acquisition systems to develop a detector diagnostic tool.

## Electron and hole centers in the UV - irradiated Bi<sup>3+</sup> - doped Ca<sub>3</sub>Ga<sub>2</sub>Ge<sub>3</sub>O<sub>12</sub> garnet

**A. Krasnikov<sup>1</sup>, V. Tsiumra<sup>2,3</sup>, L. Vasylechko<sup>4</sup>, S. Zazubovich<sup>1</sup>, Ya. Zhydachevskyy<sup>2</sup>**

<sup>1</sup>*Institute of Physics, University of Tartu, W. Ostwaldi 1, 50411 Tartu, Estonia*

<sup>2</sup>*Institute of Physics, Polish AS, Al. Lotników 32/46, 02-668 Warsaw, Poland*

<sup>3</sup>*Ivan Franko National University of Lviv, 107 Tarnavskoho str., 79017 Lviv, Ukraine*

<sup>4</sup>*Lviv Polytechnic National University, Bandera 12, 79013 Lviv, Ukraine*

**E-mail: [aleksei.krasnikov@ut.ee](mailto:aleksei.krasnikov@ut.ee)**

Bismuth - doped compounds, owing to their excellent luminescence performance and tunable luminescence properties, attract an increasing attention as promising materials for applications in different fields, e.g., in fiber lasers, broadband optical amplifiers, bioimaging, scintillators, light-emitting diodes, solar cells, etc. Among them, the materials, where a trivalent Bi<sup>3+</sup> ion substitutes for a trivalent rare-earth ion, have been studied in most detail. However, due to a relatively high cost and limited resources of rare-earths, highly effective *rare-earth-free* compounds are needed for the above-mentioned applications. The Ca<sub>3</sub>Ga<sub>2</sub>Ge<sub>3</sub>O<sub>12</sub> garnet is one of such compounds. Recently, we have carried out a detailed investigation of the Bi<sup>3+</sup> - doped microcrystalline powder of Ca<sub>3</sub>Ga<sub>2</sub>Ge<sub>3</sub>O<sub>12</sub> by the X-ray diffraction and time-resolved photoluminescence spectroscopy methods. In the luminescence spectrum of Ca<sub>3</sub>Ga<sub>2</sub>Ge<sub>3</sub>O<sub>12</sub>:Bi, the Bi<sup>3+</sup> - related ultraviolet (UV) and visible (VIS) emission bands have been observed. The complex UV emission bands (located around 3.9 eV and 3.06 eV) are ascribed to the radiative decay of the triplet relaxed excited state of Bi<sup>3+</sup> ions having different nearest surroundings. The VIS emission (2.41 eV) is shown to arise from an exciton localized around a Bi<sup>3+</sup> ion.

Under selective UV irradiation of Ca<sub>3</sub>Ga<sub>2</sub>Ge<sub>3</sub>O<sub>12</sub>:Bi in the 4.1 - 5.7 eV energy range, various types of electron and hole centers are also created. In this work, these processes are investigated by the TSL method in the 80 - 510 K temperature range. The dependences of the TSL characteristics on the irradiation energy, temperature, and duration, as well as on the emission energy are measured and analyzed. The origin of the optically created intrinsic and Bi - related electron and hole centers of different types, responsible for the observed TSL glow curve peaks, is clarified. The band gap energy of Ca<sub>3</sub>Ga<sub>2</sub>Ge<sub>3</sub>O<sub>12</sub> and the depths of electron traps are determined. The electron-hole recombination processes, resulting in the appearance of the intrinsic and Bi<sup>3+</sup> - related luminescence, are investigated.

Two mechanisms are suggested to be responsible for the photostimulated creation of the electron and hole centers in Ca<sub>3</sub>Ga<sub>2</sub>Ge<sub>3</sub>O<sub>12</sub>:Bi under irradiation in the Bi - related absorption region: (i) the release of electrons to the conduction band (CB) from the lowest-energy excited level of Bi<sup>3+</sup>, located at about 30 meV below the bottom of the CB, and the subsequent trapping of the free electrons at different intrinsic and Bi - related centers; (ii) an electron transfer from the valence band (VB) to the ground electron state of a Bi - related center. As a result of these processes, mobile holes in the VB and the electron centers, arising from the Ca<sub>3</sub>Ga<sub>2</sub>Ge<sub>3</sub>O<sub>12</sub> host and responsible for the TSL glow curve peaks located at about 138, 280, 350 and 440 K, as well as the Bi<sup>2+</sup> - type electron centers, responsible for the ≈180 K and 230 - 250 K peaks, are created. The mobile holes become trapped by Bi<sup>3+</sup> ions resulting in the formation of the Bi<sup>4+</sup> - type hole centers. The holes trapped by the regular oxygen ions and/or by the oxygen ions located close to cation vacancies V<sub>c</sub>, result in the formation of the intrinsic O<sup>-</sup> - type hole centers. The recombination of thermally released electrons with the hole centers results in the appearance of the Bi<sup>3+</sup> - related complex ≈3.95 eV emission band and the intrinsic 2.67 eV emission band, respectively.

## Charge trapping in Li doped $Y_3Al_5O_{12}$ single crystals: correlated EPR and TSL investigation

**M. Buryi<sup>1</sup>, V. Laguta<sup>1</sup>, V. Babin<sup>1</sup>, K. Bartosiewicz<sup>2,3</sup>, A. Yoshikawa<sup>3,4</sup>, K. Kamada<sup>3,4</sup>, S. Kurosawa<sup>3,4</sup>, A. Yamaji<sup>3</sup>, M. Nikl<sup>1</sup>**

<sup>1</sup>*Institute of Physics CAS, Cukrovarnicka 10, 162 00 Prague, Czech Republic*

<sup>2</sup>*Kazimierz Wielki University, Institute of Physics, ul. Powstańców Wielkopolskich 2, 85-090 Bydgoszcz, Poland*

<sup>3</sup>*Institute for Materials Research, Tohoku University, 2-1-1 Katahira, Sendai 980-8577, Japan*

<sup>4</sup>*New Industry Creation Hatchery Center, Tohoku University, 6-6-10 Aboba, Aramaki, Sendai, 9880-8579, Japan*

**E-mail: buryi@fzu.cz**

Doped with different activators, e.g., Ce (see e.g., [1]) yttrium aluminum garnets,  $Y_3Al_5O_{12}$  (YAG), serve as efficient scintillators which find implementation in different fields of science, medicine and industry for decades. In order to push their light-emitting feasibilities to the intrinsic limit, numerous approaches to the material synthesis were proposed. For example, in the last years Li co-doping appeared perspective as this resulted in the faster emission and larger light yield (LY) of YAG [2]. However, Li position in the YAG lattice is still questionable whether it is substitutional or interstitial.

Well-known drawback of the yttrium or lutetium aluminium garnets as well as the other simple and complex oxides are charge trapping defects (centers). By trapping electrons or holes they contribute to afterglow thus degrading LY. The combination of electron paramagnetic resonance (EPR) and thermally stimulated luminescence (TSL) is the powerful tool for the investigation of charge trapping centers. It is known that typical paramagnetic hole trapping defects are  $O^-$  whereas  $F^+$  centers are created by the electron trapping at an oxygen vacancy. Both defects are sensitive to the doping, i.e., the type of dopant (cation or anion) and its amount play significant role in the thermal stability of the trap. Presently we report on the peculiarities of the X-ray induced defects creation in YAG:Li(1000, 10000 ppm) with the special accent put on the presence of Li inside the garnet structure. The existence of  $O^-$  and  $F^+$  centers were observed by means of EPR. Their thermal properties were studied in detail by both EPR and TSL.

### References

- [1] M. Nikl, V. Babin, J. Pejchal, V.V. Laguta, M. Buryi, J. Mares, K. Kamada, Sh. Kurosawa, A. Yoshikawa, D. Panek, P. Bruza, K. Mann, M. Muller, *IEEE Trans. Nucl. Sci.* 63 (2016) 433–438.
- [2] P.T. Dickens, D. T. Haven, S. Friedrich, M. Saleh, K. G. Lynn, *Journal of Applied Physics* 121 (2017) 123104.

### Acknowledgments

The financial support of the Czech Science Foundation project No. 20-12885S and the Operational Programme Research, Development and Education financed by European Structural and Investment Funds and the Czech Ministry of Education, Youth and Sports (Project No. SOLID21 CZ.02.1.01/0.0/0.0/16\_019/0000760) and Japan Society for the Promotion of Science grant No. P17379 are gratefully acknowledged.

## The influence of temperature on the photoluminescence of lithium fluoride crystals

**M. Sankowska<sup>1</sup>, P. Bilski<sup>1</sup>, B. Marczewska<sup>1</sup>, W. Gieszczyk<sup>1</sup>, M. Kłosowski<sup>1</sup>,  
Ya. Zhydachevskii<sup>2</sup>**

<sup>1</sup>*Institute of Nuclear Physics, Polish Academy of Sciences PAN (IFJ PAN), Kraków, Poland*

<sup>2</sup>*Institute of Physics, Polish Academy of Sciences, Warsaw, Poland*

**E-mail: malgorzata.sankowska@ifj.edu.pl**

Lithium fluoride is a very well-known luminescent material that has been studied and used in practice for several decades. One of the most interesting phenomenon that occurs in it is creation of radiation-induced color centers (CC) and their photoluminescence (PL). Ionizing radiation produces in LiF crystals mostly F centers, which often aggregate into more complex defects, like F<sub>2</sub> and F<sub>3</sub><sup>+</sup> color centers. F<sub>2</sub> center is composed of two anion vacancies with two bounded electrons, while F<sub>3</sub><sup>+</sup> of three vacancies with two electrons. When these centers are excited with blue light (wavelength near 445 nm), they emit photoluminescence peaked at about 670 nm (related to F<sub>2</sub>) and about 525 nm (related to F<sub>3</sub><sup>+</sup>).

Concentrations of various color centers in LiF and their photoluminescence spectra were found to be significantly influenced by temperature. The available data show that this influence is very complex. Under thermal treatment, some centers begin to disintegrate, while others interact with each other creating new species. Within this work we studied the influence of temperature treatment (up to 400°C) on PL emission spectra, as well as on absorption spectra of LiF crystals. The temperature effects were observed at various stages of the process: before irradiation, during irradiation, after irradiation, and during PL measurement.

Photoluminescence of color centers creates possibility for direct visualization of the path of ionizing particles in LiF using a fluorescence microscope, and enabled the development of the technique called Fluorescent Nuclear Track Detection (FNTD). The results of investigations of the influence of temperature on microscopic images of alpha particle fluorescent tracks will be also presented.

### References

- [1] P. Bilski, B. Marczewska, Y. Zhydachevskii, Radiophotoluminescence spectra of lithium fluoride TLDs after exposures to different radiation modalities *Radiat. Meas.* 97 (2017) 14-19.
- [2] P. Bilski, B. Marczewska, W. Gieszczyk, M. Kłosowski, M. Naruszewicz, M. Sankowska, S. Kodaira, Fluorescent imaging of heavy charged particle tracks with LiF single crystals. *J. Lumin.*, 213(2019a.) 82-87.

### Acknowledgments

This work was supported by the National Science Centre, Poland (Contract No. UMO-2020/37/N/ST5/01975).

## Low temperature thermoluminescence of $\beta$ -Ga<sub>2</sub>O<sub>3</sub> Scintillator – new results and new interpretations

**M.E. Witkowski<sup>1</sup>, K.J. Drozdowski<sup>1</sup>, M. Makowski<sup>1</sup>, W. Drozdowski<sup>1</sup>, A.J. Wojtowicz<sup>1</sup>, K. Irscher<sup>2</sup>, R. Schewski<sup>2</sup>, Z. Galazka<sup>2</sup>**

<sup>1</sup>*Institute of Physics, Faculty of Physics, Astronomy and Informatics, Nicolaus Copernicus University in Toruń, ul. Grudziądzka 5, 87-100 Toruń, Poland*

<sup>2</sup>*Leibniz-Institut für Kristallzüchtung, Max-Born-Str. 2, 12489 Berlin, Germany*

**E-mail: mwit@fizyka.umk.pl**

$\beta$ -Ga<sub>2</sub>O<sub>3</sub>, which is the most stable form from five different polymorphs of gallium oxide, provides a prospective host for activation with different ions towards applications in the field of semiconductor scintillators [1-5]. Thermoluminescent glow curve analysis enables the determination of values of trap depths and frequency factors, i.e. the parameters governing the release of electrons from the traps, as well as provides some indication of trapping and retrapping rates. However, deriving correct parameters in the fitting process is always a challenge, especially when the peaks cannot be described according to the well-known Randall-Wilkins model [6]. In this Communication we present the fitted glow curves and related trap parameters obtained with a procedure which includes relevant kinetic equations that are used to compute the fitting curves numerically. The issue of retrapping is also discussed.

### References

- [1] T. Yanagida, G. Okada, T. Kato, D. Nakauchi, S. Yanagida, *Applied Physics Express* 9 (2016) 042601/1-4.
- [2] Y. Usui, T. Oya, G. Okada, N. Kawaguchi, T. Yanagida, *Optik* 143 (2017) 150-157.
- [3] N. He, H. Tang, B. Liu, Z. Zhu, Q. Li, C. Guo, M. Gu, J. Xu, J. Liu, M. Xu, L. Chen, X. Ouyang, *Nuclear Instruments and Methods in Physics Research A* 888 (2018) 9-12.
- [4] Z. Galazka, R. Schewski, K. Irscher, W. Drozdowski, M.E. Witkowski, M. Makowski, A.J. Wojtowicz, I.M. Hanke, M. Pietsch, T. Schulz, D. Klimm, S. Ganschow, A. Dittmar, A. Fiedler, T. Schroeder, M. Bickermann, *Journal of Alloys and Compounds* 818 (2020) 152842/1-7.
- [5] W. Drozdowski, M. Makowski, M.E. Witkowski, A.J. Wojtowicz, R. Schewski, K. Irscher, Z. Galazka, *Optical Materials* 105 (2020) 109856/1-6.
- [6] J.T. Randall, M.H.F. Wilkins, *Proceedings of the Royal Society of London A* 184 (1945) 366-407.

### Acknowledgments

This research has been financed from the funds of the Polish National Science Centre (NCN) and the German Research Foundation (DFG) in frames of a joint grant (NCN: 2016/23/G/ST5/04048, DFG: GA 2057/2-1).

## Novel NASICON-type phosphors doped with RE ions: structure and luminescence

**N. Krutyak<sup>1,2</sup>, D. Spassky<sup>2,3</sup>, D. Deyneko<sup>4</sup>, V. Nagirnyi<sup>2</sup>, V. Morozov<sup>4</sup>**

<sup>1</sup>Physics Department, M.V. Lomonosov Moscow State University, Russia

<sup>2</sup>Institute of Physics, University of Tartu, Estonia

<sup>3</sup>Skobeltsyn Institute of Nuclear Physics, Moscow State University, Moscow, Russia

<sup>4</sup>Chemistry Department, M.V. Lomonosov Moscow State University, Russia

**E-mail: krutyakn@yahoo.com**

Compounds based on phosphates with Na superionic conductivity (NASICON) are considered as novel phosphors for application in LEDs. It was recently shown that the NASICON-type  $\text{Na}_{3-2x}\text{Sc}_2(\text{PO}_4)_3:x\text{Eu}^{2+}$  phosphors exhibit a unique temperature stability exceeding that of traditional LED phosphors [1]. The effect is related to temperature induced modification of the process of energy transfer to  $\text{Eu}^{2+}$  connected with phase transitions. Another novel NASICON-type phosphate,  $\text{Na}_{3.6}\text{Y}_{1.8}(\text{PO}_4)_3$  doped with various activators, is also extensively studied and considered for application in LEDs [2]. Here, we present the results of the study of structure and luminescence properties of NASICON-type phosphors  $\text{Na}_{3.6}\text{A}_{1.8}(\text{PO}_4)_3$  (A = Y, Lu) doped with RE ions ( $\text{Eu}^{3+}$ ,  $\text{Dy}^{3+}$ ).

A series of  $\text{Na}_{3.6}\text{Y}_{1.8-x}(\text{PO}_4)_3:x\text{Dy}^{3+}$  ( $x = 0.01-0.4$ ),  $\text{Na}_{3.6}\text{Lu}_{1.8-x}(\text{PO}_4)_3:x\text{Dy}^{3+}$  ( $x = 0.01-0.4$ ),  $\text{Na}_{3.6}\text{Y}_{1.8-x}(\text{PO}_4)_3:x\text{Eu}^{3+}$  ( $x = 0.01-0.7$ ), and  $\text{Na}_{3.6}\text{Lu}_{1.8-x}(\text{PO}_4)_3:x\text{Eu}^{3+}$  ( $x = 0.01-0.4$ ) phosphors were synthesized by solid-state reaction. The characterization of crystal structure was performed using XRD technique. Luminescence excitation and emission spectra under excitation in the UV region were measured in the temperature range 77–500 K using a laboratory setup based on a LOT-Oriel MS-257 spectrograph. Spectra in VUV region were obtained using a specialized setup with a Shamrock 303i (Andor Technology) monochromator and optical vacuum cryostat allowing measurements at  $T = 5-300$  K.

The structure analysis confirmed that all samples were single-phased and crystallized in a NASICON-type structure (sp. gr.  $R\bar{3}$ ). The luminescence spectra under UV excitation consist of the luminescence bands corresponding to the 4f–4f intraconfigurational transitions in  $\text{Dy}^{3+}$  or  $\text{Eu}^{3+}$  ions. For the series with Dy, the decrease of luminescence intensity was observed due to concentration quenching. Different channels of energy transfer to RE ions are considered using the results of VUV luminescence spectroscopy.

It is also shown that under the VUV excitation photoluminescence spectra demonstrate an additional non-elementary broad band in the UV spectral region. The origin of the band is discussed. The high-energy band is attributed to intrinsic luminescence of excitons self-trapped at the  $\text{PO}_4^{3-}$  complexes. The onset of excitation spectrum is tentatively ascribed to the fundamental absorption edge and the bandgap is estimated as  $E_g > 7$  eV. Temperature dependence of luminescence intensity and decay kinetics were studied as well. Chromaticity characteristics were determined for the whole set of samples.

### References

- [1] Y.H. Kim et al., *Nature Materials*, 16 (2017) 543-550.
- [2] U. Farooq et al., *Journal of Alloys and Compounds*, 821 (2020) 153513.

### Acknowledgments

This work was performed within the project MOBJD613.



## Luminescence Response of YAP:Mn Crystal to the Ionizing and Visible Radiation

**S. Ubizskii<sup>1</sup>, O. Poshyvak<sup>1</sup>, D. Afanassyev<sup>1</sup>, A. Luchechko<sup>1,2</sup>, Ya. Zhydachevskyy<sup>1,3</sup>**

<sup>1</sup> Lviv Polytechnic National University, Lviv, S. Bandera St, 12, 79013, Ukraine

<sup>2</sup> Ivan Franko National University of Lviv, Universytetska St., 1, Lviv, 79000, Ukraine

<sup>3</sup> Institute of Physics of the Polish Academy of Sciences, Al. Lotników, 32/46, Warsaw, 02-668, Poland

**E-mail: Sergii.B.Ubizskii@lpnu.ua**

Optically stimulated luminescence (OSL) is used last decades as novel method of passive luminescence dosimetry and an alternative to the traditional thermo-luminescence dosimetry [1]. One of the promising material for this application is crystalline  $\text{YAlO}_3:\text{Mn}^{2+}$  (YAP:Mn) [2,3]. But despite the similarity of physical processes during irradiation and stimulated luminescence OSL has a number of features. In particular, in contrast to thermo-luminescence, in which thermal activation of shallow traps makes them inactive when deeper dosimetric traps start emptying, the charge carriers released from the latter during optical stimulation can be recaptured not only on deep traps but also on shallow ones. This peculiarity leads to long-lasting afterglow. It was previously reported [4] that glow initiated by optical stimulation of irradiated YAP:Mn has a hyperbola decay kinetics being described by Becquerel's empirical law.

The present work is devoted to investigation of afterglow after X-ray irradiation as well as one induced by optical stimulation by intense visible light produced from high power LEDs. The last is used in particular for the erasing of residual dosimetric signal optically.

Experiments have shown that the afterglow being registered up to 27 h could be produced by X-ray irradiation (45 kV, 0.3 mA) just for 10 s. Its initial level is saturating if the exposure time becomes more than 300 s. At the same time even illumination by red (660 nm) light can not only stimulate OSL but produce additional afterglow that should be taken into account in OSL dosimetric measurements based on YAP:Mn.

### References

- [1] E.G. Yukihara, S.W.S. McKeever, *Optically Stimulated Luminescence: Fundamentals and Applications*, Willey (2011).
- [2] Ya. Zhydachevskii, A. Suchocki, M. Berkowski, Ya. Zakharko, *Radiation Measurements*, 42 (2007) 625-627.
- [3] Ya. Zhydachevskii, A. Luchechko, D. Maraba et al., *Radiation Measurements*, 94 (2016) 18-22.
- [4] S. Ubizskii, D. Afanassyev, Ya. Zhydachevskii, et al., *2019 International Conference on Information and Telecommunication Technologies and Radio Electronics (UkrMiCo-2019)*, Odesa, Ukraine.

### Acknowledgments

This work was supported by the NATO Science for Peace and Security Program (project G5647), National Research Foundation of Ukraine (grant 2020.01/0248) and Ministry of Education and Science of Ukraine (project 0119U002249).

## Luminescent and structural properties of $\text{Sc}_x\text{Y}_{1-x}\text{VO}_4:\text{Eu}^{3+}$ solid solutions

V. Voznyak-Levushkina<sup>1</sup>, D. Spassky<sup>2,3</sup>, E. Zych<sup>4</sup>

<sup>1</sup>Physics Department, M.V. Lomonosov Moscow State University, Moscow, Russia

<sup>2</sup>Skobeltsyn Institute of Nuclear Physics, Moscow State University, Moscow, Russia

<sup>3</sup>Institute of Physics, University of Tartu, Estonia

<sup>4</sup>Faculty of Chemistry, University of Wrocław, Wrocław, Poland

E-mail: [spas@srd.sinp.msu.ru](mailto:spas@srd.sinp.msu.ru)

Orthovanadates with zircon structure  $\text{REVO}_4$  (RE is a rare-earth ion) are well-known due to their excellent electronic, thermal, optical, and luminescent properties. As a result, vanadates are considered for application as display and LED phosphors, non-contact luminescent thermometers, scintillation detectors, spectral converters for enhancement of solar cell efficiency and laser hosts. Optimization of vanadates properties for different applications can be achieved by using their solid solutions. The gradual change of crystal's composition realized in substitutional solid solutions allows to modify the properties of compounds. Recently it was shown that  $(\text{Sc},\text{Y})\text{VO}_4$  mixed vanadates can be considered as promising materials for application in lighting and as a new media for Raman laser converter [1,2]. Here we present the results of the study of luminescent and structural properties of  $\text{Sc}_x\text{Y}_{1-x}\text{VO}_4:\text{Eu}^{3+}$  solid solutions.

Synthesis of the vanadate  $\text{Sc}_x\text{Y}_{1-x}\text{VO}_4:\text{Eu}^{3+}$  mixed crystals ( $x=0, 0.1, 0.3, 0.5, 0.7, 0.9, 1$ ) doped with 1mol% of  $\text{Eu}^{3+}$  was carried out by the solid state method. The influence of the annealing on the samples' phase purity was investigated. The crystallinity was controlled by the methods of X-ray diffraction (XRD) and scanning electron microscopy (SEM). The XRD analysis revealed that the synthesized samples are homogenous and crystallize in the tetragonal system, I41/amd space group. The lattice parameters of the solutions were derived from the XRD data and also using a recently proposed structural model [3]. The luminescence properties were studied under UV and X-ray excitations in the temperature range 80-500 K. Emission from self-trapped excitons, defect-related complexes as well as interconfigurational transitions in  $\text{Eu}^{3+}$  has been observed. The dependence of intensity of  $^5\text{D}_0 - ^7\text{F}_0$  forbidden transition on Sc/Y ratio allows to trace the rate of crystal structure disorder, which occurs in solid solutions due to the nonhomogeneous distributions of substitutional cations. The dependence of the relative intensities of the observed emission bands on the Sc/Y ratio and temperature is analyzed taking into account the processes of energy transfer between the emission centers. The dependence of the edge of the creation of separate e-h pairs was obtained from the analysis of the excitation spectra of thermostimulated luminescence.

### References

- [1] F. Kang, H. Zhang, L. Wondraczek, et al, *Chem. Mater.* 28 (2016) 2692–2703.
- [2] A.I. Zagumennyi, S.A. Kutovoi, A.A. Sirotkin, et al., *Appl Phys B* 99 (2010) 159–162.
- [3] M.G. Brik, M. Bettinelli, E. Cavalli, *J. Solid State Chem.* 230 (2015) 49–55.

### Acknowledgments

This work is supported by the Russian Science Foundation under grant 21-12-00219.

## Recombination emission and electron trapping centers in irradiated BaSO<sub>4</sub> and CaSO<sub>4</sub>

T.N. Nurakhmetov<sup>1</sup>, Zh.M. Salikhodzha<sup>1</sup>, A.M. Zhunusbekov<sup>1</sup>, A.Zh. Kainarbay<sup>1</sup>,  
D.H. Daurenbekov<sup>1</sup>, K. B. Zhangylyssov<sup>1</sup>, T.T. Alibay<sup>1</sup>, B.M. Sadykova<sup>1</sup>,  
B.N.Yussupbekova<sup>1</sup>, D.A.Tolekov<sup>1</sup>

<sup>1</sup>L.N. Gumilyov Eurasian National University, 2 Satpayev str., Astana, Kazakhstan, Z01A3D7

E-mail: duke.ddx@yandex.ru

Two types of emission appear in irradiated sulfates of alkali and alkaline earth metals. Short-wavelength emission bands arising from the recombination of an electron with unequally located holes at 3.64 eV, 3.7-3.8 eV, 4.1-4.3 eV and 4.9-5.0 eV and long-wavelength recombination emission appears at 3.0-3.1 eV, 2.6-2.7 eV, and 2.4-2.5 eV in irradiated crystals CaSO<sub>4</sub> and BaSO<sub>4</sub>.

The appearance of intrinsic emissions in range from 3.64 eV to 4.9-5.0 eV is possibly associated with different thermal stability of localized holes SO<sub>4</sub><sup>-</sup> in different crystallographic [1] directions. The localization of holes at different energy distances above the valence band can be associated with structure of the valence band. The top of the valence band, in which the electronic transition occurs, consists of several subbands. Holes SO<sub>4</sub><sup>-</sup> created in subbands during relaxation should rise above the valence band. Thus, the spectral position of the main emission arising in the irradiated crystal of CaSO<sub>4</sub> and BaSO<sub>4</sub> upon recombination of an electron with hole centers depends on the location and surroundings of SO<sub>4</sub><sup>-</sup> radicals. It is possible that cationic and anionic vacancies are created near the radicals SO<sub>4</sub><sup>-</sup>.

Assuming that these long-wavelength emissions should be associated with the formation of electron-hole trapping centers, we measured the excitation spectrum for these emissions. It was shown that for all the investigated sulfates of alkali metals and for BaSO<sub>4</sub> and CaSO<sub>4</sub> these emissions are excited at photon energies 4.5-4.7 eV, 3.9-4.0 eV and 3.35-3.5 eV. The excitation spectrum of recombination emission of 3.0-3.1 eV, 2.6-2.7 eV and 2.4-2.5 eV is in the transparency region of the crystal matrix. Thus, the energy distances of electron-hole trapping centers are located at 4.5-4.7 eV, 3.9-4.0 eV and 3.35-3.5 eV. Recombination emission of 3.0-3.1 eV, etc., arise in sulfates with impurities in the long-wavelength region of these bands and are excited in the same spectral regions.

Phosphorescence or tunneling luminescence was detected for a number of alkali metal sulfates at 3.0-3.1 eV, 2.6-2.7 eV and 2.4-2.5 eV confirming the detected electron-hole trapping centers. It is shown that these recombination or tunneling emissions are generated by excitation in the fundamental region of crystals, where free electron-hole pairs are created.

### References

[1] R. Danby, Jh. Boas, R. Calvert, Jh. Pilbrow, *J.Phys.C.:Solid State Phys.*, 15 (1982) 2483-2493.

### Acknowledgments

This work was supported by the Science Committee of Ministry of Education and Science Republic of Kazakhstan grants IRN № AP09259303.

## TL and OSL studies of Mn<sup>2+</sup> and Eu<sup>3+</sup>-doped MgGa<sub>2</sub>O<sub>4</sub> phosphor

**A. Luचेchko<sup>1</sup>, Ya. Zhydachevskyy<sup>2,3</sup>, S. Ubizskii<sup>2</sup>, E. Bulur<sup>4</sup>**

<sup>1</sup>Ivan Franko National University of Lviv, Lviv, Ukraine

<sup>2</sup>Lviv Polytechnic National University, Lviv, Ukraine

<sup>3</sup>Institute of Physics, Polish Academy of Sciences, Warsaw, Poland

<sup>4</sup>Middle East Technical University, Ankara, Turkey

**E-mail: andriy.luchechko@lnu.edu.ua**

It is known that oxide materials with spinel structure attract great attention due to their perfect luminescent properties, good radiation damage resistance, high-temperature and chemical stability. In particular, magnesium and zing gallate (MgGa<sub>2</sub>O<sub>4</sub> and ZnGa<sub>2</sub>O<sub>4</sub>) compounds are promising materials as hosts for light emitting diodes and different kinds of display technologies as well as phosphors for various luminescent applications [1]. In the last decades, optically stimulated luminescence (OSL) has become of high interest as the readout technique applicable in radiation dosimetry that is an alternative to thermo-stimulated luminescence (TSL) [2, 3]. Thus, the TSL and OSL properties of magnesium gallate doped with manganese and europium ions have been studied in this research.

Magnesium gallate compounds doped with manganese and europium ions were synthesized by the high-temperature solid-state reaction method at 1200 °C. X-ray diffraction analysis has confirmed the single-phase composition of MgGa<sub>2</sub>O<sub>4</sub>:Mn<sup>2+</sup>,Eu<sup>3+</sup> polycrystalline samples.

Manganese ions (Mn<sup>2+</sup>) emission of MgGa<sub>2</sub>O<sub>4</sub>:Mn<sup>2+</sup> is presented by the broad band in the 475-575 nm spectral region with a maximum around 505 nm under the excitation in the band-to-band transitions region. The luminescence spectra of Eu<sup>3+</sup> ions are presented by sharp peaks which correspond to the *f-f* transition in europium ions. The TSL curve of magnesium gallate co-doped with manganese and europium ions shows a complex peak in the range 390-550 K. The fading of the TSL intensity was also investigated. The possible electron-hole recombination mechanisms are discussed. The continuous wave OSL (CW-OSL) and pulsed OSL (POSL) studies of the MgGa<sub>2</sub>O<sub>4</sub>:Mn<sup>2+</sup>,Eu<sup>3+</sup> samples were performed. The time-resolved OSL signal after 5 Gy irradiation as a function of preheating temperature is in good agreement with the TSL curve. The CW-OSL and POSL glow curves under different doses of irradiation were obtained and analyzed.

### References

- [1] A. Luचेchko, O. Kravets, *Journal of Luminescence*, 192 (2017) 11-16.
- [2] E.M. Yoshimuraa, E.G. Yuki-hara, *Radiation Measurements*, 41 (2006) 163-169.
- [3] A. Luचेchko, Ya. Zhydachevskyy et al., *Optical Materials*, 78 (2018) 502-507.

### Acknowledgments

This work was supported by the NATO Science for Peace and Security Program (project G5647), National Research Foundation of Ukraine (grant 2020.01/0248) and Ministry of Education and Science of Ukraine (project 0119U002249).

## Characterization of Lexsyg Smart automated reader for TL and OSL dosimetry using various materials

**S. Motta<sup>1</sup>, J. B. Christensen<sup>1</sup>, E. G. Yukihara<sup>1</sup>**

<sup>1</sup>Paul Scherrer Institute, Forschungsstrasse 111, 5232 Villigen PSI, Switzerland

**E-mail: [silvia.motta@psi.ch](mailto:silvia.motta@psi.ch)**

TL and OSL detectors are among the most used passive solid state detectors for personal and medical dosimetry. Several readers are commercially available for rapid readout of many TL/OSL detectors used in routine dosimetry, while other readers are mainly devoted to research. The Lexsyg Smart is an automated reader designed for TL/OSL dosimetry and luminescence dating application [1], which hosts a built-in beta source for irradiations directly in the reader. The system has been characterized for environmental dosimetry in the literature [2]. However, due to the wide range of possible applications and the absence of information regarding its performance for dosimetry, it was necessary to perform a characterization of the Lexsyg Smart automated reader. Hence, this work aims at characterizing this reader for dosimetry application using different TL/OSL materials (LiF:Mg,Ti, LiF:Mg,Cu,P, CaF<sub>2</sub>:Tm, Al<sub>2</sub>O<sub>3</sub>:C, and BeO). For that, we used a protocol which includes (i) the fitting of the TL curves into single peaks (when applicable), (ii) the choice of the reader configuration specific to each material (e.g. detection filters, heating rate, stimulation intensity), and (iii) the normalization of the obtained signal  $S$  with respect to the signal deriving from a reference irradiation  $S_R$  (using the built-in source). Such protocol eliminates the uncertainties associated with changes in the dosimeter sensitivity and mass, and in the reader sensitivity. The characterization focuses on the investigation of the reproducibility of the protocol using the automated reader, and on the determination of the dose rate of the built-in source for low doses (closed shutter configuration). The results show that, with the described protocol, it is possible to achieve a reproducibility in the range of 0.5 – 5% (experimental standard deviation), depending on the material and technique employed (TL or OSL). Depending on the desirable precision, this work helps guide the choice of the TL/OSL materials combined with the appropriate reader configuration.

### References

- [1] D. Richter, A. Richter, K. Dornich, *Geochronometria*, 42 (2015) 202-290.
- [2] S. Kreutzer, L. Martin, G. Guérin, C. Tribolo, P. Selva, N. Mercier, *Geochronometria*, 45 (2018) 56-67.

### Acknowledgments

This work was funded by the Swiss Federal Nuclear Safety Inspectorate ENSI, contracts no. CTR00491.

## Effect of exciton-like luminescence flare-up in the field of homologous cations in KCl matrix

K. Shunkeyev<sup>1</sup>, D. Sergeyev<sup>1,2</sup>, A. Maratova<sup>1</sup>, Zh. Ubayev<sup>1</sup>

<sup>1</sup>Zhubanov Aktobe Regional University, Aktobe, Kazakhstan, Aktobe, A. Moldagulova, 34  
<sup>2</sup>Begeldinov Military Institute of Air Defence Forces, Kazakhstan, Aktobe, A. Moldagulova, 39

E-mail: aida\_m@list.ru

In alkali halide crystals (AHCs), radiative relaxation of self-trapped excitons (STE) has a high luminescence quantum yield [1, 2] at low temperatures (4.2 K). However, as the temperature rises, the exciton mean free path ( $\lambda$ ) [1, 2] sharply decreases, which is the reason for the deterioration of the luminescence ability of AHC scintillators at their operating temperature (300 K). At 80 K in KCl, excitons are self-trapped without a barrier ( $\lambda = 2a$  [1, 2]) and the STE luminescence is completely quenched. However, this situation, which excludes the excitonic luminescence mechanism, creates a unique opportunity for studying recombination luminescence due to the mobility of unrelaxed holes, since their mean free path increases with increasing temperature.

The features (flare-up) of recombination luminescence in KCl-Na, KCl-Li, KCl-Sr crystals in a local deformation field (Li, Na, Sr) have been studied by the method of luminescence spectroscopy. With an increase in temperature (83  $\rightarrow$  300 K), an increase in the intensity of exciton-like luminescence with characteristic emission bands with maxima at 2.8 eV and 3.1 eV (KCl-Na), 2.7-2.8 eV (KCl-Li) and 2.6  $\div$  3.0 eV (KCl-Sr).

The activation energies estimated from the temperature dependences of the X-ray luminescence spectra of crystals are in the range of 20–40 meV, which is significantly lower than in the hopping diffusion of  $V_K$  - centers (0.54 eV).

The maximum increase in the intensity of exciton-like luminescence in the field of a light cation, for example, in KCl-Na crystal ( $10^4$  ppm), to room temperature is more than 200 times, which is comparable to the luminescence yield at a low temperature (4.2 K) for KCl crystal or scintillator CsI-Na at room temperature.

The effect of the intensification of exciton-like luminescence intensity at room temperature is interpreted by an increase in the probability of recombination assembly of electron-hole pairs in the field of local deformation (Li, Na, Sr) of KCl matrix due to the mobility of unrelaxed holes.

### References

- [1] Ch.B. Lushchik, Free and self-trapped excitons in alkali halides: spectra and dynamics, in Excitons, eds. E.I. Rashba and M.D. Sturge, North-Holland, Amsterdam, New York, Oxford, 1982. Chapter 12.
- [2] Ch. Lushchik and A. Lushchik, Evolution of anion and cation excitons in alkali halide crystals, Fiz. Tverd. Tela 60, 1478-1494 (2018), *Phys. Solid State* 60, 1487-1505 (2018).

### Acknowledgments

The work was carried out within the framework of the grant financing project of the Science Committee of the Ministry of Education and Science of the Republic of Kazakhstan (AP 08855672).

## Regularities of manganese charge state formation and luminescent properties of Mn doped Al<sub>3</sub>O<sub>3</sub>, YAlO<sub>3</sub> and Y<sub>3</sub>Al<sub>5</sub>O<sub>12</sub> single crystalline films

**A. Majewski-Napierkowski<sup>1</sup>, V. Gorbenko<sup>1</sup>, T. Zorenko<sup>1</sup>, S. Witkiewicz-Łukaszek<sup>1</sup>,  
Yu. Zorenko<sup>1</sup>**

<sup>1</sup>*Institute of Physics, Kazimierz Wielki University in Bydgoszcz, 85-090 Bydgoszcz, Poland*

**E-mail: artmaj13@gmail.com**

Nowadays Mn-doped Al<sub>2</sub>O<sub>3</sub>-Y<sub>2</sub>O<sub>3</sub>-based oxides are considered as laser media and materials for thermo- and optically-stimulated luminescent (TL and OSL) dosimetry [1–4]. This stimulates us to study of the growth process and optical properties of manganese ions in single crystalline films (SCFs) of various oxide compounds grown by liquid phase epitaxy (LPE) method [3, 4].

This work is related to the investigation of the regularities of manganese charge state formation and luminescent properties of the SCFs of Mn doped oxides with different crystallographic structure: sapphire Al<sub>2</sub>O<sub>3</sub>:Mn, perovskite YAlO<sub>3</sub> (YAP:Mn) and garnet Y<sub>3</sub>Al<sub>5</sub>O<sub>12</sub>:Mn (YAG:Mn), grown by the LPE method from the melt-solution based PbO-B<sub>2</sub>O<sub>3</sub> flux onto sapphire, YAP and YAG substrates, respectively [3, 4]. As an activating oxide, the MnO<sub>2</sub> in the concentration of 0.1-10 mole % with respect to film-forming components was used. Meanwhile, due to relatively small segregation coefficients, the real content of Mn ions in the SCFs of sapphire (0.1), YAP (0.14) and YAG (0.02), was significantly less and lies in the 0.001–1; 0.01–0.81 and 0.002–0.2 at. % ranges, respectively. Changing the oxide host structure results in variation of the optical properties of the SCF materials under study. In order to characterize them, the absorption, cathodo-luminescence (CL), thermoluminescence (TL) and photoluminescence (PL) spectra as well as the PL decay kinetics of Al<sub>2</sub>O<sub>3</sub>:Mn, YAP:Mn and YAG:Mn SCFs with different Mn concentration were investigated. The obtained spectra were analysed for determination of the preferable valence states of manganese ions which are realized in these SCFs depending on the Mn content.

In all the SCFs under study, the different valence states of manganese ions (Mn<sup>2+</sup>, Mn<sup>3+</sup>, Mn<sup>4+</sup>) were observed. The change of the structure of the host crystal lattice as well as the dopant content in these three materials strongly affect the valence states of the manganese, which can be seen in the intensity difference of their absorption, CL, PL spectra and PL decay kinetics.

We have observed that the valence of manganese ions is influenced by its location in the mentioned oxide hosts. Mn<sup>4+</sup> ions are predominantly occur in the octahedral coordination (Al<sup>3+</sup> sites) in sapphire [1], perovskite [2, 3] and garnet [4]) whereas Mn<sup>2+</sup> ions dominantly localized in cub-octahedral and dodecahedral coordination's (Y<sup>3+</sup> sites) in perovskite [2, 3] and garnet [4]). The preferable manganese state in the SCFs under study is also strongly influenced by the presence of Pb<sup>2+</sup> flux and Pt<sup>4+</sup> crucible related dopants, especially at low Mn dopant level [3, 4].

We have also found that from all the SCFs under study, the best TL properties possess YAP:Mn SCFs with mail dosimetric peaks at 400 and 570 K. Furthermore, the TL properties of these SCFs are close to the properties of YAP:Mn crystals [2, 3]. Due to very low concentration of the host defects in SCFs of oxides [3, 4], we have concluded that the different valence states of Mn ions rather than the point defects are responsible for their TL properties.

The above mentioned results have also shown that the Mn doped SCFs of oxides under study can be considered as prospective materials for development of thin-film or combined (film/substrate) phosphors not only for TL dosimetry but for photovoltaic devices as well.

### References

- [1] O. Khomenko, e. a. IEEE 8<sup>th</sup> Int. Conf. on Nanomaterials: Appl.&Prop.
- [2] Ya. Zhydachevskii, at al., J. Phys.: Cond. Matter. 18 (2006)11385.
- [3] Yu Zorenko, at al, Optical Materials 34 (2012) 1979.
- [4] Yu. Zorenko, at al, Optical Materials 36 (2014) 1680.

### Acknowledgments

The work was performed in the framework of Polish 2018/31/B/ST8/03390 and NCN2019/33/B/ST3/00406 projects.

## Evaluation thermal quenching parameters from a series of experimental thermoluminescence curves recorded with variable heating rates

G. Chernov<sup>1</sup>, M. Barboza-Flores<sup>2</sup>, V. Chernov<sup>2</sup>

<sup>1</sup>*Innovación y Servicios en Nanotecnología S.A. de C.V, Campo Bello 14, Hermosillo, Sonora, 83106 México*

<sup>2</sup>*Departamento de Investigación en Física de la Universidad de Sonora, Apartado Postal 5-088, Hermosillo, Sonora, 83190 México*

**E-mail: [chernov@cifus.uson.mx](mailto:chernov@cifus.uson.mx)**

There are a number of thermoluminescence (TL) phosphors, for which the TL peak intensity and its area decrease with the increasing of the heating rate. This effect is related to the thermal quenching (TQ) of TL emission caused by an increase in non-radiative recombination when temperature increases and is usually described by the well-known Mott-Seitz formula. Among the TL materials which exhibit thermal quenching, the most widely known are anion-defective Al<sub>2</sub>O<sub>3</sub>, CVD and HPHT diamond, quartz, long persistence strontium and calcium aluminates.

A number of methods for the evaluation of TQ parameters based on an analysis of a series of TL glow curves recorded with variable heating rates are described in literature. All of them are based on the supposition that the area under “unquenched” TL curve does not depend on the heating rate. One of such methods was developed by us [1] and applied to undoped CVD diamond. The method minimizes the sum of squared differences between the integrated “unquenched” TL curves and the unknown integrated “unquenched” TL.

Our method is simple, effective, quite general and can be applied to any series of TL glow curves consisting of several overlapped peaks and does not assume a particular type of TL kinetics. The limitation of this method is that all TL peaks should have the same temperature dependence of the TQ efficiency. The method presupposes careful measurement of the series of TL curves, therefore the stability of the TL device during the measurement of all TL glow curves as well as the stability of the TL properties of an investigated sample should be guaranteed. A way to provide needed stability of TL measurements is to use automatic systems such as the Risø TL/OSL or lexsyg research imaging TL-OSL-RF system by Freiberg Instruments, for which a fixed position of the sample in the cup guarantees good reproducibility of the experiments.

In this work, we present a reliable measurement protocol for the evaluation of the TQ parameters from a series of TL glow curves measured by using the automatic Risø TL/OSL. For preprocessing of measured TL curves and subsequent evaluation of the TQ parameters a software package was developed. The protocol and program were applied to a set of TL glow curves measured with various heating rates for an anion-defective Al<sub>2</sub>O<sub>3</sub> (TLD-500K) exposed to beta radiation.

### References

- [1] V. Chernov, G. Chernov, R. Meléndrez, M. Pedroza-Montero, M. Barboza-Flores, *Physica Status Solidi A*, 209 (2012) 1779–1785.



## Temperature dependent photoluminescence studies on Mn doped $Y_3Al_5O_{12}$ single crystalline films

**A. K. Somakumar<sup>1</sup>, Yu. Zorenko<sup>2</sup>, V. Gorbenko<sup>2</sup>, Ya. Zhydachevskyy<sup>1</sup>, A. Suchocki<sup>1</sup>**

<sup>1</sup>*Institute of Physics, Polish Academy of Sciences, Al. Lotnikow 32/46, 02-668, Warsaw, Poland*

<sup>2</sup>*Institute of Physics, Kazimierz Wielki University in Bydgoszcz, Powstańców Wielkopolskich str., 2, 85-090 Bydgoszcz, Poland.*

**E-mail: skumar@ifpan.edu.pl**

Rare-earth and transition metal doped  $Y_3Al_5O_{12}$  garnet (YAG) is considered as one of the most promising optical material for the production of scintillation detectors, solid state lasers, and phosphors for white LED. This work focused on the study of optical features of YAG garnet doped with manganese (Mn) transition metal ions. The aim of this work is systematic studies of the creation of different charge states of Mn ions (2+, 3+ and 4+) in the YAG crystalline matrix. For this purpose, the YAG single crystalline films doped with nominal content of MnO dopant of 0.1, 1 and 10 mole % were grown by liquid phase epitaxy method from the melt solutions based on the  $PbO-B_2O_3$  flux [1].

YAG-Mn films were subjected to various extended photoluminescence studies as function of temperature in 4-300K range. From all YAG:Mn samples with different Mn content, the films with lowest concentration of Mn ions (YAG:Mn(0.1%)) shown the maximum luminescence efficiency and for this reason was selected for further characterisations.

The samples studied exhibit luminescence typical for Mn ions in three oxidation states with luminescence maxima at about 590 nm ( $Mn^{2+}$ ), 615 nm ( $Mn^{3+}$ ), and 670 nm ( $Mn^{4+}$ ). [2] In addition to that the luminescence from  $Ce^{3+}$  unintentional dopant, most probably present in YAG substrate, is also visible.

The luminescence at the 670nm is transformed in to twin sharp peaks low temperatures, connected with the  ${}^2E \rightarrow {}^4A_2$  transitions of  $Mn^{4+}$  in the sample. The maximum of  $Mn^{2+}$  luminescence is achieved at 75K. Such results confirm the presence of  $Mn^{4+}$  charge state in the film under study.

The decay kinetics of emission bands related to different valence states of Mn ions exhibit different temperature behaviour. Generally, the decay kinetics have complicated three-exponential decays, in the millisecond range at low temperature.

### References

- [1] Y. Jia, Y. Huang, Y. Zheng, N. G.H. Qiao, Q. Zhao, W. Lvab, H. You. Color point tuning of  $Y_3Al_5O_{12}:Ce^{3+}$  phosphor via  $Mn^{2+}-Si^{4+}$  incorporation for white light generation. *J. Mater. Chem.*, 2012, 22, 15146.
- [2] Yu. Zorenko, V. Gorbenko, T. Zorenko, B. Kuklinski, M. Grinberg, K. Wisniewski, P. Bilski. Luminescent properties of Mn-doped  $Y_3Al_5O_{12}$  single crystalline films. *Optical Materials* 36 (2014) 1680–1684.

### Acknowledgments

This work was partially supported by the Polish National Science Center (project 2018/31/B/ST8/03390).

## Execution of personal and extremity dosimeters proficiency tests regarding dose equivalent for beta particles

**M. Y. Shih<sup>1</sup>, C. H. Chu<sup>1</sup>**

<sup>1</sup>*Health Physics Division, Institute of Nuclear Energy Research, Taoyuan City, Taiwan*

**E-mail: shihmingyuan@iner.gov.tw**

This study investigated external personal and extremity dosimeters proficiency tests in Taiwan by personal dose equivalent,  $H_p(0.07)_{\text{beta}}$ ,  $^{90}\text{Sr}/^{90}\text{Y}$  beta dose measurements, based on ANSI/HPS N13.11 and 13.32 criteria. Personal dose equivalent of beta source is calculated by absorbed dose to tissue, evaluated by the extrapolation chamber according to the ISO 6980-2. The expanded uncertainty ( $k=2$ ) was 2.4 % when  $H_p(0.07)_{\text{beta}}$  was evaluated using the ISO GUM. The experimental verification with the PTB using an ionization chamber had a difference less than 1 %. Personal dose equivalent evaluated for beta particles has a strong influence on the execution quality of the external and extremity dosimeters proficiency tests.

### References

- [1] American National Standard Institute, Health Physics Society, *ANSI/HPS N13.11 Personnel Dosimetry Performance for Testing*, (2009).
- [2] American National Standard Institute, Health Physics Society, *ANSI/HPS N13.32 Performance Testing of Extremity Dosimeters*, (2018).
- [3] International Organization for Standardization, *ISO 6980-2 Reference Beta Radiation Part 2: Calibrating Fundamentals Related to Basic Quantities Characterizing the Radiation Field*, (2004).
- [4] International Organization for Standardization, *Guide to the Expression of Uncertainty for Measurement*, (1995).

## ProGlaDos Project: TL study of protective glasses of mobile phones for retrospective dosimetry

**M. Discher<sup>1</sup>, C. Bassinet<sup>2</sup>, C. Woda<sup>3</sup>**

<sup>1</sup>Paris-Lodron-University of Salzburg, Department of Geography and Geology, Hellbrunner Str 34, 5020 Salzburg, Austria

<sup>2</sup>Institut de Radioprotection et de Sûreté Nucléaire, BP17, 92262, Fontenay-aux-Roses Cedex, France

<sup>3</sup>Helmholtz Zentrum München, Institute of Radiation Medicine, Ingolstädter Landstr. 1, Neuherberg, Germany

**E-mail: michael.discher@sbg.ac.at**

The focus of the ProGlaDos research project is in the field of retrospective dosimetry which is an essential tool for assessing an absorbed dose after a radiological overexposure. Mobile phones are useful proxies for measuring the amount of dose an individual has received. There are many studies available in characterising different elements of mobile phones (i.e. electronic components, display or touch screen glass) for physical retrospective dosimetry. However, so far these techniques are frequently destructive. This implies that, in case of a dose assessment, the phones can no longer be used, which is a major issue in terms of the acceptance within the population due to the destructive loss of the mobile phone and potential emotional damage. In order to overcome this problem, alternative materials need to be sought and further research is necessary [1].

Protective glass has now become an alternative material instead of other elements of mobile phones, such as electronic components, display or touch screen glass. This type of glass is readily available and cheap, has become very popular to protect the display screen surface of phones, can be easily replaced without complete destruction of an expensive smartphone and will thus find much greater public acceptance. Preliminary tests show the potential that this kind of glass is sensitive to ionizing radiation, and could be an alternative fortuitous retrospective dosimeter [2].

However, systematic investigations are necessary to obtain the dosimetric properties, to pool the results into a database and to develop a robust measurement protocol, which are the aims of the joint ProGlaDos Project.

In this study the systematic variation of the detection window results to different TL intensities using different combinations of filters (i.e. interference filters) of the luminescence reader system. The goal is to optimize the ratio of TL signal to background (i.e. intrinsic background signal) and compare the results to TL emission spectrometer measurements. The optimization is necessary to investigate further the dosimetric properties of protective glasses in the framework of the research project.

### References

- [1] S. Sholom, S.W.S. McKeever, J.R. Chandler, *Radiat. Meas.*, 136 (2020), p. 106382.
- [2] C. Bassinet, W. Le Bris, *Radiat. Meas.*, 136 (2020), p. 106384.

### Acknowledgments

The scientific cooperation is supported by the French Ministry of foreign affairs and the French Ministry of higher education and research (project number: 46275WC) and by Scientific & Technological Cooperation (S&T Cooperation) grant, funded by funds of the Federal Ministry of Education, Science and Research (BMBWF) Austria (project ID: FR 12/2021).

## Optically stimulated luminescence properties of commercially available KCl dietary supplement as retrospective dosimeter

**K.M. Szufa<sup>1</sup>, R. Majgier<sup>1</sup>, A.Mandowski<sup>1</sup>**

<sup>1</sup>*Department of Experimental and Applied Physics, Jan Długosz University in Częstochowa, Armii Krajowej 13/15, 42-200 Częstochowa, Poland*

**E-mail: k.szufa@ujd.edu.pl**

In a situation of radiation emergencies proper estimations of the absorbed dose to the public are crucial. Therefore numerous efforts have been made to recognize household objects or materials as potential dosimeters [1-4]. Carrying out appropriate dose estimations requires the use of materials with specific properties like a linear dose response over a dose range up to 1000 mGy when acute radiation effects occur. Potassium chloride (KCl) may be considered as such a retrospective dosimeter. KCl shows a linear dose response for dose range from 25 mGy to 1 Gy under green light (520-532 nm) stimulation [5]. Additionally other OSL properties of the KCl were well established [6-8]. It is also a household material since it is a popular dietary supplement available commercially, over the counter in many cases.

The present work introduces results of the OSL measurements of the several commercially available KCl dietary supplements in different forms: pills, capsules and powder. Special attention is paid to signal background levels and lower detection limits. Advantages and disadvantages of the commercial KCl dietary supplements as retrospective dosimeter are discussed.

### References

- [1] M. Karampiperi, N.C. Tsirliganis, N.A. Kazakis, *Applied Radiation and Isotopes* 166 (2020) 109364.
- [2] N.A. Kazakis, N.C. Tsirliganis, G. Kitis, *Applied Radiation and Isotopes* 91 (2014) 79–91.
- [3] A. Timar-Gabor, O. Trandafir, *Radiation Protection Dosimetry*, 155 (2013) 404-409.
- [4] Ch. Bernhardsson, M. Christiansson, S. Mattsson, Ch. L. Rääf, *Radiation and Environmental Biophysics*, 48 (2009) 21–28.
- [5] R. Majgier, M. Biernacka, R. Smyka, A. Mandowski, *Radiation Measurements*, 106 (2017) 1-6.
- [6] R. Majgier, M. Biernacka, A.Mandowski, *Radiation Measurements*, 127 (2019) 106142.
- [7] R. Majgier, Ch. L. Rääf, A. Mandowski, Ch. Bernhardsson, *Radiation Protection Dosimetry*, 184 (2018) 1–8.
- [8] R. Majgier, M. Biernacka, A. Mandowski, *Radiation Measurements*, 90 (2016) 242-246.

## Investigations of the thermal stability of the OSL main trap in quartz from sediments

**M. Biernacka<sup>1</sup>, A. Chruścińska<sup>1</sup>, P. Palczewski<sup>1</sup>**

<sup>1</sup> *Institute of Physics, Faculty of Physics, Astronomy and Informatics, Nicolaus Copernicus University, Grudziadzka 5/7, 87-100 Torun, Poland*

**E-mail: m.biernacka@umk.pl**

Metastable states of electrons or holes (traps) in minerals are extensively used in trapped charge dating and recently in OSL-thermochronology. The thermal stability of traps determines their suitability in both cases. An experiment recently very often used to determine the thermal stability of OSL components is to measure the thermal depletion curve of the OSL signal [1]. Such a curve is created by measuring the OSL intensity after holding the sample at a specific high temperature for different periods. It allows estimating parameters of traps taking part in OSL when one interprets the OSL thermal depletion curve correctly. Usually, it is simple when the depletion curve is a single exponential decay. Unfortunately, this is not always the case. Sometimes, other kinds of decay, e.g. the stretched exponential or stretched hyperbolic functions, can successfully fit the depletion curve. Nevertheless, the obtained trap parameter values seem unbelievable [2]. The complex nature of the observed OSL signal can be the simplest explanation for these problems. Theoretical considerations concerning the influence of a disturbance by an additional trap on the parameters obtained by thermal depletion curve analysis are presented elsewhere [3]. The participation of disturbing trap in the OSL should be excluded by applying an appropriate initial preheat or an adequate optical stimulation.

This study is focused on the second solution. A new approach to measuring the thermal depletion curve is presented. The usually used CW-OSL method is replaced with the *thermally modulated* OSL method (TM-OSL), a combination of thermal and optical stimulation. This method uses the dynamic dependence of the optical cross-section of the trap on temperature for the stimulation energy significantly below the optical trap depth. It makes it possible to generate a luminescence signal from an optically active trap, which is thermally activated at high temperatures, i.e. relatively deep trap in a much lower temperature range. Such a large shift of the luminescence signal makes it possible to "pick out" a signal related to a particular trap from a complex signal often observed at high temperatures or from an incandescence signal. Additionally, if there is thermal quenching in the material, it allows avoiding this quenching.

Here, the experiment of thermal depletion of the main OSL trap in quartz is an example of applying the approach. Recently, it was found that it is possible to separate the fast OSL component from the rest of the components in quartz when the TM-OSL method is conducted using the light with the wavelength of 620 nm [4]. The presented depletion experiments with TM-OSL allowed estimating values of the thermal activation energy  $E$  and the frequency factor  $s$  for the fast OSL component in quartz. The TL signal bleached during the TM-OSL measurement was also investigated. The determined thermal stability of the main OSL trap in quartz stays in agreement in both methods used and in three quartz samples from sediments of different origins.

### References

- [1] T-S. Wu, et al., *Radiation Measurements*, 81 (2015) 104-109.
- [2] A. Chruścińska, et al., *Radiation Measurements*, 134 (2020) 106316.
- [3] N. Pawlak, et al., other presentation at this conference.
- [4] P. Palczewski, A. Chruścińska, *Radiation Measurements*, 121 (2019) 32-36.

### Acknowledgements:

This work was supported by the National Science Centre, Poland, no. (2018/31/B/ST10/03917).

## Thermal depletion curve of the complex OSL signal

**N. Pawlak<sup>1</sup>, A. Chruścińska<sup>1</sup>**

<sup>1</sup>*Institute of Physics, Faculty of Physics, Astronomy and Informatics, Nicolaus Copernicus University, Grudziadzka 5/7, 87-100 Torun, Poland*

**E-mail: natalia@umk.pl**

There are quite a few different methods that allow determining the activation energy  $E$  (the trap depth), the frequency factor  $s$  and, in consequence, the electron lifetime  $\tau$  in the trap by the thermoluminescence measurement. This is not the case with OSL studies. The thermal stability of traps active in OSL is determined mainly by TL methods after the correlation of a defined TL peak with the source trap of OSL or by measuring the so-called thermal depletion curve of the OSL signal. The first option can be hard to apply when the correlation of traps observed in OSL and in TL is not apparent. Therefore, the second possibility is increasingly used when the exact values of the thermal parameters of traps are essential. This is the case, for example, in OSL-thermochronometry [1]. The thermal depletion curve method relies on measuring the intensity of the OSL signal after holding the sample at a certain temperature for various periods, from the shortest to one where the OSL completely disappears. Such a series of measurements is repeated for several holding temperatures. The dependence of the decay time on temperature is then used for trap parameter estimation. However, in these experiments, the shapes of decay curves are often obtained, which do not correspond to simple kinds of kinetics. Moreover, even though the theoretical curves are fitted to the experimental results with reasonable accuracy, the estimated trap parameters seem unrealistic [2]. This study demonstrates using computer simulations that such undesirable effects result from the fact that the OSL signal observed in the depletion curve measurement does not originate from a single trap. The extend of the deformation of the depletion curve shape depending on parameters of traps involved in the OSL process is investigated and the impact of these deformations on the trap parameter values determined from the simulated experiments.

The computer simulations were conducted using the Matlab environment and involved the numerical solution of differential equations that present the kinetic model of OSL. The simulations take into account all the processes occurring in the laboratory conditions: the filling of traps, the relaxation after excitation, the preheat to the selected temperature, the relaxation after preheating, the heating to the holding temperature (three different values), the annealing during a chosen period (from 0 s to 10 s), the relaxation after annealing and the optical stimulation. Results for three models are compared. The first model includes one optically active electron trap, one deep electron trap (optically and thermally inactive), and one luminescence centre. The second model has an additional electron trap that is not optically active, and in the last model, the additional “disturbing trap” is also optically active.

### References

- [1] E. Yukihiro et al., *Radiation Measurements*, 120 (2018) 274-280.
- [2] A. Chruścińska, et al., *Radiation Measurements*, 134 (2020) 106316.

### Acknowledgements:

This work was supported by the National Science Centre, Poland (project no. 2018/31/B/ST10/03917).

## Luminescent properties of microcline from the granite pegmatite of the Strzegom Massif

**R. Smyka<sup>1</sup>, E. Mandowska<sup>1</sup>, A. Mandowski<sup>1</sup>**

<sup>1</sup>*Department of Experimental and Applied Physics, Jan Długosz University  
ul. Armii Krajowej 13/15, 42-200 Częstochowa, Poland*

**E-mail: robert.smyka@doktorant.ujd.edu.pl**

Microcline belongs to a group of minerals called potassium feldspars. The feldspars constitute more than 50% of the earth's crust components. Because of their prevalence, they are widely used in ionizing radiation dosimetry, especially for the purposes of dating by optically stimulated luminescence (OSL) and infrared stimulated luminescence (IRSL) methods.

This paper presents various radioluminescence properties of microcline mineral after irradiation using <sup>90</sup>Sr/<sup>90</sup>Y beta source. The dose was ranging from ~ 1 Gy to ~ 1000 Gy. The energy stored in the mineral by ionizing radiation can be released in the form of luminescence under optical or thermal stimulation. The luminescence depends on many factors – e.g. the stimulation wavelength, annealing time and temperature, optical bleaching and others.

OSL and IRSL measurements were performed using custom made OSL Helios readers [2]. It is interesting, that the IR stimulation is much more efficient than the stimulation in the visible. The readers allow to study luminescence of minerals using various stimulation vs time profiles. Therefore, it is possible to study fading and luminescence life time at different conditions. These measurements are performed in the photon counting mode.

Spectral measurements of thermoluminescence (TL) and photoluminescence were performed using different experimental setup with a cooled CCD camera [3]. The results confirm good properties of microcline as a luminescence detector of ionizing radiation. The mineral may be considered as important tool for OSL and IRSL dating of quaternary sediments.

### References

- [1] M. Biernacka, A. Mandowski, *Radiat. Meas.*, 56 (2013) 31-35.
- [2] A. Mandowski, E. Mandowska, L. Kokot, P. Bilski, P. Olko, *Elektronika: konstrukcje, technologie, zastosowania*, 51 (2012) 136-138.
- [3] E. Mandowska, R. Majgier, A. Mandowski, *Radiat. Phys. Chem.* 173 (2020) 108876.

### Acknowledgements:

This work was supported by the National Science in Poland (2018/31/B/ST10/03966).

## ProGlaDos Project - Mobile phone screen protector glass for radiation accident dosimetry: TL investigation of the intrinsic background signal

**C. Bassinet<sup>1</sup>, M. Discher<sup>2</sup>, Y. Ristic<sup>1</sup>, C. Woda<sup>3</sup>**

<sup>1</sup>*Institut de Radioprotection et de Sûreté Nucléaire, BP17, 92262 Fontenay-aux-Roses cedex, France*

<sup>2</sup>*Paris-Lodron-University of Salzburg, Department of Geography and Geology, Hellbrunner Str 34, 5020 Salzburg, Austria*

<sup>3</sup>*Helmholtz Zentrum München, Institute of Radiation Medicine, Ingolstädter Landstr. 1, 85764 Germany*

**E-mail: celine.bassinnet@irsn.fr**

In the last decade, dosimetric properties of materials from mobile phones (electronic components, display glass and touchscreen class (e.g. [1-3]) were extensively studied by luminescence with the aim of using these items as potential emergency dosimeters in the event of a radiological accident. More recently, TL dosimetric characteristics of screen protector glasses were also investigated in a preliminary study [4]. This extra layer of material is placed on the touchscreen to protect it against physical damage. It could be easily removed and replaced without destroying the phone in case of a dose assessment. However, systematic investigations of several sets of screen protectors (i.e. different brands, from different manufacturers) are necessary to develop a robust measurement protocol, which is one aim of the joint ProGlaDos research project.

A non-radiation induced signal (i.e. zero dose signal) which partially overlaps with the radiation-induced TL signal is observed for every screen protector glass. It varies in shape and intensity from one screen protector to another. The dose could be overestimated if it is not properly taken into account. In the framework of the ProGlaDos project, this intrinsic background signal was studied in detail (TL emission spectrometer measurements, homogeneity of the zero dose signal over the surface area of screen protectors, optimization of a chemical treatment [5] to minimize its contribution). In this work, the results of this study are presented and discussed.

### References

- [1] C. Bassinet, C. Woda, E. Bortolin, S. Della Monaca, P. Fattibene, M.C. Quattrini, B. Bulanek, D. Ekendahl, C.I. Burbidge, V. Cauwels, E. Kouroukla, T. Geber- Bergstrand, A. Mrozik, B. Marczewska, P. Bilski, S. Sholom, S.W.S. McKeever, R.W. Smith, I. Veronese, A. Galli, L. Panzeri, M. Martini. *Radiat. Meas.*, 71 (2014) 475–479.
- [2] M. Discher, C. Woda. *Radiat. Meas.*, 53–54 (2013) 12–21.
- [3] J.R. Chandler, S. Sholom, S.W.S. McKeever, H.L. Hall. *J. Appl. Phys.* 126 (2019) 074901.
- [4] C. Bassinet, W. Le Bris, *Radiat. Meas.*, 136 (2020) 106384.
- [5] M. Discher, C. Woda, I. Fiedler, *Radiat. Meas.*, 56 (2013) 240-243.

### Acknowledgements:

The scientific cooperation is supported by the French Ministry of foreign affairs and the French Ministry of higher education and research (project number: 46275WC) and by Scientific & Technological Cooperation (S&T Cooperation) grant, funded by funds of the Federal Ministry of Education, Science and Research (BMBWF) Austria (project ID: FR 12/2021).



## Comparison of OSL properties of sodium sulfate and potassium sulfate

**R. Majgier<sup>1</sup>, M. Tsvirko<sup>1</sup>, A. Mandowski<sup>1</sup>**

<sup>1</sup>*Department of Experimental and Applied Physics, Faculty of Science and Technology, Jan Długosz University, ul. Armii Krajowej 13/15, 42-200 Częstochowa, Poland*

**E-mail: renata.majgier@ujd.edu.pl**

The optically stimulated luminescence (OSL) method is widely used in dosimetry of ionizing radiation. The OSL usually occurs in crystalline dielectric materials with a wide energy band gap. Only two materials are commonly used in OSL dosimetry: aluminium oxide doped with carbon ( $\text{Al}_2\text{O}_3:\text{C}$ ) and beryllium oxide ( $\text{BeO}$ ). Much more phosphors have found use in the OSL-like thermoluminescence (TL) method. One of the most efficient phosphors in TL is dysprosium-doped calcium sulphate, therefore other sulfate salts may be potential candidates for high quality phosphors. The OSL properties of sulphates is much less known. The aim of this work is to study the luminescence properties of selected sulfate salts using OSL method in order to test their dosimetric potential. As shown earlier [1], potassium sulfate doped with cerium ( $\text{K}_2\text{SO}_4:\text{Ce}$ ) shows high sensitivity to radiation (luminescent signal is higher than for  $\text{Al}_2\text{O}_3:\text{C}$ ) and it is important to continue research for this material. Another salt in this group is sodium sulfate ( $\text{Na}_2\text{SO}_4$ ), the properties of which are compared to  $\text{K}_2\text{SO}_4$  in this work.

The samples under study were prepared from analytical quality material. For the preparation of doped samples, the pure powder (potassium sulfate or sodium sulfate, respectively) was dissolved in distilled water. Then the dopant – cerium sulfate was added. The obtained crystals were then fabricated in the form of pellets (5 mm diameter x 1 mm thickness) by pressing crystalline powders at  $2 \text{ ton/cm}^2$ . To increase the luminescent signal, the pellets were annealed in a porcelain crucible in high temperature furnace. The dependence of the OSL signal on the anilation temperature was investigated for both materials. The optimal anilation temperatures for the two materials are different. In the case of  $\text{K}_2\text{SO}_4:\text{Ce}$  it is  $1000 \text{ }^\circ\text{C}$ , and in the case of  $\text{Na}_2\text{SO}_4:\text{Ce}$  –  $800 \text{ }^\circ\text{C}$ . After annealing the pellets were irradiated using  $^{90}\text{Sr}/^{90}\text{Y}$  beta source. The OSL measurements, in CW-OSL mode, were performed using custom-made reader ‘Helios 1’ [2] with green light stimulation. The intensity and stability of the OSL signal for both materials were compared – higher intensity was observed in the case of  $\text{K}_2\text{SO}_4:\text{Ce}$ , about 15 times higher at the same anilation temperature ( $800 \text{ }^\circ\text{C}$ ) and about 40 times higher at the optimal anilation temperature for each material. Better dosimetric properties (dose response, fading characteristic) were also confirmed for potassium sulfate.

### References

- [1] R. Majgier, M. Tsvirko, A. Mandowski, *Luminescence*, 36.4 (2021) 1089-1096.
- [2] A. Mandowski, E. Mandowska, L. Kokot, P. Bilski, P. Olko, B. Marczevska, *Elektronika: konstrukcje, technologie, zastosowania*, 51 (2010) 136-138.

## Investigation of feldspar luminescence decay using pulsed IRSL measurement

**E. Mandowska<sup>1</sup>, R. Smyka<sup>1</sup>, A. Mandowski<sup>1</sup>**

<sup>1</sup>*Department of Advanced Computational Methods, Jan Długosz University  
ul. Armii Krajowej 13/15, 42-200 Częstochowa, Poland*

**E-mail: e.mandowska@ujd.edu.pl**

Optically stimulated luminescence (OSL) – sometimes in the form of infra-red stimulated luminescence (IRSL), is a measurement technique used in dosimetry of ionizing radiation and luminescence dating of archaeological and geological samples [1]. Potassium feldspars are well-known materials, which are sensitive to IR stimulation. The minerals are important for dating of quaternary sediments [2].

Most of OSL and IRSL materials exhibit fading of the luminescence signal in a long-time scale. It is important to study this phenomenon, especially for its dosimetry and dating applications. The phenomenon of signal loss is quite common. It should be taken into account and some characteristic features, such as the mean lifetime should be determined.

Various measurement methods are used to investigate the loss of signal. They usually consist in making a large series (several dozen) of samples and testing the OSL/IRSL response after a sufficiently long period of time. Such a test requires a high homogeneity of the measured samples and is very time-consuming. In this article, we present a method of examining the state of an OSL detector using much simpler – pulsed OSL/IRSL method.

The measurement was performed using Helios-3 OSL Reader [3]. A sample (potassium feldspar) was initially irradiated by <sup>90</sup>Sr/<sup>90</sup>Y beta source. Then it was placed in the reader for several hours or weeks. Pulsed OSL/IRSL stimulation probes the current density of charge carriers in traps, but also decreases its population. Appropriate normalization may restore the ‘undistorted’ signal. Basic properties, assumptions, limitations and examples of the application of the method are described.

### References

- [1] E. G. Yuhikara, S. W. S. McKeever, *Optically Stimulated Luminescence: Fundamentals and Applications*, Wiley (2011).
- [2] M. Jain, C. Ankjærgaard, *Radiation Measurements* 46 (2011), 292-309.
- [3] A. Mandowski, E. Mandowska, L. Kokot, P. Bilski, P. Olko, *Elektronika: konstrukcje, technologie, zastosowania*, 51 (2012) 136-138.

### Acknowledgments

This work was supported by the National Science in Poland (2018/31/B/ST10/03966).

## Investigation of the dose-rate effects in the thermoluminescence of LiF:Mg,Ti (TLD-100)

D. Ginzburg<sup>1</sup>, L. Oster<sup>2</sup>, I. Eliyahu<sup>3</sup>, G. Reshes<sup>2</sup>, S. Biderman<sup>2</sup>, A. Shapiro<sup>2</sup>,  
D. Nemirovsky<sup>4</sup>, Y.S. Horowitz<sup>5</sup>

<sup>1</sup> Department of Biotechnology Engineering, Ben Gurion University of the Negev, Beer Sheva, Israel

<sup>2</sup> Physics Unit, Sami Shamoon College of Engineering, Beer Sheva, 84100, Israel,

<sup>3</sup> Nuclear Physics and Engineering Department, Soreq Nuclear Research Center, Yavneh, 81800, Israel

<sup>4</sup> Physics Unit, Sami Shamoon College of Engineering, Ashdod, Israel

<sup>5</sup> Physics Department, Ben Gurion University of the Negev, Beersheva, 84105, Israel

E-mail: leonido@sce.ac.il

A recent review of the pertinent literature [1] has concluded that there is little reliable experimental evidence supporting the presence, or lack of it, of dose-rate effects in the thermoluminescence of LiF:Mg,Ti (TLD-100). On the other hand, ample evidence exists that dose-rate effects may be expected on theoretical grounds in which dose-rate effects are simulated as arising from competition between excitation and recombination [2] or from a dose-rate dependence in the excitation stage and recombination stage leading to  $V_3$ - $V_k$  (two-hole to single hole) transformation [3]. In this work the response of LiF:Mg,Ti (TLD-100) is investigated in two experiments following  $^{137}\text{Cs}$  irradiation and dose-rate calibration employing ionization chambers. (i) Using two sources of different activities and variation of the sample to source distances to obtain a difference of five orders of magnitude in the dose rate from  $17.6 \text{ Gy hr}^{-1}$  and  $17.6 \times 10^{-5} \text{ Gy hr}^{-1}$ . (ii) Placing the samples under irradiation in a plastic container to determine whether low energy scattered electrons created in the sample and intervening materials are influencing the results. For the main glow peak (peak 5) no dose rate effect is observed to within a precision of  $\sim 5\%$  (1 SD). In addition, the shape of the glow curves indicating the relative intensities of the various glow peaks is close to identical under all values of dose-rate.

### References

- [1] Y.S. Horowitz, L. Oster, I. Eliyahu, *Radiat. Prot. Dosim.*, 179 (2018) 184-188.
- [2] R. Chen and P. Leung, *J. Phys. D. Appl. Phys.*, 33 (2000) 846-850.
- [3] I. Eliyahu, L. Oster, D. Ginsburg, G. Reshes, S. Biderman, Y.S. Horowitz, *Nucl. Instrum. Meths.*, B440 (2019)139-145.

### Acknowledgments

This research is supported by the Israeli Ministry of Science, Technology and Space. Project No. – Merkava, 3-16316 and by the PAZY Foundation.

# Atomistic simulation synthesis of $\text{Li}_x\text{TiO}_2$ nanoporous as anode electrode materials for energy storage in lithium ion batteries

**B. N. Rikhotso<sup>1</sup>, M. G. Matshaba<sup>1</sup>, D. C. Sayle<sup>2</sup>, P. E. Ngoepe<sup>1</sup>**

<sup>1</sup>University of Limpopo, Materials Modelling Centre, Private Bag X 1106, Sovenga, 0727, South Africa

<sup>2</sup> University of Kent, School of Physical Sciences, Canterbury, Kent, CT2 7NZ, United Kingdom

E-mail: nkatekoblesing@gmail.com

Nanoporous-Architected  $\text{Li}_x\text{TiO}_2$  show promising properties as anode materials for lithium rechargeable batteries due to their ability to store more lithium atoms along with withstand high temperature conditions at atomistic level during charging and discharging [1]. In the current study, we investigated how the nanoporous of  $\text{Li}_{0.03}\text{TiO}_2$ ,  $\text{Li}_{0.04}\text{TiO}_2$  and  $\text{Li}_{0.07}\text{TiO}_2$  behave at high simulated temperatures through amorphisation and recrystallization method [2]. Recrystallisation synthesis was performed on  $\text{Li}_x\text{TiO}_2$  nanoporous from their amorphous precursors, then proceeded by the cooling process towards 0 K. Lastly the nanoporous were heated at temperature intervals of 100 K up to 1500 K. The variation of configuration energies with time, served as an indication of crystal growth for the  $\text{Li}_x\text{TiO}_2$  nanoporous. Calculated Ti-O radial distribution functions, were used to confirm the stability interaction after cooling. Simulated X-Ray Diffraction (XRD) spectra, at low (0 K) and above high (500 K) temperatures, showed polymorphic structure in  $\text{Li}_x\text{TiO}_2$  depicting domains of both rutile and brookite in accord with experiment. Nanoporous microstructures have pure straight and zigzag patterns (figure 1) that are consistent with our XRD patterns at all concentrations of lithium atoms and temperatures. The lithium transport was analysed using diffusion coefficient, calculated as a function of temperature in order to investigate the Li diffusivity at the given temperatures stated above. An increase in temperature indicated an increase in diffusivity of  $\text{Li}_{0.03}\text{TiO}_2$ ,  $\text{Li}_{0.04}\text{TiO}_2$  and  $\text{Li}_{0.07}\text{TiO}_2$  nanoporous structures. Thus, rendering suitable anode material for Li ion batteries since it can withstand such temperatures.

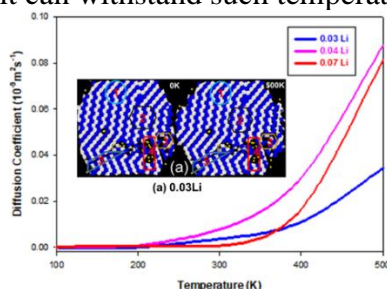


Fig.1. Lithiated snapshots of evolving microstructures of nanoporous ( $\text{Li}_{0.03}\text{TiO}_2$ ) at 0 K and 500 K with different types of defects

## References

- [1] B. N. Rikhotso, M.G. Matshaba, D.C. Sayle, P.E. Ngoepe, *Optic. Mat.*,102 (2020) 109831.
- [2] T.X.T. Sayle, C.R.A. Catlow, R.R. Maphanga, P.E. Ngoepe, D.C. Sayle, *J. Cryst.Growth.*, 294 (2006) 1198.
- [3] M.G. Matshaba, D.C. Sayle, T.X.T. Sayle, P.E. Ngoepe, *J. Phys. Chem. C.*, 26 (2016) 14001.

## Acknowledgments

This work was supported by South African Chair Initiative of the Department of Science and Technology (DST) and the National Research Foundation (NRF) and the Energy Storage Allocation from the Department of Science and Technology.

# AUTHOR INDEX

## A

Afanassyev D. ThP2-6  
 Ahmine A. TuP1-7  
 Ahrens B. FrS16-K33  
 Akhmetova A. TuP1-19  
 Alekseev V. TuS4-O16  
 Alibay T. T. ThP2-8  
 Ambrozevich S. MoS3-O10  
 Amilusik M. ThS10-O42  
 Androulidaki M. TuP1-25  
 Antonyak O. TuP1-18  
 Arhipov P. TuS4-K10,  
 TuS4-O16,  
 TuS4-O17  
  
 Auffray E. MoS1-O2,  
 ThS11-O49

## B

Babichenko S. ThS13-O55  
 Babin V. MoS1-O3,  
 TuS5-K11,  
 TuS5-O19,  
 TuS6-O28,  
 TuS7-O29,  
 TuS7-O30,  
 TuP1-26,  
 ThP2-2  
  
 Bachiri A. TuP1-3,  
 MoS2-O5,  
 TuP1-15  
  
 Barboza-Flores M. FrS14-O57,  
 ThP2-13  
  
 Bartosiewicz K. TuS4-O14,  
 ThP2-2  
  
 Bassinet C. ThP2-16,  
ThP2-21  
 .  
 Batentschuk M. FrS16-K32  
 Beitlerova A. TuS6-K12,  
 TuS6-O25,  
 TuS6-O27  
  
 Belsky A. TuP1-2,  
 ThS10-O43  
  
 Berkowski M. TuP1-23  
 WeS8-O35

Biderman S. ThP2-24  
 Biernacka M. ThP2-18  
 Bilski P. TuP1-12,  
ThS11-O46,  
 ThS12-K25,  
 ThP2-3,  
 FrS14-K28,  
 FrS14-O56,  
 FrS15-O61

Boćkowski M. ThS10-O42  
 Bohacek P. MoS1-K3  
 Bolek P. TuP1-11  
 Bondzior B. FrS14-O58  
 Bossin L. ThS11-K23  
 ThS12-O52  
 ThS12-O53

Boyaryntseva Ya. TuS4-K10,  
 TuS4-O16,  
 TuS4-O17

Brabec C. FrS16-K32  
 Brik M. G. MoS2-K5,  
 TuS6-O26

Bulur E. ThP2-9  
 Bulyk L.-I. ThS10-O44,  
 TuS6-O26

Buryi M. TuS6-O28,  
ThP2-2,  
 TuS5-K11,  
 TuS5-O19,  
 TuS7-O30,  
 WeS8-K16,  
 TuP1-13,  
 TuP1-26

Buzanov O. A. WeS8-O34,  
 ThS10-O43,  
 ThS10-O41,  
 TuP1-24

## C

Cala R. ThS11-O49  
 Chaika M. ThS10-K21  
 Chang I. FrS15-O62  
 Chepyga L. FrS16-K32  
 Cherenenko K. WeS8-O33

Chernenko K.	WeS9-O37, ThS10-O41, ThS13-O55	Dewo W.	<u>TuP1-16</u> , TuS6-K13
Chernov G.	FrS14-O57, ThP2-13	Deyneko D.	ThP2-5
Chernov V.	<u>ThP2-13</u> , FrS14-O57	Di Credico B.	TuS7-O32
Chornodolskyy Ya.	ThS10-O44, TuP1-17, TuP1-18	Discher M.	<u>FrS15-O60</u> , <u>ThP2-16</u> , FrS15-O62, ThP2-21
Christensen J. B.	ThS11-K23, <u>ThS12-O53</u> , ThS12-O52, ThP2-10,	Dolezal V.	TuS5-K11
Chrunik M. J.	ThS10-O42	Dosovitskiy G.	MoS3-O11, MoS3-O12
Chruścińska A.	<u>FrS15-K31</u> , ThP2-18, ThP2-19,	Drozdowski K. J.	ThP2-4
Chu C. H.	ThP2-15	Drozdowski W.	<u>MoS2-O5</u> , MoS2-K6, TuP1-3, TuP1-15, ThP2-4
Chukova O.	<u>TuP1-25</u>	Duffar T.	TuP1-7
Chylli M.	<u>TuS7-O31</u>	Dujardin C.	<u>TuS7-K14</u> , <u>TuP1-7</u> , ThS11-O48
Ciepielewski P.	TuS6-O26	Dunaeva E. E.	TuP1-5
Cieszko M.	TuP1-21	<b>E</b>	
Colombo C.	MoS2-O7	Eliyahu I.	ThP2-24
Comotti A.	ThS11-O48	<b>F</b>	
Corradi G.	WeS9-O37	Fabisiak K.	<u>ThS12-O51</u>
Cova F.	MoS2-O7, ThS11-O48	Fang M.-H.	WeS9-O40
Crapanzano R.	<u>TuS7-O32</u>	Fasoli M.	TuS7-O32
Čuba V.	TuS7-O29	Fedorov A.	FrS16-O64
<b>D</b>		Fedorov N.	ThS10-O43
D'Arienzo M.	TuS7-O32	Feldbach E.	WeS9-O37, ThS10-O45, TuP1-4
Danilkin M.	<u>MoS3-10</u>	Fernandez J. F.	TuP1-4
Daurenbekov D.	<u>ThP2-8</u> , TuP1-19	Fujiwara C.	<u>MoS2-O9</u> , MoS1-O4, ThS12-O50
de Marcillac P.	TuP1-7		
Děcká K.	TuS7-O29		
Demkiv T.	ThS10-O44, TuP1-17, TuP1-18		
Dendebera M.	TuP1-17, TuP1-18		
Dereń P. J.	WeS9-O39, FrS14-O58, FrS15-O63, FrS16-O65	<b>G</b>	
		Gadomski A.	<u>MoS0-K1</u>
		Gajewski J.	ThS12-K25, FrS14-O56

Galazka Z.	MoS2-K6, MoS2-O5, TuP1-3, TuP1-15, ThP2-4		
Galenin E.	<u>TuS5-O20</u> , TuS4-K10, TuS4-O16, ThS11-O49		
Galli A.	FrS15-K30		
Galunov N.	<u>MoS2-O8</u>		
Gamernyk R.	ThS10-O44, TuP1-18		
Gayshan V.	<u>TuP1-27</u>		
Gektin A.	MoS1-K4, TuP1-27		
Gerasymov Ia.	<u>TuS4-O16</u> , TuS4-K10, TuS4-O17, TuS5-O20		
Giela T.	ThS10-O42		
Gieszczyk W.	<u>FrS14-K28</u> , ThS11-O46, TuP1-12, ThP2-3		
Ginzburg D.	ThP2-24		
Giuliani A.	TuP1-7		
Gorbacheva T.	TuS4-O17		
Gorbenko V.	<u>TuS6-O27</u> , TuS6-K13, TuS6-O24, TuS6-O25, TuS6-O26, FrS16-O64, TuP1-10, TuP1-11, TuP1-12, TuP1-13, TuP1-14, TuP1-16, TuP1-20, ThP2-12, ThP2-14		
Grochot A.	ThS10-O42		
Grüne M.	FrS16-K33		
Grynyov B.	TuS4-K10		
Gundacker S.	MoS1-O2, ThS11-O49		
		<b>H</b>	
		Hajek F.	TuS5-K11
		Hanada T.	MoS2-O9, TuS5-O21, TuS5-O22, TuP1-9,
		Havlak L.	TuS5-K11
		Havlicek J.	TuS5-K11
		Hizhnyi Y.	<u>WeS8-O35</u> , <u>TuP1-23</u>
		Horowitz Y.S.	ThP2-24
		Horwacik T.	FrS14-O56
		Houel J.	TuS7-K14
		Houžvička J.	TuP1-22
		Huang W.-T.	WeS9-O40
		Hubáček T.	TuS6-O28, TuS7-O30
		Hussainova I.	TuP1-4
		<b>I</b>	
		Iida T.	MoS1-O1, TuP1-6
		Irmscher K.	MoS2-K6, MoS2-O5, TuP1-3, TuP1-15, ThP2-4
		Ishikawa S.	TuS5-O18, TuS5-O22, ThS12-O50
		Ishizawa S.	<u>ThS12-O50</u>
		Iwanowski P.	ThS10-O42
		<b>J</b>	
		Jabłońska K.	ThS10-O42
		Jakubec I.	TuS7-O29
		Jarý V.	<u>TuS7-O30</u> , TuS6-O28, TuS7-O29
		<b>K</b>	
		Kaczmarek M.	TuS6-K13
		Kaczmarek S. M.	WeS9-O40
		Kaderavkova A.	TuS7-O31

Kainarbay A.	TuP1-19, ThP2-8	Kochurikhin V.	TuS5-O18, TuS5-O21, TuS5-O22, TuP1-8, TuP1-9
Kajdrowicz T.	FrS14-O56		
Kamada K.	<u>TuS5-O18</u> , <u>TuP1-8</u> , MoS1-O1, TuS5-O21, TuS5-O22, ThS11-O46, TuP1-6, TuP1-9, TuP1-10, ThP2-2, MoS2-O9	Kodama S.	MoS2-O9, TuS5-O19
		Kofanov D.	<u>TuS4-O17</u>
		Korjik M.	MoS3-O12
		Korzhik M.	MoS3-O11
		Kosyl K. M.	ThS10-O42
		Kotomin E. A.	WeS9-K19, WeS8-K17
			WeS9-O37
Kandel R.	TuP1-26	Kovács L.	
Kapton Ł.	<u>ThS11-O47</u>	Kozlova A. P.	ThS10-O41, TuP1-5, TuP1-24
Karavaeva N.	MoS2-O8		
Kasimova V.	WeS8-O34	Kozlova N.	WeS8-O34, ThS10-O43
Khabuseva S.	MoS2-O8		
Khromiuk I.	MoS2-O8	Král J.	TuS7-O29
Kim H.	<u>FrS15-O62</u> , FrS15-O60	.Král R.	TuS5-K11, <u>TuS5-O19</u> , MoS1-O3
Kim J.-L.	FrS15-O62		
Kim K. J.	TuS5-O18, TuS5-O22, TuP1-6, TuP1-8, TuP1-9, TuS5-O21	Krasnikov A.	<u>ThP2-1</u> , WeS9-O38
		Kratochwil N.	MoS1-O2, ThS11-O49
		Krech A.	MoS2-O8
		Krutyak N.	<u>ThP2-5</u> , ThS10-O43
Kim M. C.	FrS15-O60, FrS15-O62		
		Kučera M.	<u>TuS6-K12</u> , TuS5-O23
Kirm M.	<u>ThS10-K20</u> , MoS3-O13, WeS9-O37, ThS10-O45, ThS13-O55	Kucerkova R.	TuS5-O18, TuS6-O25, TuS6-O27, TuP1-10, TuP1-14
Kiselev S.	<u>WeS8-O36</u>		
Kitaura M.	<u>WeS9-K18</u>	Kudrjajtseva I.	TuS6-O26, WeS8-O35
Klejch M.	TuS4-O15		
Klementiev K.	ThS10-O41	Kulevoy T.	WeS8-O34
Kłosowski M.	ThS11-O46, ThS12-K25, FrS14-K28, FrS14-O56, TuP1-12, ThP2-3	Kulzer F.	TuS7-K14
		Kurashima Y.	ThS12-O50
		Kurosawa S.	<u>MoS1-O4</u> , MoS2-O9, TuS4-O14, TuS5-O19, TuS5-O21,
Kochiev M.	MoS3-O10		



	TuS5-O22, ThS12-O50, TuP1-9, ThP2-2	Majewska N. Majewski-Napierkowski A. Majgier R.	<u>WeS9-O40</u> <u>ThP2-12</u> <u>ThP2-22</u> ThP2-17
Kurtsev D.	TuS4-O16, TuS4-O17, TuS5-O20	Makowski M.	<u>TuP1-15</u> , MoS2-K6, MoS2-O5, TuP1-3, ThP2-4
Kutsuzawa N.	TuS5-O21		
Kuzovkov V. N.	WeS8-K17		
<b>L</b>			
Lagov P.	WeS8-O34		
Laguta V.	<u>WeS8-K16</u> , TuS5-K11, TuP1-13, ThP2-2	Malyi T. Mandowska E. Mandowski A.	TuP1-18 <u>ThP2-23</u> , ThP2-20 <u>ThS11-K22</u> , ThP2-17, ThP2-20, ThP2-22, ThP2-23
Lalinsky O.	<u>TuS5-O23</u> , TuS6-K12	Mann S.	<u>MoS2-O6</u>
Lebbou K.	TuS4-K10, TuS4-O17	Maratova A. Marczewska B.	<u>ThP2-11</u> ThS12-K25, FrS14-K28, ThP2-3
Ledoux G.	TuS7-K14		
Lee J.	FrS15-O60, FrS15-O62	Marek J. Mares J. A.	ThS12-K24 <u>TuS6-O25</u> , TuP1-14, TuS6-O27, TuP1-10
Lee S. K.	FrS15-O62		
Lemański K.	<u>FrS14-O58</u> , FrS15-O63		
Lengyel K.	WeS9-O37	Markovskiy A.	TuP1-16, <u>FrS16-O64</u> , TuP1-21
Leniec G.	WeS9-O40		
Leśniewski T.	WeS9-O40		
Lighthart R.	TuP1-26	Marnieros S.	TuP1-7
Liu R.-S.	WeS9-O40	Martin P.	ThS10-O43
Loghina L.	TuS7-O31	Martinazzoli L.	<u>MoS1-O2</u> , ThS11-O49
Lorenzi R.	TuS7-O32		
Łoś S.	ThS12-O51	Martini M.	<u>FrS15-K30</u>
Lucchini M. T.	ThS11-O49	Maryański M.	<u>ThS12-K24</u>
Luचेchko A.	<u>ThP2-9</u> , ThP2-6	Matshaba M. G.	ThP2-25
		Meng Z.	TuS7-K14
Lushchik A.	<u>WeS8-K17</u> , TuS6-O26, WeS8-O35	Michalska P. Mihóková E. Mikhailik V. B. Miniajluk-Gaweł N.	ThS13-O54 <u>TuS7-O29</u> TuP1-26 <u>FrS15-O63</u> , FrS14-O58
<b>M</b>			
Ma C.-G.	MoS2-K5	Mitina N.	TuP1-17
Mahler B.	TuS7-K14	Miyazaki T.	TuP1-6
Mahlik S.	<u>MoS3-K8</u> , WeS9-O40	Mizukoshi K.	MoS1-O1, TuP1-6

Monguzzi A.	<u>MoS2-O7</u> , ThS11-O48	Nolte P.	FrS16-K33
Morozov V.	ThP2-5	Nones C.	TuP1-7
Moskal G.	ThS11-O47	Novati V.	TuP1-7
Mostoni S.	TuS7-O32	Nurakhmetov T.	TuP1-19, ThP2-8
Motta S.	<u>ThP2-10</u>		
Motto-Ros V.	TuP1-7		
Mrozik A.	<u>FrS15-O61</u> , <u>TuP1-12</u> , ThS11-O46	<b>O</b>	
		Ohashi Y.	TuS5-O21, TuS5-O22, TuP1-9, MoS2-O9
Murakami R.	TuS5-O18		
Mykhaylyk V.	TuP1-17		
		Olivieri E.	TuP1-7
<b>N</b>		Olko P.	<u>ThS12-K25</u>
Nagirnyi V.	<u>WeS9-O37</u> , ThS10-O45, ThS13-O55, TuP1-4, ThP2-5	Omelkov S.	MoS3-O13, ThS10-O45, TuP1-4
		Orfano M.	<u>ThS11-O48</u> , MoS2-O7
Nagorny S.	<u>TuP1-26</u>	Oster L.	<u>ThP2-24</u>
Nahorna V. V.	TuP1-26	Osvet A.	FrS16-K32
Nargelas S.	<u>MoS3-O12</u> , MoS3-O11	<b>P</b>	
Nedilko S. A.	TuP1-25	Pakari O. V.	ThS11-K23, <u>ThS12-O52</u> , ThS12-O53
Nedilko S. G.	WeS8-O35, TuP1-23, TuP1-25	Palczewski P.	ThP2-18
		Pankratov V.	<u>ThS10-O41</u> , <u>TuP1-5</u> , WeS8-O33, WeS8-O35, TuP1-24
Nemirovsky D.	ThP2-24		
Ngoepe P. E.	ThP2-25	Pankratova V.	<u>TuP1-24</u> , ThS10-O41, TuP1-5
Nikl M.	<u>MoS1-K3</u> , MoS1-O3, MoS2-O7, TuS4-O15, TuS5-O18, TuS5-O19, TuS6-K12, TuS6-O25, TuS6-O27, TuS7-O29, WeS8-K16, ThS11-O49, TuP1-10, TuP1-14, TuP1-22. ThP2-2	Paprocki K.	ThS12-O51, TuP1-20
		Paterek J.	TuS5-K11, MoS1-O3, TuS5-O19
Nisi S.	TuP1-26	Pavlov Y.	WeS8-O34
Nizhankovskiy S.	ThS13-O54, FrS16-O64, TuP1-21	Pawlak N.	<u>ThP2-19</u>
		Pedracka A.	FrS14-O56
		Pejchal J.	<u>TuS5-K11</u> , MoS1-K3, ThS11-O48
		Piasecki M.	MoS2-K5

Piotrowski T. ThS13-K27  
Poda D. V. TuP1-7  
Polák J. TuP1-22  
Polupan Ya. MoS2-O8  
Popielarski P. TuP1-11  
Popov A. I. WeS9-K19,  
WeS8-K17,  
TuP1-24

Poshyvak O. ThP2-6  
Pospíšil J. TuS4-O15  
Prochazkova-Prouzova L. TuS5-K11,  
TuP1-26

Przybylińska H. ThS10-O42,  
TuP1-23

Pushak A. TuP1-18  
Pustovarov V. A. MoS3-O13,  
TuP1-1,  
WeS8-O36

## R

Radzhabov E. WeS8-O33  
Rajendran V. WeS9-O40  
Rathaiiah M. TuS6-K12  
Rebane O. ThS13-O55,  
ThS10-O45

Redon T. TuP1-7  
Remeš Z. TuS6-O28,  
TuS7-O30

Reshes G. ThP2-24  
Reszka A. ThS10-O42

Rikhotso B. ThP2-25  
Ristic Y. ThP2-21

Rojas-Hernandez R. E. TuP1-4  
Romet I. TuP1-4,  
MoS3-O10,  
MoS3-O13,  
WeS9-O37,  
ThS10-O45,  
ThS13-O55

Rubesova K. TuS5-K11  
Rubio-Marcos F. TuP1-4  
Ruiz-Torres R. R. FrS14-O57  
Runka T. TuS6-K13,  
TuP1-16

## S

Saaring J. ThS10-O45  
Şadel M. FrS14-O56  
Sadykova B. M. ThP2-8  
Salas-Castillo P. FrS14-O57  
Salikhodzha Zh. M. TuP1-19,  
ThP2-8

Sankowska M. ThP2-3  
Šarakovskis A. ThS10-O41  
Sato H. MoS2-O9,  
TuS5-O21,  
TuS5-O22,  
TuP1-9

Sayle D. C. ThP2-25  
Schauer P. TuS5-O23  
Schewski R. MoS2-K6,  
MoS2-O5,  
TuP1-3,  
TuP1-15,  
ThP2-4

Schweizer S. FrS16-K33  
Scotti R. TuS7-O32  
Secchi V. MoS2-O7  
Seeman V. WeS8-K17  
Selyukov A. MoS3-O10  
Sergeyev D. ThP2-11  
Shablonin E. WeS8-K17  
Shakhno A. TuP1-20,  
TuP1-21

Shapiro A. ThP2-24  
Shaposhnyk A. TuS5-O20  
Shendrik R. WeS8-O33,  
TuP1-5

Shih M.-Y. ThP2-15  
Shunkeyev K. ThP2-11  
Shyichuk A. FrS14-O59  
Sidletskiy O. TuS4-K10,  
TuS4-O16,  
TuS4-O17,  
TuS5-O20,  
TuS6-O27,  
ThS11-O46,  
ThS11-O49,  
TuP1-10

Siryk Yu. TuP1-21  
Skuratov V. A. TuP1-24  
Ślosarek K. MoS0-K2

Smyka R.	<u>ThP2-20</u> , ThP2-23	Tanabe S.	<u>MoS3-K7</u>
Somakumar A. K.	<u>ThP2-14</u> , TuS6-O26	Tanaka H.	ThS12-O50
Sowa U.	FrS14-O56	Tarasenko O.	MoS2-O8
Sozzani P. E.	ThS11-O48	Tichy-Rács E.	WeS9-O37
Spassky D.	<u>ThS10-O43</u> , <u>ThP2-7</u> , MoS3-O10, WeS8-O34, ThP2-5	Tishchenko E. V.	<u>TuP1-2</u>
Stasiv V.	WeS8-O35	Tkachenko S.	TuS4-K10, TuS4-O16, TuS4-O17, TuS5-O20
Stefańska D.	<u>WeS9-O39</u> , FrS16-O65	Tolekov D. A.	ThP2-8
Stefanski M.	ThS10-K21	Tomala R.	ThS10-K21
Steinmeyer P.	TuP1-27	Toyoda S.	MoS2-O9, TuS5-O21, TuS5-O22, TuP1-9
Stelian C.	TuP1-7	Trofimova E.	<u>MoS3-O13</u>
Stolbunov V.	WeS8-O34	Tsiumra V.	<u>WeS9-O38</u> , ThS10-O42, ThP2-1
Strankowski M.	ThS10-O42	Tsvirko M.	ThP2-22
Stratakis E.	TuP1-25		
Stręk W.	<u>ThS10-K21</u>		
Suchá A.	TuS7-O29		
Suchocki A.	<u>TuS6-O26</u> , MoS2-K5, WeS8-O35, WeS9-O38, ThS10-O42, ThS10-O44, TuP1-23, ThP2-14	<b>U</b>	
Suzdal V.	TuP1-27	Ubayev Zh.	ThP2-11
Swakoń J.	FrS14-O56	Ubizskii S.	<u>ThP2-6</u> , ThP2-9
Sykora G. J.	MoS2-O6		
Syrotych Y.	<u>TuP1-10</u> , TuS6-K13	<b>V</b>	
Szczepański Z.	TuP1-21	Vainer Yu.	MoS3-O10
Szufa K.	<u>ThP2-17</u>	Vaitkevičius A.	MoS3-O11, MoS3-O12
Szybowicz M.	ThS12-O51	Vaněček V.	TuS5-K11, <u>MoS1-O3</u> , TuS5-O19, TuP1-26
<b>T</b>		Vanetsev A.	ThS10-O45
Taira Y.	WeS9-K18	Vasil'chenko E.	WeS8-K17
Takizawa Y.	<u>TuS5-O21</u> , <u>TuP1-9</u> , MoS1-O1, TuS5-O22, TuP1-8	Vasil'ev A. N.	TuS7-K14, ThS10-O43, TuP1-2, <u>MoS1-K4</u>
Tamulaitis G.	<u>MoS3-O11</u>	Vasin A. A.	TuP1-1
Tamulaitis G.	MoS3-O12	Vasylechko L.	WeS8-O35, WeS9-O38, ThP2-1
		Veber P.	TuS6-O24, TuP1-7

Vedda A.	MoS2-O7, TuS7-O32, ThS11-O48	Wlodarczyk D. Woda C.	<u>ThS10-O42</u> ThP2-16, ThP2-21
Velazquez M.	TuP1-7, TuS6-O24	Wojtowicz A. J.	<u>MoS2-K6</u> , MoS2-O5, TuP1-3, TuP1-15, ThP2-4
Vereschagina N. Villa I.	MoS3-O10 <u>TuS7-K15</u> , MoS2-O7, TuS7-O32, TuP1-7		
Vistovskyy V.	<u>TuP1-18</u> , ThS10-O44, TuP1-17	<b>X</b> Xu J.	MoS3-K7
Vlcek M. Voitenko T. Voloshinovskii A.	TuS7-O31 TuP1-25 <u>TuP1-17</u> , ThS10-O44, TuP1-18	<b>Y</b> Yajima R.	<u>TuS5-O22</u> , TuP1-8, TuP1-9
Vovk O. Voznyak-Levushkina V. Vu T. H. Q.	TuP1-21 ThP2-7 WeS9-O39, <u>FrS16-O65</u>	Yamaji A.	MoS1-O4, MoS2-O9, TuS4-O14, TuS5-O21, TuS5-O22, ThS12-O50, TuP1-9, ThP2-2
<b>W</b>			
Wachnicki L. Wang P. Watanabe S. Winiiecki J.	WeS9-O38 TuP1-26 WeS9-K18 <u>ThS13-K26</u> , ThS12-O51, ThS13-O54	Yokota Y.	MoS2-O9, TuS5-O19, TuS5-O21, TuS5-O22, TuP1-9
Winnacker A. Witkiewich-Lukaszek S.	FrS16-K32 TuP1-10, <u>TuP1-14</u> , TuS4-O16, TuS6-O24, TuS6-O25, TuS6-O27, TuP1-11, <u>ThS13-O54</u> , TuP1-12, TuP1-20, ThP2-12	Yoshikawa A.	<u>TuS4-K9</u> , MoS1-O1, MoS1-O4, MoS2-O9, TuS4-O14, TuS5-O18, TuS5-O19, TuS5-O21, TuS5-O22, ThS11-O46, ThS12-O50, TuP1-6, TuP1-8, TuP1-9, TuP1-10, ThP2-2
Witkowski M. E.	<u>ThP2-4</u> , MoS2-K6, MoS2-O5, TuP1-3, TuP1-15	Yoshino M.	<u>MoS1-O1</u> , <u>TuP1-6</u> , MoS2-O9, TuS5-O18,

	TuS5-O21, TuS5-O22, TuP1-8, TuP1-9		TuP1-12, TuP1-13, TuP1-14, TuP1-20, ThP2-12
Yukihara E. G.	<u>ThS11-K23</u> , ThS12-O52, ThS12-O53, ThP2-10	Zorenko Yu.	<u>TuS6-O24</u> , <u>TuP1-13</u> , TuS4-K10, TuS4-O14, TuS4-O16, TuS6-K13, TuS6-O25, TuS6-O26, TuS6-O27, ThS11-O46, ThS13-O54, FrS16-K32, FrS16-O64, TuP1-10, TuP1-11, TuP1-12, TuP1-14, TuP1-16, TuP1-20, TuP1-21, ThP2-12, ThP2-14
Yussupbekova B. N.	TuP1-19, ThP2-8		
<b>Z</b>			
Zabelina E.	<u>WeS8-O34</u> , ThS10-O43		
Zaichenko A.	TuP1-17		
Zajac M.	ThS10-O42		
Zajíc F.	<u>TuS4-O15</u>		
Zapadlík O.	<u>TuP1-22</u>		
Zazubovich S.	WeS9-O38, ThP2-1		
Zelenskaya O.	TuS4-O16, TuS4-O17		
Zeler J.	TuP1-11		
Zemenova P.	TuS5-K11		
Zhangylyssov K. B.	ThP2-8	Zuev M. G.	TuP1-1
Zhunusbekov A. M.	ThP2-8	Zúniga-Rivera N. J.	FrS14-O57
Zhydachevskii Ya.	ThP2-3	Zych E.	FrS14-O59, TuP1-11, ThP2-7
Zhydachevskyy Ya.	<u>FrS14-K29</u> , TuS6-O26, WeS8-O35, WeS9-O38, TuP1-23, ThP2-1, ThP2-6, ThP2-9, ThP2-14		
Zhyshkovych A.	TuP1-18		
Zloužeová K.	TuS5-O19		
Zolotarova A. S.	TuP1-7		
Zorenko T.	<u>TuP1-21</u> , TuS4-O14, TuS4-O16, TuS6-O24, TuS6-O25, TuS6-O27, FrS16-O64, TuP1-10, TuP1-11,		